

STOCK STRUCTURE OF PATAGONIAN TOOTHFISH *DISSOSTICHUS*
ELEGINOIDES (SMITT 1898, FAMILY NOTOTHENIIDAE) IN THE
SOUTHWEST ATLANTIC

A thesis submitted in fulfilment of the requirements for the degree of

DOCTOR OF PHILOSOPHY

In

ICHTHYOLOGY AND FISHERIES SCIENCE

Of

RHODES UNIVERSITY

By

BRENDON LEE

ORCID ID

<https://orcid.org/0000-0003-1682-8905>

January 2022

Supervisors: Prof. Warwick Sauer, Dr Alexander Arkhipkin and Dr Haseeb Randhawa

General Abstract

The identification of discrete self-sustaining productive units in marine populations is essential for achieving sustainable fisheries objectives. Marine fish populations frequently exhibit dynamic characteristics across their life-histories, displaying variability in spatial structure and mixing patterns, both within and among populations. The incoherent application of management boundaries on biological populations can bias stock assessment results and have important implications on sustainable fisheries management. Patagonian toothfish (*Dissostichus eleginoides*) is a long-lived, slow-growing, late-maturing, deep-sea, benthopelagic species. It forms the basis of important and highly lucrative industrial and artisanal fisheries across its distribution. Patagonian toothfish have complex life-histories characterised by high dispersal potential during the egg and larval phase, a wide depth range because of their ontogenetic migratory behaviour, and large adult size that is capable of undertaking long-distance active movements (>200 km). These characteristics provide opportunities for high levels of connectivity, and as such, the stock structure is not well understood. We applied an integrated, multidisciplinary approach to provide an improved understanding of the complex stock structure dynamics for Patagonian toothfish on the Patagonian Shelf, specifically in relation to the shelf, slope, and deep-sea plains around the Falkland Islands. Research results were focused on aspects pertaining to (1) geographic variation in phenotypic characters (otolith shape); (2) a description of the spatial-temporal distribution patterns; (3) the active movements of deep-sea adults (tag-recapture study); and (4) the identification of early life-history dispersal through otolith microstructure and microchemical chronologies. Results from the study indicate high regional connectivity during the early life-history stages derived from at least two spawning contingents into spatially discrete nursery areas (cohort groups) on the Falklands Shelf. Fish followed distinct ontogenetic pathways into deeper waters adjacent to the areas wherein juvenile settlement into a demersal habitat occurred. There is little to no evidence of mixing among cohort groups

during their ontogenetic migration into deep-sea adult habitats, reflecting a mixed population based on oceanographically defined egg and larval dispersal. The majority of the adult component of the population continue to display high site fidelity. However, between 9 and 25% of the population, consisting predominantly of larger reproductively capable adults undertake long-distance dispersal behaviour, identified as home-range relocations from the adult deep-sea habitats towards three of the known southern spawning grounds in the region. Results are suggestive of a requirement for improved collaborative efforts for regionally-based management approaches with careful consideration of local stock contingents. Future monitoring and research priorities should focus on the identification of reproductive potential, dispersal pathways and settlement patterns of stock contingents to inform the dynamics of mixed stock origins across the Patagonian region. While many aspects regarding the stock structure remain unresolved, results derived from the current studies can be used to inform the development of management measures to ensure the continued recovery and sustainable management of Patagonian toothfish within the region.

Declaration

I, Brendon Lee, hereby declare that this doctoral thesis submitted to the Department of Ichthyology and Fisheries Science, Rhodes University, is my original work and has not been previously submitted in any form to another university. I have not included ideas, phrases, passages or illustrations from another person's work without acknowledging their authorship.



Brendon Lee

14/01/2022

Date

Preface

Publications during the PhD

This thesis is comprised of four independent research chapters, integrated with a general introduction (Chapter 1), and a general discussion and conclusion (Chapter 6). Three of the research chapters have been published as stand-alone manuscripts in peer-reviewed journals, and one is under preparation for submission. As a result, there is some repetition regarding the species biology and study area among these. Although a number of collaborators contributed to each publication, in all cases, I was involved with the study design and methodology, I led the collection of data and analyses, and wrote each manuscript.

Chapter 2 - **Lee, B.**, Brewin, P. E., Brickle, P., and Randhawa, HS. (2018). Use of otolith shape to inform stock structure in Patagonian toothfish (*Dissostichus eleginoides*) in the southwestern Atlantic. *Marine and Freshwater Research*, 69: 1238–1247.

Chapter 3 - **Lee, B.**, Arkhipkin, A., and Randhawa, HS. (2021). Environmental drivers of Patagonian toothfish (*Dissostichus eleginoides*) spatial-temporal patterns during an ontogenetic migration on the Patagonian Shelf. *Estuarine, Coastal and Shelf Science*, 259: 107473.

Chapter 4 - **Lee, B.**, Skeljo, F., Randhawa, HS., Arkhipkin, A. (2022). Deep-sea movement patterns of the Patagonian toothfish *Dissostichus eleginoides* Smitt 1898, in the Southwest Atlantic. *Marine and Freshwater Research*.

Other Publication during the PhD

Brickle, P., Randhawa, H. S., Reid, M. R., **Lee, B.**, Shcherbich, Z., and Arkhipkin, A. I. (2021).

Otolith trace elemental analyses and parasites provide useful tools for the stock discrimination of *Patagonotothen ramsayi* (Regan, 1913) (Nototheniidae) on the southern Patagonian Shelf. *Fisheries Research*, 244: 106129.

Lee, B., Cockroft, K., Arkhipkin, A. I., Wing, S. R., and Randhawa, H. S. (2019). Age, growth and mortality estimates for the ridge-scaled grenadier *Macrourus carinatus* (Günther, 1878) in the southwestern Atlantic. *Fisheries Research*, 218: 174–185.

Arkhipkin, A., Brickle, P., **Lee, B.**, Shaw, P.W., McKeown, N.J. (2022). Taxonomic re-appraisal for toothfish (*Dissostichus*: Notothenioidea) across the Antarctic Polar Front using genomic and morphological studies. *Journal of Fish Biology*.

Arkhipkin, A., Shcherbich, Z., Busbridge, T., Blake, A., and **Lee, B.** (2022). Sexual dimorphism in age, growth and maturation in channel bull blenny *Cottoperca trigloides* (Forster, 1801) (Bovichtidae: Notothenioidei) on the Patagonian Shelf, Southwest Atlantic. *Polar Biology*.

Conference presentations during the PhD

Lee, B. (2018). Variability in otolith shape shows evidence of stock structure in Patagonian toothfish (*Dissostichus eleginoides*) in the Southwest Atlantic. Oral presentation. International Otolith Symposium, Keelung, Taiwan.

Technical Reports during the PhD

- Arkhipkin, A., Herrera, D., **Lee, B.**, Boag, T., Bradley, K., and Cockcroft, K. (2017). Juvenile toothfish survey, Fisheries Research Cruise ZDLT1-01-2017. Technical Report, Falkland Islands Government, Fisheries Department, Stanley, Falkland Islands.
- Arkhipkin, A., **Lee, B.**, Goyot, L., Ramos, J.E., Chemshirova, I., Roberts, G., Costa, M., Blake, A. (2019). Cruise Report ZDLM3-02-2019: Demersal biomass survey. Technical Report, Falkland Islands Government, Fisheries Department, Stanley, Falkland Islands. 44 pp.
- Lee, B.** (2019). Age structure of the common hake *Merluccius hubbsi* from Falkland Islands waters: January - December 2018. Technical Report, Falkland Islands Government, Fisheries Department, Stanley, Falkland Islands. 16 pp.
- Lee, B.** (2020). Age structure for Patagonian toothfish *Dissostichus eleginoides* from Falkland Island waters: January – December 2018. Technical Report, Falkland Islands Government, Fisheries Department, Stanley, Falkland Islands. 18 pp.
- Lee, B.** (2020). Age structure for Patagonian toothfish *Dissostichus eleginoides* from Falkland Island waters: January – December 2019. Technical Report, Falkland Islands Government, Fisheries Department, Stanley, Falkland Islands. 17 pp.
- Lee, B.** (2022). Age structure for Patagonian toothfish *Dissostichus eleginoides* from Falkland Island waters: January – December 2020. Technical Report, Falkland Islands Government, Fisheries Department, Stanley, Falkland Islands. 17 pp.
- Lee, B.** (2020). Age structure for Rock cod *Patagonotothen ramsayi* from Falkland Island waters: January – December 2015. Technical Report, Falkland Islands Government, Fisheries Department, Stanley, Falkland Islands. 15 pp.
- Lee, B.** (2020). Age structure for Rock cod *Patagonotothen ramsayi* from Falkland Island waters: January – December 2016. Technical Report, Falkland Islands Government, Fisheries Department, Stanley, Falkland Islands. 15 pp.

- Lee, B.** (2020). Age structure for Rock cod *Patagonotothen ramsayi* from Falkland Island waters: January – December 2017. Technical Report, Falkland Islands Government, Fisheries Department, Stanley, Falkland Islands. 15 pp.
- Lee, B.**, Goyot, L., Castillejos, J. E. R., Hall, J., and Zawadowski, T. (2019). Research Cruise Report: ZDLT1-12-2018. Patagonian toothfish - juvenile survey. Technical Report, Falkland Islands Government, Fisheries Department, Stanley, Falkland Islands. 10 pp.
- Lee, B.**, Shcherbich, Z., and Randhawa, H. (2018). Age validation for rock cod (*Patagonotothen ramsayi*) sampled in the Falkland Islands: a comparison of age estimates. Technical Report, Falkland Islands Government, Fisheries Department, Stanley, Falkland Islands. 5 pp.
- Lee, B.**, Shcherbich, Z., Randhawa, H. (2020). Towards the development of an ageing strategy for finfish in the Falkland Islands trawl fisheries. AGE-2020-FIN. Technical Report, Falkland Islands Government, Fisheries Department, Stanley, Falkland Islands. 24 pp.
- Lee, B.**, Skeljo. (2020). Patagonian Toothfish Tag-recapture Program Update Report: June 2016 – July 2020. TAG-2020-TOO. Technical Report, Falkland Islands Government, Fisheries Department, Stanley, Falkland Islands. 16 pp.
- Randhawa, H. S., and **Lee, B.** (2016). Toothfish tagging cruise ZDLC2-06-2016, CFL Gambler. Technical Report, Falkland Islands Government, Fisheries Department, Stanley, Falkland Islands. 20 pp.
- Randhawa, H. S., **Lee, B.**, Farrugia, T. J., and Keningale, B. (2017). Toothfish tagging cruise ZDLK3 – 06/07 – 2017. Technical Report, Falkland Islands Government, Fisheries Department, Stanley, Falkland Islands. 17 pp.
- Winter, A., **Lee, B.**, Arkhipkin, A., Tutjavi, V., and Büring, T. (2020). 2020 1st Season assessment survey Falkland calamari (*Doryteuthis gahi*): ZDLS3-S1-2020. Technical Report, Falkland Islands Government, Fisheries Department, Stanley, Falkland Islands. 17 pp.

Winter, A., and **Lee, B.** (2018). Stock assessment – Grenadier (*Macrourus carinatus*, *Coelorinchus fasciatus*). Technical Report, Falkland Islands Government, Fisheries Department, Stanley, Falkland Islands. 13pp.

Surveys during the PhD

Doryteuthis gahi pre-season research survey. (2022). Falkland Islands Government, 15 days (FV Argos Cies). Chief Scientist.

Doryteuthis gahi pre-season research survey. (2020). Falkland Islands Government, 8 days (FV Argos Cies). Chief Scientist.

Demersal finfish biomass survey. (2019). Falkland Islands Government, 8 days (RV Monteferro). Chief Scientist.

Dissostichus eleginoides juvenile recruitment research survey. (2018). Falkland Islands Government, 8 days (RV Castello). Lead Scientist.

Acknowledgements

Undertaking a long-term project such as this in a small community like the Falkland Islands is a unique experience. For myself, one of the advantages of having been based here has been the opportunity of working with so many different people from around the world as they pass through, or remain. This has been an influential factor in being able to call this place my home over the last few years, and I am extremely grateful having had the opportunity.

I would like to express my gratitude to Joost Pompert and Paul Brewin for initially providing me with the opportunity to begin this adventure by hiring me as a scientific fisheries observer in the Falkland Islands Fisheries Department. If it were not for my initial group of colleagues and friends in the observer team during my first year, I certainly would not have enjoyed myself, learnt so much and decided to stay: Marine Quintin, Jessica Jones, Francisco Sobrado, Eva Visauta, Lars Jurgens, Ross James and Denise Blake. I thank Alexander Arkhipkin and Paul Brewin for providing me with the opportunity in a more scientific role as a fisheries scientist for Patagonian toothfish biology, which would set the stage for my eventual pursual of this PhD on a part-time basis within the position.

I would like to express my gratitude to my three supervisors. To Warwick Sauer for agreeing to take me on as a student at DIFS, and for providing me with such flexibility, being based on the other side of the world. My thanks to Alexander Arkhipkin for providing me with the many opportunities to improve my skills and capabilities, and for your continued support and enthusiasm with this research over the years. I am grateful to Haseeb Randhawa, for providing me with the professional structure and support I required to pursue this research and develop as a scientist. It has been a pleasure working with you. I would like to thank Frane Skeljo for his advice and guidance over the last year. I would also like to express my gratitude to the

three examiners of this thesis for their extensive, constructive and overall encouraging feedback: Dr Julian Ashford, Professor Stephen X. Cadrin, and Professor Stephen Wing.

I am extremely thankful for the financial support for this research from Consolidated Fisheries Ltd (CFL). Thanks to the Government of South Georgia & the South Sandwich Islands and Mark Belchier at British Antarctic Survey for otoliths from South Georgia and the South Sandwich Islands; as well as colleagues at Instituto de Fomento Pesquero (IFOP), Valparaiso, Chile for otoliths from Chile which were used for otolith shape analyses. Thanks also to William Brownscombe and Stanislav Strekopytov from the Natural History Museum in London, for providing the facilities, training, skills and equipment for the otolith microchemistry component of this research. Thank you to all the Scientific Fisheries Observers as well as Rebecca Piontek and Zhanna Shcherbich for contributions towards data collection and processing of samples over the years. I would also like to thank Michael Gras, Paul Brickle, Alex Blake and Ludovic Goyot for formal and informal contributions, assistance and discussions related to this work.

I would like to express my biggest thanks to those that gave me the opportunities to nurture my interest in the natural world as a child, specifically my parents, Anita and Terry, and grandparents, Bep, George and Joey. I will never forget all the trips and experiences around the spectacular outdoor areas wherein I grew up; the many visits to the East London Museum, and library; all the books, and projects; and the never-ending encouragement to keep exploring and learning. I also thank my siblings, Shaun, Lauren and Catherine for always keeping me inspired through how you all live your lives. You all provided me with the upbringing and environment to have the unique privilege to experience, appreciate, enjoy and learn about the wonderful outdoors. Finally, I would like to say thank you to my wife, Amanda, for supporting me in my decision to undertake this PhD here in the Falkland Islands, for always believing in me and being my closest friend. I am looking forward to many more adventures together.

Table of Contents

General Abstract.....	i
Declaration.....	iii
Preface	iv
Acknowledgements.....	ix
Table of Contents.....	xi
List of Tables	xvi
List of Figures	xviii
Chapter 1 - General Introduction.....	1
1.1. Fisheries Sustainability	1
1.2. Fisheries Expansion.....	2
1.3. Fish population dynamics and stock structure.....	4
1.4. The Patagonian Shelf	7
1.5. Patagonian toothfish	12
1.5.1. Distribution.....	12
1.5.2. Fisheries and management.....	13
1.5.3. Life-history and ecology	16
1.5.4. Population connectivity	21
1.6. Research aims and structure of the thesis	23
Chapter 2 - Use of otolith shape to inform stock structure in Patagonian toothfish in the Southwest Atlantic Ocean	26
2.1. Introduction.....	27
2.2. Materials and methods.....	30
2.2.1. Data collection	30

2.2.2.	Image and shape analyses	32
2.2.3.	Statistical analysis	34
2.3.	Results.....	35
2.3.1.	Image and shape analyses	35
2.3.2.	Shape features	36
2.3.3.	Shape analyses	39
2.4.	Discussion	45
Chapter 3 - Environmental drivers of Patagonian toothfish (<i>Dissostichus eleginoides</i>) spatial-temporal patterns during an ontogenetic migration on the Patagonian Shelf		51
3.1.	Introduction.....	53
3.2.	Materials and methods.....	56
3.2.1.	Study area	56
3.2.2.	Data collection	58
3.2.3.	Variables.....	60
3.2.4.	Statistical analysis	63
3.2.5.	Temporal structure.....	66
3.3.	Results.....	67
3.3.1.	Otolith interpretation.....	67
3.3.2.	Population structure and environmental drivers	68
3.3.3.	Spatial-temporal patterns.....	72
3.3.4.	Habitat description	78
3.4.	Discussion	80
3.4.1.	Oceanographic drivers.....	81

3.4.2.	Spatial-temporal patterns.....	83
3.4.3.	Fish relationship with habitat.....	84
3.4.4.	Ecological interactions.....	86
3.4.5.	Management implications and conclusions.....	87
3.5.	Supplementary information.....	89
Chapter 4 - Deep-sea movement patterns of the Patagonian toothfish <i>Dissostichus eleginoides</i> Smitt, 1898, in the Southwest Atlantic.....		
		92
4.1.	Introduction.....	93
4.2.	Materials and methods.....	96
4.2.1.	Study area.....	96
4.2.2.	Fish tagging and recapture.....	97
4.2.3.	Data analysis.....	100
4.3.	Results.....	102
4.3.1.	Tags and recaptures.....	102
4.3.2.	Distances moved.....	105
4.3.3.	Effects on movement.....	109
4.4.	Discussion.....	110
4.5.	Supplementary information.....	118
Chapter 5 - Otolith microstructure and microchemistry reveal early life-history shifts in Patagonian toothfish <i>Dissostichus eleginoides</i> from the Patagonian Shelf.....		
		120
5.1.	Introduction.....	121
5.2.	Materials and methods.....	124
5.2.1.	Sample Collection.....	124
5.2.2.	Sample Extraction.....	124

5.2.3.	Otolith processing	126
5.2.4.	Statistical analyses	130
5.3.	Results.....	135
5.3.1.	Otolith microstructure.....	135
5.3.2.	Temporal trends in elemental profiles	138
5.3.3.	Dynamic life-history shifts	140
5.4.	Discussion	145
5.4.1.	Otolith microstructure examination.....	146
5.4.2.	Temporal trends in elemental profiles	148
5.4.3.	Timing of life-history events	153
Chapter 6 -	General Discussion	156
6.1.	Connectivity of Patagonian toothfish on the Patagonian Shelf	156
6.2.	A hypothetical life-history for Patagonian toothfish.....	157
6.2.1.	Genetic units.....	159
6.2.2.	Spawning.....	160
6.2.3.	Egg and larval dispersal and retention	162
6.2.4.	Demersal juveniles and sub-adults	164
6.2.5.	Adults	167
6.2.6.	Stock structure.....	169
6.3.	Management approaches	174
6.3.1.	Status quo management.....	174
6.3.2.	'Weakest link' management	175
6.3.3.	Spatial and temporal closures.....	176

6.3.4.	Integration of stock composition into management.....	177
6.3.5.	Alteration of stock boundaries.....	178
6.4.	Management recommendations.....	178
6.4.1.	Collaborations.....	179
6.4.2.	Research priorities.....	179
6.4.3.	Data collection and monitoring.....	181
6.5.	Conclusion.....	186
References	187

List of Tables

Table 1: Overview of Patagonian toothfish (<i>Dissostichus eleginoides</i>) and Antarctic toothfish (<i>Dissostichus mawsoni</i>) otolith samples used for shape analysis: SGP, South Georgia; SSP, South Sandwich Islands; CHP, Chile; FIPS, Falkland Islands, south (Burdwood Bank); FIPN, Falkland Islands, north; HSP, high seas; SSA, South Sandwich Islands.	32
Table 2: Summary of the ANOVA-like permutation test with 1000 iterations on Antarctic toothfish (<i>Dissostichus mawsoni</i>) and Patagonian toothfish (<i>D. eleginoides</i>) elliptical Fourier coefficients according to seven sampling regions (see Table 1 for area codes)	41
Table 3: Jackknifed correct classification matrix of the linear discriminant analysis applied to the six sampling regions for Patagonian toothfish (<i>Dissostichus eleginoides</i>) and Antarctic toothfish (<i>D. mawsoni</i> ; see Table 1 for area codes). Bold font indicates the percentage correctly classified for each region.	42
Table 4: Jackknifed correct classification matrix of the linear discriminant analysis applied to the two sampling regions for Patagonian toothfish (<i>Dissostichus eleginoides</i>) in South Georgia and the South Sandwich Islands (SGSSI; see Table 1 for area codes). Bold font indicates the percentage correctly classified for each region.....	44
Table 5: Jackknifed correct classification matrix of the linear discriminant analysis applied to the four sampling regions for Patagonian toothfish (<i>Dissostichus eleginoides</i>) along the Patagonian Shelf (see Table 1 for area codes). Bold font indicates the percentage correctly classified for each region.....	45
Table 6: Comparison of best-fitting models based on the deviance information criterion (DIC) and Watanabe Akaike's information criterion (WAIC) scores and the associated dispersion parameter estimates. Best-fit models are depicted in grey squares and in bold.....	74

Table 7: Posterior means, standard deviations and 95% credible intervals for the spatial-temporal random field estimated in the best fit age-based and full models.....	75
Table 8: Posterior means, standard deviations and 95% credible intervals for the covariates estimated in the best fit age-based models. Credible intervals of parameter estimates that do not overlap zero are depicted in grey squares and in bold.....	79
Table 9: Summary of the explanatory variables obtained from research survey programmes and Copernicus Marine Environment Monitoring Service (CMEMS).....	91
Table 10: Numbers of toothfish tagged and released within each area according to year. Three geographic regions were defined during tagging: BB = Burdwood Bank, FIS: E = Eastern Falkland Islands Slope and FIS: N = Northern Falkland Islands Slope.....	103
Table 11: Summary of the movement patterns of tagged and recaptured Patagonian toothfish individuals across the study area. Three geographic regions were defined during tagging: BB = Burdwood Bank, FIS: E = Eastern Falkland Islands Slope and FIS: N = Northern Falkland Islands Slope.	108
Table 12: Suitability assessment for tagging of fish.....	118
Table 13: Summary of samples used for otolith microstructure (age-0+) and microchemistry transects (age-1+) from shelf areas around the Falkland Islands.	125
Table 14: Parameter estimates for (1) the linear model describing the relationship between growth increment and day of capture; and the second-order polynomial regression describing (2) the length: age and (3) age:otolith distance relationships.	138
Table 15: Mean percentage (range) of drifters released between May and June 1996–2000 from (a) Burdwood Bank and (b) southern Chile, present in the northern and southern FICZ at 50–300 days (table taken from Ashford <i>et al.</i> , 2012b). Refined scenarios based on recent results have been highlighted in grey.	164

List of Figures

- Figure 1: Map of the study area identifying the main oceanographic and physical features:
 APF: Antarctic Polar Front, BB: Burdwood Bank, NSR: North Scotia Ridge, FI: Falkland Islands, CH: southern Chile. 8
- Figure 2: Polar projection depicting the distribution patterns of Patagonian toothfish. APF: Antarctic Polar Front, SGSSI: South Georgia and South Sandwich Islands. 13
- Figure 3: Catch data for Patagonian toothfish since the inception of the fisheries, showing the (A) regional (SA: South American and SO: Southern Ocean) and (B) extent of reported (black line, FAO) and estimated total catch (Pauly *et al.* 2020) accumulated for each of the two regions. 15
- Figure 4: Model depicting key life-history stages (boxes), and the approaches (Chapters) undertaken in the current research to investigate potential connectivity pathways (arrows) of Patagonian toothfish on the Patagonian Shelf. 25
- Figure 5: Sampling positions of Patagonian toothfish and Antarctic toothfish otoliths. SGP, South Georgia; SSP, South Sandwich Islands; CHP, Chile; FIPS, Falkland Islands, south (Burdwood Bank); HSP, High Seas; FIPN, Falkland Islands, north. Solid black lines reflect the territorial waters of the Falkland Islands: Falkland Islands conservation zone (FICZ, inner) and Falkland Islands outer conservation zone (FOCZ, outer). Longitudinal lines reflect the north–south direction. 31
- Figure 6: Quality of the elliptical Fourier-outline reconstruction. The dashed vertical line shows the number of elliptical Fourier harmonics needed for a 98.5% accuracy of the reconstruction. 36
- Figure 7: Captured images reflecting examples of whole toothfish otoliths obtained from (a) South Sandwich Islands: Antarctic toothfish (*Dissostichus mawsoni*) of lengths 149, 161 and 164 cm; (b) South Georgia and South Sandwich Islands: Patagonian toothfish (*D.*

<i>eleginoides</i>) of lengths 140, 135 and 80 cm; and (c) Patagonian Shelf: Patagonian toothfish (<i>D. eleginoides</i>) of lengths 102, 66 and 69 cm.....	38
Figure 8: The mean otolith shapes based on elliptical Fourier reconstruction for Patagonian toothfish and Antarctic toothfish according to the seven sampling regions (see Table 1 for area codes).....	39
Figure 9: Non-metric multidimensional scaling ordination plot of the Euclidean distances for Patagonian toothfish (<i>Dissostichus eleginoides</i>) and Antarctic toothfish (<i>D. mawsoni</i>) otolith shape indicating capture sites (see Table 1 for area codes) and regional groupings (SA–TOA, Subantarctic Antarctic toothfish; SA–TOP, Subantarctic Patagonian toothfish; Pat–TOP, Patagonian Shelf Patagonian toothfish). Stress value of the plot: 0.027.....	40
Figure 10: Linear discriminant analysis scores for the classification of Patagonian toothfish (<i>Dissostichus eleginoides</i>) by sampling region (see Table 1 for area codes).....	43
Figure 11: Map depicting the main oceanographic and topographical features of the study area. The shaded areas indicate the quadrats from which oceanographic variables were extracted from the main current systems (see Section 2.4). APF: Antarctic Polar Front; SAF: Subantarctic Polar Front; FC: Falklands Current; PC: Patagonian Current; FT: Falklands Trough; BB: Burdwood Bank. Satellite-based depictions on the right portray years of high (16 August 2016) and low (16 August 2017) influence of the Subantarctic Front over the Falklands Shelf. Locations of the combined sample sites (black dots) and INLA mesh for the SPDE model are shown on the bottom right.	58
Figure 12: The position of the sampling locations and the observed toothfish abundance for each sample year. The sizes of points reflect the numbers of toothfish caught on the log scale.	59
Figure 13: A conceptual diagram of the spatial-temporal patterns explored within the Bayesian species distribution model framework. Note that the Age-0 model only utilised data extending over a three-year time period (2015-2017) due to the absence of any catch during 2018 to 2020.	67

- Figure 14: Sectioned otolith from an (A) 13 cm age-0+, (B) 27 cm age-1+, (C) 38 cm age-2+ and (D) 51 cm age-3+ Patagonian toothfish, viewed at 20X magnification. The white dots indicate the edge of the translucent (Winter) zone of growth. The scale bar reflects 1 mm..... 68
- Figure 15: The observed (A) length frequency and (B) age frequency distributions for Patagonian toothfish sampled across the shelf waters of the Falkland Islands during February 2015 to 2020 (n = 10,511). The dotted lines reflect the progression of cohorts through time..... 70
- Figure 16: Marginal effect of age, year, depth (m), oxygen ($\text{mmol}\cdot\text{m}^{-3}$), Falkland Current ($\text{m}\cdot\text{sec}^{-1}$) and SAF:FC current velocity ($\text{m}\cdot\text{sec}^{-1}$) variables with respect to the age-disaggregated numerical abundance (Full model) of juvenile Patagonian toothfish on the Patagonian Shelf from 2015 to 2020. The estimated effect is presented in the linear predictor scale (logarithmic link) with the grey shaded area representing the 95% credible intervals..... 71
- Figure 17: Marginal effect of year with respect to the predicted age-based numerical abundance of juvenile Patagonian toothfish on the Patagonian Shelf from 2015 to 2020. The estimated effect is presented in the linear predictor scale (logarithmic link). 72
- Figure 18: Posterior mean values for the spatial random field for the age-0 model with opportunistic spatial temporal correlation for each year. Hotspots, identified as areas with abundances above the 90th percentile are circled with the blue contour line. Grey contour lines indicate the 200 m and 500 m depth contours..... 76
- Figure 19: Posterior mean values for the spatial random field for the age-1 model with progressive spatial temporal correlation for each year. Hotspots, identified as areas with abundances above the 90th percentile are circled with the blue contour line. Grey contour lines indicate the 200 m and 500 m depth contours. 76
- Figure 20: Posterior mean values for the spatial random field for the age-2 model with progressive spatial temporal correlation for each year. Hotspots, identified as areas with

abundances above the 90 th percentile are circled with the blue contour line. Grey contour lines indicate the 200 m and 500 m depth contours.	77
Figure 21: Posterior mean values for the spatial random field for the age-3 model with a persistent spatial temporal correlation for each year. Hotspots, identified as areas with abundances above the 90 th percentile are circled with the blue contour line. Grey contour lines indicate the 200 m and 500 m depth contours.	78
Figure 22: Posterior mean values and the 95% credible intervals of the fixed parameters for the linear abiotic and biotic effects for shelf-based juvenile Patagonian toothfish abundance on the Falkland Islands shelf between 2015 and 2020.	80
Figure 23: Simulation study showing the observed number of zeros (black dot) and the simulated number of zeros in 10,000 data sets that were fitted from the full BSDMs fitted with the Poisson and zero-inflated Poisson distributions with progressive spatial-temporal correlation for age.	89
Figure 24: Posterior mean values for the spatial random field for the full model with progressive spatial temporal correlation for age. Hotspots, identified as areas with abundances above the 90 th percentile are circled with the blue contour line. Grey contour lines indicate the 200 m and 500 m depth contours.....	90
Figure 25: Map depicting the bathymetric areas occupied by juvenile (Shelf, 150 – 450 m) and adult (Slope, 451 – 2500 m) Patagonian toothfish across the study area. Five geographic regions were defined: BB = Burdwood Bank, CH = southern Chile, NSR = North Scotia Ridge, FIS: E = Eastern Falkland Islands Slope and FIS: N = Northern Falkland Islands Slope. The Falkland Islands Conservation Zones and Argentinian EEZ are reflected by solid lines.	97
Figure 26: Geographic distributions of tagged Patagonian toothfish and the associated length frequency distributions within the three regions (n=4418). Solid lines depict the Falkland Islands Conservation Zones (FCZ). The three geographic regions that occur within the Falkland Islands waters are: BB = Burdwood Bank (n = 1381), FIS: E = Eastern Falkland Islands Slope (n = 1945) and FIS: N = Northern Falkland Islands Slope (n = 1092)...	99

- Figure 27: Spatial distribution of longline fishing effort (number of lines set per $0.1^\circ \times 0.1^\circ$ gridsquare; $n = 2236$) during the study period (June 2016 to October 2021) in the Falkland Islands Conservation Zones. 104
- Figure 28: Length frequency distribution (A) for Patagonian toothfish measured at recapture ($n = 232$) and (B) the frequency distribution of distances moved for fish recaptured during the study period. Note the non-linear sequence of the x-axis. 105
- Figure 29: Tag and recapture locations for Patagonian toothfish that undertook movements of (A) <50 km, (B) 51-200 km and (C) 200+ km within 450 to 2500 m bathymetric constraints. BB = Burdwood Bank, CH = southern Chile, NSR = North Scotia Ridge, FIS: E = Eastern Falkland Islands Slope and FIS: N = Northern Falkland Islands Slope. 107
- Figure 30: Results of the generalised additive model (with 95% confidence intervals) showing the effect of direction, depth-difference between tagging and recapture locations, average fish length, and tagging location on the distances moved. Rug plots display the distribution of observations. 110
- Figure 31: Photographs depicting the different steps involved in tagging fish: A) Receiving the fish in the 'dry' section of the factory where the tagging station has been set up; B) cutting of the hooks with bolt cutters to minimise injury to the fish; C) the use of applicators to apply two tags to an immobilised toothfish; D) illustration of how tags should be applied, i.e. inserted into the dorsal muscle of the second dorsal fins angled downwards and backwards with tag barb lodged behind the forward edge of 2nd and 3rd dorsal fin ray; E) fish transported by two crew members from the tagging station to the spring balance using a stretcher; and F) fish released from the stretcher over the side of the vessel from the hauling bay, head first into the water. 119
- Figure 32: Map depicting the locations and areas where age-0+ and age-1+ year old Patagonian toothfish were sampled for microstructure ($n = 62$) and trace element analysis ($n = 120$). 126
- Figure 33: Diagram depicting (A) a whole juvenile toothfish otolith showing the position (dashed lines) and (B) orientation of transverse sections and (C) daily increment counts.

- (D) Digitised representation of a transverse section from the age-0+ section of a juvenile Patagonian toothfish displaying the location of the laser line transect extending from the primordium (birth) to the edge. (D) Age-0+ otoliths were processed for microstructure analysis and inference of daily age post-hatch (dph) onto corresponding elemental profiles of age-1+ individuals..... 128
- Figure 34: (A) Relationship between the day in year of capture (from 1 January) and otolith increment counts (Increments; $R^2 = 0.64$); (B) the distribution of hatching dates over ten-day periods, back calculated from the date of capture, from daily age estimates; (C) relationship between age (days post-hatch, dph) and length ($R^2 = 0.72$); and (D) distance from otolith primordium and age (days post-hatch, dph) developed for age-0 Patagonian toothfish ($n = 60$; $R^2 = 0.99$). 137
- Figure 35: Results of the generalised additive mixed models (with 95% confidence intervals) showing the ontogenetic relationship in age (days post hatch, dph) with Sr, Mg, Ba and Mn element:Ca ratios for juvenile Patagonian toothfish. Dotted vertical line reflects the average distance observed to the hyaline zone defined as a life-history shift (LHS) marker in age-0 otolith sections analysed for microstructure ($n = 62$), and subsequently identified in otolith transverse sections from age-1 individuals used for elemental analyses (LHS_{OS} , $n = 120$). Dashed (LHS_{Sr} , LHS_{Ba} , LHS_{Mg} and LHS_{Mn}) and solid (Integrated approach, LHS_{INT}) vertical lines reflect the average changepoints estimated across elemental profiles, respectively. 140
- Figure 36: Otolith (A) Sr, (B) Ba, (C) Mn and (D) Mg element:Ca profiles for two individual (Otolith ID = JV105 and JV99) Patagonian toothfish. Grey solid lines represent the seven-point moving average of elemental ratios estimated over age (days post-hatch, dph). The grey dashed vertical lines indicate the dynamic life-history shift, as estimated for the particular individual based on changepoint analysis. 142
- Figure 37: Boxplots comparing model predictions of the daily age post-hatch (dph) that life-history shifts occur among (A) the three areas: NE - Northeast, S - South and W - West; and (B) the five markers based on changepoints estimated across element:Ca profiles

- for Sr, Ba, Mg and Mn; and from otolith microstructure observations (OS). The y-axis is reflected on the scale of the marker for Sr:Ca and area NE which were arbitrarily selected for the intercept to produce the plots..... 144
- Figure 38: Age-frequency distribution of dynamic life-history shifts for Patagonian toothfish, detected using otolith Sr:Ca, Ba:Ca, Mg:Ca, and Mn:Ca profiles. Estimated age that life-history shift occurred for each individual was based on the average changepoint estimated from all five markers. Sample sizes are indicated above each bar..... 145
- Figure 39: Map depicting the full Patagonian range occupied by Patagonian toothfish across the study area. Solid lines reflect the conservation zones of the Falkland Islands, including juvenile inshore (50 to 150 m) and sub-adult deep-sea areas (401 to 600 m) for which monitoring data are limited. Black points reflect stations from the demersal biomass trawl survey including deep-sea stations used in 2018 (DBS), and red points indicate Lolignid squid pre-season trawl survey stations. 159
- Figure 40: Hypothetical depiction of possible scenarios explaining high variability in microchemistry signatures and what this implies in terms of the retention of juveniles from discrete or continuous spawning areas. A.) Continuous spawning area with eggs and larvae spread evenly across the Falklands Shelf. B.) Discrete spawning areas with mixing taking place during the egg phase, or (C.) retention of early juveniles from a single discrete spawning area..... 161
- Figure 41: Length frequency distribution at different depths for Patagonian toothfish sampled on the Patagonian Shelf and Slope between 2015 and 2021 (n = 71897)..... 167
- Figure 42: Hypothetical life-cycle for Patagonian toothfish depicting the stock structure based on findings of this thesis. The three spawning stock contingents (NSR = North Scotia Ridge, BB = Burdwood Bank, SC = Southern Chile) that make up the metapopulation are depicted passing through areas of interest across key life-history stages. Regions of interest: BB = Burdwood Bank, FI:W = Falkland Islands west, FI:E = Falkland Islands East, FI:S = Falkland Islands South, FI:NE = Falkland Islands North East, HS = High Seas, SC = Southern Chile. Dashed lines indicate movement across areas. 173

Chapter 1 - General Introduction

1.1. Fisheries Sustainability

The sustainability of marine capture-fisheries is integral to global food security, livelihoods, and economies. Natural resource sustainability has been included as an explicit objective in a wide range of domestic, national, and international policies, legislations, and commitments undertaken by governments, conservation groups and industry throughout the world. Sustainability is commonly linked with the term sustainable development, as it is the development of resources for human use that modifies natural resources (Hilborn *et al.* 2015). The most widely accepted definition comes from the Brundtland Commission (Brundtland 1987) - *Sustainable development is development that meets the needs of the present generation without compromising the ability of future generations to meet their own needs* - a definition clearly recognising the goal of development to provide benefits to people, within the constraints of the natural world (Hilborn *et al.* 2015; Kenny *et al.* 2018). Sustainability therefore has three interacting elements: ecological, social, and economic sustainability. In the context of fisheries, the ecological component involves the single-species resource base, interacting species, and the ecosystem in which they are embedded (Quinn II and Collie 2005). However, it is important to iterate that sustainability in fisheries is determined primarily by the process of managing the inherent trade-offs that must occur between these interacting elements, according to the desired objectives relating to the resource (Hilborn *et al.* 2015).

Commitments towards the sustainability of fisheries are highlighted in the Sustainable Development Goal 14 within the 2030 Agenda for Sustainable Development to end overfishing and restoring depleted fish stocks: a commitment adopted by all member states of the United Nations (Ye and Gutierrez 2017). Evidence from global catch reconstructions suggest that marine capture fisheries reached their peak during the mid-1990's (86 - 130 million tonnes)

after which catches have either plateaued (FAO 2020) or are in decline, despite an increase in fishing effort with the expansion of industrial fisheries into the waters of developing countries (Pauly and Zeller 2016). The most common approach for assessing the biological status of a fishery resource relates to the reporting of reference points associated with maximum sustainable yield (MSY). MSY is roughly defined as the highest average amount of catch that could consistently be taken out of a fished population each year (Costello and Ovando 2019). Reference points associated with MSY are usually stated in terms of the fishing mortality at which MSY is obtained (F_{MSY}), and the stock biomass that produces MSY (B_{MSY}). Despite much controversy surrounding the term (Larkin 1976; Mace 2001; Quinn II and Collie 2005; Rindorf *et al.* 2017; Pauly and Froese 2021), MSY has been enshrined in national and international law (e.g. in the UN Convention on the Law of the Sea – UNCLOS 1982). Globally, roughly 60% of fish stocks are considered maximally sustainably fished, 7% are underfished and 30 to 35% are overexploited or collapsed (Link 2010; Branch *et al.* 2011; Costello *et al.* 2016; Ye and Gutierrez 2017; FAO 2020). The proportion of fisheries defined as overexploited have been growing over time (Costello and Ovando 2019). However, while smaller, unassessed fisheries are declining, many large, industrial fisheries appear to be doing well and in many cases rebuilding as a result of effective management (Costello *et al.* 2012; Melnychuk *et al.* 2017; Hilborn 2020).

1.2. Fisheries Expansion

Since the advent of industrial fishing, the pattern of exploitation can be characterised as one of the sequential depletion of many fish stocks (Ludwig *et al.* 1993; Hutchings 1996; Dickey-Collas *et al.* 2010), with subsequent large-scale changes in the relative abundance of various ecosystem components (Link *et al.* 2011; Christensen *et al.* 2014; Danovaro *et al.* 2020; Duarte *et al.* 2020). This has been further exacerbated through climate change (Brander 2007; Brander 2010; Campana *et al.* 2020). With declines in shallow coastal water resources, increasing demand with human population growth, and technological advances in the

development of fishing gear, historical fisheries expanded first into offshore, and then deeper waters (Koslow *et al.* 2000; Morato *et al.* 2006; Salmerón *et al.* 2015; Victorero *et al.* 2018). The expansion and subsequent depletion of fisheries into offshore waters are clearly evident in the isolated, higher latitudes of the subantarctic and Antarctic Southern Ocean (Pauly *et al.* 1998; Morato *et al.* 2006; Kock *et al.* 2007; Ainley and Blight 2009). The intensive exploitation of finfish in the region from the late 1960s onwards lead to the near extinction of shallow-water fishes, such as the marbled rock cod (*Notothenia rossii*) by the 1970s, and icefish (*Champscephalus gunnari*) by 1980 (Croxall and Nicol 2004; Ainley and Blight 2009). Fisheries then moved into deeper waters to target grenadiers (Devine *et al.* 2012; Lee *et al.* 2019a), and later, Patagonian toothfish (Constable *et al.* 2000; Morato *et al.* 2006). These occurred in a 'boom and bust' practice, and despite later area closures for the purposes of fish-stock recovery, few populations have recovered (Ainley and Blight 2009; Hollyman *et al.* 2021).

The patterns of sequential depletion of deep-sea fish is well known (Morato *et al.* 2006; Clark and Dunn 2012; Victorero *et al.* 2018). Many deep-sea species possess characteristic k-selective life-history traits including long lives, slow growth, late maturation, and low rates of natural mortality (Bergstad 1990; Kelly *et al.* 1997; Murua and Motos 2000; Rodríguez-Marín *et al.* 2002; Murua 2003; Lee *et al.* 2019a). In addition, they commonly display aggregative behaviour, particularly during key, and sensitive life-history stages such as spawning (Roberts 2002). This behaviour can inflate the perceived biomass estimates, as well as making them easy targets for trawlers during which effort is extremely difficult to control. Due to their life-history and behavioural traits, many deep-sea fisheries show a disproportionate level of overexploitation (Clarke *et al.* 2003; Morato *et al.* 2006; Devine *et al.* 2006), exacerbated by a paucity of biological and fisheries data, limiting the ability of timely assessments (Haedrich *et al.* 2001; Devine *et al.* 2006). For example, Devine *et al.* (2006) identified five species (*Antimora rostrata*, *Coryphaenoides rupestris*, *Bathyraja spinicauda*, *Notacanthus chimnitzii* and *Macrourus berglax*) of deep-sea fish in the Northwest Atlantic that had declined to such

an extent over a 17-year period (87 to 98%) that they met the IUCN criteria for being critically endangered. The depletion of deep-sea populations are therefore more rapid, and recovery much slower and less certain than for their shallow-water counterparts (Roberts 2002).

Variation in stock recovery among regions have been attributed to stronger management regimes, even for some deep-sea species. The status of many stocks from industrial fisheries in developed countries have shown strong recovery in recent years, highlighting how stringent fisheries management can be used in a framework for stock stabilization and recovery (Worm *et al.* 2009; Branch *et al.* 2011; Costello *et al.* 2016; Ye and Gutierrez 2017; Melnychuk *et al.* 2017; Costello and Ovando 2019; Hilborn *et al.* 2020). For example, some stocks of orange roughy (*Hoplostethus atlanticus*) around New Zealand (Doonan *et al.* 2015) and Australia (Kloser *et al.* 2015) that were historically overfished and substantially depleted now appear to be recovering and likely to lead to sustainable fisheries. However, prolonged intense overexploitation, especially for collapsed stocks, not only delays rebuilding but also substantially increases the uncertainty in recovery times (Neubauer *et al.* 2013).

1.3. Fish population dynamics and stock structure

The 'stock' concept as a population unit is deeply rooted in fisheries science and has formed the basis of assessment and management for well over 100 years (Baranov 1918; Russell 1931). The essential aspect of fish stock biomass dynamics, described by Russell (1931), was that the stock biomass (S) in a given year (i) has gains in the form of recruitment (R) and individual growth (G), and losses through natural (M) and fishing (F) mortality:

$$S_{i+1} = S_i + (R + G) - (F + M)$$

It was further recognised that these stocks could be divided into animals of a size liable to capture (already recruited to the fishery), and those smaller than this limit. One of the key

factors missing from Russell's formulation was the absence of terms for emigration or immigration, which were assumed to be balanced (Haddon 2011). The 'unit stock' considered in this expression was implicitly assumed to be a reproductively isolated population that are demographically independent from other populations of the same species, and young fish in the population are assumed to be entirely spawned from adults in the same population. Isolated populations are expected to exhibit demographic independence, with different trajectories of stock, recruitment, mortality, and age composition, reflecting the population parameters that are estimated by stock assessment models (Cadrin 2020). Conventional stock assessment models, therefore, make three related assumptions about spatial scope and structure: the population is closed (no immigration and emigration), homogeneous (there are no differences in vital rates across the area), and well-mixed (fishery removals from one area in a time interval affect the density of the entire population during the interval). While the methods of modelling the details of these processes have varied, the factors identified have been the main focus of single-species fisheries scientists ever since (Haddon 2011; Hawkins *et al.* 2016); informing the Beverton-Holt yield per recruit equation (Beverton and Holt 1957) and defining the terms used to understand the relationship between recruitment and stock (Shepherd 1982).

A thorough understanding of population structure is crucial when delineating stock boundaries for the development and implementation of relevant management measures. Almost all fish populations and fisheries, have some spatial structure and mixing patterns, falling along a continuum across broadly defined (1) sympatric discrete (2) spatially complex and (3) panmictic population categories (Cope and Punt 2011; Ciannelli *et al.* 2013; Brophy *et al.* 2016; Kerr *et al.* 2020). A sympatric discrete population refers to reproductively and genetically isolated populations, which may occupy overlapping habitats, at least during one phase of their life cycle. The broadly defined spatially complex population can include both metapopulations, and source-sink populations, including those structured according to the 'Member-Vagrant Hypothesis' (Sinclair and Iles 1989). In the case of a classical

metapopulation, these consist of similar, discrete locally breeding subpopulations or contingents which may be genetically connected via dispersal (Fronhofer *et al.* 2012; Hawkins *et al.* 2016). In contrast, source-sink metapopulation structures are characterised by a donor population contributing to a receptor population that would otherwise not be able to maintain persistence. The sink feature most commonly is a result of poor habitat quality limiting the ability of the receptor population to reconnect with the source (Fronhofer *et al.* 2012; Hawkins *et al.* 2016). It has been argued that many fish stocks evolve towards near total local retention of offspring, with only demographically insignificant interpopulation exchange that sufficient to preclude genetic divergence, dubbed the 'Member-Vagrant Hypothesis' (Sinclair and Iles 1989). In this context, a member captures the ecologically meaningful component of the local population, with vagrants reflecting those of evolutionary importance that are preventing speciation (Kritzer and Sale 2004). Finally, a panmictic population refers to interbreeding individuals that are heterogeneously distributed over space.

The maintenance of diversity within a structured population provides an important stabilising (portfolio) effect, conferring resilience and maintaining productivity, not just on the species alone, but across associated ecosystems (Hilborn *et al.* 2003; Schindler *et al.* 2010). Stock boundaries are, however, often an oversimplification of complex populations and do not always accurately represent biological population structure (Zemeckis *et al.* 2014; Kerr *et al.* 2017; Berger *et al.* 2021). Complexities in stock structure that are not accounted for may have important implications for stock assessments and fisheries management arrangements (Cope and Punt 2011; Zemeckis *et al.* 2014; Moore *et al.* 2020; Kerr *et al.* 2020). For example, what is assumed as a single closed stock within a defined management area may reflect multiple individual stocks (Smedbol and Stephenson 2001; Clausen *et al.* 2007). This is of particular importance when different contingents, fished as a single stock, possess varying levels of productivity (Dickey-Collas *et al.* 2010; Ying *et al.* 2011). The implementation of conservative population parameters can then lead to the under-fishing of contingents with high productivity, or over-fishing of less productive contingents should less conservative population parameters

be assumed (Tuck and Possingham 1994; Begg *et al.* 1999a; Kerr *et al.* 2017). Political boundaries cut across the distributions of many species, creating shared stocks between nations (Abrantes *et al.* 2020), and management units containing only a portion of a larger stock can also produce misleading results for stock assessments (Begg *et al.* 1999a; Gullestad and Sundby 2020). For example, climate-driven changes in species distributions can result in changes in the proportion of a catch in an area, leading to incorrect estimations of abundance (Hutchings 1996). Further, in the situation where stocks are undergoing rebuilding from past over-harvesting, differential restoration between unidentified stock components can lead to an inability to anticipate future recruitment to these stocks (Begg *et al.* 1999a; Dickey-Collas *et al.* 2010). Inappropriate assumptions of stock structure may also have implications for resilience and model-based investigations of the effects of climate change on the distribution and abundance (Ciannelli *et al.* 2013).

The inclusion of spatial structure in stock assessment models themselves are extremely data intensive (Cope and Punt 2011; Mormede *et al.* 2020). Stock identification methods are therefore frequently used to assist in identifying self-sustaining components within natural populations (Cadrin 2020), prior to conducting stock assessments, with a concomitant resolve to increase data provisions at the scale of management needs (Cope and Punt 2011; Janßen *et al.* 2018). Stock identification methods are therefore considered as essential partners to stock assessment (Zemeckis *et al.* 2014). However, the most practiced implementation of stock identification results are through alternate management measures (Kerr *et al.* 2017).

1.4. The Patagonian Shelf

This research took place on the Patagonian Shelf, with a specific focus on the shelf, slope and deep-sea plains around the Falkland Islands in the southwest Atlantic (Figure 1). The region presents a varied seafloor morphology. In the eastern Pacific, the Chilean shelf is narrow widening as it extends southwards and it bends around Cape Horn at the tip of South America.

In the southwest Atlantic, the Patagonian Shelf (0 to 200 m) extends along the southern portion of the continental shelf of eastern South America, from the tip of Tierra del Fuego (~55°S), northwards around the Falkland Islands. To the south of the Falkland Islands lies the Burdwood Bank (Matano *et al.* 2019), a shallow (50 to 200 m) underwater plateau that is separated from the Patagonian Shelf by a narrow (80 km, 400 m deep) channel to the west, extending through a deep trough (>2500 m) to the east where it aligns with the North Scotia Ridge.

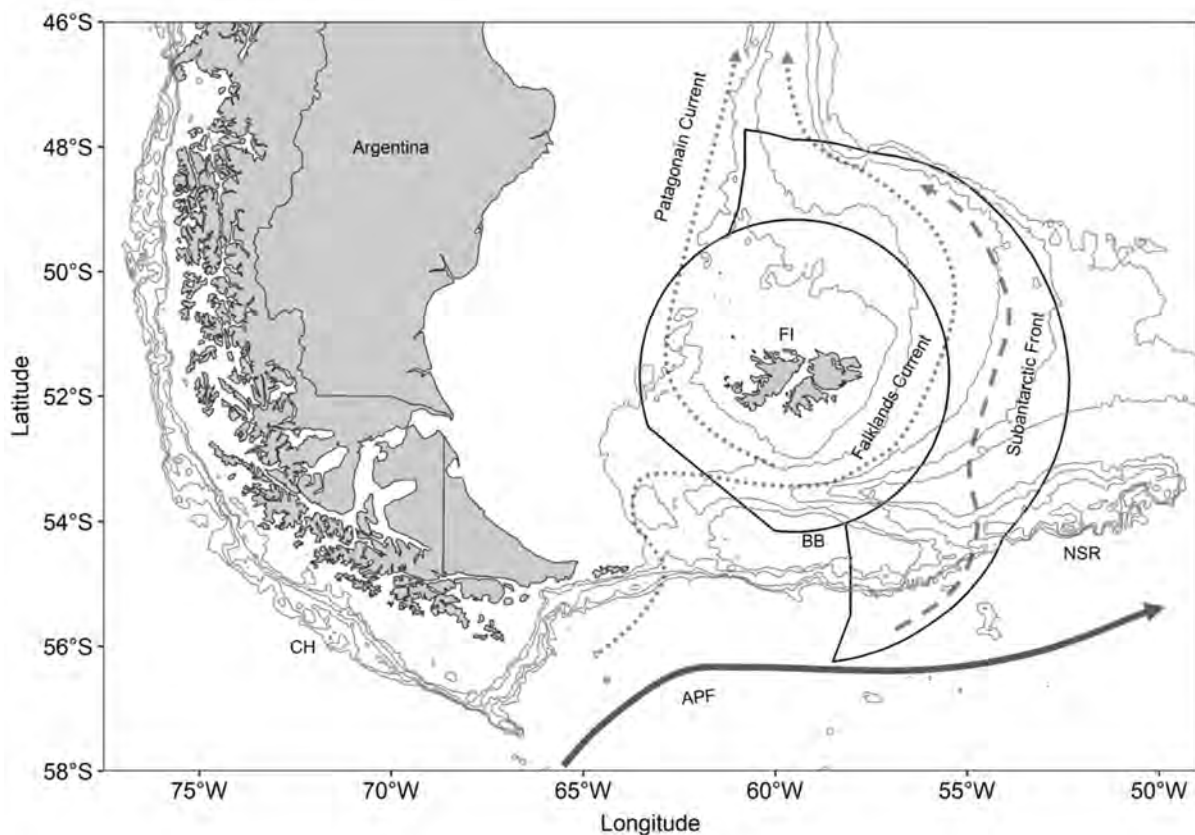


Figure 1: Map of the study area identifying the main oceanographic and physical features: APF: Antarctic Polar Front, BB: Burdwood Bank, NSR: North Scotia Ridge, FI: Falkland Islands, CH: southern Chile.

The southern extent of the Patagonian Shelf study region is defined from the Southern Ocean to the south by the Antarctic Polar Front (APF). The APF forms the strongest of a series of

eastward-flowing jets of the Antarctic Circumpolar Current (ACC), the longest (24 000 km) and strongest (130 Sverdrups, Sv, million m³/s) current in the ocean, encircling Antarctica (Clarke *et al.* 2005; Thompson 2008; Fraser *et al.* 2017). The flow (position and intensity) of the APF is constrained by bathymetry (Freeman *et al.* 2016) and is visible as a sharp change in surface water temperatures, detectable to depths of over 1000 m (Clarke *et al.* 2005). The APF forms a strong barrier to free north-south exchange of water, thus representing a distinctive biogeographical discontinuity (Clarke *et al.* 2005). The mesoscale structure of the APF however, is complex, consisting of dynamic, shifting eddies, each carrying more energy than the mean flow (Clarke *et al.* 2005; Thompson 2008; Fraser *et al.* 2017). These form an important mechanism for the transport and dispersal of parcels of water and organisms (Clarke *et al.* 2005; Fraser *et al.* 2017).

The Patagonian Shelf and Slope are among the most productive areas in the southwest Atlantic. The predominant source waters for the region are derived from the subsurface southeast Pacific Ocean, from depths greater than 500 m, upstream along the APF to the south and southeast of Chile (~55°S, 65 - 90°W; Song *et al.*, 2016). These deep waters are brought to the surface through intense wintertime convective mixing, involving a sharp deepening of the mixed layer during July-October. The source waters arrive on the Patagonian Shelf in December, during which the mixed layer shallows to less than 100 m in depth as the upper ocean is stratified in summer (Agnew 2002; Arkhipkin *et al.* 2013; Song *et al.* 2016).

The main oceanographic feature of the Patagonian Shelf is the Falkland Current, a north-flowing branch of the APF, following the continental shelf-break to the west of the Burdwood Bank and along the southern and east extent of the Falkland Islands (Croxall and Wood 2002; Arkhipkin *et al.* 2013). Along the shelf-break, the Falklands shelf waters meet the cooler and more saline waters of the Falkland Current, producing a permanent thermohaline front, known as the Falkland Current Front (Acha *et al.* 2004; Franco *et al.* 2008; Arkhipkin *et al.* 2013). Gradients of the front are seasonal and are strongest in the autumn (March – May; Acha *et*

al., 2004). During the summer (December - February) the front is characterised by mild gradients in the density and thermal field, but is weak in the salinity field. During winter (June - August), only salinity controls the density gradient. The front itself is dynamic and consists of multiple quasi-stationary meso-scale fronts (Franco *et al.* 2008), two of which are of primary importance around the Falkland Islands: the Southern Front and the North Eastern Front (Arkhipkin *et al.* 2013). The southern front is located to the south of the Falkland Islands near Beauchene Island, where the Falkland Current meets the continental slope, forming a strong upwelling at 120 to 300 m depths. The North Eastern Front represents the widest point on the Patagonian Shelf from approximately 50 to 51°S between the 150 and 200 m depth contour. In this region the apex of the shelf bends to the west with a steep slope contour to the east in contrast to the gentler slope to the north.

South of the Falkland Islands, the weaker Patagonian Current diverges to the west, extending northward (Ulibarrena and Conzonno 2015). These waters are generally less saline than those of the Falklands Current and lead to two additional meso-scale quasi-stationary frontal zones: The Western Inshore Front, located to the southwest of the Falkland Islands, and the Western Offshore Front to the northwest (Arkhipkin *et al.* 2013). The Western Offshore Front occurs as the broad valley of the Falkland Trough narrows and becomes gently shallower to the northwest of the Falkland Islands. In this region the colder more saline waters of the Patagonian Current meet the relatively warm and fresher Patagonian and Falkland Shelf waters to the north and west. The Western Inshore Front is characterised by upwelling to the shelf from the depth of 350 m and strong, almost horizontal gradients in salinity (Arkhipkin *et al.* 2013).

A second north-flowing extension of the APF, the Subantarctic Front (SAF) wraps around the eastern extent of the Burdwood Bank, flowing northward where it eventually converges with the Falkland Current and Patagonian Current at 50°S (Ashford *et al.* 2012b; Matano *et al.* 2019). Oceanographic data indicate that this current is dynamic and shifting with irregular

mesoscale eddies occasionally observed breaking through the main current stream along the northern edge of the Burdwood Bank, and linking up with the Falklands Current to the south of the Falkland Islands around Beauchene Island (Song *et al.* 2016; Fraser *et al.* 2017). In the south, persistent uplifting of micronutrient rich deep waters, driven by tidal forcing occurs around the Burdwood Bank. This leads to strong phytoplankton plumes emanating from the Burdwood Bank.

High densities of macroplanktonic euphausiid and hyperiid amphipods occur in frontal zones around the Falkland Islands, attracting and sustaining important fish and squid resources (Agnew 2002; Arkhipkin *et al.* 2013), taken by multinational fishing fleets operating in the region. The most important commercial stocks are seasonal foraging migrants such as short-fin squid *Illex argentinus*, hoki *Macruronus magellanicus*, hakes *Merluccius hubbsi* and *M. australis*, and kingclip *Genypterus blacodes* (Laptikhovsky *et al.* 2013). Other commercial species inhabit and reproduce in Falkland waters include Patagonian squid *Doryteuthis gahi*, southern blue whiting, *Micromesistius australis*, red cod, *Salilota australis*, Patagonian toothfish, *Dissostichus eleginoides*, rock cod, *Patagonotothen ramsayi*, and a diversity of skate species (Agnew 2002; Arkhipkin *et al.* 2013; Laptikhovsky *et al.* 2013). The region also hosts outstanding populations of foraging marine mammals and seabirds (Croxall and Wood 2002; Bonnet-Lebrun *et al.* 2020), including albatross (e.g. *Thalassarche melanophris*, *Diomedea exulans*), penguins (e.g. *Eudyptes chrysocome*, *Spheniscus magellanicus*), petrels (e.g. *Procellaria aequinoctialis*, *Macronectes giganteus*), pinnipeds (e.g. *Arctocephalus australis*, *Otaria flavescens*), whales (e.g. *Balaenoptera borealis*) and dolphins (e.g. *Cephalorhynchus commersonii*), many of which are ecologically linked with fish biomass and ecosystem health (Ainley and Blight 2009; Velarde *et al.* 2019).

1.5. Patagonian toothfish

1.5.1. *Distribution*

The Patagonian toothfish *Dissostichus eleginoides* Smitt 1898 (family Nototheniidae) is a large (>200 cm TL, >150 kg weight), benthopelagic predatory fish. They have a wide geographic distribution in the Southern Ocean, occurring across the continental shelf, slope, and deep-sea plains of southern Patagonia and Chile; on plateaus surrounding subantarctic islands (e.g. South Georgia, Kerguelen, Heard and McDonald Islands), banks and seamounts (Figure 1; Eastman, 1993; Collins *et al.*, 2010). On the Patagonian Shelf, they are broadly distributed in the eastern Pacific as far north as Ecuador, off the narrow Chilean Shelf extending southwards, around Cape Horn, and over the Argentinean and Falklands Shelf in the southwest Atlantic northwards to 30°S. South of the Falkland Islands, they occur over the Burdwood Bank and across the North Scotia Ridge.

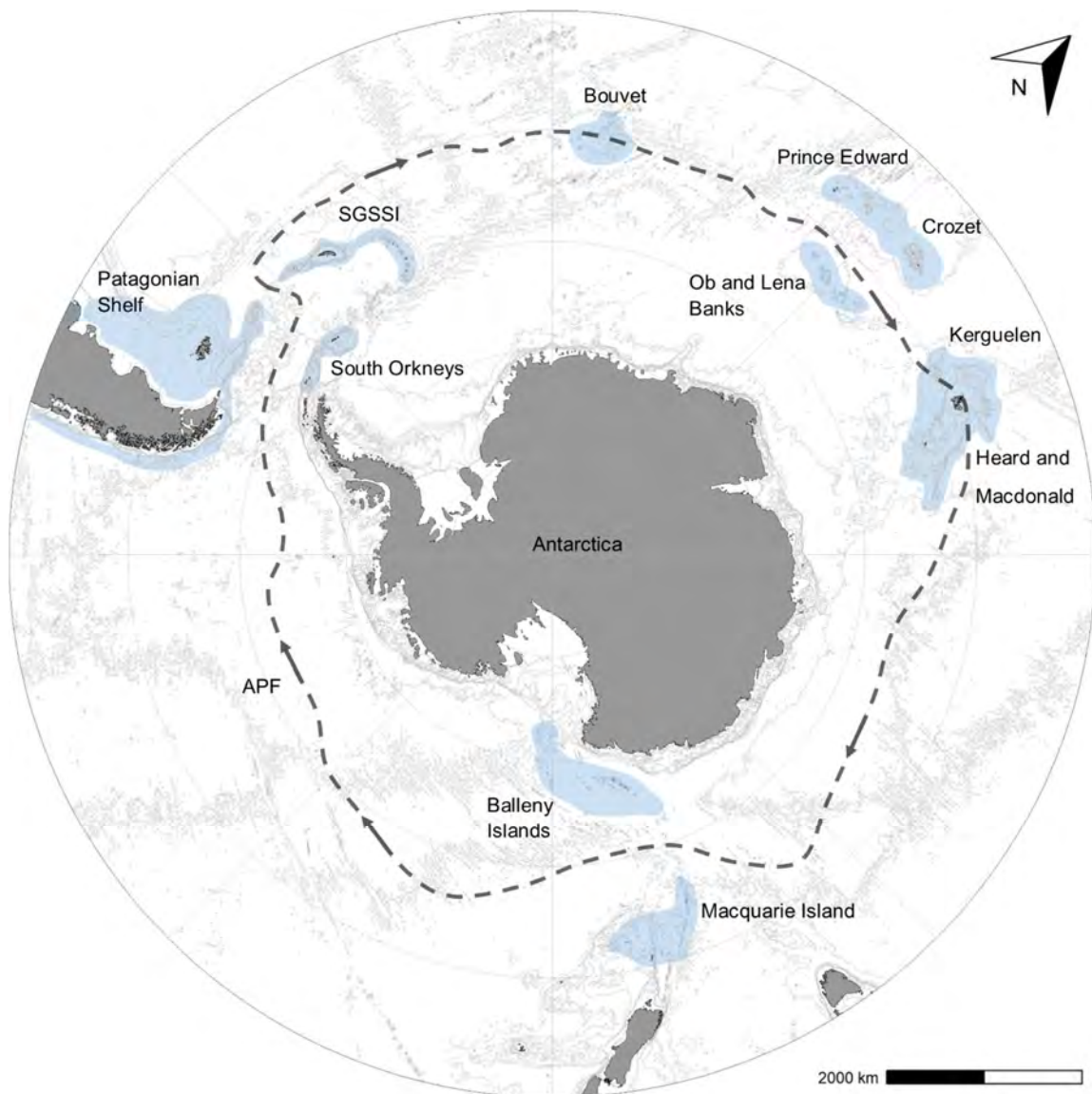


Figure 2: Polar projection depicting the distribution patterns of Patagonian toothfish. APF: Antarctic Polar Front, SGSSI: South Georgia and South Sandwich Islands.

1.5.2. Fisheries and management

Patagonian toothfish have an early history of overexploitation (Agnew 2000; Bialek 2003; Sovacool and Siman-Sovacool 2008). Catches across their range increased exponentially from just over 1000 tonnes in 1977 to 60 000 tonnes in 1992 (Figure 3A). During the 1990s reported catches ranged between 30 000 and 45 000 tonnes, although it has been suggested that these may have been underestimated by as much as 10 to 50% in some areas as a result

of illegal and unreported catch (Figure 2B; Collins *et al.*, 2010; Victorero *et al.*, 2018; Pauly *et al.*, 2020). As a result of the development and enforcement of robust management measures since 2004 (Croxall and Nicol 2004; Kock *et al.* 2007), stocks have partially recovered or are in recovery across much of their range. This included the introduction of a Catch Documentation Scheme, in which the fish are tracked from the point of landing and throughout the trade cycle (Bialek 2003). Continued uncertainties associated with the influence and extent of catch depredation by marine mammals (Moreno *et al.* 2008; Brown *et al.* 2010; Van Den Hoff *et al.* 2017); and the bycatch of juveniles in trawl fisheries remains a concern (Laptikhovsky and Brickle 2005; Victorero *et al.* 2018).

Fisheries for Patagonian toothfish now form the basis for important industrial and artisanal fisheries with global catches remaining stable at 20 000 to 25 000 tonnes/year (Tuck *et al.* 2003; Croxall and Nicol 2004; Moreno *et al.* 2006; Grilly *et al.* 2015). In the Southern Ocean, CCAMLR has responsibility for the conservation and sustainable exploitation of marine living resources, including fisheries for Patagonian toothfish. CCAMLR regulates fishing activities through a suite of annually agreed Conservation Measures (CMs) that are legally binding on the 26 member states (Collins *et al.* 2021). The CCAMLR area of competence roughly corresponds with waters south of the APF, including some areas under national jurisdiction (e.g. France: Kerguelen).

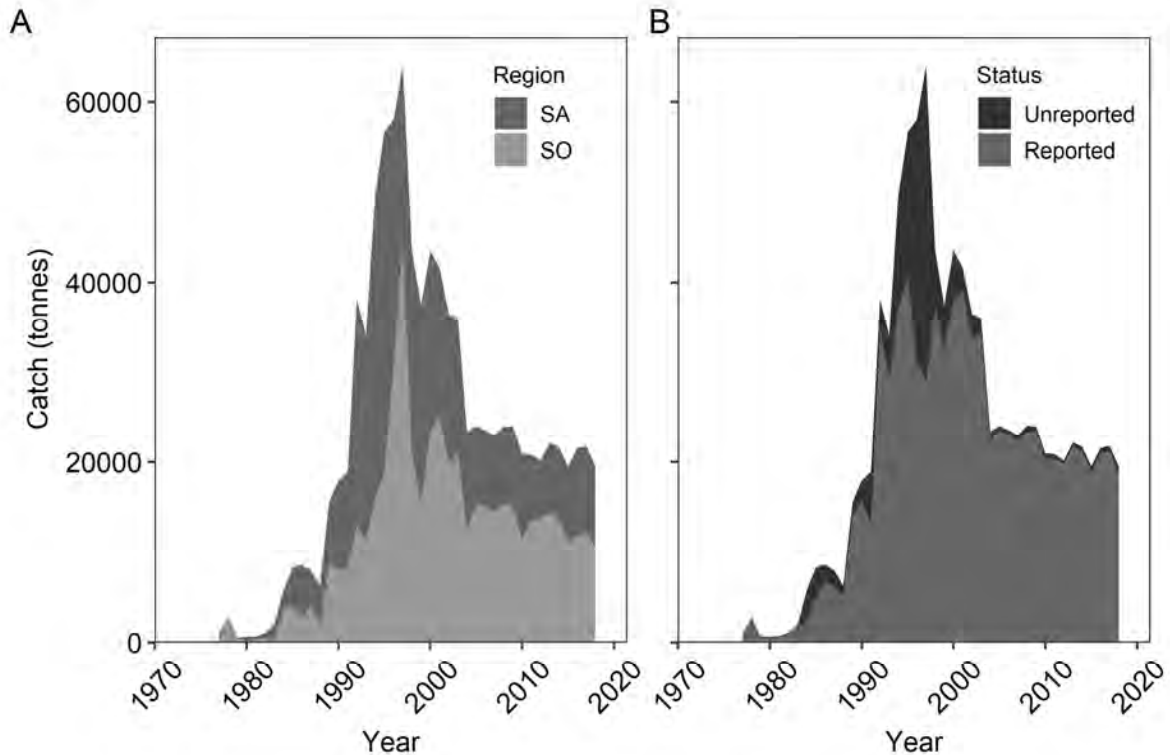


Figure 3: Catch data for Patagonian toothfish since the inception of the fisheries, showing the (A) regional (SA: South American and SO: Southern Ocean) and (B) extent of reported (black line, FAO) and estimated total catch (Pauly *et al.* 2020) accumulated for each of the two regions.

On the Patagonian Shelf, outside of CCAMLR waters, the species is managed independently by nations according to international boundaries. The species is also targeted by international fleets on the high seas, outside of national jurisdictions. For example, Korean vessels fishing to the north and northeast of the Falkland Islands, and over the North Scotia Ridge have captured a total of nearly 12, 000 tonnes between 2013 and 2019 (Park *et al.* 2021). Catches over the Patagonian Shelf have followed the global pattern, peaking at over 40 000 tonnes in 1995, prior to the implementation of stringent management measures since 2004. Management advice for Patagonian toothfish in the Argentinean, Chilean and Falkland Islands fisheries are based on statistical catch-at-age models which are used to estimate relative biomass (Henriquez *et al.* 2016; Skeljo and Winter 2020). The Chilean Patagonian toothfish

stock is targeted both by industrial and artisanal longline fisheries (Moreno *et al.* 2006). The stocks are categorised as overfished, with overfishing occurring (Henriquez *et al.* 2016). Off Argentina, Patagonian toothfish are predominantly (98%) targeted by a deep-sea trawl fishery. The spawning stock biomass is currently estimated to be at 30.3% of the unfished state, corresponding to their defined precautionary biological reference point. Based on this, their management authority has maintained a 3700 tonnes TAC, with the stock considered to be in a rebuilding state (Godelman *et al.* 2021). In the Falkland Islands, both the targeted longline fishery as well as the bycatch components arising through the shelf-based inshore trawl fisheries are accounted for in the modelling framework (Skeljo and Winter 2020). A total allowable catch (TAC) is then decided in accordance to a set of harvest control rules. The TAC has been set at 1040 tonnes since 2015, with a spawning stock biomass maintained at between 40 to 45% of the unfished state. The stock stands at an acceptable level of abundance, and is projected to increase under the current fishing pressure (Skeljo 2020). To date, models have assumed that single self-replenishing stocks of Patagonian toothfish occur within political boundaries. Defining stock structure is therefore a key research priority for fisheries management and essential for planning effective adaptation of the fisheries to climate change.

1.5.3. Life-history and ecology

Patagonian toothfish appear to be a moderately long-lived species, reaching ages of over 50 years (Horn 2002). Growth during the early life-history is fast (12 – 15 cm TL per year), slowing down (1.5 – 2.5 cm TL per year) as adults (Laptikhovsky *et al.* 2006b; Arkhipkin and Laptikhovsky 2010). Age validation studies have used lead-radium dating (Andrews *et al.* 2011) and marginal increment analysis (Horn 2002) to validate the annual periodicity of increment formation in the otoliths of Patagonian toothfish from the youngest age classes to at least 30 years old. Females grow at a faster rate and reach larger sizes than males. Around the Falkland Islands, the mean maximum length (L_{∞}) of females and males were 121.7 cm,

and 107.7 cm, respectively (Laptikhovsky *et al.* 2006b). These estimates were within the range of those estimated for both male ($L_{\infty} = 95.9$ to 134.3 cm) and female ($L_{\infty} = 103.5$ to 158.7 cm) fish from around Kerguelen and within the New Zealand subantarctic (Horn 2002; Ashford *et al.* 2005a).

The macroscopic assessment of Patagonian toothfish gonads generally follows a five-stage scale defined by Kock and Kellermann (1991). In the Falkland Islands, however, gonad maturity stage is assigned according to an eight-stage scale: I and II – immature-resting, III and IV - maturing, V - mature, VI – gravid, VII – spent, and VIII – recovering (Nikolsky 1963). Through the histological examination of female Patagonian toothfish gonads, four broad stages of reproductive development were described around the Falkland Islands (Boucher 2018): Immature (never spawned), Developing (ovaries beginning to develop, but not yet ready to spawn), Spawning capable (fish are able to spawn), Regressing (ending of spawning), and Skipped Spawning (oocyte development had started, but been arrested).

Evidence suggests that not all fish that have reached maturity participate in spawning annually (Arana 2009; Boucher 2018), a characteristic also described in other Patagonian toothfish populations at Kerguelen (Yates *et al.*, 2018) and South Georgia (Everson and Murray 1999). Around the Falkland Islands, the majority of the Patagonian toothfish female population (55.8 to 85.6%) consist of non-spawning individuals remaining in a regressing phase of reproductive development during the spawning period (Boucher 2018). On Kerguelen, the occurrence of female fish of all size classes with low gonado-somatic index and low macroscopic gonad stage during the spawning season also suggests that a proportion of mature females do not spawn every year. This life-history aspect has been described as prominent in northern and central Chile (north of 47°S), and north of 53°S in the Atlantic, where there is no evidence of spawning taking place (Laptikhovsky *et al.* 2006a; Arana 2009; Boucher 2018).

Based on the distribution of macroscopically (macroscopic stage ≥ 3) and histologically (spawning capable) assessed mature individuals, spawning of Patagonian toothfish has been described in discrete areas off southern Chile (Arana 2009), the Burdwood Bank (Laptikhovsky *et al.* 2006a; Boucher 2018), and the western edge of the North Scotia Ridge (Laptikhovsky *et al.* 2006a). Off southern Chile, spawning is thought to occur from July to September, although based on the occurrence of post-spawning individuals, this season may be more protracted (Arana 2009). Although more prominent outside of the spawning areas, evidence of follicular atresia, a characteristic of skipped-spawning has been described across the Patagonian distribution, occurring in as many as 22.1% of the female Patagonian toothfish around the Falkland Islands (Rideout 2000; Arana 2009; Boucher 2018).

On the Burdwood Bank, spawning occurs between 800 and 1000 m depths, with a minor peak during May and a Major peak in July and August (Laptikhovsky *et al.* 2006a; Boucher 2018). Spawning behaviour, characterised by vertical movements into shallower waters (900 to 1200 m), has been described through satellite-derived tagging observations on the Burdwood Bank during March, and May to August (Brown *et al.* 2013a). During the same study, fish from the northern adult habitats of the Falkland Islands Slope and deep-sea plains did not display spawning behaviour during the spawning months.

Based on maturity being reached from stage III+ of the macroscopic scale, length at 50% maturity across spawning areas was estimated at 89 to 90 cm for females and 81 to 86 cm for males (Laptikhovsky *et al.* 2006a; Arana 2009). However, a comparison of histological and macroscopic staging of Patagonian toothfish around Kerguelen found that 65% of macroscopic stage II (developing or resting) fish contained either recent post-ovulatory follicles, or atresia; indicating they were likely to have spawned at some time in the past, or that oocyte development had commenced in the past and had been arrested (Yates *et al.*, 2018). This result closely matches the occurrence of large numbers of female fish around the Falkland Islands in a regressing stage of development (Boucher 2018). This suggests that

age-at-maturity estimates on the basis of stage III+ fish being mature may result in biased estimates. Based only on histologically assessed fish, length-at-maturity around the Falkland Islands was indeed estimated at a smaller size, 79.1 cm, compared to those based on macroscopic assessments (Boucher 2018).

Annual spawning migrations have been inferred for Patagonian toothfish from foraging areas on the Patagonian shelf and slope to the north and east of the Falkland Islands to spawning areas on the Burdwood Bank (Laptikhovsky *et al.* 2006a). Results from archival pop-up tags, however, indicate high site fidelity, although these were limited by a small sample size ($n = 16$) and the deployment only on large fish (>127 cm; Brown *et al.*, 2013a). The same study also identified seasonal bathymetric movements, with fish inhabiting deeper waters during December (post-spawning). Similar seasonal differences have been recorded through seasonal changes in length distributions for adult Patagonian toothfish off southern Chile. The absence of larger fish from depths targeted for fishing (1000 to 1200 m) late in the year (November - December) has been attributed to localised behavioural patterns such as vertical migrations, reduced feeding (post-spawning), and the recruitment of smaller fish into the fishery (Arana 2009).

Fecundity ranges from ~50 000 to 550 000 eggs per individual and increases with fish size (Chikov and Melnikov 1990; Kock and Kellermann 1991). The egg and larval life-history phases across the species distribution is not well understood (Evseenko *et al.* 1995). Based on 39 specimens collected over 11 years, from across their distribution, these stages are thought to be pelagic, occurring in the upper 500 m of the water column (Evseenko *et al.* 1995; North 2002). The egg and larval phase are also thought to be protracted extending up to 105 and 90 to 230 days, respectively (North 2002; Andrews *et al.* 2011). Observations of egg development of laboratory-reared Patagonian toothfish identified a hatch period of 30 to 33 days, although this would be expected to be more protracted under natural conditions (Mujica *et al.* 2016). The protracted egg and larval periods, when combined with strong oceanographic

features that are prevalent in the region, provide the opportunity for high dispersal across large geographic areas, potentially contributing to population connectivity (Cowen and Sponaugle 2009; Ramesh *et al.* 2019; Álvarez-Noriega *et al.* 2020).

Recruitment of juvenile Patagonian toothfish in the region is variable, with strong year classes occurring every 4–5 years (Laptikhovsky and Brickle 2005). Juveniles of <15 cm TL (0+ year old fish) occur in shallow waters at the extent of, and inshore of the 200 m depth contour (Laptikhovsky *et al.* 2006a; Arkhipkin and Laptikhovsky 2010). Lengths of Patagonian toothfish increase with depth, with large adults occurring as deep as 2000 m (Arkhipkin and Laptikhovsky 2010). Similar downslope ontogenetic migrations have been described across their range (Belchier and Collins 2008; Péron *et al.* 2016), however, due to the lack of large shelf areas available for foraging, Patagonian toothfish are thought to descend much earlier in comparison to their life-history on the Patagonian Shelf (Laptikhovsky *et al.* 2006a).

Ontogenetic migrations and related trophic changes are reflected in both the parasite assemblages and diet of Patagonian toothfish across their size and depth distribution (Arkhipkin *et al.* 2003; Brickle *et al.* 2006b). Patagonian toothfish sampled from the shelf (<200 m) and deep-sea (>1000 m) were found to possess different parasite communities. Those caught at intermediate depths (200 to 600 m) were found to have parasite communities that were intermediate, containing a mixture of shelf and deep-sea communities. Juvenile fish are active nektonic predators, taking mainly near-bottom fish (*Patagonotothen ramsayi*) and squid (*Doryteuthis gahi*). During their ontogenetic migration as sub-adults (500 to 1000 m deep) they feed on larger benthic species (Morids, Macrourids and Skates), becoming typical opportunistic predators as large adults (>1000 m depth) where they mainly feed on small and relatively inactive fish, squid and crustaceans.

1.5.4. Population connectivity

Patagonian toothfish populations are genetically structured at a regional and sub-regional scale. Strong genetic heterogeneity has been shown across the APF using both microsatellite and mitochondrial DNA analyses (Shaw *et al.* 2004; Rogers *et al.* 2006; Canales-Aguirre *et al.* 2018). These results have suggested the APF as a major barrier to larval dispersal with deep-water troughs and distance inhibiting movements of adults. Genetic differentiation using nuclear markers have also been described among populations inhabiting island groups to the south of the APF, indicating stock separation and limited mixing (Smith and McVeagh 2000; Appleyard *et al.* 2002; Rogers *et al.* 2006; Toomey *et al.* 2016).

Trace element analysis undertaken from the edge and nucleus of Patagonian toothfish otoliths have indicated a sharp population boundary in the vicinity of the APF, with large-scale variation in trace element concentrations from Patagonian populations in relation to subantarctic Islands to the south (Ashford *et al.* 2005b; Ashford *et al.* 2006). This prior evidence of population isolation across the APF has also been corroborated through heterogeneity in whole otolith $\delta^{18}\text{O}$ and $\delta^{13}\text{C}$ isotopes (Ashford and Jones 2007). Further, there is no reported evidence of tagged fish being recaptured after movements across the APF (Williams *et al.* 2002; Marlow *et al.* 2003; Agnew *et al.* 2006; Brown *et al.* 2013a). Medium-scale movements undertaken by tag-recaptured fish have, however, been reported between the South Sandwich Islands to South Georgia (>740 km; Roberts and Agnew, 2008); and from Heard Island to Kerguelen (>210 km) and Crozet (>1025 km; Williams *et al.*, 2002). This reflects that adult Patagonian toothfish are capable of large-scale movements, although these appear to be infrequent. Juvenile Patagonian toothfish are negatively buoyant, however, adults are inferred to become neutrally buoyant at maturity, therefore reducing the energy needed for large-scale movement (Eastman 1993).

Despite the geographical expanse of the region, Patagonian toothfish populations on the South American continental shelf shows no significant genetic structuring. However, genetic markers vary greatly in their ability to resolve the extent to which the population consists of a single or multiple phenotypic or contingent stocks (Beebee and Rowe 2008). Population connectivity may be driven through aspects of their biology (e.g. dispersal during a protracted egg and larval period) and the continuity of the deep-sea habitat in the region enabling the active migration or movement in adults (Canales-Aguirre *et al.* 2018). Connectivity may also be driven through their ontogenetic migrations from nursery areas to their deep-sea habitats. On the Patagonian Shelf, these migrations are thought to occur over an extended period compared to other areas of their range that contain narrow shelves (Laptikhovsky *et al.* 2006a). Otolith microchemistry, however, was used to identify distinct nucleus and edge signatures among areas sampled around the Falkland Islands and Chilean Shelf, suggesting more restricted connectivity and the possibility of more than one South American population (Ashford *et al.* 2005b; Ashford *et al.* 2006). The parasite fauna of juvenile Patagonian toothfish indicated spatial separation between individuals inhabiting areas to the northwest and southeast of the Falklands Shelf (Brown *et al.* 2013b). High site fidelity and limited connectivity was also described for large adults, monitored over nine month time periods using archival satellite pop-up tags (Brown *et al.* 2013a). These results are contradictory to the annual spawning migrations described by Laptikhovsky *et al.* (2006a).

Particle simulations in a wind-driven oceanographic model identified wide dispersal of Patagonian toothfish eggs and larvae, from spawning areas on southern Chile and the Burdwood Bank across the Patagonian Shelf (Ashford *et al.* 2012b). In combination with otolith trace element analyses, models predicted recruitment of juveniles from southern Chile to the northern Patagonian Shelf, and region of mixed recruitment from southern Chile and the Burdwood Bank to the south of the Falkland Islands (Ashford *et al.* 2012b). These results are therefore suggestive of large-scale connectivity driven through early life-history dispersal. The absence of spawning in the northern extent of their range, combined with the prospect of high

site fidelity (in the absence of annual spawning migrations) identifies important questions in terms of connectivity and the closure of the adult – spawning - recruitment life cycle. There is growing evidence that the spatial structure and population dynamics of Patagonian toothfish may be more complex than currently assumed.

1.6. Research aims and structure of the thesis

The aim of this project was to provide an improved understanding of the stock structure dynamics for Patagonian toothfish on the Patagonian Shelf, specifically in relation to the shelf, slope, and deep-sea plains around the Falkland Islands. To achieve this, an integrated approach was used whereby a range of complementary methods were incorporated to improve our understanding of life-history stages identified as potential pathways of population connectivity. In this way, it was aimed to identify the nature and extent of resource sharing on a spatial and temporal basis (Figure 4).

In Chapter 2, the focus was on identifying the use of variability in otolith shape as a tool for stock identification studies in Patagonian toothfish. The aim was to investigate this technique as an alternative tool for population discrimination compared to more traditional, yet costly and labour-intensive genetic and otolith microstructure-based approaches. The strength of this method in discriminating two closely related *Dissostichus* species (Patagonian toothfish and the closely related Antarctic toothfish, *Dissostichus mawsoni*), as well as geographically discrete Patagonian toothfish populations displaying known genetic heterogeneity was investigated. These techniques were then applied on specimens attained from across localised spawning and adult foraging habitats, to provide insights into the stock structure of Patagonian toothfish across the study area on the Patagonian Shelf. It was thought that differences or similarities in the shape of otoliths across localised regions would infer the extent of connectivity that takes place within the region.

Ontogenetic migrations were identified as a life-history stage that could lead to increased connectivity between nursery areas and sub-adult habitats. In Chapter 3 a series of spatial-temporal models were developed to define the spatial units within which early life-history stages occur in shelf waters around the Falkland Islands. The temporal dynamics of these units in the presence of variable interacting environmental (e.g. temperature, currents), chemical (e.g. salinity, oxygen), physical (e.g. depth), and ecological (e.g. inter- and intra-specific competition) drivers were investigated to improve our understanding of (1) recruitment, (2) nursery areas habitats, and (3) ontogenetic migratory pathways.

In Chapter 4 movement patterns during the adult life-history stages were explored using a medium to long-term tag-recapture programme. Connectivity in the adult component of the stock across the region remains largely unresolved, and the presence or absence of active movements of adults has important repercussions in terms of closing the life cycle and providing a linkage between the adult (non-spawning) component on the northern extent of their range with southern spawning areas.

Information on the timing and location of larval and early juvenile settlement patterns is scarce. Variability in these patterns may provide important information on the extent that newly settled juveniles arise from single, or multiple discrete spawning areas. This was investigated in Chapter 5 through an integrated approach using otolith microstructure to provide temporal inference to otolith geochemical profiles. In Chapter 6 available research was incorporated with the findings of the current project to describe a tentative life cycle for Patagonian toothfish on the Patagonian Shelf, with a specific focus on aspects relating to the stock structure within the region. Using this information, a selection of viable approaches was reviewed that can be considered for sustainable fisheries management. Finally, a range of recommendations were provided with a focus on the development of collaborations, future research priorities, and monitoring that can contribute to the sustainable management of the stock through an

improved understanding of the stock structure dynamics and inform the movement towards an ecosystem-based approach to fisheries management.

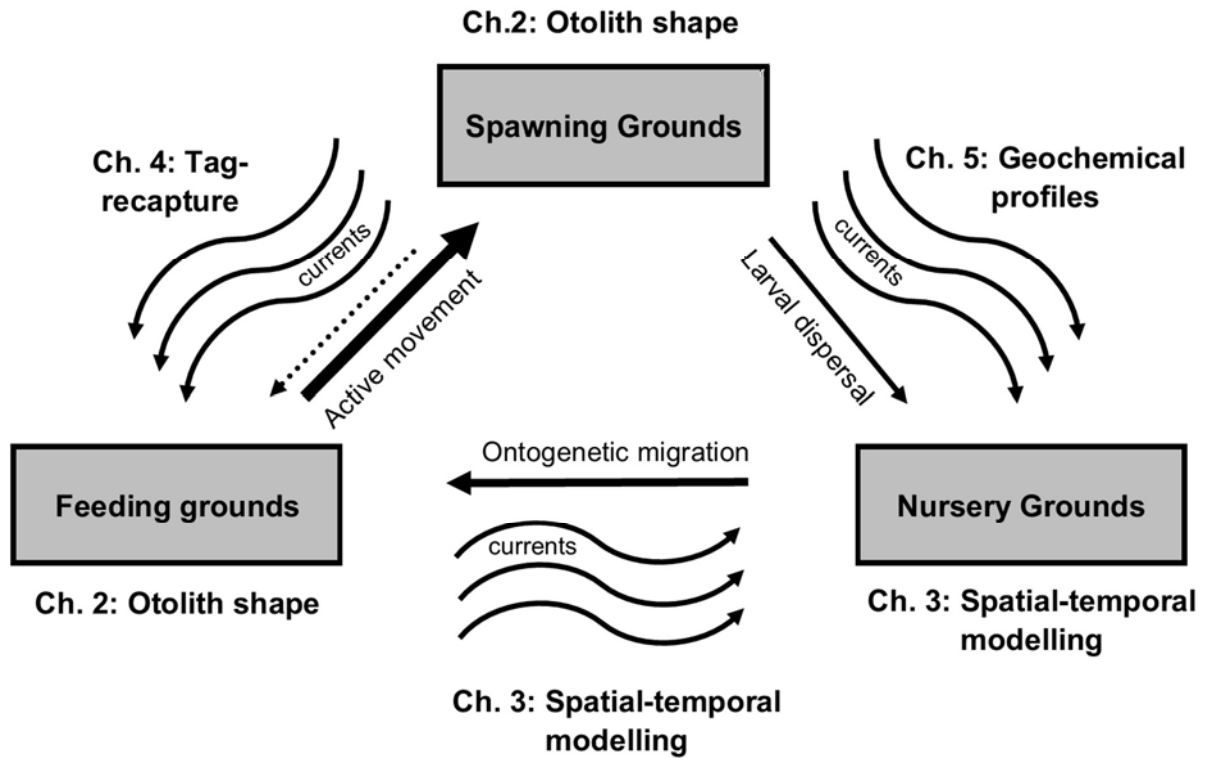


Figure 4: Model depicting key life-history stages (boxes), and the approaches (Chapters) undertaken in the current research to investigate potential connectivity pathways (arrows) of Patagonian toothfish on the Patagonian Shelf.

Chapter 2 - Use of otolith shape to inform stock structure in Patagonian toothfish in the Southwest Atlantic Ocean

Abstract

An analysis of patterns in otolith shape is an effective tool for discriminating among fish stocks. Otolith shapes of Patagonian toothfish (*Dissostichus eleginoides*) and Antarctic toothfish (*D. mawsoni*) were investigated for geographic variability within seven regions across the Patagonian Shelf, and South Georgia and the South Sandwich Islands (SGSSI). Otolith shape was characterised by its elliptical Fourier coefficients (EFCs), corrected for fish length before being analysed, using multivariate methods. Non-metric multidimensional scaling analysis suggested the following three main groupings: Patagonian Shelf, SGSSI, and the third for Antarctic toothfish. This result was supported by ANOVA-like permutation tests, indicating significant ($P < 0.001$) differences in otolith shape among these three groupings. Linear discriminant analysis (LDA) cross-validation analyses of the EFCs resulted in otoliths being correctly classified to the sampling region from which they came, with an accuracy ranging from 78.95 to 100%. LDA cross-validation analyses on sampling regions within SGSSI and the Patagonian Shelf were able to classify individuals back to their sampling region with an accuracy of greater than 89.74 and 78.95% respectively. These results have provided some alternative insights into the stock structure of Patagonian toothfish across southern South America, South Atlantic and SGSSI.

2.1. Introduction

Fisheries assessments are based on the assumption that the stocks upon which they are applied are self-sustaining productive units (Begg and Waldman 1999, King 2007). The identification of stocks and the dynamics of linkages among them are therefore fundamental for their effective management (Begg *et al.* 1999a). There are a variety of methods for investigating stock structure and linkages in fish populations. For instance, genetic differentiation forms the basis for inferences concerning stock discrimination (Campana and Casselman 1993). However, genetic analyses are not always sufficient to delineate stock units for management (Lowe and Allendorf 2010). An analysis of population structure relies on a multidisciplinary approach in which a variety of complementary methods such as tagging experiments (Brown *et al.* 2013a), parasite loadings (Brickle *et al.* 2006b; Brown *et al.* 2013b), variability in life-history characteristics (Begg *et al.* 1999b; Barrios *et al.* 2017), and otolith microchemistry (Ashford and Jones 2007; Sturrock *et al.* 2012) can all be utilised.

Variation in the shape of fish otoliths has been shown as a useful tool for discriminating among fish stocks (eg. Stransky *et al.* 2008; Neves *et al.* 2011; Vieira *et al.* 2014). Although retaining its unique taxonomic characteristics, otolith shape can vary in relation to disparate environmental and genetic factors (Cardinale *et al.* 2004; Vignon and Morat 2010), or differences in body condition or growth (Rodgveller *et al.* 2017; Mapp *et al.* 2017). Whereas genetic differences influence the shape of the otolith itself, the environment alters their rates of growth, which in turn may modify the otolith shape (Cardinale *et al.* 2004). Shape differences can be identified by visual assessments (Rodgveller *et al.* 2017). However, advances in image-analysis tools have facilitated a shift to a more complex geometric approach to morphometric analyses (Stransky 2014). For instance, geometric-outline methods quantify boundary shapes through Fourier analyses. Elliptical Fourier analysis is one of the most powerful and most widely used techniques in describing otolith shape (Stransky *et al.* 2008; Keating *et al.* 2014; Brophy *et al.* 2016; Mahe *et al.* 2016a; Rodgveller *et al.* 2017).

Outputs can subsequently be analysed using standard multivariate methods to detect patterns of variance, discriminate groups, and classify individuals to groups (Mérigot *et al.* 2007; Claude 2008; Hüsey 2008; Keating *et al.* 2014; Mahe *et al.* 2016a).

Notothenioids of the genus *Dissostichus* provide important fishery resources throughout their range. Antarctic toothfish (*D. mawsoni* Norman, 1937) is found at high latitudes around Antarctica, whereas Patagonian toothfish (*D. eleginoides* Smitt, 1898) occurs further north across islands, seamounts and shelf areas of the subantarctic (Collins *et al.* 2010). Its distribution spans the Antarctic Polar Front (APF) and extends north over the Patagonian Shelf in the Atlantic Ocean, off Chile in the Pacific and to 40° S in the south west Indian Ocean. There is some overlap in the distribution of the two species in intermediate areas, including in the Atlantic region of the subantarctic over the South Sandwich Islands.

Patagonian toothfish is highly fecund (North 2002), and has a prolonged epipelagic egg (\pm 30-90 days) and larval phase ($>$ 60 days; Evseenko *et al.* 1995; Mujica *et al.* 2016). Juveniles exploit demersal habitats on the continental slope at depths greater than 50 m before undertaking a characteristic ontogenetic migration into deeper water where adults reside and spawn (Laptikhovsky *et al.* 2006a; Collins *et al.* 2010; Brigden *et al.* 2017). Data obtained from pop-up satellite tags suggest strong site fidelity in adult toothfish (Brown *et al.* 2013a). However, there are some exceptional observations of long-distance movements of adults (Collins *et al.* 2010; Brown *et al.* 2013a). Life-history traits of Patagonian toothfish therefore suggest a potential for high levels of connectivity through advection by currents during the protracted egg and larval stages of development (North 2002) or infrequent long-distance migrations of adults.

Patagonian toothfish populations found on the Patagonian Shelf are genetically distinct from the populations on South Georgia and South Sandwich Islands (SGSSI; Shaw *et al.* 2004; Rogers *et al.* 2006), with limited genetic structure observed within each of those locations.

Research utilising wind-driven global circulation models and otolith microchemistry suggest complex localised population structures (Ashford *et al.* 2005b; Ashford *et al.* 2012b). Along the Patagonian Shelf, the existence of separate spawning populations off southern Chile and south of the Falkland Islands on the Burdwood Bank has been proposed (Laptikhovsky *et al.* 2006a; Arana 2009). Within the South Georgia region, localised circulation has been linked to spawning grounds and the retention of propagules in the region (Brigden *et al.* 2017). As such, the connectivity between juvenile recruits and non-spawning and spawning adults requires further investigation.

Geographic variation in the shape of toothfish otoliths has not been investigated previously. Given the potential for a wide-spread dispersal of juveniles, the generally high site fidelity of adults, and variability in environmental conditions that occurs across the distribution of these species, stock or environmentally driven differences in otolith shape may exist. These could prove useful as a tool to aid stock identification of toothfish in the South Atlantic Ocean. Specifically, the objectives of the study were to (1) validate the use of otolith shape analyses as a tool for population discrimination in Patagonian toothfish by effectively discriminating between two closely related *Dissostichus* species (Patagonian toothfish vs Antarctic toothfish), (2) evaluate whether otolith shape can be used to accurately discriminate between geographically discrete population groups (Patagonian Shelf vs South Georgia and the South Sandwich Islands), (3) use these methods to investigate localised subdivisions within the population structure of Patagonian toothfish within each of the Patagonian Shelf and South Georgia and the South Sandwich Islands regions and (4) investigate the potential for connectivity both across geographically discrete populations and within localised subdivisions of toothfish across the study area.

2.2. Materials and methods

2.2.1. Data collection

In total, 459 Patagonian and 37 Antarctic toothfish were randomly sampled between 2008 and 2011 by scientific observers aboard commercial toothfish longline vessels (fisheries dependent) operating within six geographically distinct regions (Table 1). As a component of standard observer protocols, otoliths are collected from Patagonian toothfish that cover the length distribution of the total catch. Patagonian toothfish were collected from south west of Chile (CHP), north of the Falkland Islands (FIPN), south of the Falkland Islands over the Burdwood Bank (FIPS), South Georgia (SGP), the South Sandwich Islands (SSP), and a region on the high seas (HSP) directly to the north of the Falkland Islands, beyond the Falkland Islands Outer Conservation Zone. Antarctic toothfish were collected from the South Sandwich Islands (SSA; Figure 5).

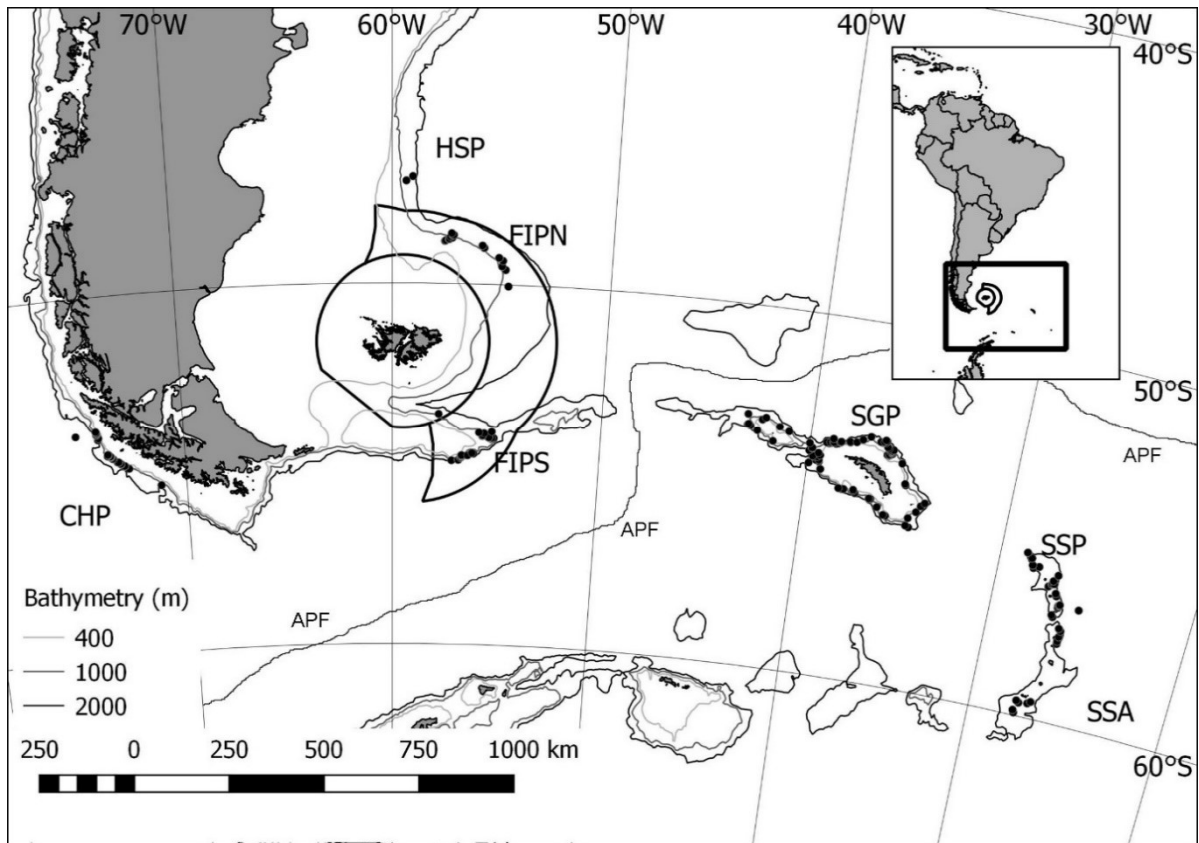


Figure 5: Sampling positions of Patagonian toothfish and Antarctic toothfish otoliths. SGP, South Georgia; SSP, South Sandwich Islands; CHP, Chile; FIPS, Falkland Islands, south (Burdwood Bank); HSP, High Seas; FIPN, Falkland Islands, north. Solid black lines reflect the territorial waters of the Falkland Islands: Falkland Islands conservation zone (FICZ, inner) and Falkland Islands outer conservation zone (FOCZ, outer). Longitudinal lines reflect the north–south direction.

For each fish, total body length was measured to the nearest centimetre and weight was recorded to the nearest gram. Sex and maturity were determined at the time of sampling by macroscopic examination of gonads. Toothfish from South Georgia, South Sandwich Islands and Chile were macroscopically staged according to the methods described by Kock and Kellermann (1991), and the High Seas, and Falkland Islands fish were staged according to Laptikhovsky *et al.* 2006a). Only adult fish (\geq Maturity stage III for both scales) were included in the study, so as to minimise the potential effect of rapid growth during the early stages of ontogenetic development (prior to sexual maturity) on otolith shape (Campana and Casselman

1993; Mahe *et al.* 2016b). Sagittal otoliths were removed, cleaned of membranes and tissues and stored dry for further examination. Only right otoliths that did not show any clearly visible growth deformations or damage were used for analyses.

Table 1: Overview of Patagonian toothfish (*Dissostichus eleginoides*) and Antarctic toothfish (*Dissostichus mawsoni*) otolith samples used for shape analysis: SGP, South Georgia; SSP, South Sandwich Islands; CHP, Chile; FIPS, Falkland Islands, south (Burdwood Bank); FIPN, Falkland Islands, north; HSP, high seas; SSA, South Sandwich Islands.

Species	Region	Capture site	N	Sampling year	Length range (cm)
<i>D. mawsoni</i>	Subantarctic	SSA	37	2011	127 - 178
<i>D. eleginoides</i>	Subantarctic	SGP	3	2005	71 - 81
			32	2008	70 - 90
			81	2009	70 - 90
			1	2012	77
<i>D. eleginoides</i>	Subantarctic	SSP	134	2011	65 - 171
<i>D. eleginoides</i>	Patagonian Shelf	CHP	38	2008	55 - 71
<i>D. eleginoides</i>	Patagonian Shelf	FIPN	16	2008	68 - 110
			58	2010	85 - 150
<i>D. eleginoides</i>	Patagonian Shelf	FIPS	77	2009	58 - 71
<i>D. eleginoides</i>	Patagonian Shelf	HSP	19	2011	76- 97

2.2.2. Image and shape analyses

High contrast otolith images were taken with an Olympus SZX12 stereo dissection microscope (Olympus Corporation, Tokyo, Japan) mounted with an Olympus DP70 camera (Olympus Corporation, Tokyo, Japan) with a PC interface. Sagittal otoliths were mounted horizontally along the longest axis with the sulcus groove down and the rostrum pointing to the left and photographed at 3.5 x magnification under reflected light on a black background. Otolith

images were enhanced to improve contrast and remove visual artefacts by using the ImageJ software package version 1.50e (version 1.50e, National Institute of Health, USA, <https://imagej.net/ImageJ>; Rueden *et al.*, 2017).

The digital images were read into R version 3.3.3 (R Core Team, 2019, <https://www.r-project.org>) and the contours of each otolith were extracted using the 'ShapeR' (Libungan and Pálsson 2015) library. The shape of each otolith was aligned to a common centre, oriented to remove discrepancies in positioning, scaled to centroid size and recorded as a matrix of x and y coordinates. Elliptical Fourier analysis (EFA) was used to fit a closed curve to an ordered set of data points in a two-dimensional plane (Tracey *et al.* 2006). It uses an orthogonal decomposition of a curve into a sum of harmonically related ellipses. These ellipses can be combined to reconstruct an arbitrary approximation of a closed shape (see Lestrel [1997] for detailed description of the methodology). Elliptical Fourier analyses were conducted to fit Fourier harmonics to each otolith outline until 98.5% (Libungan and Pálsson 2015) of the variance in the otolith shape could be reconstructed. Subsequent analyses were conducted on the set of elliptical Fourier coefficients (EFCs).

Elliptical Fourier coefficients were standardised for fish length by using functions in the 'ShapeR' library, defined according to the methods described by Leonart *et al.* (2000). An analysis of covariance (ANCOVA) was used on EFCs (the response variable) to determine whether there was a significant interaction between fish length and the sampling region (referred to as the grouping factor; Agüera and Brophy 2011; Libungan *et al.* 2015). If there was a significant ($P < 0.05$) interaction between fish length and the grouping factor on a specific EFC, the coefficient in question was excluded from subsequent analyses. A Bonferroni adjustment was conducted to account for an increased Type 1 error as a result of multiple testing of the different coefficients (Armstrong 2014). A regression coefficient was then calculated as a function of fish length for each grouping factor. The remaining EFCs were standardised using the common within-group slope according to the methods described by

Leonart *et al.* (2000). To visualise the shape differences among population groups, average otolith shapes for each sampling region were plotted by means of the reproduced outlines of the averaged normalised EFCs. The distributions of the EFCs were visually assessed for normality prior to statistical analyses in R. These appeared to be normally distributed, and as such no further transformations were performed.

2.2.3. Statistical analysis

Elliptical Fourier coefficients were transformed to a Euclidean-distance dissimilarity matrix. Other distance indices were used for comparison but indicated no significant deviation from the multivariate patterns derived from Euclidean distances. Non-metric multidimensional scaling (nMDS, Kruskal 1964) was then used to ordinate the matrices to visualise broad patterns in the location or relative dispersion of potential groupings across the data. Non-metric multidimensional scaling was performed using the MASS package in R (Venables and Ripley 2002). Non-metric multidimensional scaling has been demonstrated as a particularly robust and useful unconstrained ordination procedure for ecology that reduces dimensions by minimising a stress function without the use of *a priori* hypotheses (Anderson and Willis 2003).

Analysis of variance (ANOVA)-like permutation tests (Legendre *et al.* 2011) with 1000 iterations were used to test the hypothesis that otolith shape differed according to: (1) species, (2) geographic region (Patagonian Shelf and South Georgia and the South Sandwich Islands) and (3) sampling sites within geographic regions. The assumption of normal distribution common to parametric tests such as ANOVA and MANOVA was redundant in this study, as the non-parametric permutation tests used maintain type I error and are robust when data are non-normal (Tracey *et al.* 2006). To validate the observed grouping structure, a linear discriminant analysis (LDA) was applied to the EFCs using the MASS and ade4 (Dray and Dufour 2007) libraries in R. LDA is a parametric constrained ordination procedure that fits a linear combination of coefficients so as to maximise the ratio of variability between *a priori*

groups (Venables and Ripley 2002). A jack-knife (leave-one-out) cross-validation procedures were used to estimate classification success into sampling sites. This method randomly selects an individual specimen to be excluded from the data set, with the remaining samples being used to generate a model to predict the group of the specimens left out providing a reasonable and nearly unbiased measure of how distinct the groups are in multivariate space (Anderson and Willis 2003). This analysis will both identify the level of localised characteristic otolith shape shared among fish sampled in the same region, as well as identify the potential for mixing of individuals between sampling areas as signified by percentage of misclassification.

Linear Discriminant Analysis was also used to visualise and compare otolith shape for Patagonian toothfish within and among sampling sites. The projections of individuals along the first two axes of the LDA were examined graphically. Groupings according to sampling sites were displayed by ellipses where the centres are the means (between variances) and the ellipses the within variances. A jack-knife cross-validation procedure was used to estimate classification success separately for the Patagonian Shelf and South Georgia and the South Sandwich Islands sampling sites.

2.3. Results

2.3.1. *Image and shape analyses*

The Fourier power equation showed that over 99% of the variability in shape was captured by 32 Fourier harmonics, consisting of 128 coefficients (EFCs). Of these, 98.5% of the otolith variation could be explained by the first 12 harmonics (Figure 6). The first three EFCs of the first harmonic were used to standardise the otolith outline orientation, size, and starting point (Lestrel 1997), leaving 45 EFC for analyses. ANCOVAs showed no significant interactions

between fish length and sampling region ($P > 0.05$) and as such all the remaining EFCs were included and standardised with regards to fish length.

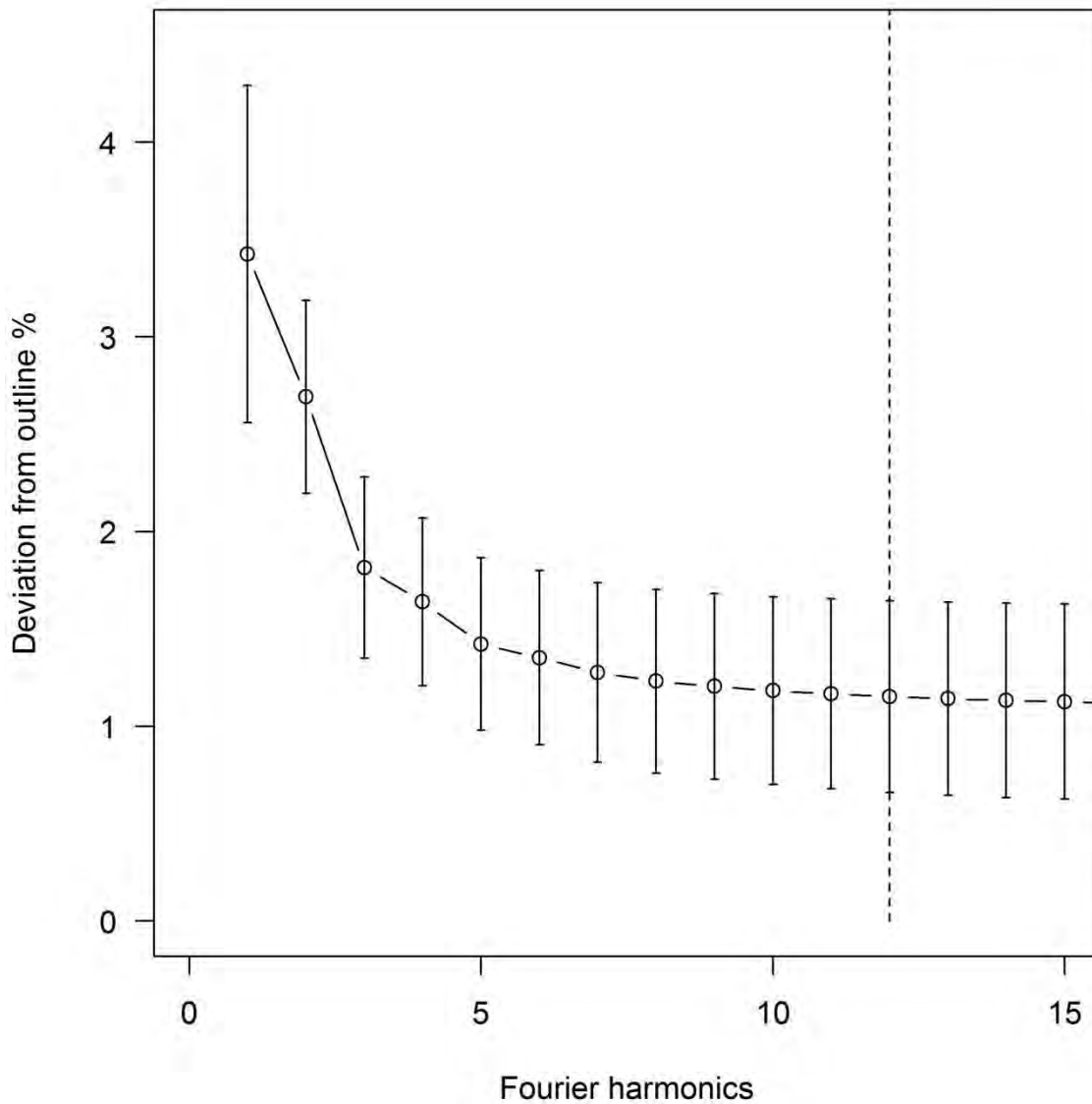


Figure 6: Quality of the elliptical Fourier-outline reconstruction. The dashed vertical line shows the number of elliptical Fourier harmonics needed for a 98.5% accuracy of the reconstruction.

2.3.2. Shape features

Three distinct otolith shapes could be observed visually (Figure 7). Otoliths obtained from Antarctic toothfish were discernible as a result of their rounded shape with a distinct hook to

their rostrum. Patagonian toothfish otoliths obtained from fish caught in South Georgia and the South Sandwich Islands displayed an intermediate shape between that obtained from Antarctic toothfish and the elongated shape clearly evident in the otoliths obtained from fish caught on the Patagonian Shelf (Chile, Falkland Islands and High Seas). Despite these general observations of observed shape, a high degree of visual variability was evident in the otoliths obtained from fish even within the same sampling sites.

The observed variability in the otolith shape was clearly demonstrated using reconstructions of the otolith outline on the basis of the average elliptical Fourier harmonics among the seven sampling regions (Figure 8). Differences were most evident in the distances of the dorsal and ventral surfaces from the centroid. The distances were greatest for Antarctic toothfish otoliths (SSA), giving these a distinctly rounder average shape. The otoliths from Patagonian toothfish sampled along the Patagonian Shelf (Chile, Falkland Islands and High Seas) were distinctly dorso-ventrally narrow giving these an elongated appearance. Patagonian toothfish sampled from sites within the subantarctic region (South Georgia and the South Sandwich Islands) displayed an intermediate shape between those sampled along the Patagonian Shelf and Antarctic toothfish captured in the South Sandwich Islands. Minor differences in shape were also clearly evident within these regional groupings, most notably along the antirostrum, excisura major and rostrum areas of the otolith.

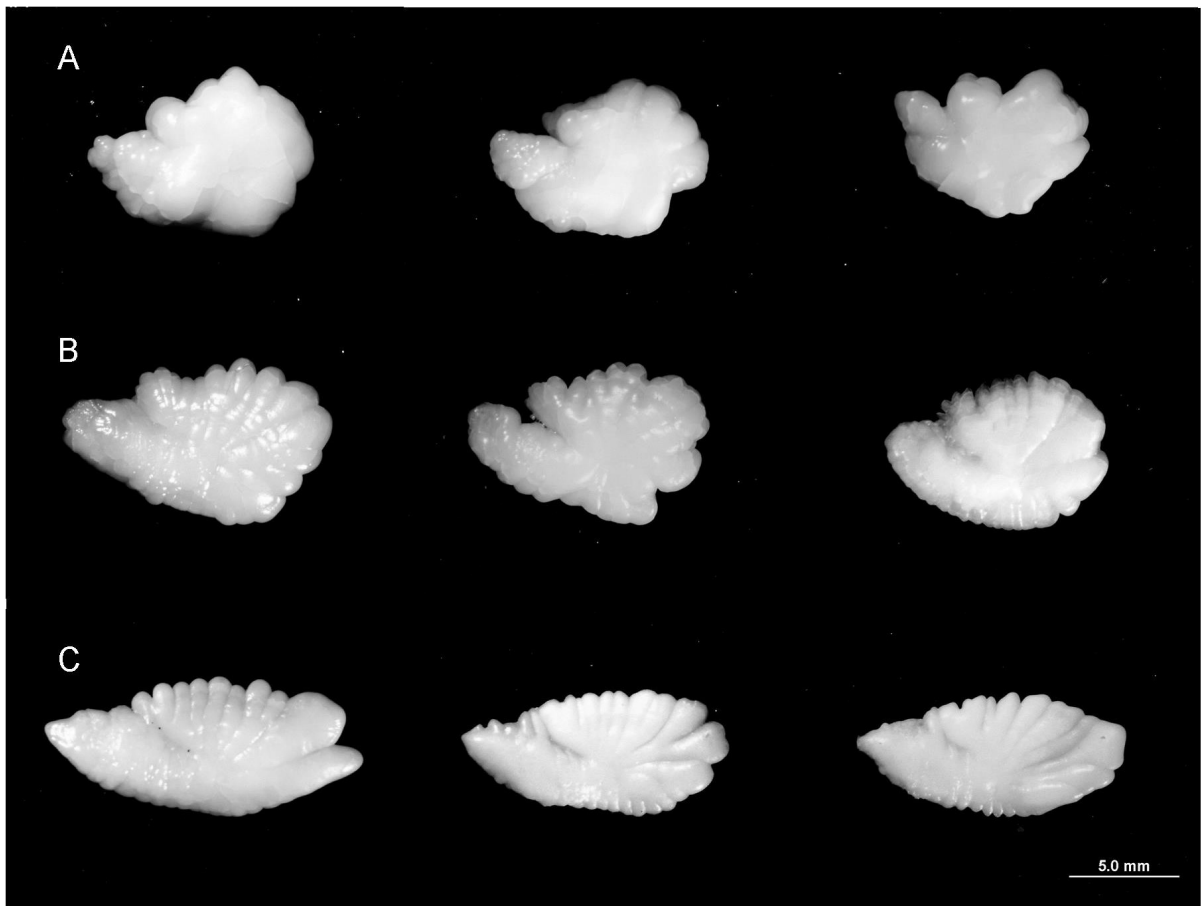


Figure 7: Captured images reflecting examples of whole toothfish otoliths obtained from (a) South Sandwich Islands: Antarctic toothfish (*Dissostichus mawsoni*) of lengths 149, 161 and 164 cm; (b) South Georgia and South Sandwich Islands: Patagonian toothfish (*D. eleginoides*) of lengths 140, 135 and 80 cm; and (c) Patagonian Shelf: Patagonian toothfish (*D. eleginoides*) of lengths 102, 66 and 69 cm.

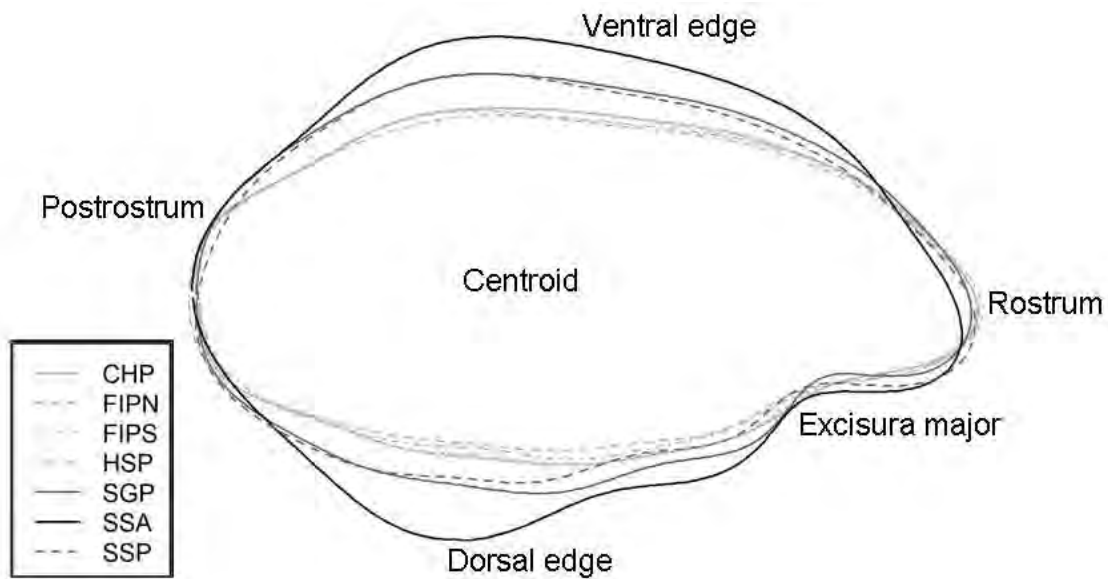


Figure 8: The mean otolith shapes based on elliptical Fourier reconstruction for Patagonian toothfish and Antarctic toothfish according to the seven sampling regions (see Table 1 for area codes).

2.3.3. Shape analyses

The nMDS ordination plot of the Euclidean distances between the EFCs of each capture site suggested the following three main groups of shapes: Subantarctic Antarctic toothfish (SSA), subantarctic Patagonian toothfish (South Georgia and South Sandwich Islands) and Patagonian Shelf Patagonian toothfish (Chile, Falkland Islands and High Seas; Figure 9). The Patagonian Shelf areas form relatively dense clusters compared with the more widespread distribution pattern observed for the subantarctic Patagonian toothfish and Antarctic toothfish clusters.

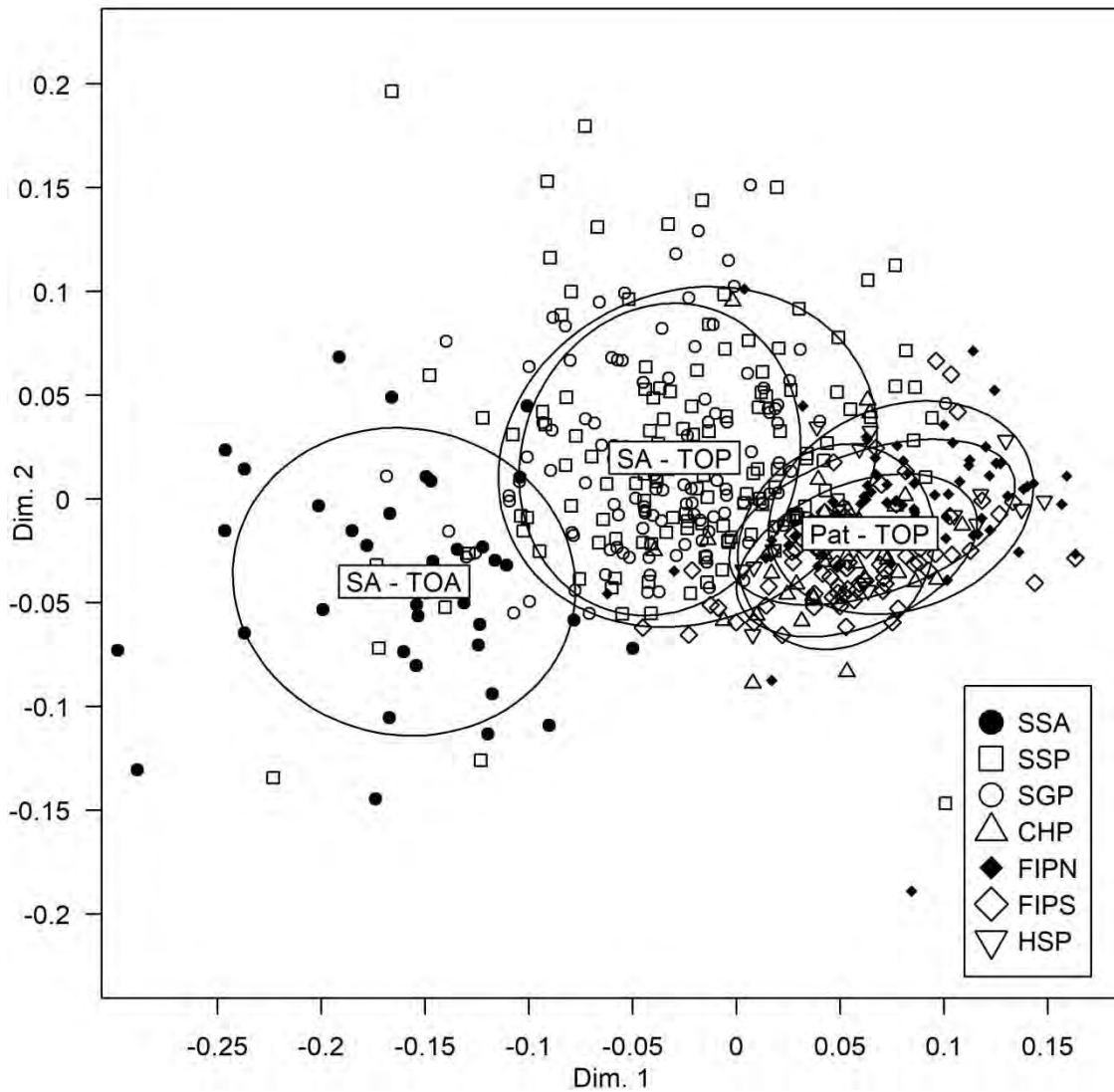


Figure 9: Non-metric multidimensional scaling ordination plot of the Euclidean distances for Patagonian toothfish (*Dissostichus eleginoides*) and Antarctic toothfish (*D. mawsoni*) otolith shape indicating capture sites (see Table 1 for area codes) and regional groupings (SA–TOA, Subantarctic Antarctic toothfish; SA–TOP, Subantarctic Patagonian toothfish; Pat–TOP, Patagonian Shelf Patagonian toothfish). Stress value of the plot: 0.027.

The results of the ANOVA-like permutation test (Table 2) and jack-knife classification of the LDA for the capture regions (Table 3) validated the patterns observed in the nMDS analysis. Permutation tests indicated significant ($F=107.55$; $P<0.001$) differences in otolith shape between the Antarctic toothfish and Patagonian toothfish sampling regions. Similarly, LDA

cross-validation showed that the subantarctic Antarctic toothfish grouping could be correctly classified to the capture site with 100% accuracy, validating the use of these methods for stock discrimination in toothfish in the study region.

Table 2: Summary of the ANOVA-like permutation test with 1000 iterations on Antarctic toothfish (*Dissostichus mawsoni*) and Patagonian toothfish (*D. eleginoides*) elliptical Fourier coefficients according to seven sampling regions (see Table 1 for area codes)

Comparison	Reason	df	Variance	F	P
All populations		6	2.50	56.21	<0.001
SSA vs SSP, SGP, CHP, FIPN, FIPS, HSP	Genetic: Different species	1	1.09	107.55	<0.001
SSP, SGP vs CHP, FIPN, FIPS, HSP	Geographic: Subantarctic and Patagonian Shelf	1	1.19	159.91	<0.001
SSP vs SGP	Both within SGSSI	1	0.055	6.089	<0.001
CHP vs FIPN	Both within Patagonian Shelf	1	0.072	14.45	<0.001
CHP vs FIPS	Both within Patagonian Shelf	1	0.072	18.54	<0.001
CHP vs HSP	Both within Patagonian Shelf	1	0.017	3.75	<0.005
FIPN vs FIPS	Both within Patagonian Shelf	1	0.084	17.81	<0.001
FIPN vs HSP	Both within Patagonian Shelf	1	0.010	1.78	<0.113
FIPS vs HSP	Both within Patagonian Shelf	1	0.027	6.44	<0.001
Residual		489	3.62		

Permutation tests also showed significant ($F=159.91$; $P>0.001$) differences in the otolith shape from fish captured in the subantarctic and the Patagonian Shelf capture regions. The majority of misclassification percentages, likewise, occurred within the sampling areas of the Patagonian Shelf (up to 21.05%), as well as within the subantarctic (up to 8.96%), supporting the significant separation of these groups from each other and higher within-group similarities. The exception was with regards to a high degree of misclassification between the FIPN (6.76%) and SSP (8.96%) capture regions. This closer relationship is evident in the LDA

ordination plot for Patagonian toothfish which shows a slight overlap in the within-group variances between these two sampling sites (Figure 10).

Table 3: Jackknifed correct classification matrix of the linear discriminant analysis applied to the six sampling regions for Patagonian toothfish (*Dissostichus eleginoides*) and Antarctic toothfish (*D. mawsoni*; see Table 1 for area codes). Bold font indicates the percentage correctly classified for each region.

Region	Predicted region (%)						
	CHP	FIPN	FIPS	HSP	SGP	SSP	SSA
CHP	100	0	0	0	0	0	0
FIPN	0	82.43	5.41	5.41	0	6.76	0
FIPS	0	0	100	0	0	0	0
HSP	0	21.05	0	78.95	0	0	0
SGP	0.85	0	0	1.71	89.74	7.69	0
SSP	0.75	8.96	0	0.75	8.96	80.60	0
SSA	0	0	0	0	0	0	100

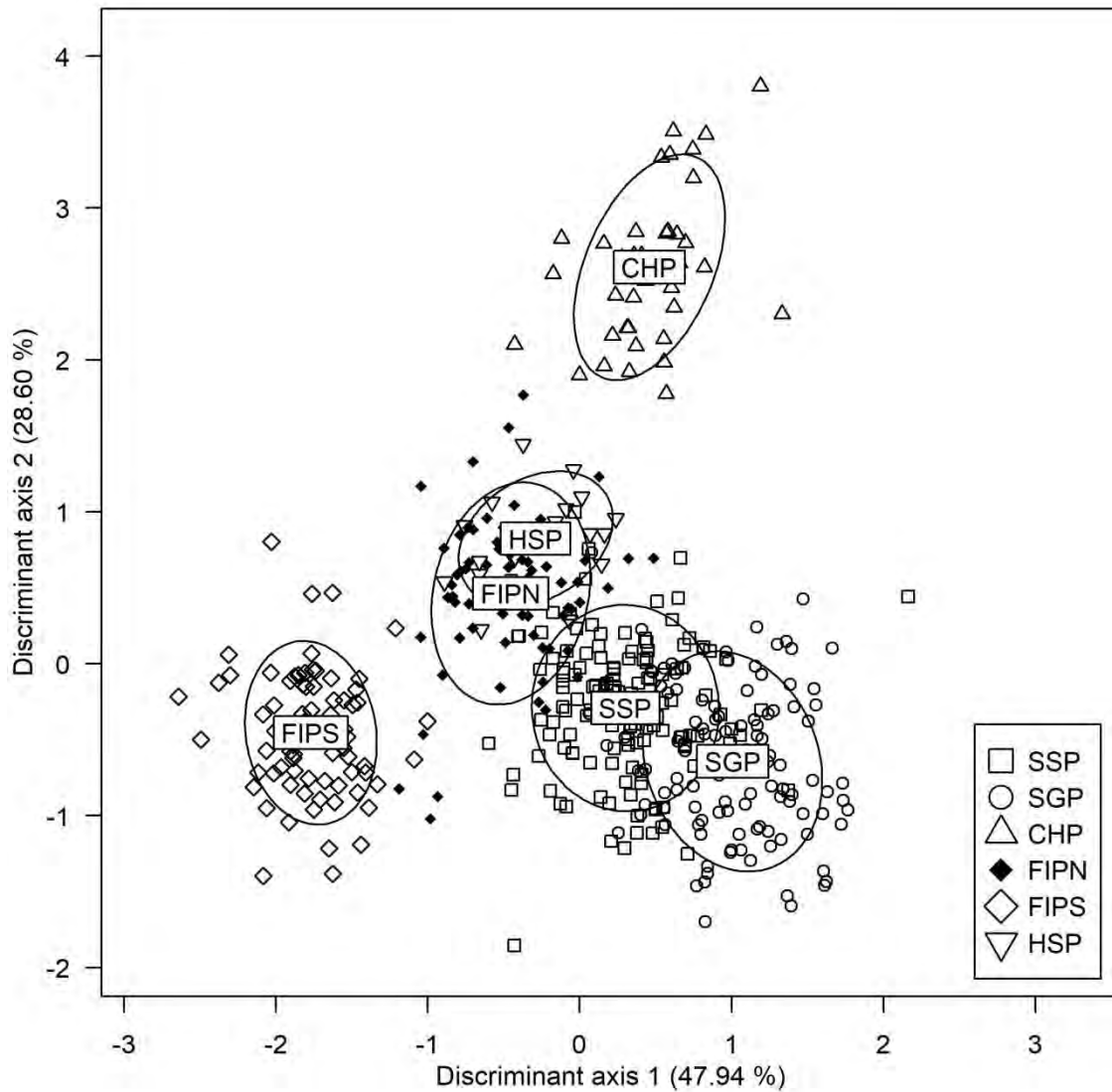


Figure 10: Linear discriminant analysis scores for the classification of Patagonian toothfish (*Dissostichus eleginoides*) by sampling region (see Table 1 for area codes).

Within the South Georgia and the South Sandwich Islands and Patagonian Shelf sampling regions, the similarities shown in the nMDS analysis were not as clear and linkages were not always supported by the results of the LDA ordination and jack-knife classification procedure. The nMDS analysis as well as the degree of overlap in the LDA ordination plot provided strong evidence for the linkages between the South Georgia and the South Sandwich Islands sampling regions. Despite the evidence, otoliths were classified to their correct sampling site with an accuracy of up to 91.04% (Table 4). This degree of separation between fish captured

in South Georgia and the South Sandwich Islands was confirmed by significant ($F=6.089$; $P<0.001$) differences in the otolith shapes between these two sampling sites.

Table 4: Jackknifed correct classification matrix of the linear discriminant analysis applied to the two sampling regions for Patagonian toothfish (*Dissostichus eleginoides*) in South Georgia and the South Sandwich Islands (SGSSI; see Table 1 for area codes). Bold font indicates the percentage correctly classified for each region

Region	Predicted region (%)	
	SGP	SSP
SGP	89.74	10.26
SSP	8.96	91.04

Within the Patagonian Shelf, Chilean fish could be classified to the correct sampling region with an accuracy of 100% (Table 5) with the LDA ordination plot not indicating linkages with any of the other sampling regions. Similarly, evidence from the LDA jack-knife classification matrix suggested a minimal degree of linkages between the northern (5.41%) and southern (1.30%) Falkland Island sampling regions. In contrast the High seas fish displayed clear overlap with the northern Falkland Islands sampling region resulting in a misclassification of 26.32%. The clear linkages between these two sites were validated by permutation tests indicating no significant ($F=1.78$; $P>0.113$) differences in otolith shape between these two sampling regions.

Table 5: Jackknifed correct classification matrix of the linear discriminant analysis applied to the four sampling regions for Patagonian toothfish (*Dissostichus eleginoides*) along the Patagonian Shelf (see Table 1 for area codes). Bold font indicates the percentage correctly classified for each region

Region	Predicted region (%)			
	CHP	FIPN	FIPS	HSP
CHP	100	0	0	0
FIPN	1.35	87.84	5.41	5.41
FIPS	0	1.30	98.70	0
HSP	0	26.32	0	73.68

2.4. Discussion

The present study showed strong patterns in geographic variation of otolith shape on the basis of elliptical Fourier descriptors and suggested that deviations in shape can be used to inform our understanding of the population structure and ecology of Antarctic and Patagonian toothfish in the southwestern Atlantic. Research into the genetic structure of Patagonian toothfish in the southern Atlantic Ocean has identified geographically discrete populations occurring throughout its range (Smith and McVeagh 2000). Because of the unique life-history and biological characteristics evident in this species, the complexity of subdivisions and connectivity between and within these population groupings remains unclear.

Variation in otolith shape indicated clear differentiation among Antarctic toothfish, Patagonian toothfish from South Georgia and the South Sandwich Islands and Patagonian toothfish from the Patagonian Shelf. The clear separation of Antarctic toothfish from Patagonian toothfish (0% misclassification) validated the use of this methodology for toothfish-stock discrimination. Otolith shape has previously been used with success to discriminate species displaying known genetic heterogeneity. Zischke *et al.* (2016) utilised LDA cross-validation techniques to

achieve a predictive accuracy of over 96% for four species of mackerel (*Scomberomorus* spp.). Similarly high rate of classification success were reported among and within species of hakes showing strong genetic heterogeneity (Torres *et al.* 2000). Levels of otolith classification success have been shown to increase with the extent of genetic discreteness or geographic separation (Castonguay *et al.* 1991). The clear separation between toothfish of South Georgia and the South Sandwich Islands and the Patagonian Shelf on the basis of differentiation in otolith shape supported prior evidence from otolith microstructure (Ashford *et al.* 2006), stable isotopes (Ashford and Jones 2007) and genetics (Shaw *et al.* 2004; Rogers *et al.* 2006) describing population isolation between Patagonian toothfish found off the Patagonian Shelf and those found on South Georgia. The separation between these two geographic regions has been attributed to the APF acting as a barrier to larval dispersal, in conjunction with the geographic distance and deep-water troughs inhibiting the active migration of sedentary adults (Shaw *et al.* 2004).

The current study showed significant differences in the otolith shape of toothfish caught within population groups of known genetic homogeneity (Patagonian Shelf; Shaw *et al.* 2004) and geographic mixing (South Georgia and the South Sandwich Islands; Roberts and Agnew 2008). This was despite the nMDS analysis not revealing any visual separation between the capture regions within these groups. In unconstrained ordination techniques such as nMDS, certain patterns of overall dispersion can sometimes hide real differences in multivariate space among groups (Anderson and Willis 2003). Constrained methods, such as LDA, highlight dispersion trends potentially overlooked by unconstrained methods. Patagonian toothfish caught in South Georgia and the South Sandwich Islands recorded success rates of up to 91.04% in allocating fish to their respective capture regions. Similarly, Patagonian Shelf toothfish could be correctly allocated to their sampling region with an accuracy of over 73.68%. The high levels of classification success obtained from the LDA imply that phenotypic differentiation reflected in the otolith shapes is sufficient to suggest geographic isolation between the sampling regions. Spatial delineation of toothfish over the Patagonian Shelf is

supported by Ashford *et al.* (2012) who found strong heterogeneity in the nucleus and edge chemistry of juvenile toothfish otoliths caught in shallow waters (<500 m) to the north and south of the Falkland Islands. This was attributed to spawning areas off southern Chile and the Burdwood Bank supporting immigration through egg and larval dispersion, to different regions of the Falkland Island territorial waters (Falkland Islands Conservation Zone and Falkland Islands Outer Conservation Zone). The ratios of chemical elements found in the edge chemistry were consistent with previously observed environmental characteristics in the regions from which the fish were captured. Similarly, using otolith microchemistry, Ashford *et al.* (2005) was able to spatially isolate toothfish according to sampling areas within South Georgia indicating strong environmental gradients within small geographical areas.

The success in discriminating local population groupings of toothfish along the Patagonian Shelf and South Georgia and the South Sandwich Islands may be related to their life-history characteristics in combination with the oceanographic environment in which they occur. Differences in otolith shape may be caused by both environmental (such as eg. temperature and feeding conditions) and genetic (stock) influences (Cardinale *et al.* 2004). Hüsey (2008) concluded that although otolith shape development consists of an ontogenetic component in the form of increasing size and crenulation, feeding level was a major variable affecting the size and number of lobes formed. Studies have suggested that particular environmental conditions such as food availability, depth, water temperature and substrate type influence the metabolism and body condition of fish (Cardinale *et al.* 2004; Mérigot *et al.* 2007; Vignon and Morat 2010), altering the rates of somatic and otolith growth and, thus, affecting otolith shape (Campana and Casselman 1993; Ferguson *et al.* 2011). Differences in otolith shape among capture regions containing genetically homogenous individuals is, therefore, indicative of the environment a fish has experienced during its life history, and groups of fish that maintain distinct distributions for part or all of their lives can, therefore, be discriminated. In the present study, the marine environments across the study region display high variability in terms of their chemical and physical properties (Ashford *et al.* 2006; Ashford *et al.* 2012b). Toothfish have a

high fecundity and long egg and larval phase (Evseenko *et al.* 1995; North 2002). This, in combination with the hydrographic dynamics prevalent in the region (Ashford *et al.* 2012b), may result in genetically homogenous individuals spread across the Patagonian Shelf from an early stage of development (Ashford *et al.* 2012b). Evidence suggests strong site fidelity in adult toothfish (Marlow *et al.* 2003; Brown *et al.* 2013a). The aforementioned environmental variability throughout the Patagonian Shelf and South Georgia and the South Sandwich Islands might therefore drive variability in otolith shape which is moulded throughout the life of individual sedentary fish.

Shape analysis on its own does not have sufficient power to determine whether the misclassification of individuals is a result of imprecision of the methodology, individual variability, linkages as a result of ecological factors (Campana and Casselman 1993), or a combination of the above (Tracey *et al.* 2006). In the current study, ecological linkages could occur during the dispersal of eggs, larvae and juveniles, or through the movement of adults. Fish from the HSP had a classification success of 73.68%, in which 26.32% were misclassified to the FIPN. This high level of misclassification can be somewhat expected given the lack of any geographical or oceanographic boundaries and the close distances between the two capture regions. In South Georgia and the South Sandwich Islands, despite significant differences in their otolith shape, 10.26% of fish from South Georgia were misclassified as being from South Sandwich Islands. Roberts and Agnew (2008) reported that a single fish tagged near the South Sandwich Islands was recaptured in the South Georgia fishery. This reflects that some large-scale movements (740 km), although infrequent, occur between these two regions. It can be speculated that these rare movements are the cause of misclassification in otolith shape between these two regions.

High levels of misclassification were also evident, across the APF, between individuals from the South Sandwich Islands (8.96%) and those from the north of the Falkland Islands Zone (6.76%). Although research has explored the genetic structure of Patagonian toothfish across

the southwestern Atlantic (Smith and McVeagh 2000; Shaw *et al.* 2004; Rogers *et al.* 2006; Toomey *et al.* 2016), these works have not directly compared samples from both the Falkland Islands and the South Sandwich Islands together. Rogers *et al.* (2006) indicated how a single individual of 33 sampled from the northern region of the Falkland Islands showed a “Southern Ocean” haplotype, although this was inferred as either having arisen through a sampling error on the fishing vessel, in subsequent labelling of samples or through the active migration of a single adult. Similarly, analysis of a 12S mitochondrial sequence showed that 9 of 230 (4%) sampled South Sandwich Patagonian toothfish individuals were found to have a northern haplotype, characteristic of Patagonian toothfish populations living to the north of the APF (Roberts 2012). Research has indicated that the APF may not be the impermeable barrier of north-south dispersal in the Southern Ocean, to the extent that was once thought. Oceanographic data have shown that the APF is, in fact, made up of many small jets (Thompson 2008), with mesoscale eddies having been observed pushing southward into Antarctic waters (Ansorge and Lutjeharms 2003). Fraser *et al.* (2017) provided evidence that shallow-water marine organisms can push through the front with observed eddies by rafting, supporting the prediction of biological permeability of the APF. These results suggest that, in theory, the misclassification occurring in the South Sandwich Islands could be a result of toothfish eggs or larvae undertaking southward traverses of the APF, with observed eddies into subantarctic waters, although future research would be required to investigate the likelihood of this possibility further. In opposition to this, similarities in otolith shape that are reflected as misclassification may not conclusively indicate connectivity, because this may alternately indicate homogeneity in certain environmental conditions driving similarities in otolith shape between two distinct population groupings (Stransky *et al.* 2008). This reinforces the importance of analysing and interpreting the results of otolith-shape analyses in the context of a multidisciplinary framework, including genetic, tag-recapture, or otolith microchemistry analyses.

Consistent differences were clearly detectable among population groups, both with statistical analyses of EFCs, as well as with the naked eye. The successful discrimination of toothfish into population groups of known genetic differentiation validated that an analysis of otolith shape, described using EFCs, can be a powerful, cost-effective and objective tool for examining population structure in this deep-sea marine species. However, further evidence is required to identify to what extent this reflects localised stock delineation. A comparison of otolith shape among size classes, ages or life-history stages according to sex and year may contribute to understanding the potential of this method in stock discrimination. A multidisciplinary approach through the collaborative use of other methods such as otolith microchemistry, hydrographic modelling, or tagging is further required to identify the strength of this method in establishing and validating local isolation in the stock structure across the Patagonian Shelf and South Georgia and the South Sandwich Islands.

Chapter 3 - Environmental drivers of Patagonian toothfish (*Dissostichus eleginoides*) spatial-temporal patterns during an ontogenetic migration on the Patagonian Shelf

Abstract

Understanding the spatial and temporal dynamics in marine fish populations is essential for the development of effective adaptive management strategies. Many marine fish species undergo ontogenetic shifts in abundance, with the utilization of productive shelf-based habitats during early life-history stages. For instance, in the shelf ecosystem around the Falkland Islands, a dynamic Patagonian toothfish population undertakes an early life-history ontogenetic migration after recruitment from spawning areas off southern Chile and the Burdwood Bank. To better understand the spatial-temporal dynamics for this species, Bayesian species distribution models were used to (1) identify oceanographic drivers of recruitment success; (2) assess the spatial-temporal distribution patterns; and (3) describe the habitat preferences and ecological interactions during a six-year study period (2015–2020) on the Patagonian Shelf. The presence of seasonal mesoscale eddies linking the Subantarctic Front with the Falkland Current appear to be of primary importance for the survival of toothfish eggs and larvae on the shelf after transport from offshore spawning areas over the Burdwood Bank and southern Chile. Results indicate persistent recruitment hotspots for newly-settled Patagonian toothfish to the northwest, along with opportunistic areas to the south and northeast of the Falkland Islands, coinciding with the main areas of upwelling and high productivity. During years of low recruitment, juveniles are largely constrained to sheltered inshore regions to the northwest of the Falkland Islands. Spatial distribution patterns during post-settlement ontogenetic migrations are progressive, characterised by age-structured hotspots that differ according to depth, current velocity, oxygen, mixed-layer thickness, the

abundance of competitors (icefish – *Champscephalus esox*) and prey (rock cod – *Patagonotothen ramsayi*). The temporal shift in the range and intensity of hotspots is linked to levels of recruitment and subsequent cohort strength, which in turn appears to be driven by oceanographic processes. Understanding the environmental influences on recruitment dynamics is a key step in assessing connectivity within these discrete spatial groups on the Patagonian Shelf, and how their variability can influence the adult population over time.

3.1. Introduction

Understanding spatial patterns in marine fish populations are essential for the effective movement towards ecosystem-based fisheries management (Link 2010; Fogarty 2014). Spatial patterns can be highly variable in time due to the influence of different environmental and ecological processes. Physical (e.g. temperature, current dynamics), chemical (e.g. salinity) and structural (e.g. bathymetry, habitat availability) environmental factors can influence stocks through changes in physiology, distribution and migration patterns, and mortality rates (Link 2010). Ecological processes such as competition and predator-prey interactions may also influence population dynamics, abundance and distribution of a species (Leach *et al.* 2016; Pennino *et al.* 2019; Coll *et al.* 2019). While this information can be implemented and used to provide stock assessment advice directly (Booth 2000), they are more commonly incorporated for use as contextual information in the designation of essential fish habitat, aiding conservation management, and informing marine spatial planning (Fiorentino *et al.* 2003; Young and Carr 2015; Fonseca *et al.* 2017; Liu *et al.* 2018; Janßen *et al.* 2018).

Many marine fish species undergo ontogenetic shifts in habitats and are subject to multiple anthropogenic and environmental pressures throughout their life cycle (Barbeaux and Hollowed 2017; Kraufvelin *et al.* 2018; Wheeland and Morgan 2020). Within such species, aspects such as egg and larval dispersal may be significant, varying on both temporal and spatial scales under different physical influences, often transcending economic boundaries (Cowen *et al.* 2007). Early life-history spatial patterns and abundance are the first step of a chain of successive events, making it vital for understanding and interpreting the adult population structure (Grorud-Colvert and Sponaugle 2009; Félix-Hackradt *et al.* 2013; Cooper and Nichol 2016). The identification of areas within which key early life-history processes occur and the linkages between them through transport and migrations may therefore be critical for predicting population connectivity.

Species distribution models (SDMs) are the primary tools to provide quantitative information for the prediction and identification of species temporal and spatial patterns, through linking occurrence and abundance with environmental variables and other ecological processes. Currently, there is a wide range of modelling approaches used for predicting species distributions (Guisan and Zimmermann 2000; Norberg *et al.* 2019; Stock *et al.* 2020). The implementation of Bayesian hierarchical species distribution models (B-HSD) in fisheries ecology has been widely used in recent years, including the protection of vulnerable life-history stages (Paradinas *et al.* 2015; Paradinas *et al.* 2017), the identification of high density discard hot-spots (Stock *et al.* 2020), or the protection of vulnerable habitats (Rufener *et al.* 2017; Fonseca *et al.* 2017; Pennino *et al.* 2019; Coll *et al.* 2019; Paradinas *et al.* 2020), including those vulnerable to bycatch (Ward *et al.* 2015). B-HSD models allow spatial and temporal components to be incorporated as random variables, reducing the influence of these on the effects of other variables (Martínez-Minaya *et al.* 2018). This allows for the spatial structure of the data to be incorporated into the modelling process preventing violation of the independence assumption.

The Patagonian toothfish *Dissostichus eleginoides* Smitt, 1898 (family Nototheniidae) has a distribution spanning the Antarctic Polar Front (APF), extending north over the Patagonian Shelf in the Southwest Atlantic, and off the continental shelf of Chile in the Pacific (Eastman 1993; Collins *et al.* 2010). It is a large (~200 cm TL), benthic-pelagic species inhabiting island plateaus, seamounts and the continental shelf/slope across a wide range of depths from 50 m down to 2500 m (Arkhipkin and Laptikhovskiy 2010). Validated age estimates have confirmed long lifespans (>50 years), slow growth (Horn 2002; Andrews *et al.* 2011), and complex, long reproductive cycles with late maturity (10 – 17 years; Boucher, 2018; Yates *et al.*, 2018). These life-history traits make them vulnerable to overexploitation (Koslow *et al.* 2000; Norse *et al.* 2012; Victorero *et al.* 2018). The species is a sought-after resource due to its high commercial value and abundance (Sovacool and Siman-Sovacool 2008; Grilly *et al.* 2015). In the Falkland Islands, a Marine Stewardship Council (MSC) certified longline fishery targets

the adult component of the population in deep waters between 800 and 2000 m. Juvenile Patagonian toothfish are also reported annually as bycatch in the shelf-based (<400 m depth) finfish and squid trawl fisheries (Laptikhovsky and Brickle 2005; Randhawa 2020), although the extent and consistency of these remain unclear.

The population occurring over the Patagonian Shelf is genetically homogenous (Shaw *et al.* 2004; Canales-Aguirre *et al.* 2018). However, genetic markers vary greatly in their ability to resolve the extent to which the population consists of a single or multiple phenotypic or contingent stocks (Beebee and Rowe 2008; Ashford *et al.* 2012b; Lee *et al.* 2018). Spawning occurs annually between June and August within two geographically discrete areas off the far southern tip of Chile (Arana 2009); and the Burdwood Bank to the south of the Falkland Islands (Laptikhovsky *et al.* 2006a). Eggs hatch in September and October (unpublished data). Regional current systems are thought to be influential in the dispersal of pelagic eggs (± 30 -90 days) and larvae (>60 days) into inshore (<200 m) nursery areas, including around the Falkland Islands (Evseenko *et al.* 1995; Ashford *et al.* 2012b; Mujica *et al.* 2016). The recruitment and settlement of post-larval Patagonian toothfish typically occurs during the late austral summer (January – February; Arkhipkin and Laptikhovsky, 2010). Juvenile fish then undertake a characteristic ontogenetic migration into deeper waters where adults reside and spawn (Arkhipkin and Laptikhovsky 2010). Rock cod (*Patagonotothen spp.*) are the predominant prey source for juvenile toothfish (Arkhipkin *et al.* 2003), where they undertake intense competition with icefish (*Champsocephalus esox*), during the early life-history stages (Brown 2011).

The observed recruitment of juvenile Patagonian toothfish into nursery areas around the Falkland Islands show large-scale variability in abundance. Years of high recruitment are thought to support the fishery over an extended time period (Laptikhovsky and Brickle 2005), making their protection during these vulnerable life-history stages of fundamental importance for the effective management of the species. The spatial patterns of juvenile settlement areas

and the temporal persistence of these as recruitment hotspots remain equivocal. Further, the spatial and temporal structure of subsequent ontogenetic migrations, and the extent to which they follow distinct pathways across the Patagonian Shelf into deeper waters where adults reside and spawn, is not well understood. In the current study, Bayesian hierarchical spatial-temporal models were applied to describe the abundance and spatial patterns of age-disaggregated Patagonian toothfish juveniles on the shelf waters around the Falkland Islands using a six-year time series of fisheries independent bottom trawl surveys (2015 - 2020). In particular, the aims of the study were to (1) identify the environmental and ecological variables that influence these patterns and (2) assess the spatial-temporal persistence (stability) of nursery area hotspots and subsequent ontogenetic migration pathways into their adult deep-water habitats.

3.2. Materials and methods

3.2.1. Study area

The study area was located in the highly productive waters of the Patagonian Shelf of the Southwest Atlantic surrounding the Falkland Islands (48 - 55°S and 53 - 64°W), where key toothfish early life-history stages occur (Figure 11). The region presents varied seafloor morphology, including the extensive shallow Patagonian Shelf, 80 – 400 m to the west of the Falkland Islands, becoming increasingly constricted in the east where it deepens into the Patagonian Slope. South of the Falkland Islands lies the Burdwood Bank (200 m depth), a shallow underwater plateau partially linked to the Patagonian Shelf by a narrow (90 km) shallow (400 m) channel to the west. This channel widens to the north and deepens (2000 m) to the east into the Falklands Trough (Matano *et al.* 2019). The oceanography in the region is largely driven by the Antarctic Polar Front (APF) which carries cold, nutrient rich waters of subantarctic origin through the Drake Passage off the southern tip of South America (Agnew 2002; Arkhipkin *et al.* 2013; Song *et al.* 2016). Upon encountering the Burdwood Bank, two

north flowing branches of the Antarctic Circumpolar Current wrap around its edges forming the Falklands Current to the west and the Subantarctic Front (SAF) to the east (Ashford *et al.* 2012b; Matano *et al.* 2019). The Falklands Current follows the shelf break extending around the southern and eastern edge of the Falkland Islands, with the weaker Patagonian Current diverging to the west (Croxall and Wood 2002; Arkhipkin *et al.* 2013). The SAF passes along the southern shelf edge of the Burdwood Bank, before extending north through a trough (2000 m deep) in the North Scotia Ridge to align subsequently with the 2000 m isobaths along the Patagonian Slope, and eventually converging with the Falklands Current at 50°S (Ashford *et al.* 2012b). Oceanographic data indicate that this current is dynamic and shifting with irregular mesoscale eddies occasionally observed breaking through the main current stream along the northern edge of the Burdwood Bank, and linking up with the Falklands Current (SAF-FC) to the south of the Falkland Islands around Beauchene Island (Song *et al.* 2016; Fraser *et al.* 2017).

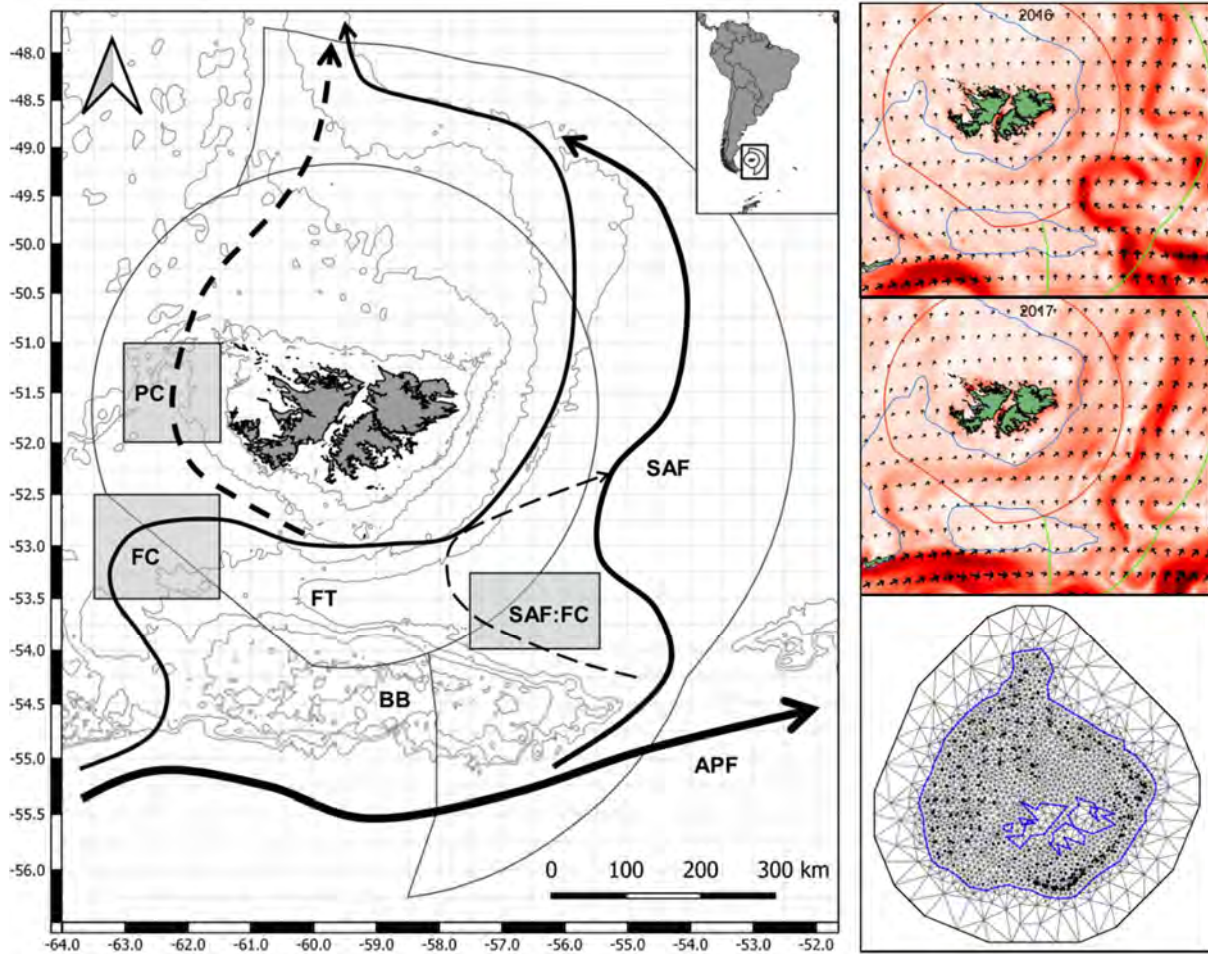


Figure 11: Map depicting the main oceanographic and topographical features of the study area. The shaded areas indicate the quadrats from which oceanographic variables were extracted from the main current systems (see Section 2.4). APF: Antarctic Polar Front; SAF: Subantarctic Polar Front; FC: Falklands Current; PC: Patagonian Current; FT: Falklands Trough; BB: Burdwood Bank. Satellite-based depictions on the right portray years of high (16 August 2016) and low (16 August 2017) influence of the Subantarctic Front over the Falklands Shelf. Locations of the combined sample sites (black dots) and INLA mesh for the SPDE model are shown on the bottom right.

3.2.2. Data collection

Data on toothfish were collected during two multi-annual research survey programmes: Demersal biomass surveys, and Patagonian longfin squid (*Doryteuthis gahi*) pre-season

surveys; which together cover the trawling grounds around the Falkland Islands shelf (Gras *et al.* 2018; Winter *et al.* 2020). During all surveys, comprehensive data associated to each trawl station were collected. Geographic locations (Latitude, Longitude) of sampling stations, depth and trawl dimensions (door distance, footrope length, bridle length) were recorded. The Swept-area (m^2) of each trawl was estimated as the product of trawling distance and width (Gras *et al.* 2018).

Catch information including catch composition (by species) and catch weights (to the nearest g) was recorded (Figure 12). For toothfish and other selected species, random samples of 100 individuals were measured to the nearest lowest cm, and sex and maturity were macroscopically assessed. Otoliths were extracted from a subsample of male and female toothfish to cover the length distribution of the catch for each survey.

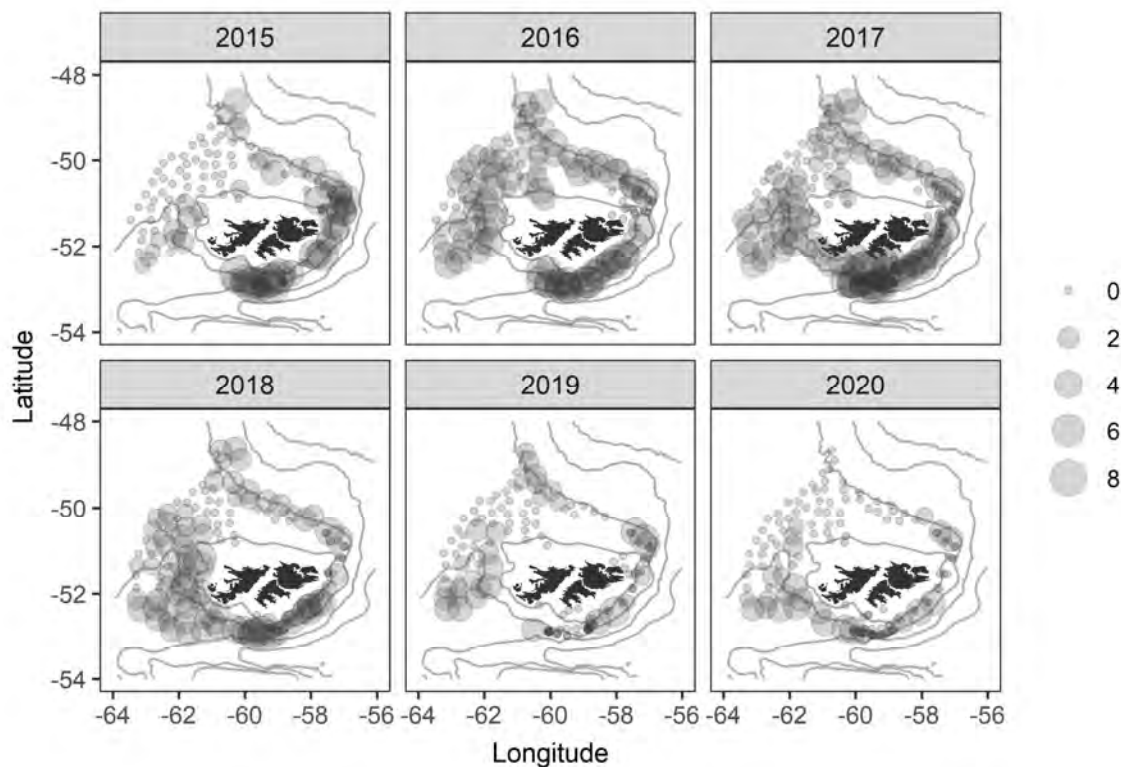


Figure 12: The position of the sampling locations and the observed toothfish abundance for each sample year. The sizes of points reflect the numbers of toothfish caught on the log scale.

Demersal biomass surveys - Demersal biomass research surveys were carried out over a 21-day period during the late austral summer (February) from 2015 to 2020. During the survey, 79 fixed stations were replicated for each year according to a systematic transect design based on the division of the shelf area into 0.5 longitude by 0.25 latitude decimal degree grid squares. Each station was allocated to an individual grid square to ensure coverage of the entire study area. Additionally, 12 to 31 floating stations were undertaken each year and were used to broaden the spatial area or cover additional areas of interest in deeper (>300 m) or shallower (<100 m) waters of the shelf. Typically, 83 to 102 trawl stations of 45 - 60 minutes took place each year. The gear consisted of a bottom trawl net (20 to 30 m horizontal opening) with a 40 mm mesh liner in the cod end.

Patagonian longfin squid pre-season surveys - Pre-season surveys for the Patagonian longfin squid *Doryteuthis gahi* were carried out over a 14-day period during the late austral summer (February) of the same years as the demersal biomass surveys. Surveys consisted of 39 fixed-station trawls of 120 minutes located on a series of 15 transects perpendicular to the shelf break to the south and east of the Falkland Islands. An additional 19 to 21 floating stations were undertaken each year to further investigate areas of high-density or high-variability biomass or to investigate additional areas of interest in deeper (>300 m) or shallower (<100 m) waters. A bottom trawl net (30 to 100 m horizontal net opening, mesh size = 40 mm) with a cod end mesh liner was used for the surveys.

3.2.3. Variables

Juvenile Patagonian toothfish were present in 497 (53.79%) of the 924 hauls sampled in the study area between 2015 and 2020. For each year of the study period, between 90 and 120 otoliths from fish covering the length distribution of the sampled catch were extracted and processed for ageing (n = 643) as described by Horn (2002) and Arkhipkin and Laptikhovskiy (2010). In the laboratory, otoliths were embedded in polyester resin and transversely sectioned

using a Buehler Isomet low-speed saw equipped with a diamond-edge blade (Buehler Ltd, Esslingen am Neckar, Germany). Transverse sections were mounted on glass slides with coverslips and examined at 20x magnification for ageing under an Olympus BX-50 microscope. The number of completed annuli between the nucleus and otolith edge were enumerated by two independent age readings without reference to biological or catch information. If the successive readings were in agreement this estimate was used as the final age for the otolith. If the readings differed, a third consensus reading was taken and compared to the previous two age estimates. If all three age readings differed, the otolith was excluded from the analyses. The reproducibility of age estimates were described using an index of average percent error (APE) following the method of Beamish and Fournier (1981). Observed age estimates were used to derive age-length keys for each year. These were applied to length frequency data ($n = 10,511$) to obtain an age estimate for each sampled fish ($n = 23,134$ individuals). Age frequencies from the sampled fish were raised to the total catch for each station to get a separate value of the catch for each annual cohort.

The response variable therefore consisted of the numerical abundance of age-disaggregated Patagonian toothfish for each station from 2015 to 2020. Only Patagonian toothfish aged 0+, 1, 2 or 3 were included in the analyses (see section 3.3.1). Twelve covariates were considered that may help explain the abundance and distribution patterns for juvenile Patagonian toothfish (supplementary information: Table 9). These included four habitat-based oceanographic variables: (1) sea bottom temperature (degrees Celsius, °C); (2) sea bottom current velocity ($\text{m}\cdot\text{sec}^{-1}$); (3) oxygen concentration ($\text{mmol}\cdot\text{m}^{-3}$); and (4) mixed layer thickness (m); one topographical feature: (5) depth (m); three oceanographic-based recruitment drivers: (6) SAF-FC, (7) Falklands Current and (8) Patagonian Current surface water velocities ($\text{m}\cdot\text{sec}^{-1}$); two biotic interactions: (9) rock cod and (10) icefish abundance (kg/m^2); (11) age (years) and (12); the year of capture. All covariates were also investigated for interactions with age.

The habitat-based environmental variables and oceanographic-based recruitment drivers were obtained from the Global Ocean Physical Reanalysis (GLORYS12 V1) and Global Biogeochemical Hindcast (BIORYS2 V4) numerical modelling products, both available from Copernicus Marine Environment Monitoring Service (CMEMS, <http://marine.copernicus.eu/>). GLORYS data are available as daily averages distributed on a standard regular grid at 1/12° latitude-longitude resolution from the ocean surface to the sea-floor (50 depth levels). BIORYS data provides monthly average measurement at a horizontal resolution of 1/4° across 75 vertical depth levels. CMEMS environmental data have been built to provide a realistic representation of environmental and biogeochemical information in comparison with in situ observations (Le Traon *et al.* 2019). These data have been extensively applied, and validated for use in marine fisheries research (Lauria *et al.* 2017; Lezama-Ochoa *et al.* 2020; Andrews and Leroux 2020) including traditionally data-poor areas across the shelf of the southwestern Atlantic Ocean (Eg. Chemshirova *et al.*, 2021; Franco *et al.*, 2020). Despite the extensive coverage and use provided by satellite data, the limitations regarding the lower temporal and spatial resolution and resultant uncertainties in averaged estimates of these variables should be acknowledged in comparison with directly obtained in situ observations (Robinson *et al.* 2011). For more detailed information on these data, the reader is referred to the user manual (Perruche 2019; Fernandez and Lellouche 2021) and quality information documentation (Perruche *et al.* 2019; Drévilon *et al.* 2021).

Daily habitat-based variables were averaged across a ten-day (30 day for oxygen) time period prior to and including the date that each corresponding trawl station occurred. The depth and mid-point coordinates for each trawl station was aligned with the nearest depth and grid point of their respective oceanographic variables. The topographical feature depth was taken as the average between the start and end point recorded at each trawl station. Biotic interspecific interactions related to the abundance of local scale prey (rock cod), and competitors (icefish) were estimated based on the total catch (kg) divided by the swept area (m²) at each sample station.

The presence of strong current velocities at the SAF-FC interface was hypothesised to result in stronger recruitment cohorts compared to years when these are absent or less abundant. Surface water velocity data ($\text{m}\cdot\text{sec}^{-1}$) were extracted from c. 18,500 km^2 ($0.75\text{-}1^\circ\text{S} \times 1.75\text{-}2^\circ\text{W}$) quadrats located over the observed pathways of the Falklands Current ($52.5^\circ - 53.5^\circ\text{S}$; $60^\circ - 62^\circ\text{W}$), the Patagonian Current ($51^\circ - 52^\circ\text{S}$; $61.5^\circ - 63^\circ\text{W}$), and the SAF-FC ($53.25^\circ - 54^\circ\text{S}$; $55.5^\circ - 57.5^\circ\text{W}$; Figure 11). Data were extracted for the time periods corresponding to the peak periods (August-September) of toothfish egg and larval dispersal and linked to the station data based on birth year (cohort). In order to capture data related to spatial areas and temporal periods exclusively from within the main current flow, the mean current velocity was estimated only from data points in each quadrat that were greater than the 0.75-quantile during each prescribed time period. This approach would actively select data from faster flowing water movement within each area at a given time.

3.2.4. Statistical analysis

All data manipulations and analyses were undertaken using R software (R Core Team 2021). The explanatory variables were explored for outliers, and the presence of collinearity using Pearson correlation coefficients and variance inflation factors (VIF) according to the protocols described by Zuur et al. (2010). A square root transformation was taken on the icefish and rock cod abundance variables to reduce the spread of the data. Continuous explanatory variables were standardised (difference from the mean divided by the corresponding standard deviation) to avoid numerical estimation problems and improve interpretation of the parameters (Zuur *et al.* 2017).

A total of five Bayesian species distribution models (BSDM) were applied to the age-disaggregated shelf-based Patagonian toothfish numerical abundance data in terms of explanatory variables for combined (Full model) and separate age classes (Age-based models). The natural logarithm of swept area was used as an offset variable in all models

tested. BSDMs were fitted using the integrated nested Laplace approximation (INLA) approach, implemented using the R-INLA package (http://www.r_inla.org; Martins et al., 2013), in R software. INLA is a computationally efficient method for fitting a large class of latent Gaussian models (which includes spatial-temporal models) in a Bayesian framework (Rue *et al.* 2009). Spatial correlated random effect terms were included in the modelling framework using the Stochastic Partial Differential Equations (SPDE) approach (Lindgren *et al.* 2011). In this approach, a continuously indexed Gaussian field was approximated with a Matérn covariance function by a Gaussian Markov random field (GMRF). A Delaunay triangulation which consists of a dense triangular grid is constructed on the spatial domain. This grid which is also called a mesh forms the structure on which the representation of the field is based (Figure 11). To avoid increased variance occurring at the borders of the latent field (an edge effect), the mesh was extended beyond the boundary of the sample sites (Zuur *et al.* 2017).

The expected values of toothfish abundance (Y) at each sampling station i , during the defined time period t were related to covariates based on the zero-inflated Poisson (ZIP) and zero-inflated negative binomial (ZINB) model equations:

$$Y_{it} \sim ZIP(\mu_{it}, \pi) \text{ or}$$

$$Y_{it} \sim ZINB(\mu_{it}, \pi, k)$$

$$\log(\mu_{it}) = \beta_0 + \log(Offset_{it}) + X_{it}\beta + f(X_{it}) + w_{it}$$

$$\log(\pi) = \gamma_0$$

where π is the probability of 'false' zeros, and μ is the mean abundance of toothfish (including the 'true zeros'). The negative binomial dispersion parameter, k , allows for extra variation and was set to 1, a so-called geometric distribution. The parameter β_0 , is the intercept and β represents the coefficients which quantifies the effect of the explanatory covariates X . Smooth

term, $f()$ were fitted to nonlinear explanatory covariates represented by a cubic regression spline with 3 to 7 knots to describe biologically realistic response terms. The terms w represents the spatial (temporal) correlated random effects (SRF) term for the model. This term is a latent variable that change in space and time, thus capturing any spatial and temporal patterns that are not already explained by the covariates (Zuur *et al.* 2017; Zuur and Ieno 2018).

Penalised complexity priors (PC priors) were imposed on the model range and marginal standard deviation hyperparameters of the SRF (Fuglstad *et al.* 2019). Specifically, these were set when defining the SPDE as follows: (1) the probability that the spatial effect range was smaller than 25 km was 0.0001, and (2) the probability that the spatial effect standard deviation was greater than 1.4 was 0.001. Default priors were assigned for all fixed effect parameters, which are approximations of non-informative priors designed to have little influence on the posterior distribution. Starting from the full model that contained all explanatory variables in each part, the most parsimonious model was selected using step-wise backwards selection on the basis of the lowest Deviance Information Criterion (DIC; Spiegelhalter *et al.*, 2002) and widely applicable information criterion (WAIC; Watanabe, 2010).

Model validation was undertaken by obtaining the Pearson residuals, calculating the dispersion statistic and comparing this to 1 (a value greater than one indicates overdispersion and a value less than one means underdispersion). The dispersion statistic was calculated as the sum of squared Pearson residuals divided by sample size minus the number of parameters. As a second approach to assess over- or under- dispersion and to test whether the model was capable of dealing with the number of zeros in the observed data, a simulation study was undertaken during which 10,000 simulations from the posterior distributions of the regression parameters were used to generate simulated toothfish abundance data. For each simulation the regression parameters were extracted and the fitted values calculated. Using the fitted values, a new set of toothfish abundance data for the given mean were simulated.

The number of zeros generated for each simulated data set was calculated and compared to the number of zeros in the observed data (Supplementary information: Figure 23). Sample variograms of the residuals were also plotted to identify whether any correlation remained in the residuals (Zuur *et al.* 2017).

3.2.5. Temporal structure

Different spatial-temporal patterns were explored for the five models described above (Figure 13). For each of the five models, a single SRF that was constant across all temporal groupings was fitted (BSDM-Constant). Fixed effect (categorical) terms for respective temporal variables were included in the BSDM framework. This structure assumes a temporally persistent spatial distribution while making allowance for intensity trends on the temporal scale. For the full (age-disaggregated) model, separate SRFs for each age component were fitted, grouped across the study period (BSDM-Age). This structure assumes that spatial patterns vary for each age class but are persistent across sample years. Finally, age-specific temporal models with separate SRFs estimated for each year were explored (BSDM-Year).

For each of the temporal models, opportunistic and progressive spatial structures were applied as described according to Martínez-Minaya *et al.* (2018), Paradinas *et al.* (2020, 2017), and Zuur *et al.* (2017). A progressive spatial-temporal distribution was implemented using an “exchangeable” SRF. The structures in this model are uniformly correlated with the extent of this relationship reflected in the temporal correlation parameter Φ , with values closer to 1 indicating higher temporal dependency. An opportunistic spatial distribution allows for the SRF to be independent for each temporal component while sharing a common covariance function to avoid overfitting (i.e. based on the same hyperparameters of the SRF). The identification of hotspots was based on the 90th percentile of the abundance in the SRF for each model tested. The 90th percentile reflects the most abundant 10% predicted within the study area.

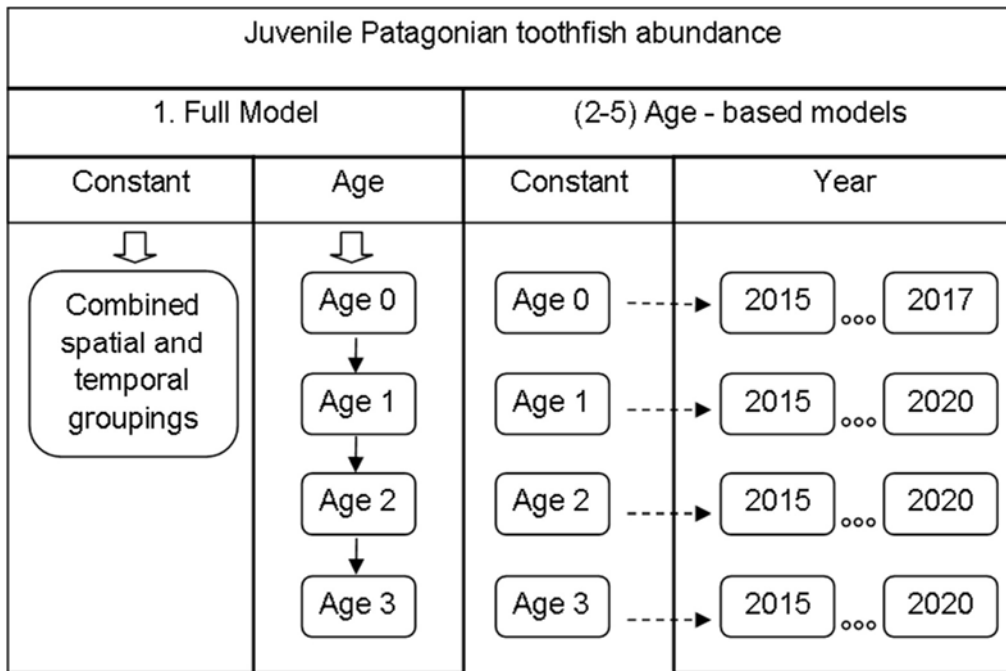


Figure 13: A conceptual diagram of the spatial-temporal patterns explored within the Bayesian species distribution model framework. Note that the Age-0 model only utilised data extending over a three-year time period (2015-2017) due to the absence of any catch during 2018 to 2020.

3.3. Results

3.3.1. Otolith interpretation

Sectioned otoliths of juvenile Patagonian toothfish showed clear, discernible growth rings, comprised of alternating translucent and opaque growth zones in all the sampled otoliths (Figure 14). During the first three to four years, zones were relatively broad and often contained macrostructures within the individual annuli. Macrostructures were clearly distinguishable from annuli due to their smaller diameter and diffuse banding structure. The banding structure of annuli in fish greater than four years became increasingly narrow and difficult to discern due to the likely formation of the transition zone as described by (Horn 2002). Age estimates were obtained from all 643 of the otoliths aged. Agreement was reached

between the two age readings for 86.31% of the otoliths, 12.60% differed by one year and 0.93% differed by two years. These differences were largely attributable to the interpretation of the margin as completed or uncompleted annuli in fish greater than 4 years of age. The reproducibility of age estimates for shelf-based juvenile Patagonian toothfish was high (APE = 2.27%) and the age estimates can therefore be considered as reliable (Campana 2001).

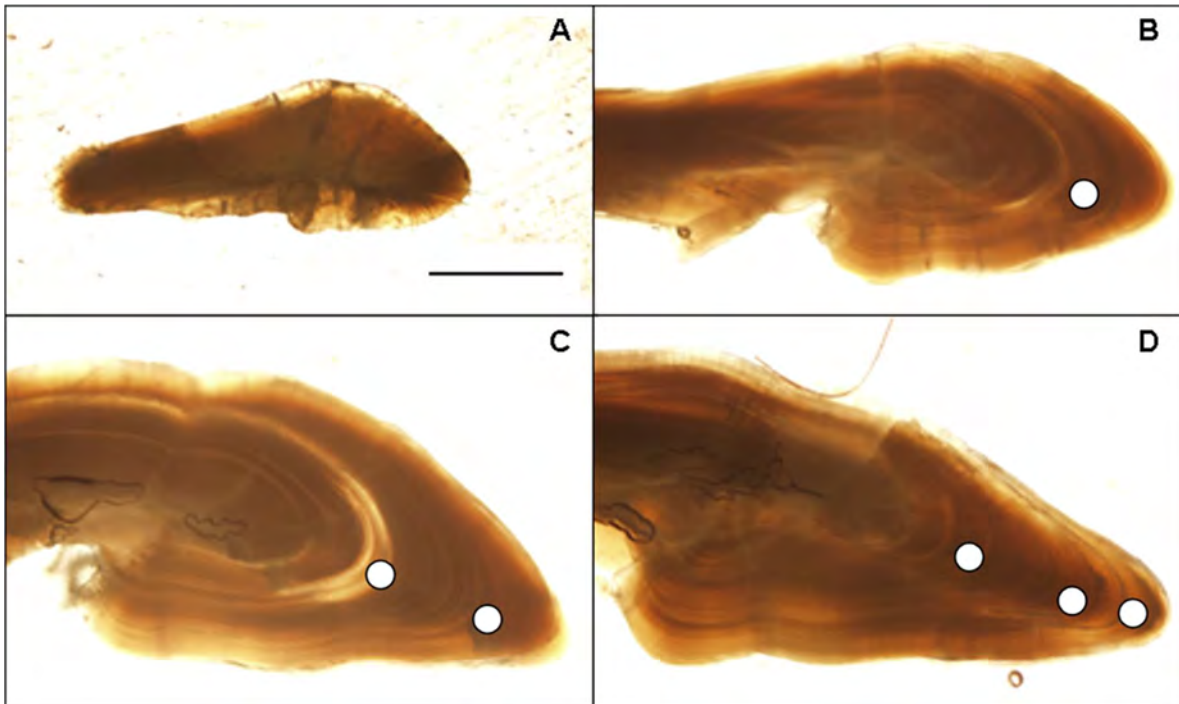


Figure 14: Sectioned otolith from an (A) 13 cm age-0+, (B) 27 cm age-1+, (C) 38 cm age-2+ and (D) 51 cm age-3+ Patagonian toothfish, viewed at 20X magnification. The white dots indicate the edge of the translucent (Winter) zone of growth. The scale bar reflects 1 mm.

3.3.2. Population structure and environmental drivers

The majority of the Patagonian toothfish across the shelf (97.58%; $n = 22,575$) consisted of fish less than four years old (Age-0 = 12,185, Age-1 = 6,231, Age-2 = 3,227, Age-3 = 932). A distinct progression of multimodal, age structured cohorts were clearly visible in the length frequency distributions for fish aged between 0+ and 3+ years passing through the shelf population over the study period (Figure 15). There was high variability in the annual age

structure composition of the shelf population during the study period. Differences in annual age structure appeared to be driven by high and low recruitment cohorts entering the fishery. High recruitment cohorts occurred during 2015 and 2017 (modal length of 10 to 14 cm) which can be tracked through subsequent study years as age-1 (2016 and 2018; modal length 30 – 33 cm), age-2 (2017 and 2019; modal length 44 – 50 cm) and age-3 (2018 and 2020; modal length 56 cm) fish. Low recruitment cohorts that occurred from 2018 to 2020 are further reflected in weaker progressive cohorts of age-1 fish during 2019 and 2020, respectively, and age-2 fish during 2020. The 2016 recruitment cohort was intermediate in abundance, with progressive cohorts of age-1 (2017) and age-2 (2018) fish reflected in the length- and age-frequency histograms.

Demographic variables of importance from the full BSDM showed abundance estimates of shelf-based Patagonian toothfish were greatest for early juvenile (age-0 and age-1) fish, declining with increasing age thereafter (Figure 16). Abundance estimates showed a strong increase from 2015 to 2016, remaining stable until 2017 and then declining until 2020. The year effect for the age-specific models indicated high variability in age-specific patterns, with strong 2015 and 2017 year-classes passing through the population and maintaining the steady overall abundance that was observed over the study period (Figure 17). The years 2018 to 2020 had low recruitment levels (age-0 abundance) which were reflected in low abundance levels for age-1 (2019 and 2020) and age-2 (2020) predictions. The low abundance estimates for age-1, 2 and 3 fish during 2015 indicate that recruitment levels had likely been low between 2012 and 2014.

The presence of mesoscale eddies, identified through increased current velocities, linking the Subantarctic Front with the Falklands Current to the south of the Falkland Islands was a key driver of increased recruitment levels and subsequent abundance in older age-classes on the Shelf (Figure 16). In contrast, increased current velocities of the Falklands Current had a negative influence on recruitment levels and subsequent abundance on the shelf.

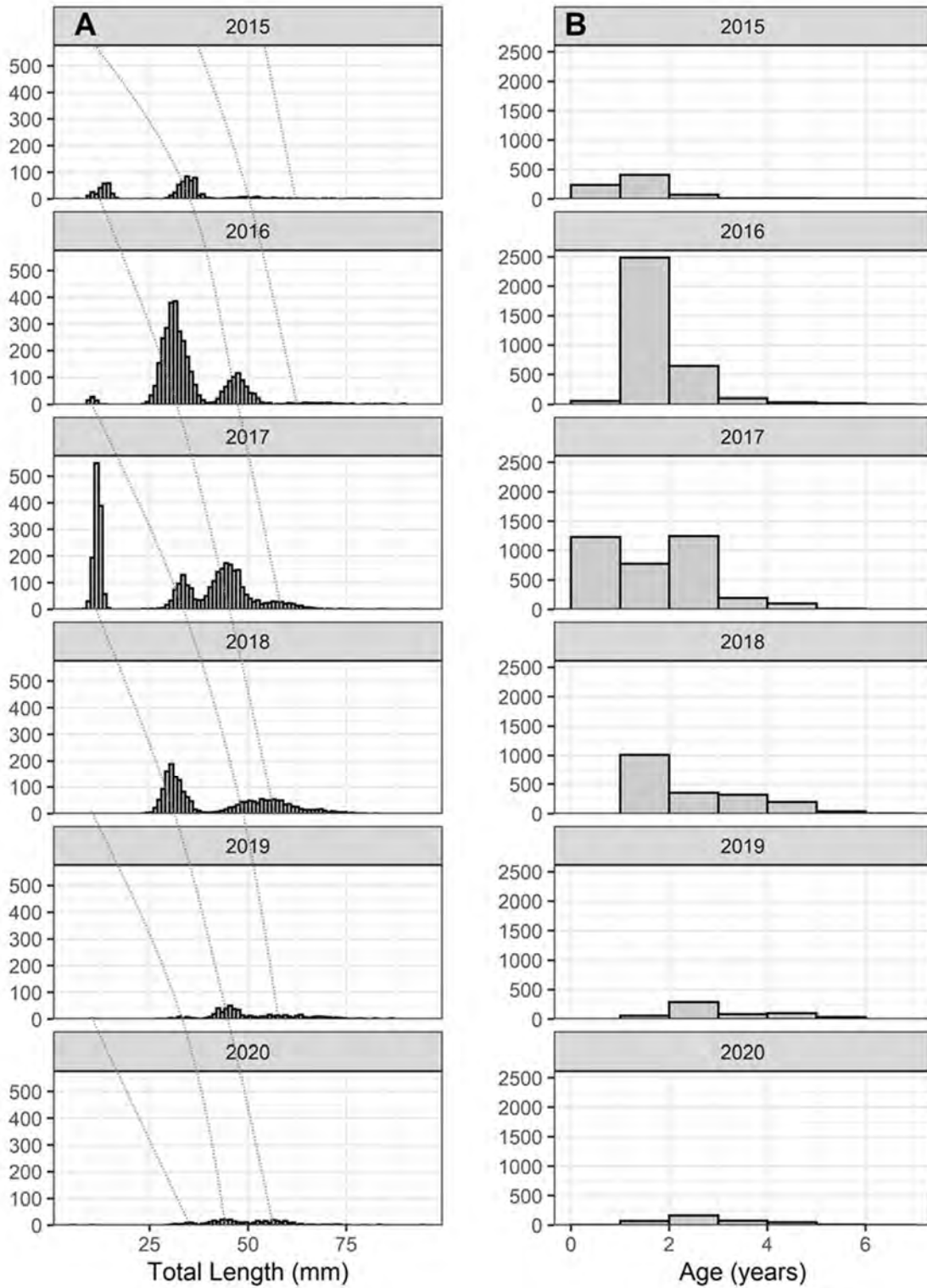


Figure 15: The observed (A) length frequency and (B) age frequency distributions for Patagonian toothfish sampled across the shelf waters of the Falkland Islands during February 2015 to 2020 ($n = 10,511$). The dotted lines reflect the progression of cohorts through time.

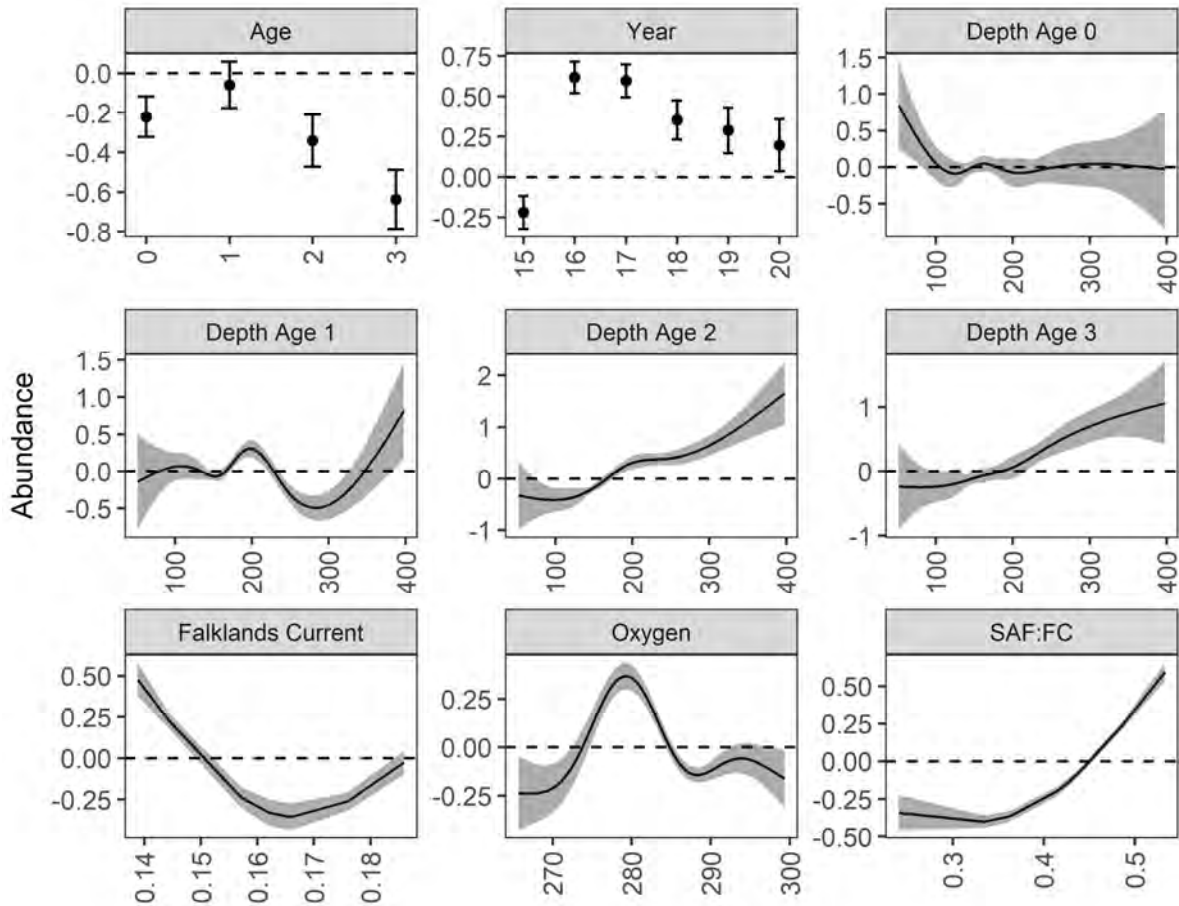


Figure 16: Marginal effect of age, year, depth (m), oxygen (mmol.m^{-3}), Falkland Current (m.sec^{-1}) and SAF:FC current velocity (m.sec^{-1}) variables with respect to the age-disaggregated numerical abundance (Full model) of juvenile Patagonian toothfish on the Patagonian Shelf from 2015 to 2020. The estimated effect is presented in the linear predictor scale (logarithmic link) with the grey shaded area representing the 95% credible intervals.

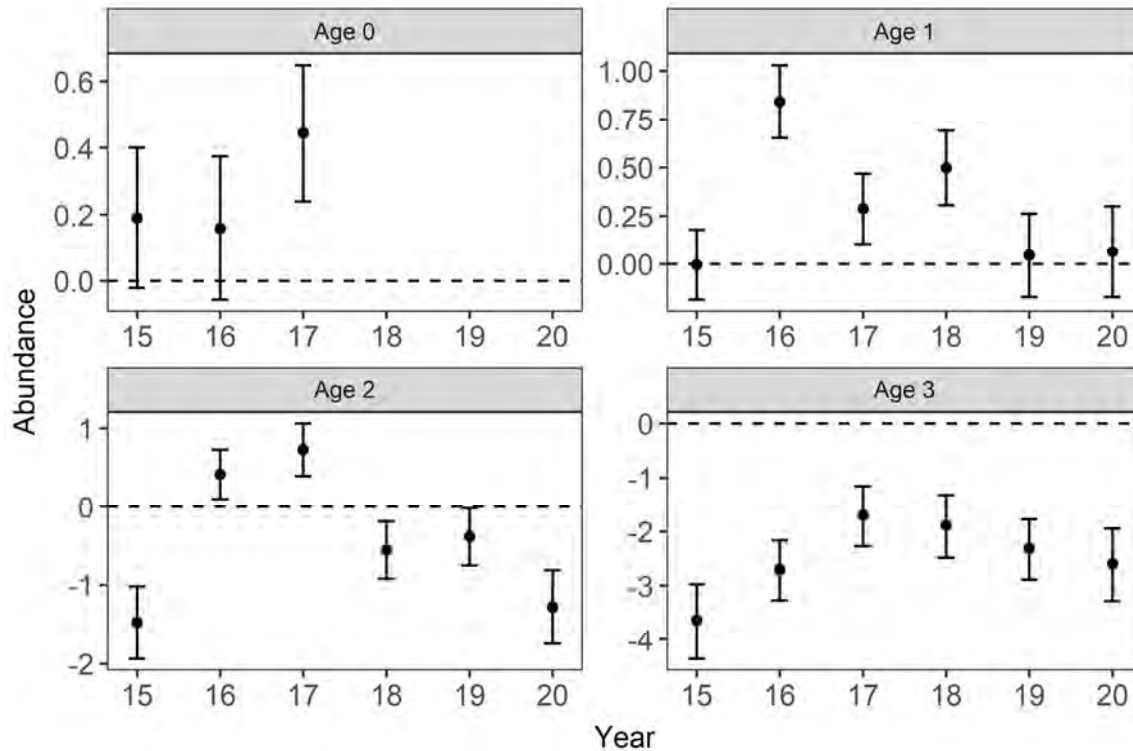


Figure 17: Marginal effect of year with respect to the predicted age-based numerical abundance of juvenile Patagonian toothfish on the Patagonian Shelf from 2015 to 2020. The estimated effect is presented in the linear predictor scale (logarithmic link).

3.3.3. Spatial-temporal patterns

The shelf-based component of the Patagonian toothfish population displayed a progressive age-based spatial structure (Table 6, supplementary information: Figure 24). As opposed to a uniform persistent population, the low temporal correlation parameter ($\Phi = 0.27$) indicated substantial differences in the spatial patterns for each age class, indicative of the high annual variability at each age across the study period. The extent of annual variability in spatial patterns decreased with age (Table 7). Age-0 fish were distributed opportunistically, indicating virtually independent spatial patterns for each of the three years modelled (Figure 18). High variability in the spatial patterns during the three years were clear with hotspots occurring in inshore waters (<200 m) to the south, east, northeast and northwest during 2015, to the north and northwest during 2016 and to the south, west and northwest during 2017. Thus, the only

consistent hotspot across the sample period was to the northwest, although the spatial extent and intensity of this hotspot varied for each year.

Patagonian toothfish at age-1 and age-2 displayed progressive spatial patterns. Substantial spatial variability remained among the sampled years for age-1 ($\Phi = 0.34$, Figure 19) compared to age-2 fish ($\Phi = 0.45$, Figure 20). A consistent hotspot was evident during all years adjacent to the 200 m depth contour to the west of the Falkland Islands progressing into deeper waters to the southwest for age-2 fish. This area was constricted and the only identified area of abundance for age-1 (2019 and 2020) and age-2 (2020) Patagonian toothfish from the extremely low 2018 and 2019 recruitment cohorts. Progressive spatial patterns from the high 2015 and 2017 recruitment cohorts contained distinct hotspots in abundance to the south of the Falkland Islands for age-1 (2016 and 2018) and age-2 (2017 and 2019) fish. Further, the high 2015 and intermediate 2016 recruitment cohort also contained hotspots in abundance to the north of the Falkland Islands for both age-1 (2016 and 2017) and age-2 (2017 and 2018) fish. The spatial patterns for age-3 Patagonian toothfish were temporally persistent across the study period containing two distinct hotspots extending into deeper waters at the shelf-slope interface: to the southwest of the Falkland Islands at the western extent of the Falklands Trough; and to the north of the Falkland Islands (Figure 21).

The progression of high and low recruitment cohorts with increasing age showed a number of consistent down-slope migratory pathways into deeper waters. The largest of these consisted of newly recruited Patagonian toothfish from the west and northwestern inshore nursery areas migrating down the slope across the wide southwestern shelf to enter their adult areas at the western extent of the Falklands Trough. Patagonian toothfish from the northern and northeastern nursery areas undertook either an eastern or northern pathway on either side of the wider shelf extension to the northeast of the Falkland Islands. During years of high recruitment, newly recruited fish to the southern nursery areas appeared to either link up with

the ontogenetic migration pathway to the southwest, or to migrate in a more southerly direction directly into the Falklands Trough to the west of Beauchene Island.

Table 6: Comparison of best-fitting models based on the deviance information criterion (DIC) and Watanabe Akaike's information criterion (WAIC) scores and the associated dispersion parameter estimates. Best-fit models are depicted in grey squares and in bold.

Model	Distribution	Level of persistence	Structure	DIC	WAIC	Dispersion
Full (age)	ZIP	Combined	Persistent	2873.21	3782.61	1.87
		Age	Opportunistic	240.89	330.88	1.2
		Age	Progressive	0.00	0.00	1.19
Age-0	ZINB	Combined	Persistent	28.98	48.88	2.06
		Year	Opportunistic	0.00	0.00	1.55
		Year	Progressive	3.31	7.13	1.6
Age-1	ZIP	Combined	Persistent	704.71	1,360.77	1.29
		Year	Opportunistic	12.04	19.20	0.87
		Year	Progressive	0.00	0.00	0.87
Age-2	ZIP	Combined	Persistent	791.23	1,104.97	1.4
		Year	Opportunistic	208.99	262.01	0.85
		Year	Progressive	0.00	0.00	1.27
Age-3	ZIP	Combined	Persistent	0.00	0.00	1.49
		Year	Opportunistic	232.94	214.62	0.94
		Year	Progressive	212.13	184.80	0.89

Table 7: Posterior means, standard deviations and 95% credible intervals for the spatial-temporal random field estimated in the best fit age-based and full models.

Model	Parameter	Mean	SD	2.5% quant.	97.5% quant
Age-0	Pi	0.72	0.03	0.65	0.77
	Range	30.71	7.64	16.61	45.95
	s.d	0.88	0.08	0.70	1.01
Age-1	Pi	0.48	0.03	0.42	0.52
	Range	44.82	6.10	32.47	55.95
	s.d	1.00	0.05	0.90	1.09
	Temp	0.34	0.06	0.23	0.47
Age-2	Pi	0.40	0.01	0.37	0.42
	Range	35.51	3.28	30.44	43.21
	s.d	0.69	0.03	0.65	0.76
	Temp	0.45	0.07	0.33	0.60
Age-3	Pi	0.21	0.00	0.20	0.22
	Range	37.26	2.48	33.92	43.24
	s.d	1.10	0.11	0.90	1.30
Full (age)	Pi	0.62	0.01	0.60	0.64
	Range	20.86	1.47	18.06	23.86
	s.d	1.03	0.03	0.97	1.10
	Temp	0.27	0.05	0.15	0.37

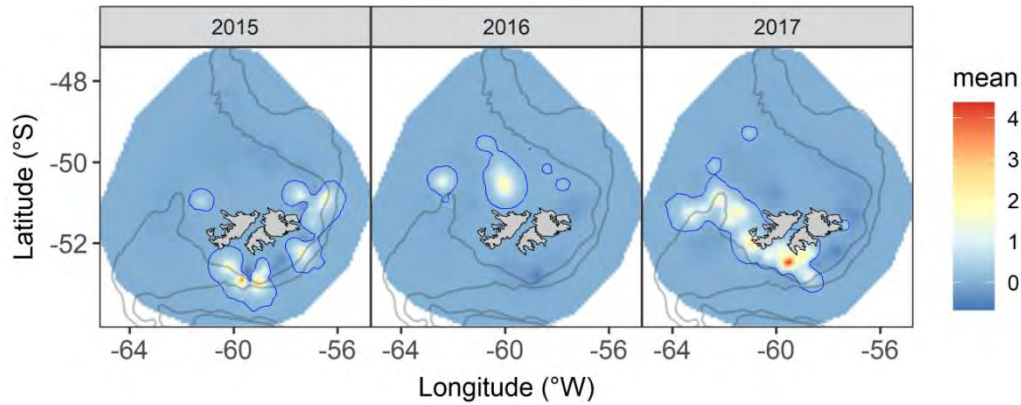


Figure 18: Posterior mean values for the spatial random field for the age-0 model with opportunistic spatial temporal correlation for each year. Hotspots, identified as areas with abundances above the 90th percentile are circled with the blue contour line. Grey contour lines indicate the 200 m and 500 m depth contours.

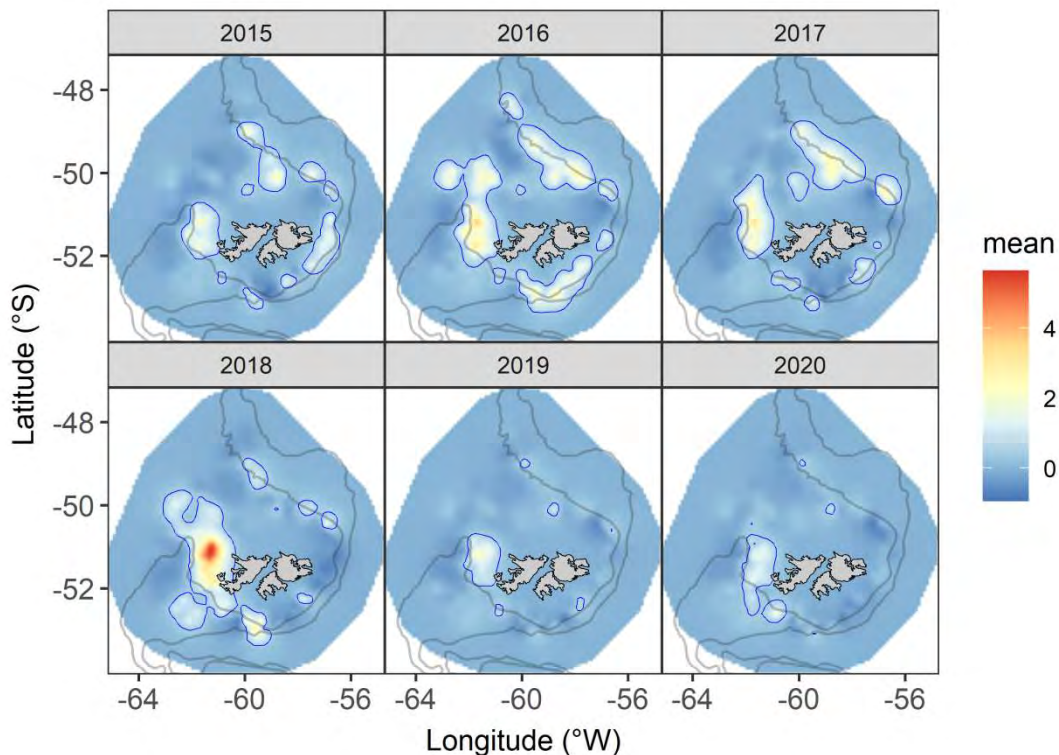


Figure 19: Posterior mean values for the spatial random field for the age-1 model with progressive spatial temporal correlation for each year. Hotspots, identified as areas with abundances above the 90th percentile are circled with the blue contour line. Grey contour lines indicate the 200 m and 500 m depth contours.

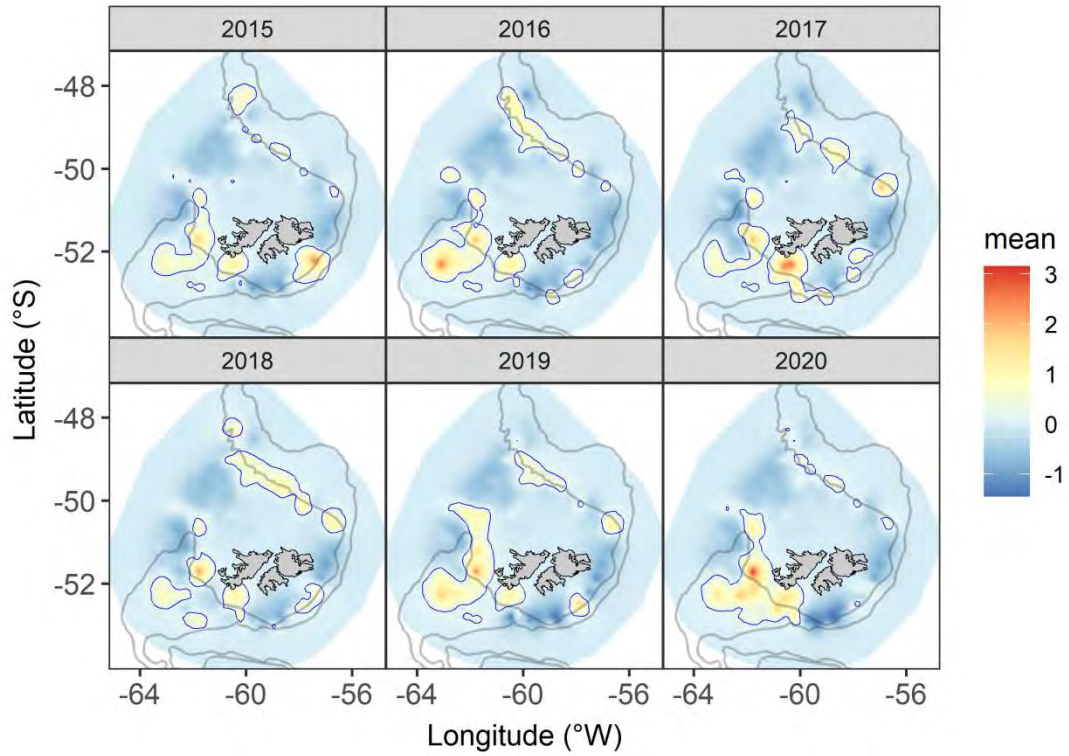


Figure 20: Posterior mean values for the spatial random field for the age-2 model with progressive spatial temporal correlation for each year. Hotspots, identified as areas with abundances above the 90th percentile are circled with the blue contour line. Grey contour lines indicate the 200 m and 500 m depth contours.

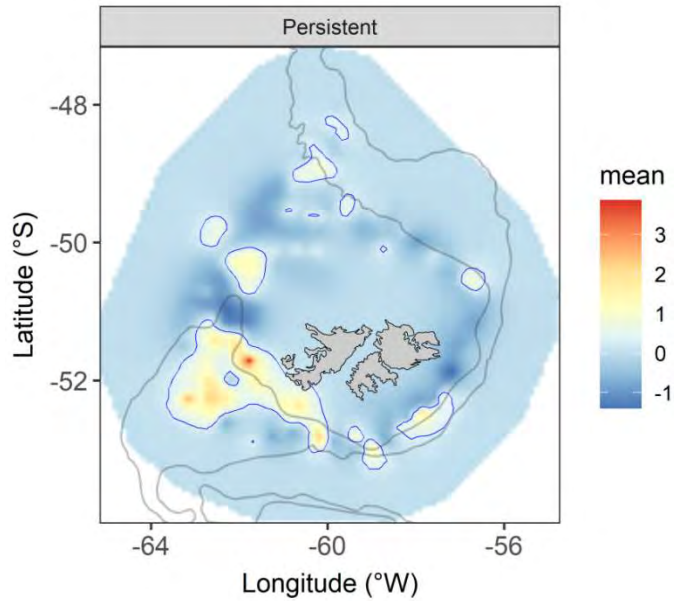


Figure 21: Posterior mean values for the spatial random field for the age-3 model with a persistent spatial temporal correlation for each year. Hotspots, identified as areas with abundances above the 90th percentile are circled with the blue contour line. Grey contour lines indicate the 200 m and 500 m depth contours.

3.3.4. *Habitat description*

Functional response curves for oxygen from all five models indicated a distinct range preference of moderate to high oxygen concentrations for all age-classes (Figure 16). Both the full and age-based BSDM results (Table 8) indicated age-dependent associations of juvenile Patagonian toothfish with environmental (depth, current velocity, and mixed layer thickness) and ecological variables (rock cod and icefish abundance). Response curves for depth showed that younger fish occurred in shallower waters compared to older fish (Figure 16). Age-0 toothfish occurred in the greatest abundance at depths less than 120 m, age-1 fish between 150 and 220 m, with age-2 and age-3 fish occurring at depths greater than 180 m and 200 m respectively. The fit of the depth smoother for age-0 fish also indicated a distinct positive effect at depths between 250 to 300 m. Model results suggest that newly recruited, age-0 toothfish have a habitat preference for slower current velocities and a deeper mixed

layer thickness compared to older fish (Figure 22). Newly recruited Patagonian toothfish occurred in areas with high icefish abundance, a relationship that decreased with increasing age. Rock cod abundance did not influence the abundance of age-0 toothfish, but had a strong influence on the abundance of age-1 toothfish, which steadily decreased with increasing age.

Table 8: Posterior means, standard deviations and 95% credible intervals for the covariates estimated in the best fit age-based models. Credible intervals of parameter estimates that do not overlap zero are depicted in grey squares and in bold.

Model	Parameter	Mean	SD	2.5% quant.	97.5% quant
Age-0	Intercept	0.19	0.11	-0.02	0.40
	mlt	0.14	0.07	0.01	0.28
	vel	-0.05	0.07	-0.18	0.08
	CHE	0.49	0.06	0.38	0.60
Age-1	Intercept	0.00	0.09	-0.19	0.18
	mlt	-0.05	0.05	-0.15	0.05
	CHE	0.11	0.03	0.05	0.17
	PAR	0.43	0.03	0.37	0.50
Age-2	Intercept	-1.47	0.23	-1.94	-1.02
	vel	-0.06	0.07	-0.20	0.07
	CHE	-0.24	0.13	-0.50	0.01
	PAR	0.17	0.05	0.07	0.27
Age-3	Intercept	-3.65	0.35	-4.35	-2.97
	mlt	-0.13	0.08	-0.29	0.03
	vel	-0.19	0.09	-0.36	-0.03
	CHE	-0.71	0.36	-1.48	-0.05

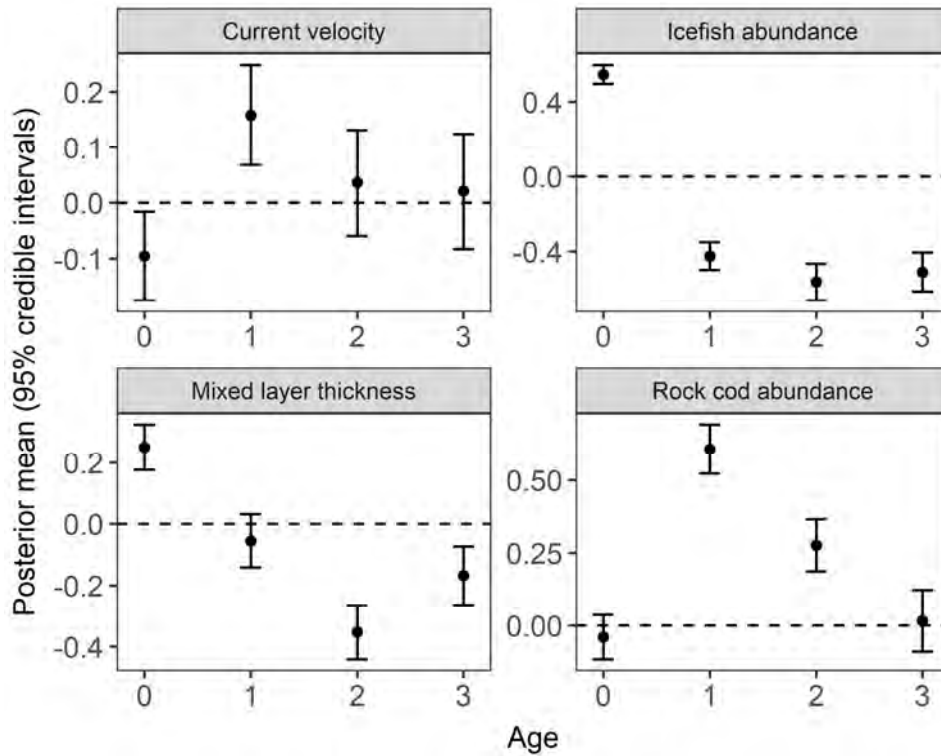


Figure 22: Posterior mean values and the 95% credible intervals of the fixed parameters for the linear abiotic and biotic effects for shelf-based juvenile Patagonian toothfish abundance on the Falkland Islands shelf between 2015 and 2020.

3.4. Discussion

The results of the present study showed that Bayesian species distribution models were appropriate to describe the age-based ontogenetic migrations of Patagonian toothfish on the shelf around the Falkland Islands. Increased current velocity of mesoscale eddies linking the Subantarctic Front from the east of the Burdwood Bank to the Falklands Shelf was identified as a key oceanographic driver of recruitment and juvenile abundance onto the shelf. Spatial-temporal patterns for newly recruited juveniles (age-0+) were characterised as opportunistic (temporally independent), becoming increasingly persistent (stable) with age, following discrete ontogenetic migratory pathways. Juvenile Patagonian toothfish inhabited areas with high oxygen concentrations, with age-specific preferences for environmental (depth, current velocity, mixed layer thickness), and ecological (abundance of competitors and prey) drivers.

The main advantage of using the Bayesian spatial-temporal models is that they account for spatial structure that remains unexplained by the covariates. This is through the use of spatial random field that can be modelled over time, thus capturing the dynamic nature of ecological systems (Soriano-Redondo *et al.* 2019). In the current study, the spatial structure was a proxy for the age-based ontogenetic migratory process, with progressive age-classes remaining adjacent to the opportunistic areas within which large recruitment pulses occurred, even though there were apparently suitable areas elsewhere across the western, southern and northeastern shelf. In ecological terms, the factors affecting the spatial structure are likely to be related to the extent that oceanographic features influence larval dispersal to, and survival within productive upwelling areas that occur around the Falkland Islands (Agnew 2002; Croxall and Wood 2002; Arkhipkin *et al.* 2013). This would explain why the vertically segregated age-structured hotspots aggregate in clusters around these areas, benefiting from the availability of prey to drive their early rapid growth. The increasing temporal autocorrelation obtained in the age-based models, identifies the extent of recruitment variability that occurs in the population, with increasingly stable populations and distinct, predictable ontogenetic migration pathways to the adult population inhabiting the deep-waters of the Patagonian Slope. These results suggest that the abundance and spatial patterns during the early life-history of Patagonian toothfish may have evolved through multiple interactions of environmental, physiological, and ecological processes, resulting in niche expansion and reduction in inter-cohort competition (Polis 1984; Péron *et al.* 2016). It is important to note that due to the complexity of ecological systems, the spatial-temporal autocorrelation structure could also be capturing other aspects that were not included in the study.

3.4.1. Oceanographic drivers

The shelf-based population of Patagonian toothfish was dominated by juveniles of between 0+ and 4 years. The age structure composition was temporally variable, and characterised by large recruitment pulses, such as those that occurred during 2015, 2016 and 2017, largely

supporting the shelf population thereafter. The presence of variable recruitment pulses around the Falkland Islands were reported by Laptikhovsky and Brickle (2005) as occurring every 4-5 years, although the potential oceanographic or other drivers of these were not investigated. Wide fluctuations in year-class strength may be due to the protracted epipelagic egg and larval phase, rendering this species as particularly sensitive to the influence of large, basin-scale oceanographic features (Doyle and Mier 2016). At South Georgia, periods of increased recruitment were strongly related to lower temperatures during the spawning period, which was thought to be driven by large-scale climatic events such as El Niño Southern Oscillation (Belchier and Collins 2008). Off the northern US west coast, recruitment in sablefish (*Anoplopoma fimbria*), a species following a similar life-history strategy to that of Patagonian toothfish, was found to be related to colder conditions during the spawner pre-conditioning period (Tolimieri *et al.* 2018). This result was attributed to stronger upwelling events leading to higher productivity and food availability, and subsequent larval survival. Further, increased cross- and long-shore current systems during the egg and larval periods of development lead to higher recruitment through increased larval retention from their spawning areas (Tolimieri *et al.* 2018). In the current study, high recruitment cohorts were explained through increased current velocities that occurred along the northern shelf edge of the Burdwood Bank. It is within this region that temporally variable mesoscale eddies have been observed linking the north flowing waters of the Subantarctic Front with the Falklands Current oceanographic system to the south of the Falkland Islands (Matano *et al.* 2019). This suggests that the increased influence of cold subantarctic waters over the Falklands Shelf may be leading to (1) increased productivity and food availability for subsequent egg and larval survival, (2) increased egg and larval retention from the spawning areas over the Burdwood Bank, or (3) a complex interaction of these two aspects. Variable levels of egg and larval survival or retention during early life-history stages in particular would play a key role in determining year-class strength, thus defining the abundances and spatial patterns in subsequent age groups.

3.4.2. *Spatial-temporal patterns*

Juvenile Patagonian toothfish spatial patterns differed across their early life-history with high temporal variability at recruitment becoming increasingly persistent with age. Despite this variability four persistent hotspots in abundance could be identified within spatially discrete areas to the northeast, northwest, south and southwest of the Falkland Islands. These were consistent with previously described quasi-stationary mesoscale frontal zones that occur through the upwelling of subantarctic waters onto the shelf (Arkhipkin *et al.* 2013). Cold subantarctic waters being forced up onto the shelf create areas of high productivity along the inshore shelf-break in waters <200 m deep. This supports persistent and predictable macrozooplankton densities, such as euphausiids (*Euphausia lucens* and *E. vallentini*), amphipods (*Themisto gaudichaudii*) and decapods (*Munida gregaria*), providing preferential habitat and feeding conditions, particularly for newly recruited fish and squid (Agnew 2002; Croxall and Wood 2002). It is also within the deeper waters surrounding these areas that larger demersal predators congregate (Agnew 2002). These patterns were consistent for the interpretation of juvenile Patagonian toothfish spatial structure around the Falkland Islands. Newly recruited Patagonian toothfish (age-0) inhabited the shallow inshore areas of these upwelling's where they likely competed with other small predators (eg. icefish) to feed on the abundant prey, such as post-larval rock cod. Progressive age-components of the stock appeared to remain in discrete spatial groups adjacent to these upwelling areas. The spatial patterns between increasing age components reflected their increasing movement into deeper waters from their original respective nursery areas. These results suggest a lack of large-scale connectivity between inshore populations after settlement onto the shelf, although this may require further investigation.

The primary differences observed in the spatial patterns among lower recruitment cohorts (i.e. 2018-2020) across all age components included (1) a contraction of the distribution range, (2) the stronger fragmentation of areas of abundance, and (3) the absence of noticeable

abundance hotspots to the south and east of the Falkland Islands. Range contraction and fragmentation has been associated with decreases in abundance due to species concentrating in their preferred habitat as density dependent effects decline (Nye *et al.* 2009; Pennino *et al.* 2019). The increased influence of productive subantarctic waters on these frontal zones may therefore be leading to increased larval survival, particularly in the southern and eastern shelf where this influence is likely to be most pronounced.

3.4.3. Fish relationship with habitat

Age-classes were vertically segregated on the shelf with newly recruited toothfish occurring in the shallowest depths, and older fish being found at increasingly greater depths. Downslope ontogenetic migratory behaviour has been described for Patagonian toothfish across their geographical range including South Georgia (Belchier and Collins 2008), the Kerguelen Plateau (Péron *et al.* 2016) and around the Falkland Islands (Arkhipkin and Laptikhovsky 2010). Around the Kerguelen Plateau, juvenile Patagonian toothfish of <60 cm occurred along the extended shelf and bank areas moving progressively downwards to 600 m as they grow (Péron *et al.* 2016). Depth is an important physiological limitation that influences the distribution of fish and acts as a proxy because of its close relationship with other environmental variables (eg. temperature, oxygen and salinity) and biological factors (eg. food availability, predation and competition; Parra *et al.*, 2017). The shelf-based habitat of juvenile Patagonian toothfish (age up to 4 years, 60-70 cm) around the Falkland Islands was described as a major feeding ground prior to their ontogenetic migration into deeper waters of the continental slope and abyssal plains (Croxall and Wood 2002; Arkhipkin and Laptikhovsky 2010). The highly productive shelf-based waters are thought to provide optimal feeding conditions, along with the warmer water temperatures supporting rapid growth (Agnew 2002; Arkhipkin and Laptikhovsky 2010). In the current study, available predictors such as bottom temperature and salinity were excluded during data exploration and model backwards selection due to correlation with depth. Environmental variables were derived from global data

sets that likely do not reflect higher spatial and temporal resolution compared to data obtained from field observations such as depth (Parra *et al.* 2017).

Juvenile Patagonian toothfish occurred in a relatively narrow range of moderate to high dissolved oxygen throughout their shelf-based life-history. The Falklands Current and Subantarctic Front carries oxygen rich waters across the western, southern and eastern shelf adjacent to and offshore of the 200 m depth contour (Arkhipkin *et al.* 2019). These areas are consistent with the persistent abundance of post-recruitment (ages-1 to 3) Patagonian toothfish particularly during strong year-classes driven by the increased influence of the SAF:FC, but also during low year-class cohorts although restricted largely to the west and southwestern shelf. In contrast, the confluence of the comparatively warmer waters of the southwards flowing Argentine Shelf Drift derived from the Brazil Current lead to low oxygen levels in the shallower (<200 m) waters to the north and northwest of the Falkland Islands. It is within this variable region of influence that little to no Patagonian toothfish occurred throughout their shelf-based life-history. Research has indicated that Patagonian toothfish have a very low oxygen affinity comparable to Antarctic and an exception to non-Antarctic notothenioids (Coppola *et al.* 2015). This is thought to have evolved as a result of the lack of hypoxic zones in the cold Antarctic waters, making Patagonian toothfish potentially vulnerable to even mildly low oxygen levels. The association of newly recruited age-0+ Patagonian toothfish with shallow-water inshore habitats closest to the coast potentially make them more vulnerable to the dynamics of the Falklands Current and Subantarctic Front, and the extent that these carry oxygenated waters up onto the inshore shelf. During years of high influence, oxygen levels may be less restricted inshore of the 200 m depth contour providing improved conditions for juvenile survival. Dissolved oxygen has been described as a key variable of importance in defining the abundance and spatial patterns of cape hakes off the west coast of South Africa (Kainge *et al.* 2017; Mbatha *et al.* 2019). Low oxygen levels were shown to have a detrimental effect on inshore recruitment levels, with less severe effects on larger fish living in deeper more oxygen rich waters.

The shallow-water nursery area habitats of age-0 toothfish were also defined by lower current velocities and an increased mixed layer thickness (proxy for productivity) compared to older juvenile fish. Mixing of inshore shelf waters with subantarctic waters at upwelling zones that occur around the Falkland Islands creates a band of increased productivity, reflected in the increased mixed layer of the habitat occupied by the newly recruited toothfish (Arkhipkin *et al.* 2013). Lower current velocities for newly recruited juvenile habitats are also likely linked to their occurrence and abundance inshore of the continental shelf at shallower depths. The predominant current systems around the Falkland Islands dominate the continental shelf-slope interface, only encroaching onto the inshore shelf as comparatively weakened eddy systems with little water movement (Agnew 2002). These current systems would lead to increased current velocities at the depths within which older juvenile toothfish occur.

3.4.4. Ecological interactions

Favourable environmental conditions may also be indirectly reflected in the importance of biotic variables in describing juvenile abundance patterns. Rock cod are the main prey item for juvenile Patagonian toothfish (< 60 cm) at depths less than 500 m (Arkhipkin *et al.* 2003), and have been identified as a wasp-waist species that plays a key role in the trophodynamics within the region (Ricciardelli *et al.* 2020). The absence of rock cod as a variable of importance for age-0 toothfish can be explained through the selectivity of the fishing gear, and their inclusion in the model as biomass (mass, kg) as opposed to numerical abundance. Rock cod sampled within the inshore nursery areas generally consisted of small, newly recruited individuals of between 4 and 7 cm TL. Their numerical abundance in large numbers can be clearly confirmed through their occurrence in the stomach contents of their predators (e.g. toothfish) as well as through secondary catch in association with trawled up benthic invertebrates and kelp (pers. obs.). Despite their numerical abundance, biomass would be low as considered within the BSDMs. Further, due to their small size, newly recruited rock cod, would not be fully selected for by the fishing gear used within the surveys, likely not capturing

the true extent of their importance within these inshore areas. The rapid growth of Patagonian toothfish, and their downslope migration were reflected in the importance of fully selected, larger rock cod in defining post-settlement (age-1 – 2) juvenile toothfish abundance and spatial patterns, highlighting the continued importance of this species within the shelf-based ecosystem as a prey species for higher trophic level species. The importance of rock cod decreased with increasing age, whereby the diet of juvenile toothfish evolved towards larger, less active fishes such as *Antimora rostrata*, near-bottom macrourids and skates, that occur in waters beyond the depth range within which rock cod commonly occur (Arkhipkin *et al.* 2003).

The relevance of icefish as a factor affecting the abundance and spatial distribution of juvenile toothfish within their nursery areas (age-0 fish), reflects strong spatial-temporal overlap during this early life-history stage of development. This result could be argued on the grounds that small rock cod recruits are the main prey item for both species (Arkhipkin *et al.* 2003). This would imply an indirect effect, whereby icefish abundance does not necessarily have a causal relationship in driving abundance of juvenile toothfish in their nursery areas, but simply that both species favour similar environmental settings and prey (Pennino *et al.* 2019). This abundance of newly recruited Patagonian toothfish and icefish are therefore inextricably linked to habitat conditions, and the abundance of their main prey (i.e. rock cod). Rapid growth, larger size and their downslope ontogenetic migration out of the inshore areas occupied by icefish may be a reflection of their changing diet to larger benthic fish and squid species that occur in deeper waters, reflecting a notable population impact of this interaction.

3.4.5. Management implications and conclusions

The results of the current study have further provided some key environmental and ecological predictors that impact on the abundance and spatial patterns for the juvenile component of a dynamic Patagonian toothfish population on the Patagonian Shelf. The predictive ability of

these models will only be strengthened by continuing the fishery independent data collection time series, to further capture the complexity and natural variability within the underlying systems (Ludwig *et al.* 1993).

Variable recruitment as observed in the current study highlights the vulnerability of the species to over-exploitation. These findings suggest an emphasis on management measures that (1) reduce the impact of fishing on age truncation (Barnett *et al.* 2017), and (2) provide protection for high recruitment cohorts through an appropriate spatial management approach. The maintenance of old-growth age structure is recognised as a bet-hedging response to variable environments where larval survival and successful recruitment may be uncommon, an aspect of particular importance for species at the margin of their ranges (Francis *et al.* 2007). Long-lived spawners provide a storage effect whereby a stock will persist as long as enough adults outlive periods unfavourable to successful spawning and recruitment.

These results indicate the importance of further research into the role of regional oceanographic variability in driving primary productivity in key areas around the Falkland Islands, and how these may be influential in driving Patagonian toothfish recruitment. Future research considerations should work towards the development of an improved understanding of how the variability in these systems influence the lower trophic levels, and how this may impact the survival of juvenile fish species within these highly productive upwelling areas. Further, research objectives should be aimed at the identification of the extent of any potential adult migratory behaviour from non-spawning to spawning areas amongst the adult component of the population, as well as the extent of connectivity within discrete spatial groups in the shelf-based population as defined in the current study.

3.5. Supplementary information

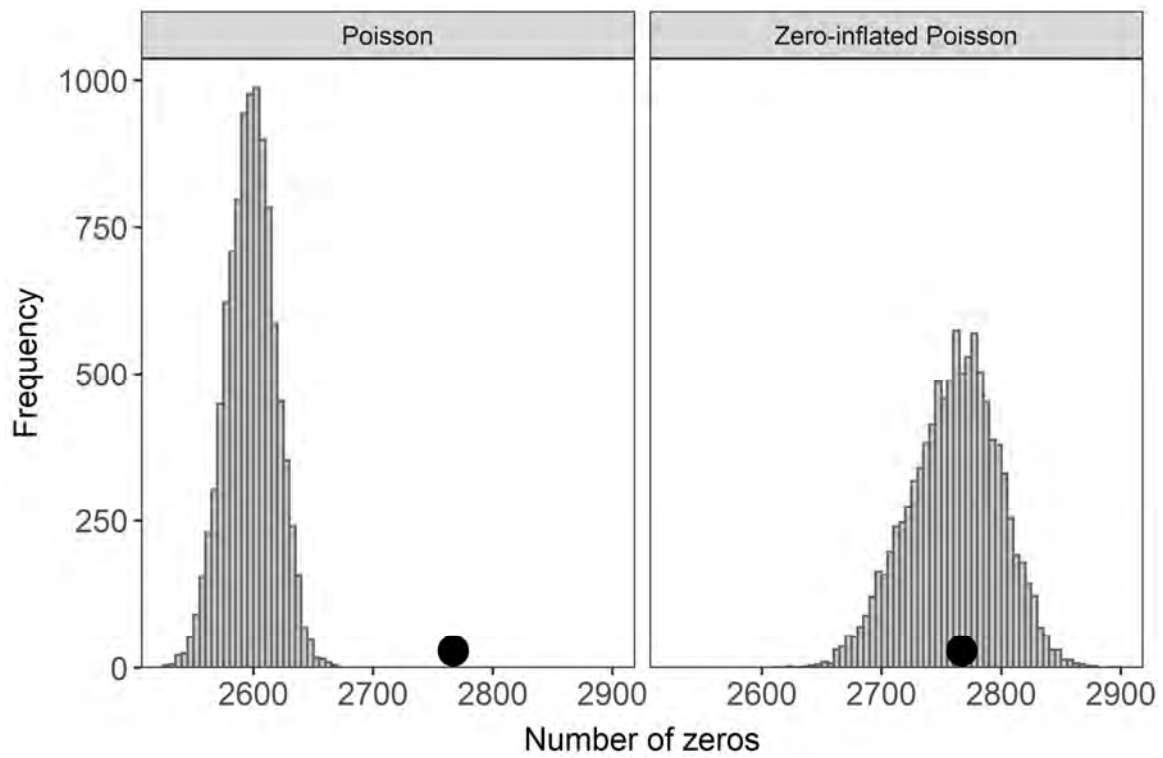


Figure 23: Simulation study showing the observed number of zeros (black dot) and the simulated number of zeros in 10,000 data sets that were fitted from the full BSDMs fitted with the Poisson and zero-inflated Poisson distributions with progressive spatial-temporal correlation for age.

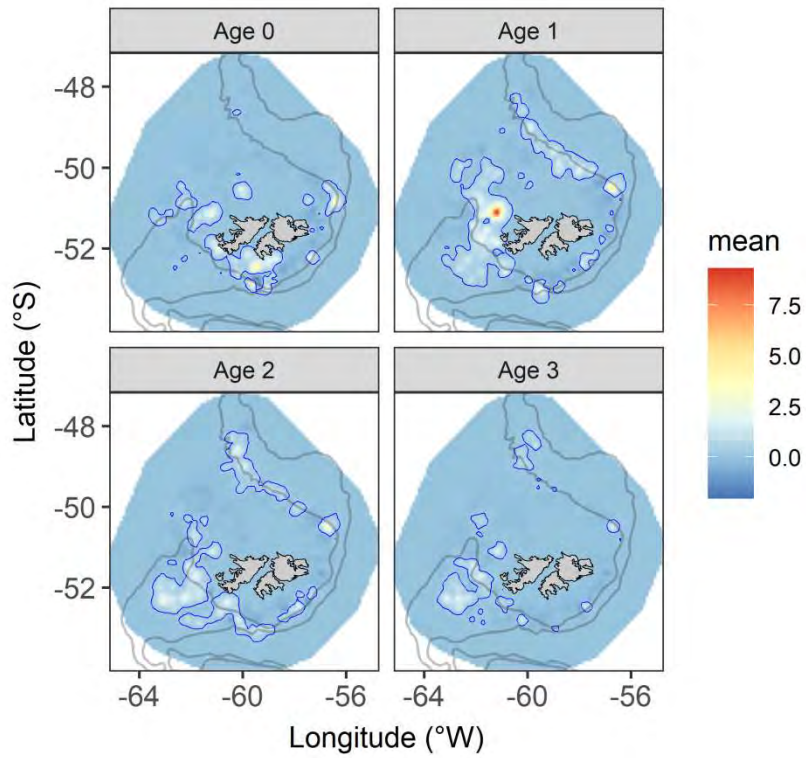


Figure 24: Posterior mean values for the spatial random field for the full model with progressive spatial temporal correlation for age. Hotspots, identified as areas with abundances above the 90th percentile are circled with the blue contour line. Grey contour lines indicate the 200 m and 500 m depth contours.

Table 9: Summary of the explanatory variables obtained from research survey programmes and Copernicus Marine Environment Monitoring Service (CMEMS).

Variable	Variable name	Units	Average	Min	Max	Spatial resolution	Temporal resolution
SA	Swept area	m ²	536,834	18,228	2,000,538	Trawl Station	Daily
SBT	Sea bottom temperature	°C	5.64	3.74	10.02	0.02 x 0.02	10 day mean
SBV	Current velocity	m.sec ⁻¹	0.041	0.00076	0.21	0.02 x 0.02	10 day mean
MLT	Mixed layer thickness	m	15.69	10.52	36.95	0.02 x 0.02	10 day mean
DO	Oxygen Concentration	mmol m ⁻³	284.84	265.69	299.33	0.25 x 0.25	Monthly mean
Depth	Depth	m	171.91	52.00	398.00	Trawl mid-point	Daily
SAF-FC	Subantarctic Front-Falkland Current interface velocity	m.sec ⁻¹	0.43	0.24	0.53	18,481.5 km ²	Dispersal period (August-September)
FC	Falkland Current velocity	m.sec ⁻¹	0.16	0.14	0.19	24,642 km ²	Dispersal period (August-September)
PC	Patagonian Current velocity	m.sec ⁻¹	0.10	0.091	0.12	18,481.5 km ²	Dispersal period (August-September)
PAR	Rock cod abundance	cpue sqrt(kg.m ⁻²)	0.00082	0	0.033	Trawl station	Daily
CHE	Icefish abundance	cpue sqrt(kg.m ⁻²)	2.17x10 ⁻⁵	0	0.0014	Trawl station	Daily

Chapter 4 - Deep-sea movement patterns of the Patagonian toothfish *Dissostichus eleginoides* Smitt, 1898, in the Southwest Atlantic

Abstract

Knowledge on movement patterns within marine fish populations are essential for understanding key aspects of biology, distribution and population connectivity. Many deep-sea fish species possess complex life-history patterns with distributions occurring across vast areas. The nature of connectivity at different life-history stages in a dynamic Patagonian toothfish population on the Patagonian Shelf, Slope and deep-sea plateau around the Falkland Islands remains speculative. The aim of the current study was to elucidate the movement patterns as well as the extent that these are driving connectivity during the adult life-history stages of Patagonian toothfish in the region. A six-year tag-recapture program was executed and data were analysed using generalised additive models. Tagging and recapture results indicated that the majority of individuals (78%) displayed high site fidelity (<50 km). However, 10% of individuals undertook large-distance movements across oceanographic and physical boundaries. These were characterised by large (>120 cm) fish inhabiting the slope and deep-sea plains (north of 52°S) undertaking southward (direction = 150 - 240°) home-range relocations to spawning areas on the Burdwood Bank, North Scotia Ridge and southern Chile. The results suggest a metapopulation structure with low frequency of seasonal spawning, with important considerations in terms of the spawning stock dynamics, and the development of regional management agreements across their Patagonian distribution.

4.1. Introduction

Movement is a key component of animal ecology, defining the spatial and temporal scale of biotic interactions, response to the environment, and anthropogenic pressures experienced by individuals, groups and populations (Nathan *et al.* 2008). Many marine fish species possess complex life cycles where the scale and pattern of movement varies across and within life-history stages (Allen *et al.* 2018). These include the passive dispersal of eggs and larvae, ontogenetic habitat relocations, daily foraging activities, seasonal (predictable) migrations, and erratic nomadic movements (Shaw 2020). The patterns and drivers of these movements are essential for understanding key aspects of biology, distribution and population structure in the presence of environmental change; thus, informing the development of management and conservation strategies.

Deep-sea, apex predators in particular, frequently exhibit such complex life-histories, which combined with slow growth, long life and low natural mortality, make them potentially vulnerable to over-exploitation if not carefully managed (Koslow *et al.* 2000; Stevens *et al.* 2000; Roberts 2002; Devine *et al.* 2006; Drazen and Haedrich 2012). This can be further exacerbated when the movement of animals occurs across political boundaries, requiring an accurate description of transboundary and shifting spatial use to inform multilateral management through international or regional cooperation (Howey *et al.* 2017). Despite this, and while technological developments are providing ground-breaking insights, little is known about the movement patterns in many deep-sea fish species (Hussey *et al.* 2018).

Approaches to studying movement and connectivity patterns in deep-sea marine fish populations include the use conventional and electronic tagging experiments (Edwards *et al.* 2019), genetic techniques (Canales-Aguirre *et al.* 2018), oceanic circulation modelling (Ashford *et al.* 2012a; Mori *et al.* 2016), analyses of life-history and catch data from surveys (Parker *et al.* 2019; Lee *et al.* 2021), and the chemistry (Ashford *et al.* 2012b) and

morphometrics (Lee *et al.* 2018) of fish otoliths. The utilisation of conventional tags continues to be an important and cost-effective method for assessing the effective boundaries of populations for fisheries management purposes around the world (Hall 2014; Bartes *et al.* 2021). In particular, the implementation of tag-recapture programmes have been used to study the movement behaviour in several deep-sea, long-lived fish species including sablefish *Anoplopoma fimbria* in the Northeast Pacific (Kimura *et al.* 1998; Maloney and Sigler 2008), Antarctic toothfish *Dissostichus mawsoni* in the Ross and Amundsen Seas (Petrov and Tatarskiy 2010; Hanchet *et al.* 2015) and Patagonian toothfish *D. eleginoides* off South Georgia (Marlow *et al.* 2003; Agnew *et al.* 2006; Collins *et al.* 2010) and the Kerguelen Plateau (Williams *et al.* 2002). Conventional tags have several limitations (Hall 2014), including a reliance on the reporting of accurate data by individuals, often without scientific training in data collection protocols. Further, recaptured fish provide only the start and end point of the movement, with no knowledge of the pathway and extent of movement in between these points. Nonetheless, while the ability of a species to survive the tagging procedure should be carefully considered, the use of conventional tags is far less invasive compared to satellite tags, they are not limited by battery power to a finite life-span, and can therefore be used across life-history stages and on a wide temporal scale. These data can provide extremely useful information on individuals and support inferences about the contributions of adult movements to lifetime paths within populations (Allen *et al.* 2018).

Patagonian toothfish is a large (up to 230 cm and 200 kg), long-lived (over 50 years), benthopelagic predator of the family Nototheniidae (Eastman 1993; Collins *et al.* 2010). It is distributed across underwater plateaus, seamounts, and islands of the Southern Ocean, extending north around the southern continental shelf and slope of South America (Collins *et al.* 2010). The species supports important commercial fisheries across its range (Tuck *et al.* 2003; Payne *et al.* 2005; Laptikhovskiy and Brickley 2005; Moreno *et al.* 2006; Grilly *et al.* 2015). Patagonian toothfish exhibits changes in spatial distribution through wide-ranging and complex movement patterns across their life-history (Arkhipkin and Laptikhovskiy 2010; Péron

et al. 2016). However, many aspects related to their ecology, such as connectivity, reproductive behaviour and habitat-use remain poorly understood (Péron *et al.* 2016).

Genetic homogeneity for Patagonian toothfish across the Patagonian Shelf suggests connectivity within the region, although the extent that this occurs through egg and larval dispersal, ontogenetic migrations or the active movement of adults remains unclear (Appleyard *et al.* 2002; Shaw *et al.* 2004; Rogers *et al.* 2006; Canales-Aguirre *et al.* 2018). Further, genetic markers vary greatly in their ability to resolve the extent of population level mixing (Beebee and Rowe 2008), particularly for long-lived species such as Patagonian toothfish. Spawning of Patagonian toothfish occurs between June and August from the southern region of Chile, over the Burdwood Bank and North Scotia Ridge to the south of the Falkland Islands (Laptikhovsky *et al.* 2006a; Arana 2009). The egg and larval periods are protracted (Evseenko *et al.* 1995; North 2002; Mujica *et al.* 2016) providing opportunities for extensive dispersal across the region through the prevailing current systems (Ashford *et al.* 2012b; Ramesh *et al.* 2019; Álvarez-Noriega *et al.* 2020). Juvenile recruitment occurs on the inshore Patagonian shelf waters, including in hotspots associated with productive upwelling around the Falkland Islands (Agnew 2002; Croxall and Wood 2002; Arkhipkin *et al.* 2013). Juvenile fish then undertake an extended (3-6 year) down-slope ontogenetic migration into their deep-sea (800 to 2500 m) adult habitat (Arkhipkin and Laptikhovsky 2010; Lee *et al.* 2021). These migrations are thought to occur along distinct pathways adjacent to their respective juvenile recruitment hotspots (Lee *et al.* 2021).

Previous studies have suggested annual spawning migrations from deep-sea foraging habitats to the spawning areas on the Burdwood Bank (Laptikhovsky *et al.* 2006a). In contrast, reproductive studies within the region have suggested that large proportions of the population may skip spawning, making it uncertain as to whether the slope-based component of the population contribute to the spawning stock at all (Ashford *et al.* 2012b; Boucher 2018). Through the use of pop-up satellite archival tags, Brown *et al.* (2013a) revealed strong site

fidelity combined with seasonal bathymetric movements, foraging behaviour, and spawning activities, although sampled specimens were limited to large adult individuals (>127 cm) over a short to medium time period (<180 days).

Effective management and conservation of fish species requires knowledge of movement patterns driving connectivity across life-history stages. Using the results of a 6-year tag-recapture program, the current study aimed to investigate the movement patterns of Patagonian toothfish, with particular attention to potential connectivity between foraging areas along the slope and deep-sea habitats to the east and north of the Falkland Islands, and the southern spawning areas.

4.2. Materials and methods

4.2.1. Study area

The study area was located across the Patagonian Shelf edge (150 – 400 m; 214, 887 km²), Slope and deep-sea plains (400 to 2500 m; 459, 410 km²) in the southwestern Atlantic and south-eastern Pacific (Figure 25). The study area was divided into five broad regions based on the occurrence of key life-history events, and prominent geographic or oceanographic features forming barriers to active migrations of adult fish. These included the three known regional spawning areas for Patagonian toothfish that supply juvenile recruits around the Falkland Islands, specifically: (1) the narrow continental slope of southern Chile; (2) the Burdwood Bank, a shallow (~200 m depth) underwater plateau isolated from the South American continental shelf by a narrow (90 km; 450 m deep) passage to the west, and from the Falkland Islands to the north by the Falklands Trough (>2000 m deep); and (3) the North Scotia Ridge, which lies to the east of the Burdwood Bank from which it is separated by the Subantarctic Front and a deep (2000 m) trough. The Falklands Slope represents the immediate continental slope and deep-sea plains extending around the Falkland Islands and

was sub-divided into: (4) the eastern and southern portion where it constricts and deepens into the Falklands Trough; and (5) the northern extent, as it constricts and bends to the west.

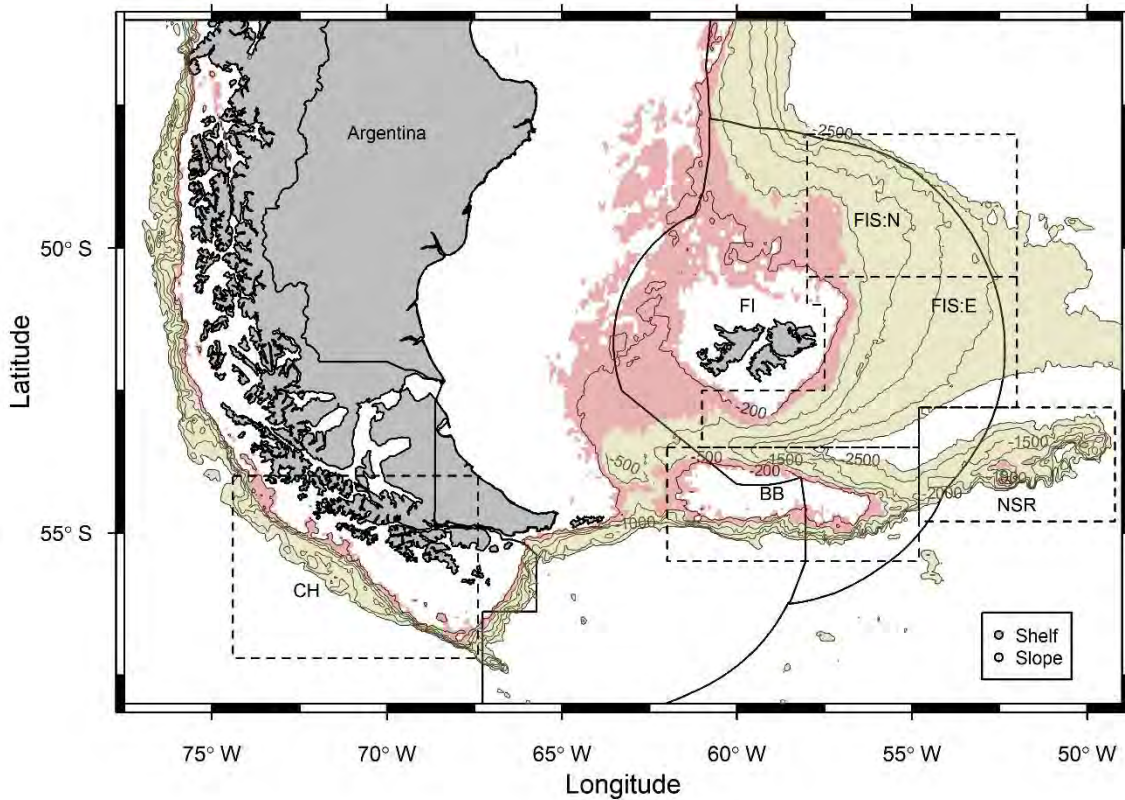


Figure 25: Map depicting the bathymetric areas occupied by juvenile (Shelf, 150 – 450 m) and adult (Slope, 451 – 2500 m) Patagonian toothfish across the study area. Five geographic regions were defined: BB = Burdwood Bank, CH = southern Chile, NSR = North Scotia Ridge, FIS: E = Eastern Falkland Islands Slope and FIS: N = Northern Falkland Islands Slope. The Falkland Islands Conservation Zones and Argentinian EEZ are reflected by solid lines.

4.2.2. Fish tagging and recapture

The tag-recapture programme was developed and implemented as a collaborative project between scientists from the Falkland Islands Fisheries Department (FIFD) and industry (Consolidated Fisheries Ltd, CFL), which operates a single commercial long-liner using an

'umbrella' system at depths greater than 600 m (Brown *et al.* 2010). The 'umbrella' system was developed to reduce the loss of hooked toothfish to depredation by cetaceans, with hooks set in clusters and an umbrella of buoyant netting set above each cluster. The umbrella floats above the hooks whilst the gear is on the seabed, but when the gear is recovered, it folds over the hooks and hooked fish, protecting it from depredation. All Patagonian toothfish were tagged within the Falkland Islands Conservation Zones (FCZ) on the Burdwood Bank and the Patagonian Slope (regions 2, 4 and 5). Tagging was undertaken by scientific staff during pulsed-tagging research surveys and commercial fishing operations between June 2016 and October 2021 (Figure 26). The specific objective of pulsed-tagging surveys was to tag large numbers of toothfish across the study area during a limited time period. Five pulsed-tagging research surveys took place during which between 407 and 1161 toothfish were tagged from stratified locations covering the study area, over an 11 to 23 day time period (Randhawa and Lee 2016; Randhawa *et al.* 2017; Farrugia and Keningale 2018; Farrugia *et al.* 2018; Skeljo and Pearman 2021). In addition to the pulsed-tagging trips, FIFD Fisheries Observers tagged a maximum of 25 toothfish per week during commercial fishing activities.

During tagging activities, all specimens were handled rapidly, and with extreme care to avoid additional stress (see supplementary information; Figure 31). All fish captured were hauled onboard without the assistance of a gaff, the hooks removed and initially assessed for major injury or damage (see supplementary information; Table 12). Once a fish had been identified as suitable for tagging, it was tagged using two (small = 75 mm, large = 80 mm) external spaghetti-dart tags with a plastic head (Floy tag & Manufacturing Inc, USA). All tags were inscribed with a unique numeric code, a postal address and email address for the FIFD. A sharp, disinfected, hollow applicator was used to insert the two tags into the dorsal musculature below and on either side of the posterior dorsal fin spines, ensuring that the barb of the tag was locked behind a pterygiophore. Fish were transported on purpose-made PVC stretchers to the release site on the hauling bay, released headfirst into the water and observed so that the likely fate could be recorded: Likely survival – swimming in downward

motion; Unclear – floating but with swimming motion; Likely mortality – floating, no apparent movement.

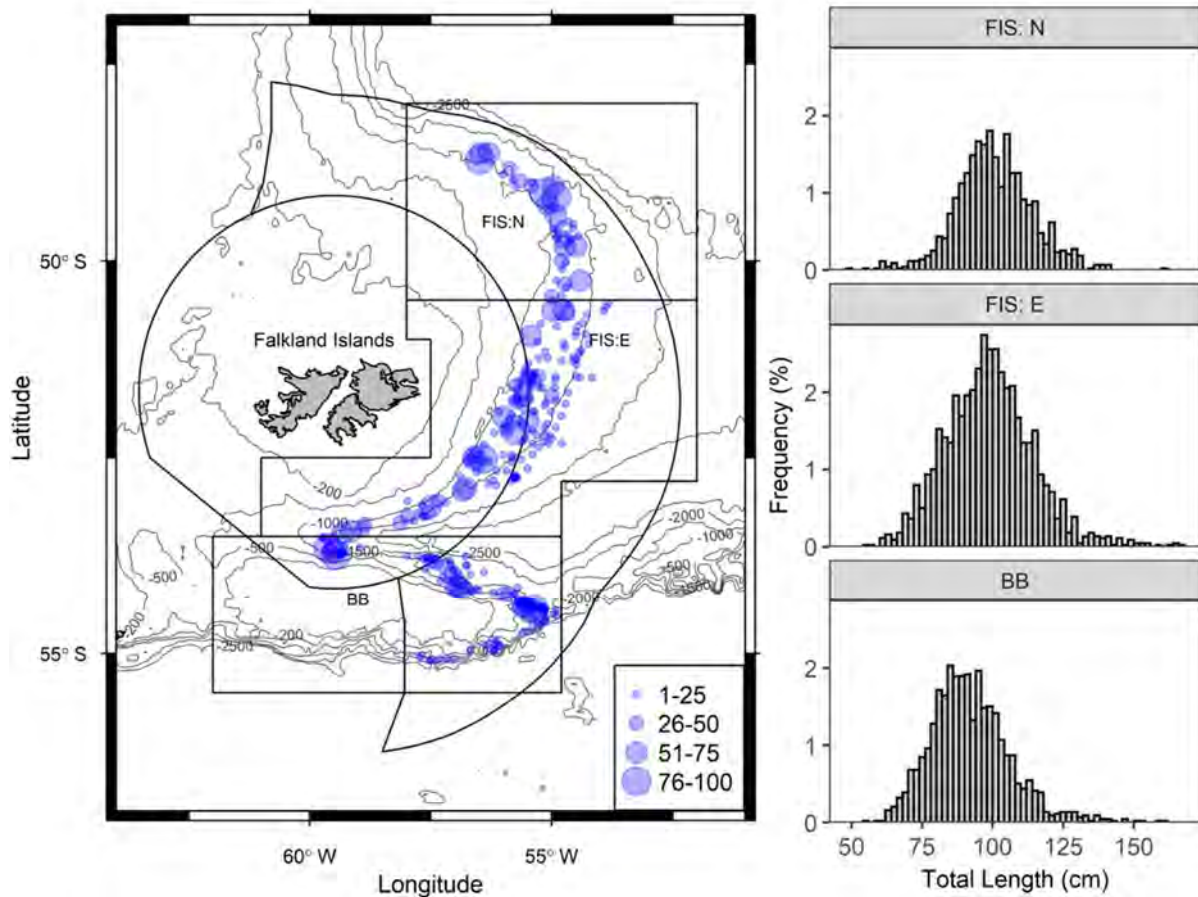


Figure 26: Geographic distributions of tagged Patagonian toothfish and the associated length frequency distributions within the three regions ($n=4418$). Solid lines depict the Falkland Islands Conservation Zones (FCZ). The three geographic regions that occur within the Falkland Islands waters are: BB = Burdwood Bank ($n = 1381$), FIS: E = Eastern Falkland Islands Slope ($n = 1945$) and FIS: N = Northern Falkland Islands Slope ($n = 1092$).

For the recaptures of tagged fish within the FCZ, we relied primarily on commercial fishing operations, with data being collected either by fishers or FIFD fisheries observers (49.84% FIFD fisheries observer coverage of the fishery during the study period). As a component of the science-industry collaborative research surveys, fishers were provided with training for the accurate collection of data from recaptured fish. Comprehensive data associated with all

sampling (tagging and recapture) stations were collected, including date of capture, geographic location (Latitude, Longitude), and depth (m). All specimens were measured to the nearest lower cm (total length TL) and weighed (g). Recaptured individuals were assessed macroscopically for sex and maturity, and the otoliths extracted, cleaned and stored dry in paper envelopes. Additional information recorded for recaptured individuals included any damage or infection at the tagging site, as well as the pre-anal fin length (PAL). On five occasions the tail of the recaptured individual had already been cut during factory processing prior to the tag being noticed. During these occasions, the TL of the fish was estimated using the linear PAL-TL relationship estimated using the total recaptured fish sample.

Extensive fishing effort for Patagonian toothfish also occurs in the national waters of Chile and Argentina and on the high seas to the east and north of the FCZ (for example by the Korean longliner fleet; Park *et al.*, 2021). For the recaptures outside of the FCZ we relied on the reporting by fishing fleets operating in these regions, specifically through collaborative work with Chile and the High Seas Korean fleet.

4.2.3. Data analysis

All data manipulations and analyses were undertaken using R software (R Core Team 2021). The distance moved and potential migration route for individually tagged and recaptured fish were calculated based on a least-cost path calculation using the 'marmap' package version 1.0.5 (Pante and Simon-Bouhet 2013). A constrained least-cost path involves identifying the shortest distance in which a Patagonian toothfish could have moved according to specified depth constraints. Potential movement patterns (distance and path) were constrained according to the bathymetric preferences of adult Patagonian toothfish based on their known depth distribution. Based on their size, all fish were considered adults. While adult Patagonian toothfish occur in deeper waters (>800 m) of the Patagonian Slope, they are also infrequently recorded on the edge of the slope at shallower depths between 500 and 800 m. In the current

study, least-cost movement of fish was constrained between depths of 450 and 2500 m. These depths reflect the minimum (469 m) and maximum (2364 m) depth ranges observed for tagged and recaptured fish throughout the study period.

Eight covariates were considered that may help explain the movement patterns of adult Patagonian toothfish. These included the average length of the fish ($\text{Length} = (\text{TL}_{\text{tagged}} + \text{TL}_{\text{recapture}}) / 2$; cm), the time spent at liberty ($\Delta\text{Liberty}$; days), the direction of movement from 0 to 360° between tagging and recapture (Direction ; degrees), the difference in depth at the recapture and tagging locations ($\Delta\text{Depth} = D_{\text{recapture}} - D_{\text{tagging}}$; m), the sex of the fish (sex ; Male, Female), the month of recapture (Month), the tagging area (Lon , Lat) and the relative condition factor of the fish at tagging ($C_i = W_i / \widehat{W}_i$; where W_i is the recorded weight of the fish i and \widehat{W}_i is the predicted mean weight of the fish i given its observed length for the population under investigation (Blackwell *et al.* 2000; Ogle 2016)). The covariates were explored for outliers, and the presence of collinearity using Pearson correlation coefficients (<0.5) and variance inflation factors (<3 ; VIF) according to the protocols described by (Zuur *et al.* 2010).

Generalised additive models (GAM) were applied to the movement data to estimate and predict the distances moved by Patagonian toothfish with respect to the covariates. GAMs are non-parametric or semi-parametric generalizations of multiple linear regressions. GAMs have the advantage of being able to model non-linearity in the relationship between the response and predictor variables by using non-parametric smoothing functions. One common choice is the so called ‘smoothing splines’, which are splines with knots at each distinct value of the variable. Statistical modelling was performed in the R package ‘mgcv’ version 1.8-34 (Wood 2017). The log-normal and gamma distribution with a log link function were both explored, as the response variable was both continuous and strictly positive. The gamma distribution was however dismissed due to evidence of patterns in the residuals indicating minor heterogeneity, as based on model validation procedures described below. The movement distance for each recaptured fish i was related to the covariates, according to the full model of the form:

$$\log(\text{Distance}_i) \sim \beta_0 + s(\text{Length}_i) + s(\Delta\text{Depth}_i) + cc(\text{Direction}_i) + te(\text{Lon}_i, \text{Lat}_i) + \Delta\text{Liberty}_i + \text{Sex}_i + \text{Month}_i + \text{Condition}_i + \varepsilon_i$$

$$\log(\varepsilon) \sim N(0, \sigma^2)$$

where β_0 is the intercept, s represents the thin plate regression spline smoothers, cc represents the cyclic cubic regression spline smoother used for direction (penalised cubic regression splines using knots for binding minimum and maximum values together), and te represents tensor product smooth between latitude and longitude at the tagging location. The degree of smoothness of the splines were estimated by generalised cross-validation (GCV).

Starting from the full model that contained all covariates, the most parsimonious model was selected using step-wise backwards selection on the basis of the lowest Akaike Information Criterion, adjusted for small sample sizes (AICc; Burnham and Anderson, 2002). The final model was validated by extracting the residuals and visually inspecting these for normality (histograms and Q-Q plots), homogeneity (residuals vs fitted values), independence (residuals vs each covariate), and influential observations (Zuur, 2016).

4.3. Results

4.3.1. Tags and recaptures

A total of 4418 Patagonian toothfish individuals were tagged and released between June 2016 and October 2021 (Table 10). Tagging effort was evenly distributed across the study area (Figure 26A). The greatest quantity of fish ($n = 1945$, 44%) were tagged in the largest region, the eastern slope, at depths ranging from 737 to 1764 m. A further 1381 (31%) Patagonian toothfish were tagged within the spawning region over the Burdwood Bank at depths from 804 to 2100 m, while 1092 (25%) individuals were tagged between 946 and 1426 m depths to the northeast of the Falkland Islands. The length frequency distributions of tagged fish were similar

throughout the three areas (Figure 26B). Fish tagged along the eastern slope had a mean length of 98 cm (s.d. = 16 cm), compared to 100 cm (s.d. = 13) further north. Fish tagged on the Burdwood Bank were slightly smaller overall with a mean length of 91 cm (s.d. = 15 cm).

Table 10: Numbers of toothfish tagged and released within each area according to year. Three geographic regions were defined during tagging: BB = Burdwood Bank, FIS: E = Eastern Falkland Islands Slope and FIS: N = Northern Falkland Islands Slope.

Year	Numbers tagged			Total
	BB	FIS: E	FIS: N	
2016	66	201	170	437
2017	128	371	186	685
2018	661	810	718	2189
2019	94	33	0	127
2020	122	49	0	171
2021	310	481	18	809
Total	1381	1945	1092	4418

Within the FCZ, the spatial distribution of fishing effort corresponded with the areas wherein fish were tagged, across the extent of sub-adult and adult life-history stages (Figure 27). During the 6-year study period the fishing generally occurred on 200 days per year, with lower effort recorded over the spawning period (June to August; mean \pm s.d. = 9.44 ± 12.52 days per month) compared to the rest of the year (18.87 ± 11.65 days per month), due to the routine closure of the Burdwood Bank spawning area to fishing. However, limited tagging and recapture effort still occurred over the Burdwood Bank during the closure via pulsed-tagging research surveys.

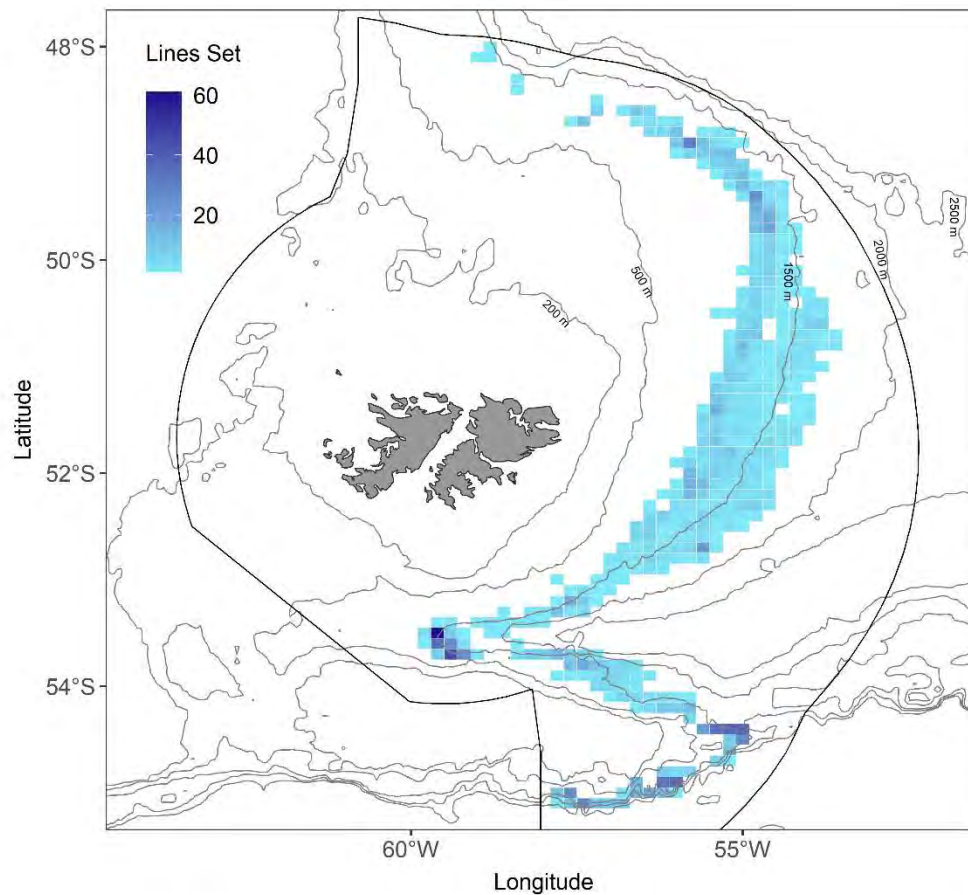


Figure 27: Spatial distribution of longline fishing effort (number of lines set per $0.1^\circ \times 0.1^\circ$ gridsquare; $n = 2236$) during the study period (June 2016 to October 2021) in the Falkland Islands Conservation Zones.

A total of 232 toothfish have been recaptured since the inception of the tagging program in the Falkland Islands, indicating a recapture rate of 5.25%. Of these 44% of the recaptured fish were reported while a FIFD observer was onboard, compared to 56% otherwise. Given the ~50% observer coverage of the fishery, this suggests no recapture reporting bias by commercial fishers in the FCZ. The length distribution of recaptured fish was similar to that of those that were tagged offset by growth while at liberty (mean = 108.19 cm, s.d. = 12.89; Figure 28A). The depths wherein fish were recaptured ranged from 469 to 2364 m (mean = 1344.48 m). Time at liberty ranged from 22 to 1877 days (0.10 – 5.14 years) with an average of 729.14 days (2.00 years; standard error = 27.39 days).

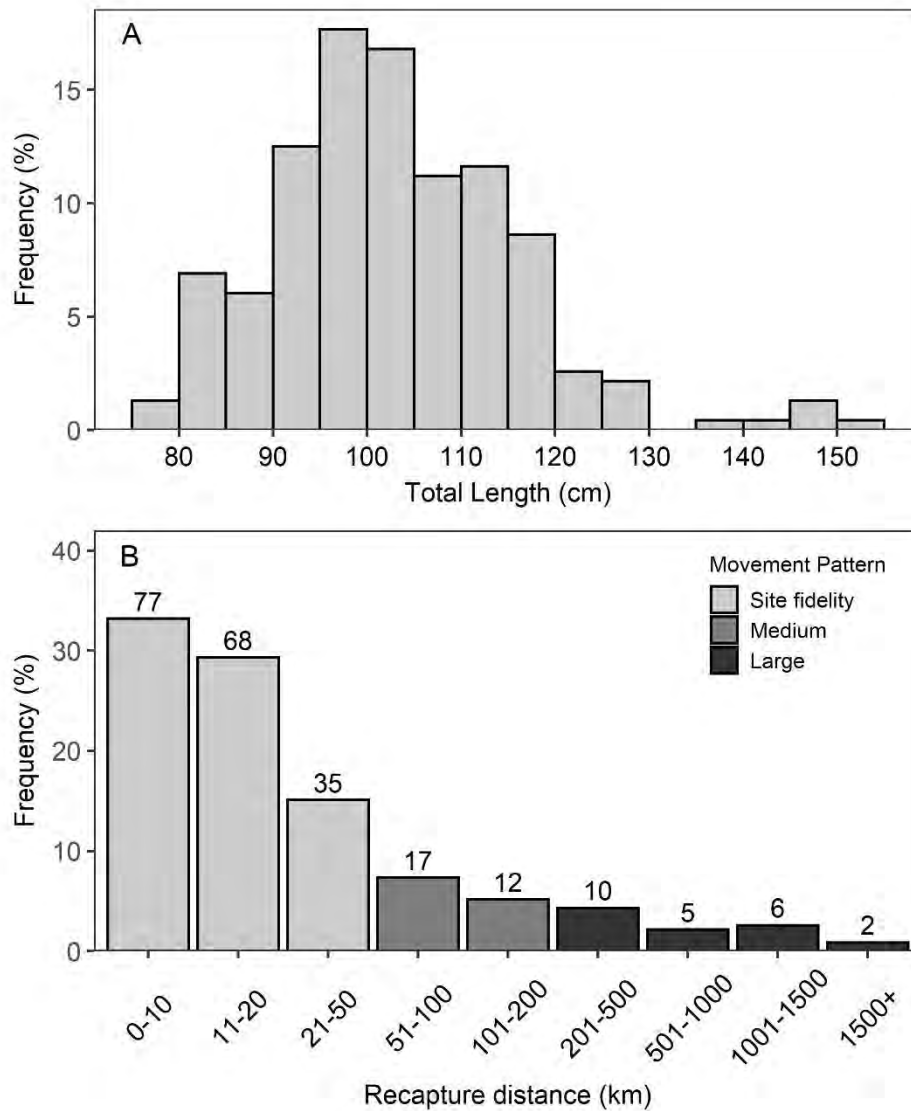


Figure 28: Length frequency distribution (A) for Patagonian toothfish measured at recapture ($n = 232$) and (B) the frequency distribution of distances moved for fish recaptured during the study period. Note the non-linear sequence of the x-axis.

4.3.2. Distances moved

Most recaptured fish (78%; $n = 180$) showed high site fidelity with movements of less than 50 km (Figure 28B). A further 13% of the recaptured fish ($n = 29$) displayed medium movements of between 51 to 200 km distances. A comparatively small, yet significant component (10%; n

= 23) of the recaptured fish displayed large-scale movement behaviour, with distances travelled between 201 to 1896 km.

The extent of movement patterns appeared to differ according to the area wherein fish were tagged (Figure 29; Table 11). Of the three areas, fish tagged in the spawning area on the Burdwood Bank had the highest site fidelity (85%; n = 39) and the lowest proportion of medium (9%; n=4) and large-scale (6%; n = 3) movements. Medium and large-scale movements from Burdwood Bank involved both southerly migrations to the southern slope edge as well as eastern lateral movements onto the north Scotia Ridge, which involved crossing a deep oceanic trough. No northwards movements were captured in the data from fish tagged on the Burdwood Bank moving across the Falklands Trough onto the Falklands Slope (Figure 29).

In contrast, fish tagged on the northern and eastern Falklands Slope had a higher proportion of medium (11%; n = 11 and 16%; n = 14, respectively) and large-scale (10%; n = 10 and 11%; n = 10, respectively) movements. Fish tagged on the northern Falklands Slope generally undertook medium-scale movements in a southerly direction (82%; n = 9). While fish tagged on the eastern and southern extent of the Falklands Slope undertook medium-scale movements in both southerly (50%; n = 7) and northerly (50%; n = 7) directions, these did not extend across any geographical or oceanographic boundaries and appeared to extend predominantly into deeper waters. Recaptured individuals suggest adults move in a southerly direction, including thirteen individuals that undertook movements into the spawning areas off southern Chile (n=7), and the southern extent of the Burdwood Bank (n=6; Figure 29). A single fish tagged to the north of the Falklands Slope was recaptured 1009 km away on the eastern extent of the north Scotia Ridge. (Figure 29).

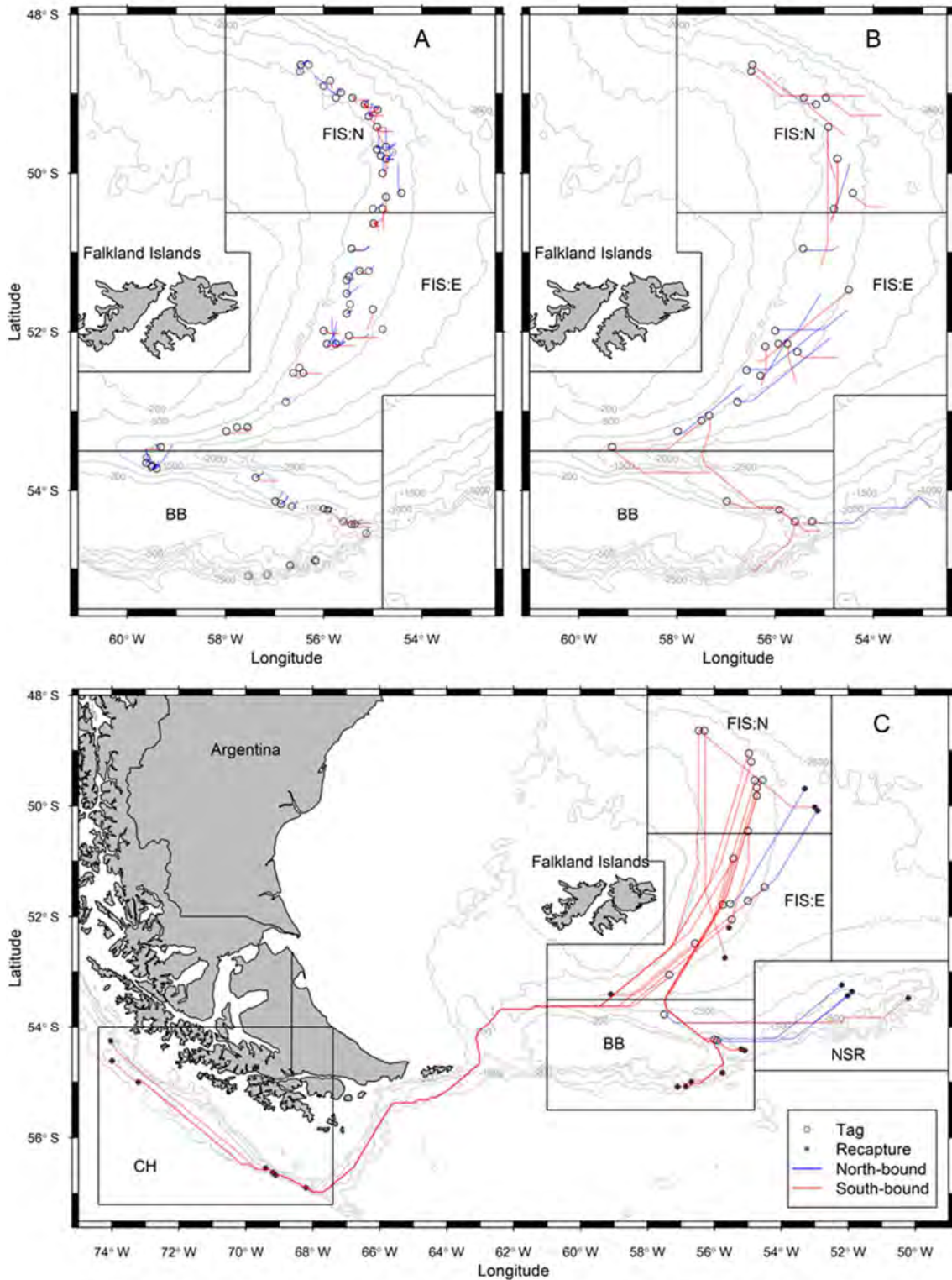


Figure 29: Tag and recapture locations for Patagonian toothfish that undertook movements of (A) <50 km, (B) 51-200 km and (C) 200+ km within 450 to 2500 m bathymetric constraints. BB = Burdwood Bank, CH = southern Chile, NSR = North Scotia Ridge, FIS: E = Eastern Falkland Islands Slope and FIS: N = Northern Falkland Islands Slope.

Table 11: Summary of the movement patterns of tagged and recaptured Patagonian toothfish individuals across the study area. Three geographic regions were defined during tagging: BB = Burdwood Bank, FIS: E = Eastern Falkland Islands Slope and FIS: N = Northern Falkland Islands Slope.

Regions		Recapture (%)									Total
		Low			Medium		Large				
		0-10	11-20	21-50	51-100	101-200	201-500	501-1000	1001-1500	1501+	
Tagging	FIS: N	32.65	31.63	14.29	9.18	2.04	3.06	3.06	2.04	2.04	98
	FIS: E	31.82	23.86	17.05	6.82	9.09	4.55	2.27	4.55	0.00	88
	BB	36.96	34.78	13.04	4.35	4.35	6.52	0.00	0.00	0.00	46
Total		33.19	29.31	15.09	7.33	5.17	4.31	2.16	2.59	0.86	232

4.3.3. *Effects on movement*

The distances that Patagonian toothfish moved between tagging and recapture were significantly affected by the depth-difference between tagging and recapture locations, the direction moved and the area wherein fish were tagged. The average fish length showed a weakly significant effect on distances moved. The length, depth, direction, and area covariates kept in the best-fit model explained 60.5% of the deviance. The sex of the fish, condition, month of recapture and the time at liberty had no significant effect on the distances moved. Patagonian toothfish from the northern extent of the Falklands slope (north of 52°S), and those moving in a southerly direction (150 to 240°) travelled greater distances (Figure 30). Further, those moving into greater depths during their time at liberty indicated larger movement distances. The average length of Patagonian toothfish had a minor positive effect on the distances moved with larger fish (>120 cm) moving greater distances compared to smaller individuals.

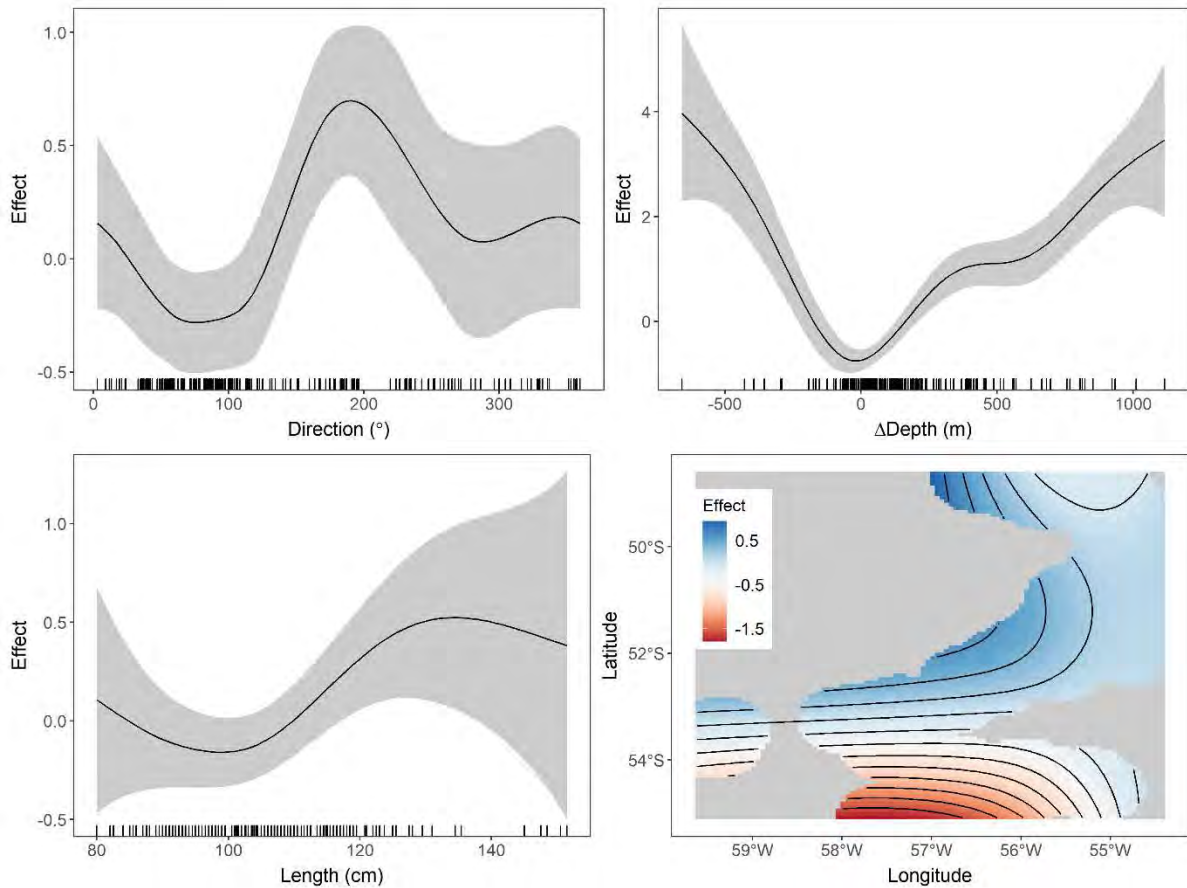


Figure 30: Results of the generalised additive model (with 95% confidence intervals) showing the effect of direction, depth-difference between tagging and recapture locations, average fish length, and tagging location on the distances moved. Rug plots display the distribution of observations.

4.4. Discussion

This study provides the first description of the regional movement patterns of a deep-sea apex predator, the Patagonian toothfish, on the Patagonian Slope and deep-sea plateau to the east of the Falkland Islands. While genetic homogeneity in the Patagonian toothfish population across the South American continental shelf has previously been described (Shaw *et al.* 2004; Canales-Aguirre *et al.* 2018), the extent of connectivity pathways driving this has remained uncertain (Beebee and Rowe 2008), and was thought to largely be a result of egg and larval dispersal through the prevailing regional current systems (Ashford *et al.* 2012b; Lee *et al.*

2021). Through the use of a six-year tag-recapture program, the first direct observations of movements were provided from foraging areas on the Falklands Slope to the spawning areas off the Burdwood Bank and North Scotia Ridge in the southwest Atlantic and southern Chile in the south-eastern Pacific. Research results reveal high levels of individual movement variation that were defined according to three patterns of movement: high site fidelity (Pattern 1: <50 km movement), the dominant pattern across the study area; medium-scale (Pattern 2: 51-200 km) localised movements; and large-distance (Pattern 3: 201-2000 km) dispersive movements (home-range relocations) across physical and oceanographic barriers. Understanding the patterns of movement helps explain the connectivity between the adult component of the stock inhabiting the slope with the southern spawning areas. These findings provide evidence in support of the hypothesis of a single Patagonian toothfish metapopulation across the Patagonian Shelf and Slope with levels of connectivity occurring across multiple life-history stages.

High site fidelity, defined as movements of less than 50 km, was the dominant movement pattern (78%) observed across the study area. High site fidelity has been consistently reported for Patagonian and Antarctic toothfish across their range. Results from a tagging program undertaken in the Ross and Amundsen Seas for the closely related Antarctic toothfish revealed that 50% of recaptured fish displayed movements of less than 50 km, with a further 20% moving less than 100 km (Hanchet *et al.* 2015). Very little movement has also been reported for Patagonian toothfish around South Georgia (Marlow *et al.* 2003) and Heard Island on the Kerguelen Plateau (Williams *et al.* 2002). The use of satellite linked archival tags over a six-month assessment period on the Burdwood Bank and Falklands Slope revealed movements of less than 50 km for 79% of fish (Brown *et al.* 2013a). Further, differentiation in the otolith shape of Patagonian toothfish from southern Chile, the Burdwood Bank and the northern Falklands Slope was attributed to partial geographic isolation of fish from each of these areas, at least until the age at which maturity is reached (Lee *et al.* 2018).

Large-distance movements across geographic and oceanographic barriers were observed in ~10% of the recaptured Patagonian toothfish. These were characterised by individuals from the slope (north of 52°S) undertaking southbound movements (150-240°) towards the spawning areas over the Burdwood Bank, North Scotia Ridge and southern Chile. Similar migratory behaviour has been reported for Antarctic toothfish in the Ross Sea, where long-distance movements, although limited, were reported almost exclusively from slope based foraging areas towards northern spawning grounds (Hanchet *et al.* 2015). Hanchet *et al.* (2008) hypothesised that spent adults return to the continental slope in post-spawning migrations. However, active large-distance movements are unlikely due to strong current speeds. Individuals are therefore thought to rely on large-scale ocean circulation to facilitate adult connectivity from the spawning areas on the Pacific-Antarctic Ridge to feeding grounds on the Ross Sea slope (Ashford *et al.* 2012a). While the southbound movements observed in the current study may be an emergent result due to geographic constraints (driven by recaptures reported in Chile), this appears to be unlikely due to the almost complete absence of observed northbound movements across Falkland Conservation Zone during the 6-year tag-recapture programme.

Based on the distribution of pre-spawning and spawning fish, Laptikhovsky *et al.* (2006a) hypothesised seasonal migrations of Patagonian toothfish between foraging areas on the slope and spawning areas on the Burdwood Bank. Tag-recapture data only record the time and location of release and recapture and reveal nothing about the location of the fish in the intervening time periods. Despite this limitation, results of the current study are suggestive of high levels of site fidelity, and an absence of any northerly direction return migrations from the spawning areas to the slope. Further, the lack of influence of time at liberty in describing movement distances is indicative that limited movements are not simply restricted to individuals recaptured over short or within-seasonal time periods. These results, combined with those obtained with otolith shape analyses (Lee *et al.* 2018) and movement patterns derived from satellite tags (Brown *et al.* 2013a) described above appear to imply that large-

scale, annual spawning migrations undertaken on a seasonal basis are unlikely. In turn, these large-distance movements may therefore be reflecting a home-range relocation, at least over the time period covered during the current study. This is a key finding in identifying that at least a limited component of the Patagonian toothfish across the region may be contributing to the southern spawning population, and that those dispersed during their early life-history stages to the north and east of the slope are not lost from the population as non-breeding vagrants as discussed by Ashford *et al.* (2012b). This hypothesis would still be consistent with the absence of any fish in spawning condition on the slope and deep-sea plains to the north and east of the Falkland Islands (Laptikhovsky *et al.* 2006a).

High site fidelity and the lack of seasonal spawning migrations may, however, have important consequences on the contribution of fish occupying the slope towards the spawning stock. The Burdwood Bank and North Scotia Ridge are considered the only spawning grounds of toothfish in the vicinity of the Falkland Islands (Laptikhovsky *et al.* 2006a). This is supported by satellite derived tagging observations of spawning behaviour in toothfish on the Burdwood Bank that was not present in those on the slope (Brown *et al.* 2013a). Fish displaying high site fidelity on the slope may therefore represent a significant proportion of the population not participating in spawning every season. Further investigation is therefore required on the extent of the population across their range that are (1) spawning capable, (2) skipping spawning, and the (3) number of successive seasons that may be skipped. The planned continuation of the tag-recapture programme on a longer time scale may also provide further information on the occurrence and extent of both southern movements to spawning grounds and any return migrations.

What drives high site fidelity in adult Patagonian toothfish? During their older life-history stages in particular, Patagonian toothfish contain reduced amounts of red muscle tissue for sustained low speed swimming which is thought to be a constraint on regular large-scale migrations in the species (Brown *et al.*, 2013a). Along the subantarctic Kerguelen Plateau, high site fidelity

has been associated with skipped spawning (Yates *et al.* 2018), a reproductive feature also reported in Northeast Arctic cod (Skjæraasen *et al.* 2012), Alaskan sablefish (Tolimieri *et al.* 2018) and Pacific halibut (Loher and Seitz 2008). The occurrence of skipped spawning in Patagonian toothfish has been described as a potential energy saving mechanism, leading to increased survival or spawning success in subsequent years (Skjæraasen *et al.* 2012; Yates *et al.* 2018). Such a life-history strategy may be evolutionarily attractive on the Patagonian Shelf and Slope due to the energy requirements necessary not just for reproductive development, as in the case of the Kerguelen Plateau, but also the large distances that adult fish are required to move to reach the spawning grounds. This behaviour may have developed as a result of: (1) the wide dispersal of eggs and larvae through the prevailing currents in the region (Ashford *et al.* 2012b); (2) the ontogenetic migration of juveniles and sub-adults into deeper waters adjacent to areas of recruitment, often large distances from spawning areas (Arkhipkin and Laptikhovsky 2010; Lee *et al.* 2021); and (3) the continuity of the deep-sea habitat along the continental shelf of South America facilitating the movement of fish large and fit enough to undertake such a journey (Canales-Aguirre *et al.* 2018). The latter hypothesis is consistent with the results of the current study indicating that only fish significantly larger (>120 cm) than the lengths at 50% maturity for both male (81-86 cm) and female (89-90 cm) fish undertook large distance migrations (Laptikhovsky *et al.* 2006a; Arana 2009).

The temporal and spatial scale of medium-scale movements captured in the current study likely cover a range of patterns including (1) localised foraging, (2) predictable ontogenetic migrations and (3) dispersal (Quinn and Brodeur 1991). In particular, at least some of the medium-scale movement may reflect incomplete home-range relocations whereby individuals were recaptured prior to reaching their destination on the southern spawning grounds. These are reflected in the continued southern movement trend observed for fish, particularly those tagged in the north of the slope. Regarding potential foraging-induced movements, Patagonian toothfish are known to switch their prey type according to season or life-history stage (Arkhipkin *et al.* 2003; Troccoli *et al.* 2020). For example, individuals specialising in

migratory prey (such as squid and southern blue whiting), may undertake movement patterns consistent with this prey, while those targeting sedentary species as more opportunistic predators (such as the crustaceans) may possess a greater degree of site fidelity. Further, differences in food availability can also be a driver of movement patterns, dictating whether, when and where a species migrates. This may be evident in near-far searching with individuals displaying a higher degree of site fidelity in areas with good foraging opportunities (stayers), and moving greater distances (leavers) otherwise (Murray *et al.* 2019; Shaw 2020). Interspecific interactions can also lead to movements of groups within a population to escape infection from local build-up of parasites or pathogens. Examination of parasites for post-juvenile Patagonian toothfish has shown significantly greater abundances of certain taxa in the north of their Falklands Slope distribution (Brown *et al.* 2013b). This may be an influence of the increased movement behaviour from fish on the north of the slope.

The significance of depth as a predictor of movement distance is indicative that some of the observed movements may be related to the continuous downslope ontogenetic migration characteristic across the Patagonian toothfish life-history. These downslope migrations are thought to occur as a result of a combination of inter- and intraspecific competition, abiotic factors, and individual traits (Arkhipkin and Laptikhovsky 2010; Shaw 2020; Lee *et al.* 2021). Around the Kerguelen Plateau, Patagonian toothfish undertake a gradual migration from shallow to deep waters as fish grow, except at intermediate depths of between 600 and 1200 m where fish were consistently between 75 and 80 cm, coinciding with the length at which maturity is reached (Péron *et al.* 2016). Ontogenetic migratory behaviour is known to occur during the juvenile and pre-adult life-history stages around the Falkland Islands (Lee *et al.* 2021), where the productive shelf-based waters provide optimal feeding conditions, along with warmer water temperatures to support rapid growth (Agnew 2002; Arkhipkin and Laptikhovsky 2010; Lee *et al.* 2021). Although these migrations have been less well studied for older fish inhabiting depths greater than 400 m, dietary data suggests a distinct shift in prey and feeding strategy towards a less active more opportunistic diet on species inhabiting deeper waters

(Arkhipkin and Laptikhovsky 2010). In contradiction to this result, change in depth may not be a causative explanatory factor of movement distance, as assumed in the GAM, and simply be a correlated response of long-distance movement.






Recapture rates were high across the study area (5.25%), indicating that Patagonian toothfish survived the tagging procedure well. Similar recapture rates (4 – 6%) have been reported for Antarctic toothfish in the Ross and Amundsen Seas fisheries (Hanchet *et al.* 2015). High survivorship in Patagonian toothfish has previously been reported by those tagged with dart (Marlow *et al.* 2003; Agnew *et al.* 2006) and satellite tags, with sperm whale predation identified as the predominant risk during the release procedure (Brown *et al.* 2013a). The current study used experienced scientific personnel operating according to stringent guidelines for the handling, tagging and release of fish, predominantly undertaken during dedicated surveys. Further, commercial fishers have been involved with the tag-recapture programme from conception, and have received training in the accurate collection of data for recaptured fish, should a scientific fisheries observer not be available. The development of these protocols through a strong industry-science based partnership gives us a level of confidence that recapture reporting rate is at or close to 100% within the territorial waters of the Falkland Islands. Recapture reporting outside of the Falkland Islands Conservation Zones were reliant on reporting by vessels fishing on the high seas (e.g. South Korea) or within the jurisdiction of other nations (e.g. Chile and Argentina) and hence may be subject to non-reporting bias. More comprehensive reporting from the areas outside of FCZ may therefore show that the large-scale home-range relocations are more frequent than what was thought, and would therefore not undermine the conclusions drawn from these. The presence and potential importance of toothfish dispersal into southern Chile, the high seas (North Scotia Ridge), and in all likelihood, Argentina, identifies the need for improved cooperation and regional management for fisheries across the region. Such an approach should include considerations relating to the region-wide expansion of the tag-recapture programme. Further,

aspects relating to the reproductive biology, specifically with regards to skipped spawning and the contribution of the biomass to the spawning stock also requires further investigation.

The guidelines and protocols that have been established for the tag-recapture programme proved to be effective, providing a high-quality data set containing important information on the movement patterns of Patagonian toothfish in the southwest Atlantic. The planned extension of the tag-recapture programme into an ongoing, long-term study will, in time, provide an extensive dataset from which further insights can be drawn on regional stock structure dynamics and associated movement patterns for this deep-sea marine predator. In particular, local movement patterns in a metapopulation stock structure may be vital in understanding potential vulnerabilities of specific spawning stock contingents.

4.5. Supplementary information

Table 12: Suitability assessment for tagging of fish

Assessment Category	Do not tag	Example
Hook injuries	Hook injury outside the mouth areas (outside the lips, jaw, or cheek), or in the back of the mouth or throat.	
Gills	Gills pink or white. Gills must be bright red as per photo on the right.	
Bleeding	Any visible bleeding from gills, or excessive bleeding elsewhere	
Body	Visible damage to fish body with open wounds	
Organs	Visible damage to eye or penetration of body cavity, including by crustaceans (amphipods/lice/hagfish)	
Scales	Abrasions or single area of recent scale loss equal to or exceeding the area equivalent to the fish tail	

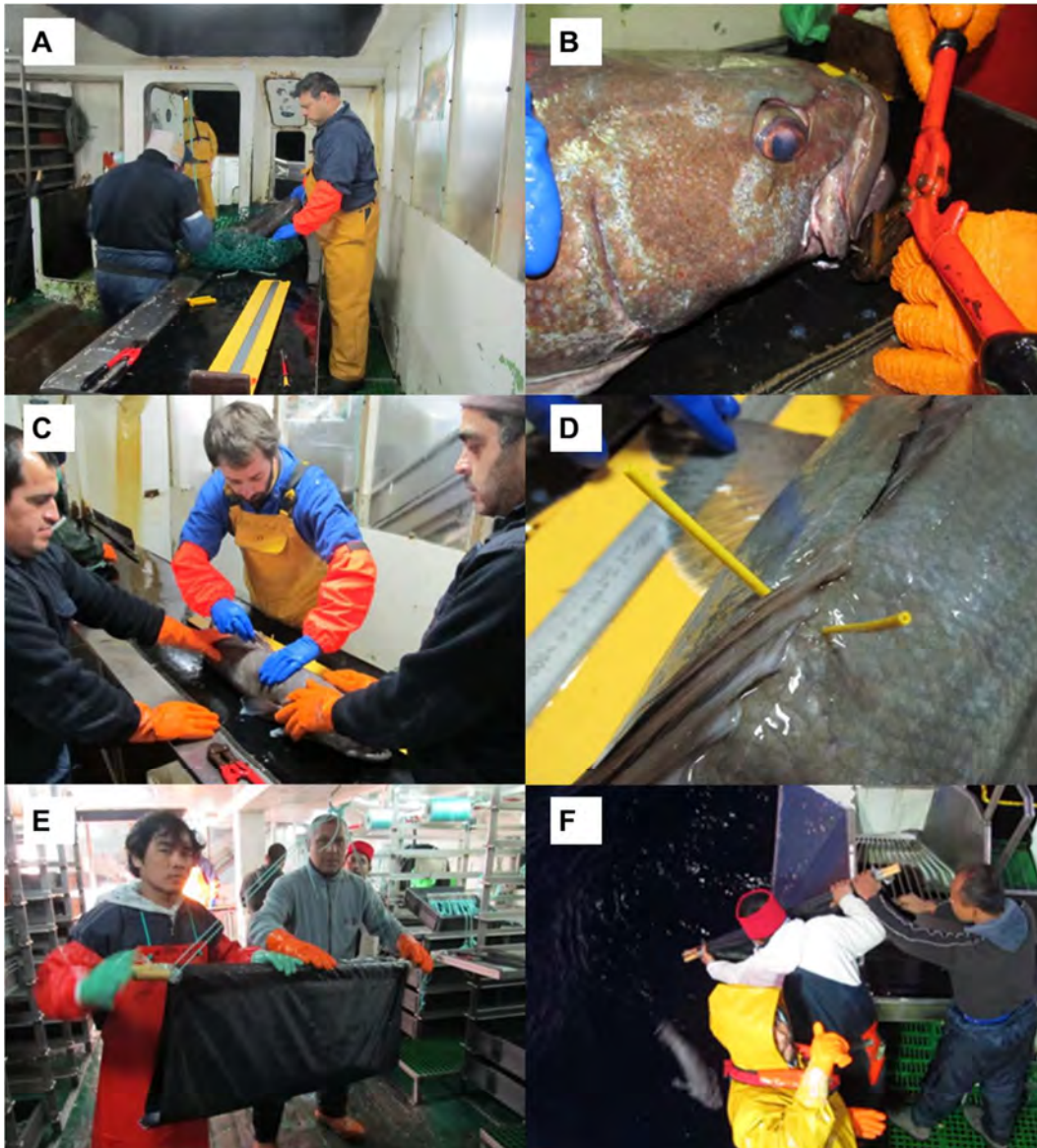


Figure 31: Photographs depicting the different steps involved in tagging fish: A) Receiving the fish in the 'dry' section of the factory where the tagging station has been set up; B) cutting of the hooks with bolt cutters to minimise injury to the fish; C) the use of applicators to apply two tags to an immobilised toothfish; D) illustration of how tags should be applied, i.e. inserted into the dorsal muscle of the second dorsal fins angled downwards and backwards with tag barb lodged behind the forward edge of 2nd and 3rd dorsal fin ray; E) fish transported by two crew members from the tagging station to the spring balance using a stretcher; and F) fish released from the stretcher over the side of the vessel from the hauling bay, head first into the water.

Chapter 5 - Otolith microstructure and microchemistry reveal early life-history shifts in Patagonian toothfish *Dissostichus eleginoides* from the Patagonian Shelf

Abstract

Many long-lived, deep-sea species of the higher latitudes, such as Patagonian toothfish, possess protracted egg and larval phases leading to dispersal across large geographical areas. The timing of ontogenetic life-history shifts is vital for understanding dispersal potential, a key driver of spatial patterns and stock structure of the species on the Patagonian Shelf. However, life-history phases prior to their settlement into a demersal habitat remain elusive and largely unexplored. We applied a complimentary approach using otolith microstructure and trace element analysis (by LA-ICMPS) to infer time-resolved elemental profiles that reflect the early ontogeny of juvenile Patagonian toothfish from key nursery areas on the Patagonian Shelf. Results revealed significant ontogenetic shifts in elemental profiles across the early life-history of Patagonian toothfish. From these, key biological benchmarks were identified, including (1) the hatch date distribution (mid-September to late October; mean = 3 October); (2) the dispersal period of pelagic larvae until their entry onto the Patagonian shelf (0 to 40 days post-hatch); (3) the transition phase from the shelf extent to inshore waters (<100 m depth; 40 to 75 days post-hatch); (4) settlement into a demersal habitat (100 days post-hatch); and (5) subsequent migration into juvenile nursery areas (<150 m depth; 120 days post-hatch). Finally, these benchmarks were shown to occur significantly earlier in fish sampled in discrete nursery areas to the west of the Falkland Islands ($F = 7.90$, $df = 2$, $P = 0.0006$). The results of the current study provide important considerations in terms of the complexity and protracted nature of early life-history stages, the reliance of recruitment upon stable environmental patterns and the potential for a mixed stock origin on the Patagonian Shelf.

5.1. Introduction

Many demersal fish species utilise disparate habitats across their spawning, larval, juvenile and adult life-history stages (e.g. Kurth *et al.*, 2019). The progressive changes in habitat use reflects the evolving physiological (e.g. growth and associated metabolic changes), environmental (e.g. temperature, salinity, oxygen tolerance), and ecological (e.g. trophic level, species interactions through competition and predation) requirements of a species across their development (Galaiduk *et al.* 2017; Hernandez *et al.* 2021), known as an ontogenetic shift or migration.

Ontogenetic shifts that occur during the early life-history stages, in particular, remain an elusive, yet critical period for many fish species. For example, deep-sea spawning species from the higher latitude regions frequently possess protracted egg and larval phases which occur in combination with strong oceanographic features (Cowen and Sponaugle 2009; Ramesh *et al.* 2019; Álvarez-Noriega *et al.* 2020). These aspects can lead to dispersal across a wide geographical area, resulting in a decoupling of the spawning and juvenile habitats within a population. Understanding the nature and timing of ontogenetic migrations across life-history stages are therefore important considerations for assessing demographic structure, natal origin and connectivity within fish populations, aspects that are important for defining stock integrity (Sanchez *et al.* 2020; Wells *et al.* 2020).

Patagonian toothfish *Dissostichus eleginoides* Smitt, 1898 (family Nototheniidae) is a demersal fish distributed around all subantarctic islands and the southern tip of South America (Eastman 1993; Collins *et al.* 2010). Patagonian toothfish are moderately slow growing, long-lived (50+ years; Andrews *et al.*, 2011; Horn, 2002) and late maturing (10-17 years; Boucher, 2018; Yates *et al.*, 2018). The species forms the basis of important commercial fisheries across their range (Tuck *et al.* 2003; Croxall and Nicol 2004; Grilly *et al.* 2015).

Genetic evidence suggests a single population across the Patagonian Shelf, independent to those to the south of the Antarctic Polar Front (APF; Smith and McVeagh, 2000; Shaw *et al.*, 2004; Rogers *et al.*, 2006; Canales-Aguirre *et al.*, 2018). Two Patagonian toothfish spawning groups are found within Patagonian population (1) off the far southern continental slope of Chile (Arana 2009); and (2) over the Burdwood Bank to the south of the Falkland Islands (Laptikhovsky *et al.* 2006a; Boucher 2018). Large-scale dispersal of eggs and larvae across the eastern Patagonian Shelf is driven by regional and localised oceanographic systems; in particular the APF and its two north-flowing extensions: the Falkland Current which carries cold, nutrient rich waters around the southern and eastern shelf edge of the Falkland Islands, and the weaker Patagonian Current which diverges to the west (Croxall and Wood 2002; Arkhipkin *et al.* 2013). Mesoscale eddies linking the Subantarctic Front with the Falklands Current to the south of the Falkland Islands have also been described as influential (Lee *et al.* 2021). In the Falkland Islands, demersal juveniles are first encountered in shallow waters (<150 m) during late January to early February at 10 to 15 cm TL (Arkhipkin and Laptikhovsky 2010), after which they are known to undertake a lengthy (3 – 6 year) ontogenetic migration into deeper waters (1000 – 2500 m) with increasing age (Péron *et al.* 2016; Lee *et al.* 2021).

Prior to their recruitment and settlement, on the shelf as juveniles, only sparse information is known in terms of their life-history, habitat and trophic ecology. The egg (30 to 105 days) and larval period (90 to 200 days) are thought to be protracted (North 2002; Mujica *et al.* 2016), with pelagic larvae inhabiting the upper 250 m of the water column (Evseenko *et al.*, 1995; North, 2002). The wide shelf-extent that occurs around the Falkland Islands (50 – 400 m; 579,148 km²) provides spatially discrete and temporally variable nursery hotspots for Patagonian toothfish (Laptikhovsky and Brickle 2005; Lee *et al.* 2021). Area specific recruitment from discrete spawning grounds has been suggested (Ashford *et al.* 2012b; Lee *et al.* 2021). During high juvenile recruitment periods, nursery area hotspots provide for opportunistic biological information to be collected during rarely observed life-history stages. However, this aspect of their biology also makes them vulnerable as bycatch to commercial

fishing operations that occur across the shelf extent (Laptikhovsky and Brickle 2005; Lee *et al.* 2021), highlighting the importance of research during this key ontogenetic phase.

Elemental concentrations in otoliths may reflect the ambient properties of the surrounding water, such as temperature, salinity, ambient elements, which are mediated by physiological factors (Campana 1999; Izzo *et al.* 2016a). The continued and predictable growth of otoliths throughout the lifetime of the fish allows time resolved environmental histories to be reconstructed (Campana and Thorrold 2001). In this way, otolith elemental concentrations can be used as natural tags, providing information on population structure, including movements, and trophic position across the life-history of a species (Fraile *et al.* 2016; Wright *et al.* 2018; Rogers *et al.* 2019; Hegg *et al.* 2019; Sanchez *et al.* 2020; Wells *et al.* 2020; Avigliano *et al.* 2021). Many otolith microchemistry-based studies have focused on the analysis of grouped or independent points taken from the core and edge of the otolith. While such research provides an excellent snapshot for these life-history stages themselves, they lose the high-resolution time-series that can be provided through an analysis of line-transects from the primordium (birth) through to the otolith edge (capture). Line transects therefore have the potential to provide high resolution life-history information, including the timing and patterns of movements within and across more inconspicuous life-history stages during time periods wherein the sampling of individuals is impracticable.

The aims of the current study are to use data derived from otolith microstructure and chemical profiles to improve our understanding of the early life-history for Patagonian toothfish occurring on the Patagonian Shelf around the Falkland Islands. The specific objectives of the study were to: (1) develop a relationship between daily ages and distances along otolith transverse sections for inference of a temporal axis onto otolith elemental transects, (2) describe and quantify elemental trends across the early life-history stages during larval dispersal and settlement into a demersal habitat, (3) use otolith microstructure and patterns in elemental transects to quantify life-history shifts, and (4) interpret what these results may mean in terms

of the life-history and population structure for Patagonian toothfish around the Falkland Islands.

5.2. Materials and methods

5.2.1. Sample Collection

Juvenile Patagonian toothfish were sampled from the inshore shelf to the shelf-edge (50 – 400 m) around the Falkland Islands (48-55°S and 53-64°W) in the south western Atlantic between January and March 2015 to 2019 (Figure 32). Data were collected during fisheries independent research (January), demersal biomass (February) and Patagonian longfin squid pre-season (February) bottom trawl surveys. Details regarding the survey designs and gear used are described in Lee et al. (2021). Additional fisheries dependent samples (January - March) were collected by Falkland Islands Fisheries Department (FIFD) fisheries observers deployed on commercial fishing vessels operating bottom trawls during the same period. Comprehensive data associated with each trawl station were collected, including depth and geographical coordinates (Latitude, Longitude). Total lengths of each fish were measured to the nearest cm, and fish were weighed to the nearest 0.1 g. Sex and maturity stage were assigned by macroscopic assessment of the gonads. Otoliths were removed, cleaned and stored in individual microcentrifuge tubes containing ethanol within labelled paper envelopes. Storage of otoliths in ethanol has been demonstrated to not influence elemental concentrations (Hedges *et al.* 2004).

5.2.2. Sample Extraction

Juvenile Patagonian toothfish otolith samples (n=182) were extracted from the data collected to meet criteria based on the year of birth (cohort), age of fish and the area of capture (Figure 32; Table 13). The length frequency distributions for juvenile Patagonian toothfish follow a

distinct progression of multimodal, age structured cohorts during their shelf-based life-history (Lee et al., 2021). As such, the age and birth years of fish could be reliably predicted for data extraction and later validated using ageing procedures (see section 2.2). In order to limit the influence of temporal confounding, individuals were selected from four birth years (2013 to 2016). Fish aged 0+ and 1+ were included for each birth year. Sample locations were grouped into three areas to the west, south and northeast of the Falkland Islands based on spatially discrete, annually variable recruitment (age-0+) and juvenile (age-1+) abundance hotspots (Lee et al., 2021).

Table 13: Summary of samples used for otolith microstructure (age-0+) and microchemistry transects (age-1+) from shelf areas around the Falkland Islands.

Method	Area	Birth year				n
		2013	2014	2015	2016	
Microstructure (Age-0+)	NE	0	10	0	10	20
	S	0	10	0	10	20
	W	0	2	10	10	22
	n	0	22	10	30	62
Trace element analysis (Age-1+)	NE	10	10	10	9	39
	S	11	10	10	10	41
	W	10	10	10	10	40
	n	31	30	30	29	120
Total		61	52	40	59	182

While all selected otolith samples were processed for trace element analyses, the availability of otoliths from age-0+ individuals varied among years, areas and number of growth increments (distance along transect). When available, a sample of ten otoliths that align with each of the criteria (birth year, age class and area) were selected and processed for subsequent analyses. In the case that ten fish were not available, all available otoliths were used. To minimise the number of missing values that were present in the data set, and ensure a balanced sample design, only otoliths from age-1+ fish, consisting of the age-0 component (primordium to the formation of the first winter annulus) were analysed for otolith chemistry (hereafter referred to as the otolith core region). Age-0+ otolith samples were therefore only

included for microstructure analyses for the development of an otolith age:distance relationship for inference onto the core region of age-1 fish.

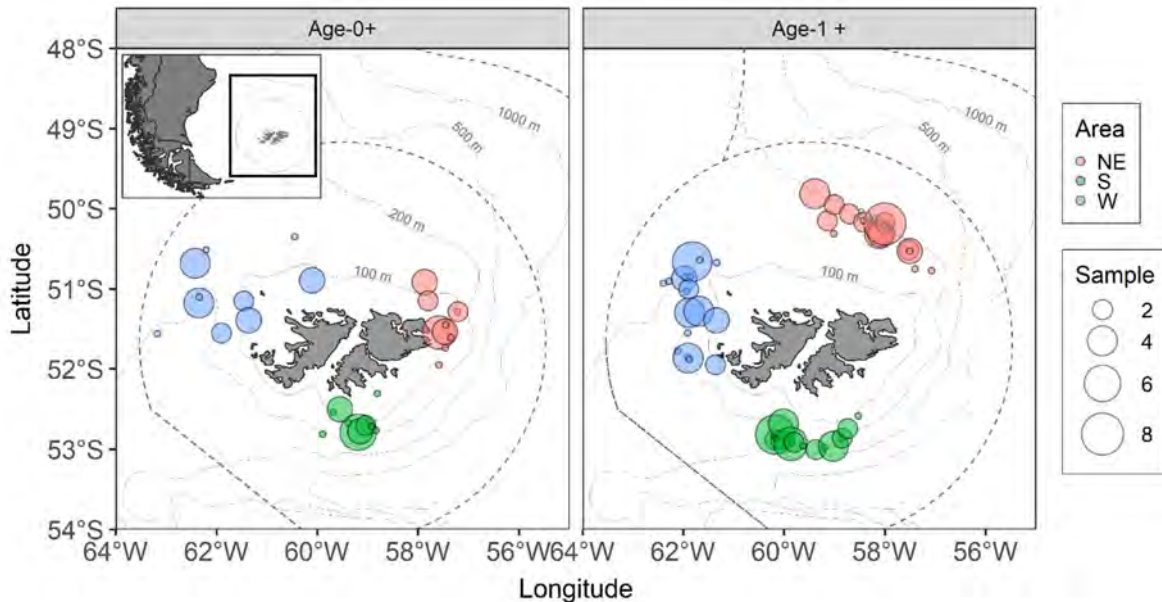


Figure 32: Map depicting the locations and areas where age-0+ and age-1+ year old Patagonian toothfish were sampled for microstructure ($n = 62$) and trace element analysis ($n = 120$).

5.2.3. Otolith processing

Otolith samples were randomised and embedded in polyester resin blocks. A series of 2-5 transverse sections of ~ 0.375 mm thickness was taken from the core area of each otolith using a Buehler Isomet low-speed saw (Buehler Ltd., Illinois, USA) to expose the primordium and inner structure (Figure 33A). Otolith sections for each individual fish were visually assessed, and the thin section considered best-centred on the primordium was selected and fixed to glass analysis slides using polyester resin (Figure 33B). Once the resin had cured, analysis slides containing otolith sections were polished with P2400 wet paper, rinsed with distilled water and stored in secure boxes until subsequent analyses.

Microstructure

The second otolith from each age-0+ fish (n=62) was processed for microstructure examination. Preparation of otoliths were undertaken under reflected light using an Olympus SZX12 dissection microscope at 10 to 25X magnification. Otoliths were mounted, concave side down on a glass slide in thermoplastic resin (Crystal Bond 509, AREMCO Products, INC., USA). Preparations were ground and polished by hand using P1200 and P2400 wet silicon carbide paper to form an even plane from the central nucleus to the otolith edge. Otoliths were then flipped over concave side up and the process repeated to obtain thin sections within which increments could be observed (Figure 33C).

Otoliths were examined at 200 - 400X magnification under transmitted light using an Olympus BX-51 microscope, fitted with an Olympus DP70 camera. The number of increments observed between the primordium and the otolith edge were independently enumerated twice by the primary reader (BL) and once by a secondary reader (AA) without knowledge of the biological or catch data of the specimen. The final age estimate was considered as the average of the three age estimates.

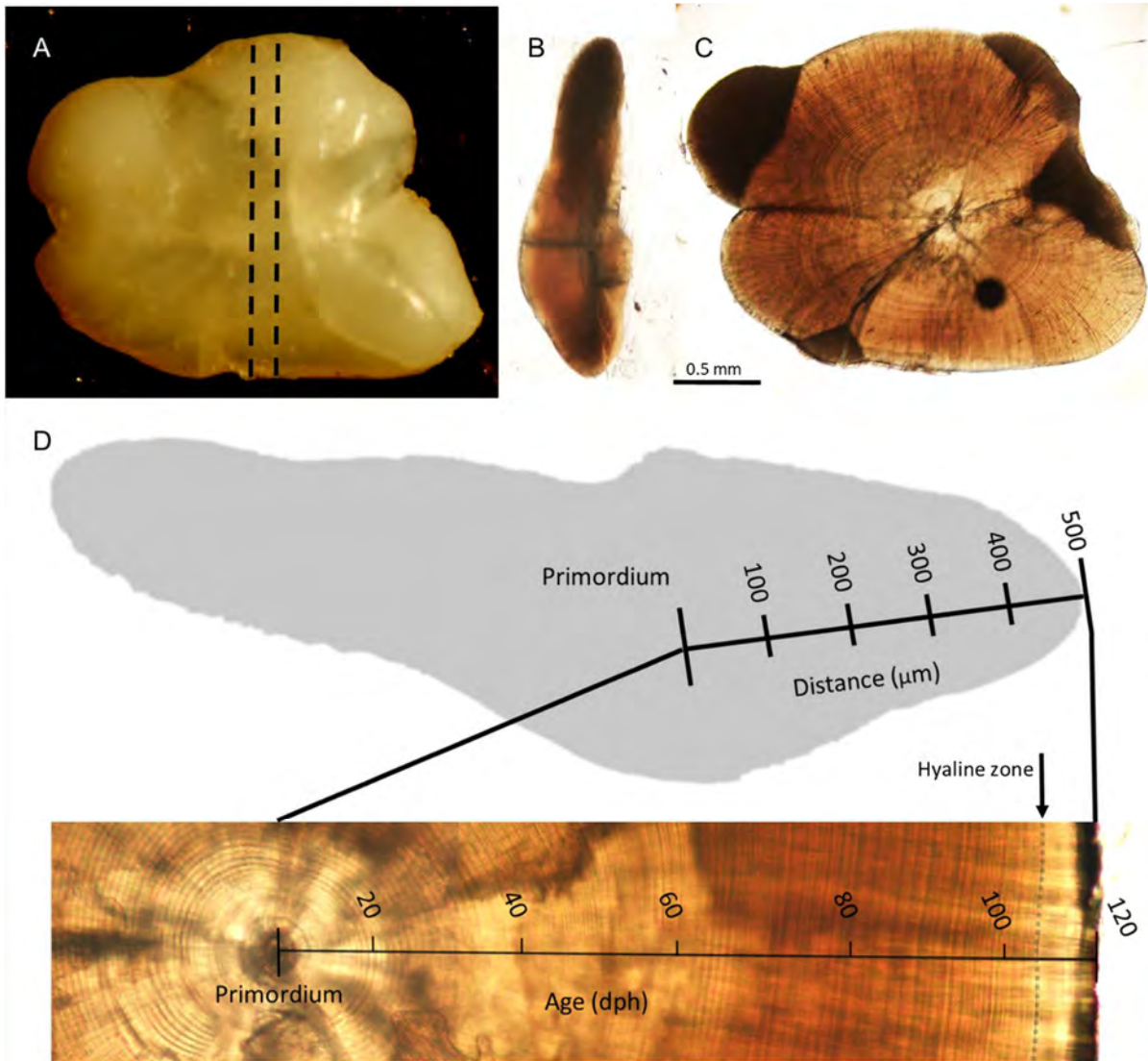


Figure 33: Diagram depicting (A) a whole juvenile toothfish otolith showing the position (dashed lines) and (B) orientation of transverse sections and (C) daily increment counts. (D) Digitised representation of a transverse section from the age-0+ section of a juvenile Patagonian toothfish displaying the location of the laser line transect extending from the primordium (birth) to the edge. (D) Age-0+ otoliths were processed for microstructure analysis and inference of daily age post-hatch (dph) onto corresponding elemental profiles of age-1+ individuals.

Trace element analysis

Otolith trace element analyses were performed on otolith transverse sections by laser ablation-inductively coupled plasma mass spectrometry (LA-ICP-MS) at the Natural History Museum, London, United Kingdom. The system consisted of an ESI New Wave Research 193 laser system used in conjunction with an Agilent 7500cs ICP-MS. Each otolith was sampled using line transects following a path from the primordium (birth) towards the dorsal edge of each transverse section (end of life), parallel to the edge of the sulcus (Figure 33D). This provides an elemental life-history profile of each of the sampled fish (hereafter referred to as LA profile). Each otolith was sampled using a 50 μm diameter laser beam, at a repetition rate of 10 Hz, a laser flux of 10 mJ/cm^2 and a scan speed of $10 \mu\text{m/s}^{-1}$. Analysis slides were placed in a sealed ablation chamber with ^4He atmosphere and viewed remotely on a computer monitor. After processing each otolith section, the chamber was purged with Argon gas for approximately 60 s to eliminate any background gases that may have contained contaminants.

Time-resolved intensities from the ICP-MS were converted to elemental concentrations (ppm) equivalents using Lolite software with ^{43}Ca as the internal standard and a Ca index value of 40.04% weight (based on the average Ca concentration extracted from otoliths). Prior to ablating each otolith section, background counts of each elemental isotope were measured in the blank sample gas for 30 s. This provided average background counts of the analysed elemental isotopes, which were subtracted from the sample counts for each ablation. Counts of elemental isotopes were calibrated against the National Institute of Standards and Technologies 612 and 610 standard reference material (NIST-SRM). The NIST-SRM was analysed at the beginning and end of each daily analytical session and after every three to five otolith line transects to account for instrumental drift. NIST 612 was used as the primary calibration standard, with the accuracy and precision assessed using replicates of NIST 610 as an unknown. Concentrations were then converted to element:Ca molar ratios R_E , $\mu\text{mol mol}^{-1}$ based on the molar mass of each element (M_E , g mol^{-1}) and calcium ($M_{\text{Ca}} = 40.078 \text{ g mol}^{-1}$).

Otolith transverse sections used for trace element analyses were immersed in water and examined under 40X magnification using an Olympus BX-51 compound microscope (Olympus Corporation, Tokyo, Japan), fitted with an Olympus DP70 camera and Olympus CellSens Software. These examinations were undertaken to validate the annual age of the otolith samples used for microstructure and LA-ICPMS. In addition, the distance between the primordium and the formation of the first annual increment, and otolith edge was measured along LA profiles.

5.2.4. Statistical analyses

All data manipulations and statistical analyses were performed in R software, version 4.0.5 (R Core Team 2021). Data manipulations and plots were undertaken using the ‘tidyverse’ version 1.3.1 (Wickham *et al.* 2019) and ‘patchwork’ version 1.1.1 (Thomas Lin Pedersen 2020) packages. Packages used for statistical analyses are specified in the paragraphs below.

Otolith microstructure

The reproducibility of growth increment (GI) estimates was described using the coefficient of variation (CV) and an index of average percent error (APE) following the method of Beamish and Fournier (1981) using the FSA package, version 0.9.1 (Ogle 2016):

$$APE = 100 \left[\frac{1}{N} \sum_{j=1}^N \left(\frac{1}{R} \sum_{i=1}^R \frac{|X_{ij} - X_j|}{X_j} \right) \right]$$

where N is the number of GIs counted; R is the number of times each fish’s otolith was read; X_{ij} the average GIs calculated for the j th fish from all reading; and X_j the reading for the j th fish.

Total number of GI were plotted against the date of capture (days since January 1) to confirm daily formation of growth increments. The data were fitted with a linear regression model of which the regression slope (m) was compared to 1 to validate the interpretation of the number of GIs as a daily age post-hatch (dph). A value that equals 1 infers a single growth increment is formed for each day of life. From the ageing data and the date of capture, the distribution of hatching dates of specimens was then back-calculated for the pooled sample.

For a description of the daily growth patterns of age-0+ fish, the relationship between length and age was fitted with a second-order polynomial regression:

$$TL_i \sim \alpha + \beta * dph_i + \beta * dph_i^2 + \varepsilon_i$$

$$\varepsilon_i \sim N(0, \sigma^2)$$

where α is the intercept and β reflects the second-order polynomial parameter estimates for the daily age post-hatch variable.

Cumulative age estimates were also recorded at 50 μm intervals from the primordium to the dorsal edge of each otolith, the same axis from which LA profiles were taken. The relationship between distance from the otolith core and cumulative daily age post-hatch was determined from the pooled data by fitting a second-order polynomial regression:

$$dph_i \sim \alpha + \beta * Distance_i + \beta * Distance_i^2 + \varepsilon_i$$

$$\varepsilon_i \sim N(0, \sigma^2)$$

where α is the intercept and β reflects the second-order polynomial parameter estimates.

Temporal trends in elemental profiles

Element:Ca ratios were analysed for Strontium (Sr^{88}), Barium (Ba^{137}), Magnesium (Mg^{24}), and Manganese (Mn^{54}) from across the age-0+ region of LA profiles. Distances from hatching to the extent of the core region for each LA profile were converted to ages based on the daily age post-hatch:Distance relationship. One issue that arises when interpreting a laser scan is data spacing (Hoover *et al.* 2012). As a result of the laser sampling along the defined otolith transects at a constant speed, the resulting data are distributed equally in both laser-space and laser-time. The number of data points contained within each standardised growth increment, therefore, varies.

Generalised additive mixed models (GAMMs) were fitted to describe temporal patterns (daily age post-hatch) in the elemental profiles for each of the four elemental ratios (Sr, Ba, Mg, Mn) and to see if profiles differed between birth years and areas of capture (Zuur *et al.* 2009). GAMMs were fitted using the 'mgcv' package, version 1.8-34 (Wood 2017). The response variables and variables were explored for outliers, and explanatory variables investigated for the presence of collinearity using Pearson correlation coefficients (>0.5) and variance inflation factors (VIF, >3) according to the protocols described by Zuur *et al.* (2010). Elemental ratios outside of 3 S.D points of the mean of each elemental profile were subsequently removed from the data as outliers. Areas of the otolith sections that had been contaminated by polyester resin were easily identifiable through large spikes in Mg and Mn and removed from the data for all elements. Preliminary data exploration indicated that a Gaussian distribution could be assumed for the response variables. To incorporate the dependency among observations of the same otolith, otolith ID was treated as a random variable. Issues of residual autocorrelation, identified with an autocorrelation function plot, were accounted for by the incorporation of a lag-one autoregressive parameter in the error structure (AR-1) using the 'itsadug' version 2.4. package in R (van Rij *et al.* 2020). The degree of correlation between

the errors was specified manually based on the estimate from each original model (excluding the AR-1 structure). Models were specified as follows:

$$(RE_{ij}) \sim \alpha + OtolithID_i + s(dph_{ij}) + Area_{ij} + YearBirth_{ij} + \varepsilon_{ij}$$

$$\varepsilon \sim N(0, \sigma^2)$$

Where RE is the element:Ca molar ratio, α is the intercept, and $s()$ is a smooth term, fitted to the daily age post-hatch covariate and represented by a cubic regression spline. Otolith ID is the random intercept that is assumed to be normally distributed with mean 0 and variance σ^2 . The index i refers to Otolith ID ($i = 1$ to 180) and j to the observation within an otolith ID ($j = 1$ to 325). The term ε_{ij} is the within-otolith variation and is assumed to be independently normally distributed with mean 0 and variance σ^2 .

GAMMs were fitted, estimating degrees of freedom (df) for the age smoother by generalised cross-validation. Best fit models were selected using backwards selection on the basis of the lowest value of Akaike Information Criterion adjusted for small sample sizes (AICc; Burnham and Anderson, 2002), providing that there were no discernible patterns in residuals.

Dynamic life-history shifts

Otolith microstructure revealed the formation of a prominent hyaline zone laid down near the edge of the otolith of all specimens (Marker 1: LHS_{OS}; Figure 33). This zone was clearly visible in corresponding otolith transverse sections. The distance along LA profiles that the LHS_{OS} occurred was measured and converted to daily age post-hatch, based on the otolith distance: daily age post-hatch relationship.

The statistical procedure ‘change point analysis’ was used to generate four additional markers of LHS for each LA profile: Sr - LHS_{Sr}, Ba - LHS_{Ba}, Mg - LHS_{Mg} and Mn - LHS_{Mn}. Change point analysis is a statistical tool used for estimating the points at which the statistical properties of a sequence of observations change. The application of this technique to time series data has the ability to identify the point of dynamic regime shifts (Möllmann *et al.* 2021) and, through changes in individual otolith elemental ratios, transition periods in early life-history stages (Hegg *et al.* 2019; Rooker *et al.* 2021). We considered a changing functional relationship in elemental ratios that occur in the core region of Patagonian toothfish elemental profiles to reflect dynamic life-history shifts that occur between the hatching of pelagic larvae in the oceanic environment, to the occurrence of early juveniles in nursery areas on the Patagonian Shelf.

Each of the four elemental ratios were smoothed across the core region of individual fish otoliths (n = 120) by calculating a 7-point moving average (n = 480; 120 fish otoliths * 4 elemental ratios). Change point analysis was applied to each smoothed elemental profile by testing for single change points in the mean and variance using the Binary Segmentation (BinSeg) algorithm in the ‘change point’ package, version 2.2.2 (Killick and Eckley 2014).

A linear mixed-effects model was used to determine whether the timing of life-history shifts for Patagonian toothfish (LHS), differed according to (1) the five methodological approaches (markers) used: LHS_{OS}, LHS_{Sr}, LHS_{Ba}, LHS_{Mg} and LHS_{Mn}; (2) the three areas of capture: W, NE and S; and (3) the four birth years examined: 2013, 2014, 2015, 2016. Otolith ID was included as a random intercept to account for a lack of independence for LHS estimated from the same otolith:

$$(LHS_{ij}) \sim \alpha + OtolithID_i + Marker_{ij} + Area_{ij} + YearBirth_{ij} + \varepsilon_{ij};$$

$$\varepsilon \sim N(0, \sigma^2)$$

where α is the model intercept, and otolith ID is the random intercept that is assumed to be normally distributed with mean 0 and variance σ^2 . The index i refers to Otolith ID ($i = 1: 180$) and j to the observation within an otolith ID ($j = 1:5$). The term ε_{ij} is the within-otolith variation and is assumed to be independently normally distributed with mean 0 and variance σ^2 .

Best fit models were selected using backwards selection on the basis of the lowest value of Akaike Information Criterion adjusted for small sample size (AICc; Burnham and Anderson, 2002). The optimal model was visually inspected for homogeneity of the residuals by plotting the residuals against the fitted values. Normality of the residuals and random effects was inspected through QQ-plots of the normalised residuals.

Given that otolith microstructure (LHS_{OS}) and elemental profiles for Sr:Ca, Ba:Ca, Mg:Ca and Mn:Ca may reflect environmental or physiological drivers that identify life-history shifts differently, an integrated changepoint (LHS_{INT}) was estimated for each individual fish otolith. This was based on the average life-history shift estimated according to the five markers. The age-frequency distribution for LHS_{INT} was plotted for inspection of patterns.

5.3. Results

5.3.1. Otolith microstructure

Three independent growth increment (GI) counts were successfully performed on 60 age-0+ individuals, with corresponding APE and CV of 4.17% and 6.62%, respectively. These values indicate a medium to high level of reproducibility, providing validity to the methods of otolith preparation for microstructure analyses. Growth increments, typically consisting of bipartite rings with alternating discontinuous (dark) and incremental (light) zones, were clearly visible in the otolith microstructure preparations (Figure 33D). A well-defined (hatch) check was present 4 to 6 increments after the primordium, which was separated by a second strong

growth check (GC) 8 to 11 increments thereafter. Otolith microstructure revealed the formation of a prominent hyaline zone laid down near to and extending to the edge of the otolith of all specimens. This zone was also clearly identifiable in transverse sections of otoliths from age-0+ fish, and the age-1+ fish that were used in elemental analyses.

GI counts for juvenile Patagonian toothfish ranged from 102 to 175 (mean \pm SD = 130 ± 16.54 GIs) and showed a significant linear relationship with day of capture (Table 14; Figure 34A). The slope (\pm 95% CI) of the fitted linear model ($m = 0.98 \pm 0.19$) was not significantly different from 1 ($F = 0.035$, $P = 0.85$), thus validating GI counts as daily age post-hatch (dph). The linear model fit was used to predict the mean (\pm 95% CI) date of first increment formation as 03 October (\pm 8.47 days). This was reflected in the hatch date distribution (Figure 34B). The range of hatch dates were distributed between 10 September and 30 October, with a clear modal peak occurring over the first 10 days of October. Fish ranged in length from 6-15 cm with total length showing an initial rapid increase with age, which slowed down after 145 days post-hatch (25 February; Figure 34C). The decrease in growth rate coincided with the end of the austral summer, given the 03 October hatch date. The daily age post-hatch:Distance relationship was well-represented by the fitted second-order polynomial regression, meaning that the age along elemental transects could reliably be predicted as a result (Table 14; Figure 34D).

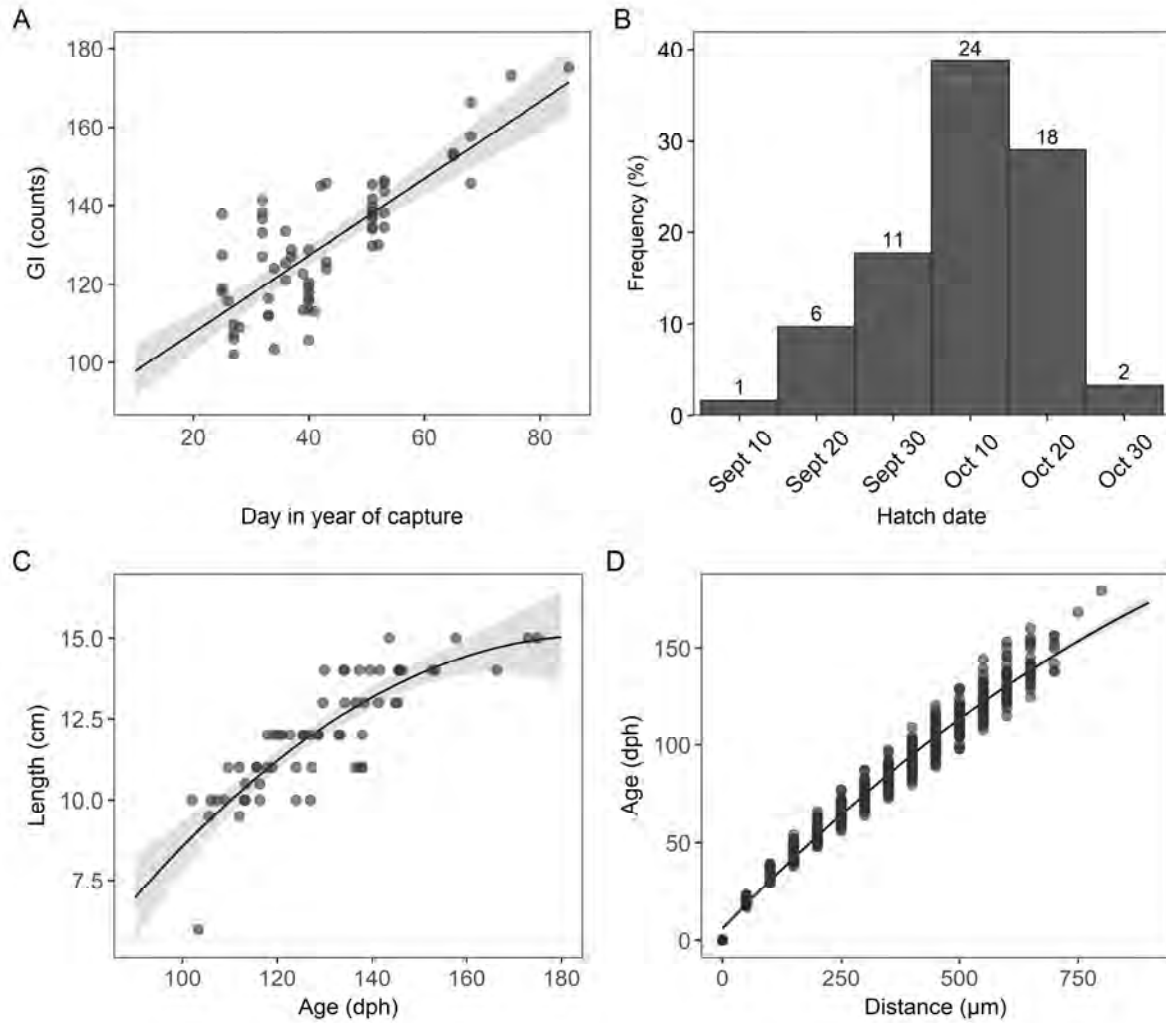


Figure 34: (A) Relationship between the day in year of capture (from 1 January) and otolith increment counts (Increments; $R^2 = 0.64$); (B) the distribution of hatching dates over ten-day periods, back calculated from the date of capture, from daily age estimates; (C) relationship between age (days post-hatch, dph) and length ($R^2 = 0.72$); and (D) distance from otolith primordium and age (days post-hatch, dph) developed for age-0 Patagonian toothfish ($n = 60$; $R^2 = 0.99$).

Table 14: Parameter estimates for (1) the linear model describing the relationship between growth increment and day of capture; and the second-order polynomial regression describing (2) the length: age and (3) age:otolith distance relationships.

Model	Parameter	Estimate	s.e.	t	P	R ²
1	Intercept	87.94	4.29	20.48	<0.0001	0.64
	Day of capture	0.98	0.096	10.24	<0.0001	
2	Intercept	-1.50	6.03	-2.48	0.02	0.72
	Age	0.32	0.09	3.56	0.0008	
	Age ²	-8.6*10 ⁻⁴	3.3*10 ⁻⁴	-2.57	0.01	
3	Intercept	5.9	0.53	11.05	<0.0001	0.99
	Distance	0.25	3.86*10 ⁻³	65.14	<0.0001	
	Distance ²	-7.33*10 ⁻⁵	5.93*10 ⁻⁶	-12.35	<0.0001	

5.3.2. Temporal trends in elemental profiles

Elemental profiles for all GAMMs showed noticeable ontogenetic shifts across the first 200 days post-hatch (Figure 35). For Sr:Ca, the final GAMM model containing days post-hatch and year of birth as significant terms explained 56.80% of the deviance. Sr:Ca ratios during 2013 were lower compared to subsequent years (2014 - 2016). Sr:Ca ratios were highest during the first 30 to 40 days post-hatch, showing a prominent decline over the next 70 to 80 days. Sr:Ca ratios were at their lowest between 100 and 120 days prior to displaying an increase until day 200.

For Ba:Ca ratios, the final model explained 36.8% of the deviance and contained significant terms for daily age, and birth year. Ba:Ca ratios were higher during the 2014 and marginally lower during the 2015 birth years. The daily age smoother for Ba:Ca showed a general decline,

which increased from day 60 to 110 days. The decline in Ba:Ca ratios reached their minimum from 110 days, gently increasing thereafter.

GAMMs describing temporal trends in Mg:Ca ratios included significant terms for birth year, explaining 85.4% of the deviance. The 2016 birth year contained marginally higher Mg:Ca ratios compared to 2013, 2014 and 2015. The daily age smoother predicted for Mg:Ca displayed an initial decline, stabilising from 90 to 160 days before sharply dropping until day 200.

Both year of birth and area were included in the final model describing temporal trends in Mn:Ca ratios. The smoother for Mn:Ca ratios (deviance explained = 32.20%) showed almost the opposite pattern to that predicted for Sr:Ca profiles. Mn:Ca ratios were low over the first 20 days post-hatch, before steadily increasing until 80 days post-hatch. A peak maximum was reached between 80- and 110-days post-hatch after which the ratios decline to their minimum at 170 days post-hatch. Fish born in 2015 and 2016 had lower Mn:Ca ratios compared to those born in 2013 and 2014, while fish captured in the south had higher Mn:Ca ratios in the LA profiles.

The strong significance of the random effect for fish ID reflected high variability in the elemental ratios across individuals that was not described by any of the parametric terms included in the model.

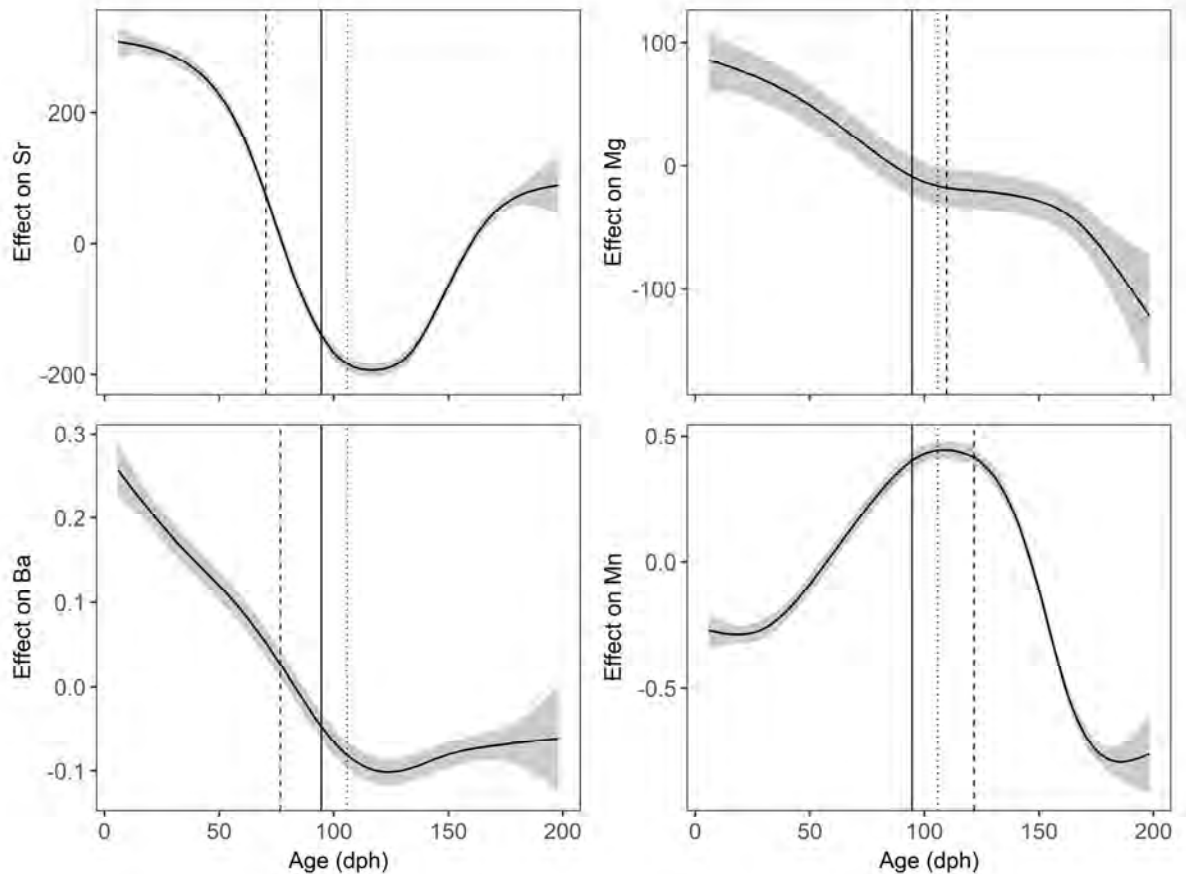


Figure 35: Results of the generalised additive mixed models (with 95% confidence intervals) showing the ontogenetic relationship in age (days post hatch, dph) with Sr, Mg, Ba and Mn element:Ca ratios for juvenile Patagonian toothfish. Dotted vertical line reflects the average distance observed to the hyaline zone defined as a life-history shift (LHS) marker in age-0 otolith sections analysed for microstructure ($n = 62$), and subsequently identified in otolith transverse sections from age-1 individuals used for elemental analyses (LHS_{OS}, $n = 120$). Dashed (LHS_{Sr}, LHS_{Ba}, LHS_{Mg} and LHS_{Mn}) and solid (Integrated approach, LHS_{INT}) vertical lines reflect the average changepoints estimated across elemental profiles, respectively.

5.3.3. Dynamic life-history shifts

High levels of individual variation were present in the life-history shifts estimated along element-specific profiles, nonetheless, common patterns were evident (Figure 36). Mean changepoints estimated along Sr:Ca profiles (mean \pm s.d. = 70.4 ± 23.80 days post-hatch)

indicated life-history shifts as ratios declined between the maximum peak (0 to 50 days post-hatch) and minimum values that occurred after 110 days post-hatch. A similar pattern was evident in the changepoints estimated along Ba:Ca profiles (mean \pm s.d. = 76.70 ± 41.00 days post-hatch); which tended to occur along the inflection point where the decline in Ba:Ca ratios towards their minimum values increased. Mean changepoints estimated along Mg:Ca LA profiles (mean \pm s.d. = 110.00 ± 42.30 days post-hatch) occurred at the base of the initial decline, within a stabilised zone along LA profiles. Mn:Ca profiles reflected mean changepoints at the extent of the maximum ratios, prior to the steep decline (mean \pm s.d. = 122.00 ± 42.80 days post-hatch). Life-history shifts estimated from otolith microstructure observations (mean \pm s.d. = 106.00 ± 15.10 days post-hatch) occurred at the local minima (for Sr, Ba and Mg) or maxima (for Mn), after the initial decline and incline over the first 90 to 110 days post-hatch (Figure 35).

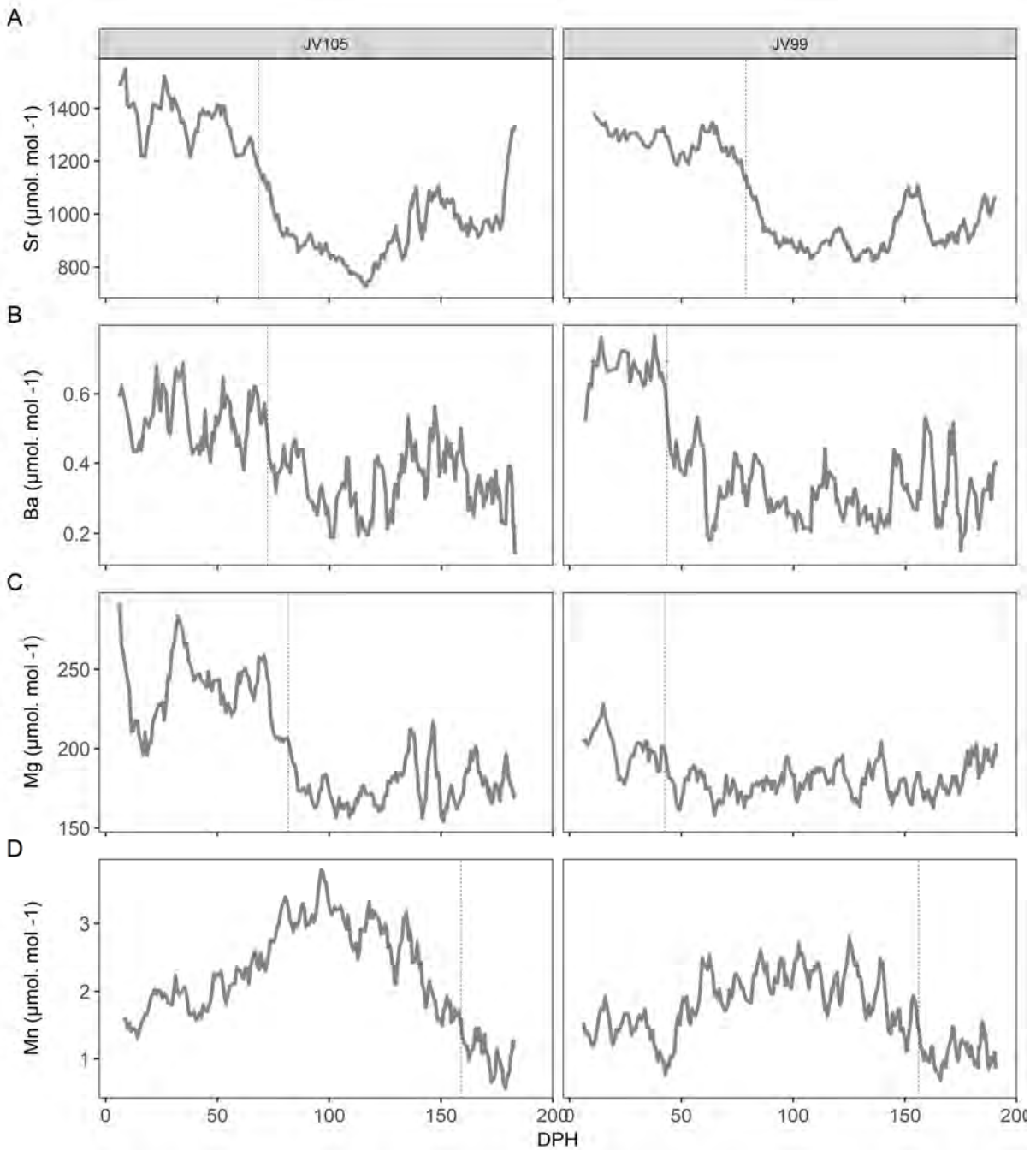


Figure 36: Otolith (A) Sr, (B) Ba, (C) Mn and (D) Mg element:Ca profiles for two individual (Otolith ID = JV105 and JV99) Patagonian toothfish. Grey solid lines represent the seven-point moving average of elemental ratios estimated over age (days post-hatch, dph). The grey dashed vertical lines indicate the dynamic life-history shift, as estimated for the particular individual based on changepoint analysis.

The final linear mixed-effects model showed that there was a significant effect of marker ($F = 53.09$, $df = 4$, $P < 0.0001$) and area ($F = 7.90$, $df = 2$, $P = 0.0006$) on the timing that life-history shifts occurred. The standard deviation of the random intercept for otolith ID was 8.55 days post-hatch.

The year of birth of sampled fish did not improve the fit of the final model. The predicted daily age that changepoints occurred were significantly earlier for the capture area to the W ($t = -3.41$, $P = 0.0009$), with no differences taking place between the NE and S ($t = 0.04$, $P = 0.97$) of the Falkland Islands (Figure 37A). Differences in changepoints estimated according to the five markers occurred in two main groupings (Group 1: Sr:Ca and Ba:Ca; Group 2: Mg:Ca, Mn:Ca and OS; Figure 37B). Those estimated from Sr:Ca and Ba:Ca elemental profiles were similar ($t = 1.44$, $P = 0.15$), with both occurring earlier compared to all the other markers ($P < 0.0001$). Changepoints estimated from Mg:Ca profiles showed no differences compared to those derived from otolith microstructure observations ($t = 0.88$, $P = 0.38$). Changepoints estimated from Mn:Ca profiles occurred later than those estimate from Mg ($t = 2.79$, $P = 0.005$) and otolith microstructure ($t = 3.66$, $P = 0.0003$) derived life-history shifts.

Integrated changepoints estimated for each fish across all five markers (mean \pm s.d. = 96.9 ± 18.1 days post-hatch) contained three modal peaks occurring at 66-75, 91 - 95 and 101 -105 days post-hatch (Figure 38).

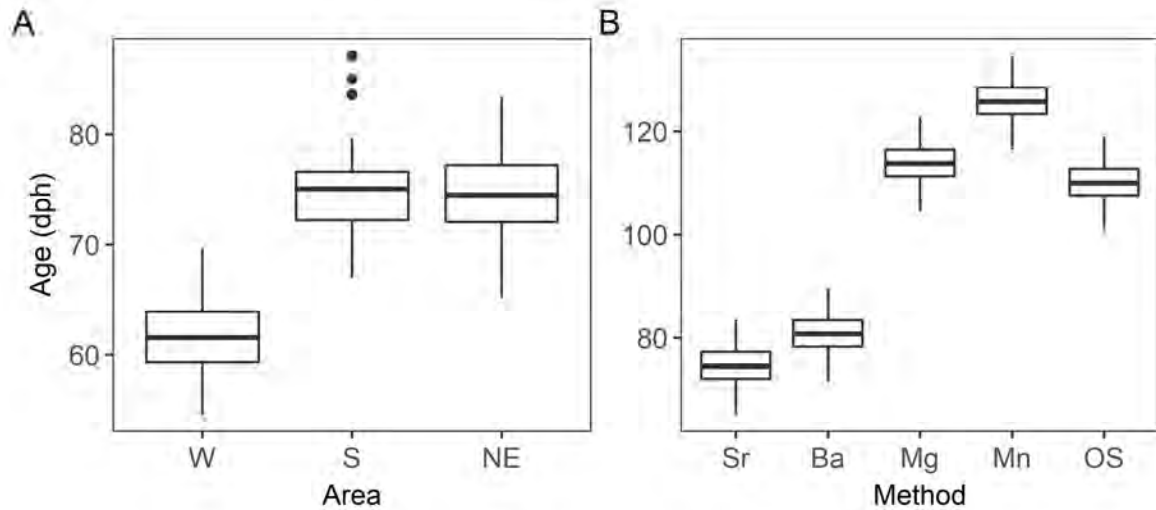


Figure 37: Boxplots comparing model predictions of the daily age post-hatch (dph) that life-history shifts occur among (A) the three areas: NE - Northeast, S - South and W - West; and (B) the five markers based on changepoints estimated across element:Ca profiles for Sr, Ba, Mg and Mn; and from otolith microstructure observations (OS). The y-axis is reflected on the scale of the marker for Sr:Ca and area NE which were arbitrarily selected for the intercept to produce the plots.

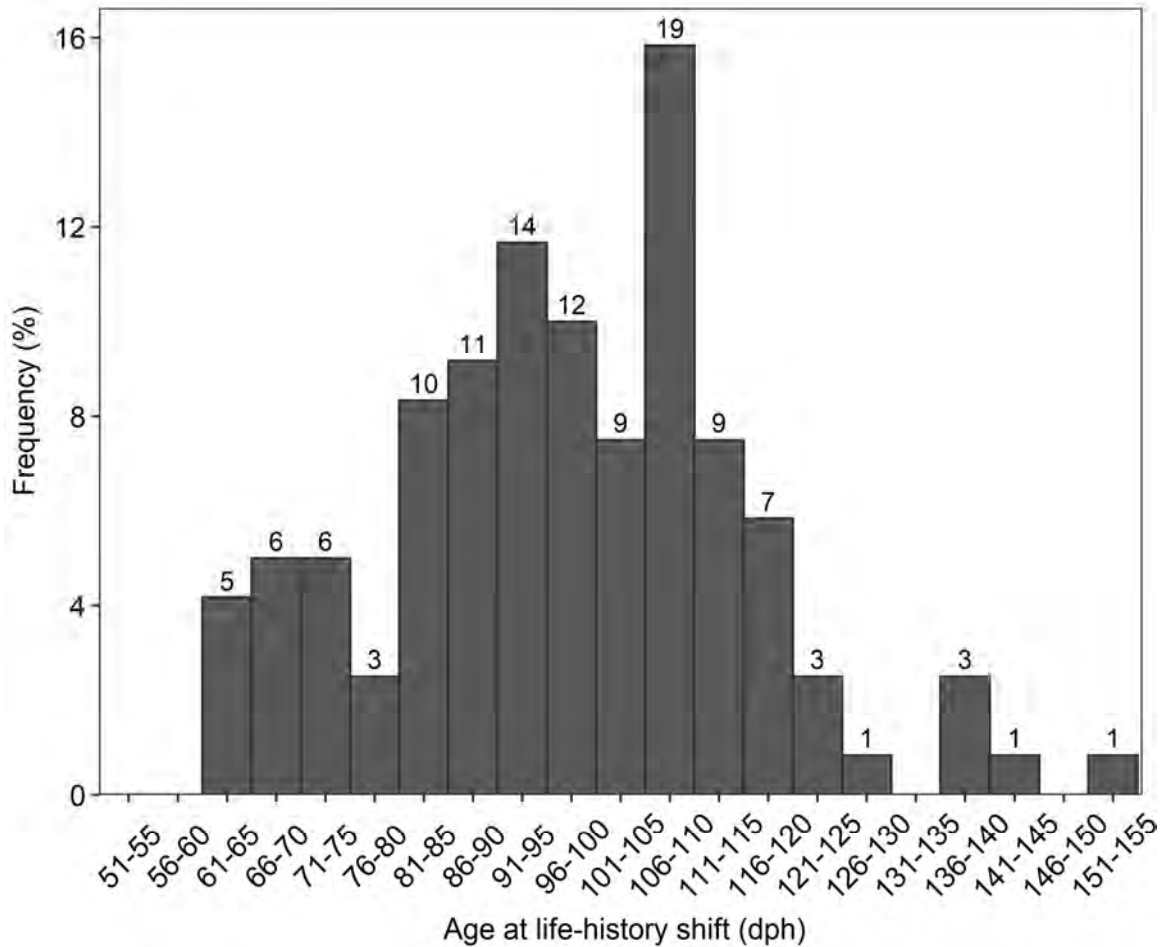


Figure 38: Age-frequency distribution of dynamic life-history shifts for Patagonian toothfish, detected using otolith Sr:Ca, Ba:Ca, Mg:Ca, and Mn:Ca profiles. Estimated age that life-history shift occurred for each individual was based on the average changepoint estimated from all five markers. Sample sizes are indicated above each bar.

5.4. Discussion

In the current study, a novel approach was used, based on otolith microstructure and microchemical analyses, to investigate previously unobserved life-history stages in juvenile Patagonian toothfish. Divergences in the observed otolith microstructure patterns and age-resolved elemental profiles were linked to biological benchmarks that coincide with reported life-history shifts; including: (1) the dispersal of pelagic larvae from cold deep, oxygen rich waters, (2) their entry onto the Patagonian shelf, (3) settlement into a demersal habitat, and

(4) subsequent active migration into juvenile nursery areas. These results provide an important contribution to understanding ontogenetic development during a critical period in the life-cycle for this iconic deep-sea predator.

5.4.1. Otolith microstructure examination

Results of the current study provided the first confirmed evidence of daily increment formation on the otoliths of juvenile Patagonian toothfish, and a description of early growth patterns in the species. Previous research investigating aspects related to the age and growth in Patagonian toothfish have focussed on the adult component of the life-history (5 to 30 years), with annual formation of growth zones validated through the use of marginal increment analysis (Horn 2002) and lead-radium dating (Andrews *et al.* 2011). Few studies have investigated otolith microstructure of other notothenioid fish. Validation of daily growth increment formation has been undertaken for two known species, mackerel icefish *Chamsocephalus gunnari* (Morley *et al.* 2005) and *Trematomus newnesi* (Radtke *et al.* 1989). Daily growth increment formation has, however, been assumed in many other species, for example, *Patagonotothen ramsayii* and *Eleginops maclovinus* (Brickle *et al.* 2005; Brickle *et al.* 2006a), as well as in the larvae of the closely related Antarctic toothfish *D. mawsoni* (La Mesa 2007).

The methods used to prepare and age juvenile toothfish otoliths provided clear growth increments from hatching through to in excess of 185 days. Following the otolith primordium, a presumed hatch check was identified after 4 to 6 increment counts, followed by a strong growth check, 8 – 12 days thereafter. These features are consistent with descriptions of the otoliths from larval Antarctic toothfish in the Ross Sea (9 to 11 days) and mackerel icefish off South Georgia (14 to 37 days; La Mesa, 2007; Morley *et al.*, 2005). This second strong growth check was identified as a signal, defining a shift from subsistence on endogenous yolk

supplies to exogenous feeding. A study on the embryonic and early larval development of laboratory-reared Patagonian toothfish described the absorption of the yolk sac and shift to exogenous feeding to occur between 15 and 18 days after hatching (Mujica *et al.* 2016), aligning closely with the results described in the current study.

The distribution of back-calculated hatch dates indicated a discrete hatch period occurring over September and October, with a mean date of birth on the 3 October (± 8.47 days). Given the July to September spawning period described off southern Chile and the Burdwood Bank (Laptikhovsky *et al.* 2006a; Arana 2009), this would mean a 30 to 90 day phase of egg development. Laboratory reared Patagonian toothfish eggs hatch between 30 and 33 days post-fertilization (Mujica *et al.* 2016), although in the wild this period may be more protracted. North (2002) described a later hatch period for Patagonian toothfish, extending from November through to mid-December, with egg development taking 3.5 months. These results were based on an examination of the intercept from a generated length-date of capture relationship, constructed from 43 larval specimens, taken in pelagic surveys off South Georgia, Shag Rocks and the Burdwood Bank between 1987 and 2001. The earlier hatch date estimated in the current study may be due to a combination of large-scale environmental differences between the two regions of study, as well as strong genetic heterogeneity among the two Patagonian toothfish populations that have been shown to occur across the APF (Shaw *et al.* 2004; Rogers *et al.* 2006).

Two clear limitations were (1) the coupling of high recruitment years for daily increment validation (2014 to 2016 birth years), and the relatively short time-frame from which daily growth observations were extracted (102 to 185 days). Observations of length-frequency distributions for age-0+ Patagonian toothfish, highlights the consistent increase in length across birth years used in the current study (Lee *et al.* 2021). This leads to the assumption that a single batch of juveniles were selected from each of the three years, that align over the total time period. Further, samples from early-life-history stages of age-0+ Patagonian

toothfish remain rare and are generally limited to the periods of collection during research specific surveys (February). By the time juvenile toothfish begin to get captured at depths targeted by commercial fisheries within the region (largely from July), their increased development and growth makes the preparation of otoliths for daily increment counts extremely challenging, and subsequent age estimates unreliable (BL pers. obs.). This factor provides a distinct constraint on the time period during which samples can be obtained for analyses.

5.4.2. Temporal trends in elemental profiles

Elemental profiles derived from the otoliths of Patagonian toothfish showed clear changes during the first year of life. The integrated usage of otolith microstructure and changepoint analyses served as a novel approach for the identification of life-history shifts during this key, yet unknown period. Patagonian toothfish occupy a range of divergent habitats across their early life-history including: an oceanic pelagic phase dominated by systems affiliated with the APF; an inshore shelf-based pelagic phase dominated by the influence of the Falkland Current and Patagonian Current; a settlement phase into an inshore demersal habitat; and an ontogenetic migration into deeper waters characterised by upwellings of oceanic driven systems. Given the distinct physical and chemical properties inherent in these water bodies, divergences in the elemental profiles would likely predict the timing of movements across these environments, as well as physiological changes that occur across their development that are linked to these movements.

Sr is incorporated into the otolith in proportion to that of ambient seawater composition and has been shown to display a positive relationship with salinity (Fraile *et al.* 2016) and a negative relationship with water temperature (Ashford *et al.* 2012b); providing a strong basis for the reconstruction of fish life-history profiles in fish. High Sr:Ca ratios characterise oceanic areas in the APF, with lower ratios occurring over the shelf around the Falkland Islands

(Ashford *et al.* 2012b). The initial stable high Sr:Ca ratios over the first 30 to 40 days post-hatch were therefore interpreted to reflect an oceanic habitat, dominated by the cold APF. During this time period, Patagonian toothfish would be at a larval life-history stage of development (Mujica *et al.* 2016) during which they are known to be pelagic, occurring within the upper 50 to 250 m of the water column, over depths of up to 3000 m (North 2002). Movement during this life-history stage is considered to largely exist through passive dispersal through the prevailing currents in the region. The steep decline in Sr:Ca ratios over the following 70 to 80 days would likely reflect the entry of pelagic larvae onto the warmer (decreasing Sr:Ca ratios) inshore shelf waters of the Falkland Islands (LHS_{Sr}), followed by their settlement into a demersal habitat within inshore warmer waters (110 to 130 days post-hatch; LHS_{Os}). Following this phase, increases in Sr:Ca over the next 70 days may be an interactive indication of their initial ontogenetic migration into deeper (100 to 150 m), colder waters, and a seasonal effect as a result of the completion of the austral summer (mid-April given an October hatch date). Such ontogenetic migratory behaviour has been displayed through analyses of length-frequency distributions (Belchier and Collins 2008; Arkhipkin and Laptikhovskiy 2010) and spatial modelling of nursery areas relative to early juvenile (age-1) habitats (Lee *et al.* 2021).

Ba:Ca ratios are also thought to be under strong environmental control (Izzo *et al.* 2016a; Busbridge *et al.* 2020), previously being inversely linked to temperature and salinity and positively related to upwellings of nutrients (Izzo *et al.* 2016b; Heimbrand *et al.* 2020). Ba:Ca ratios in the otoliths of Patagonian toothfish have previously been linked to nitrate-fuelled productivity in the APF (Ashford *et al.* 2005b; Ashford *et al.* 2012b). In the current study, Ba:Ca elemental profiles were indicative of similar life-history patterns to those observed across Sr:Ca elemental profiles. High, but declining Ba:Ca ratios over the first 60 days post-hatch indicate an early life-history period undertaken in the productive waters of the APF, and the passive dispersal of larvae into north-flowing regional systems of the Falklands Current or Patagonian Current. The steep increase in the decline of Ba:Ca ratios between 60- and 100-

days post-hatch may be indicative of the subsequent passive dispersal and active movement of larvae and early juveniles onto the inshore waters of the Falklands Shelf (LHS_{BA}). Low Ba:Ca ratios from 100 to 130 days post-hatch may subsequently be a reflection of settlement into a demersal habitat in shallow inshore waters (LHS_{OS}). As reflected in Sr:Ca ratios, the incline of Ba:Ca ratios over the next 70 days may be indicating their subsequent ontogenetic migration into their juvenile nursery areas. Following settlement, age-0+ Patagonian toothfish around the Falkland Islands have been recorded in spatially discrete nursery areas corresponding to the areas sampled in the current study. These areas correspond to quasi-stationary mesoscale frontal zones that occur through the upwelling of subantarctic waters onto the shelf (Croxall and Wood 2002; Arkhipkin *et al.* 2013; Lee *et al.* 2021), and are characterised by cold, highly productive and oxygen rich waters driving increased Ba:Ca and Sr:Ca concentrations (and declining Mn:Ca ratios – see below).

Results of the current study indicated an initial decline in Mg:Ca ratios (0 to 100 days post-hatch; LHS_{Mg} and LHS_{OS}), a period of stable concentrations (100 to 150 days post-hatch) followed by further declines (150 to 200 days post-hatch). The incorporation of Mg into the otolith has been suggested as driven by physiological controls, indicative of high metabolic activity and somatic and otolith growth (Sturrock *et al.* 2015; Limburg *et al.* 2018; Heimbrand *et al.* 2020). This was supported by both otolith elemental and microstructure results from the current study, whereby the general decline in Mg:Ca ratios correspond with initial fast growth of larval fish slowing down with increasing daily age. Ashford *et al.* (2005, 2007) associated high Mg:Ca concentrations with circulation between the Burdwood Bank and southern Patagonian Shelf. This is further indication of the oceanic influence of larval Patagonian toothfish over the first 30 to 90 days post-hatch.

Mn:Ca ratios in otoliths have been related to physiological influences in some fish species, with somatic growth being described as being of particular importance (Sturrock *et al.* 2014; Grønkjær 2016; Izzo *et al.* 2016a; Busbridge *et al.* 2020). Enriched otolith Mn:Ca ratios off

South America have also been linked to authigenic activity at the ocean-sediment interface, or resuspension from anoxic sediments (Ashford *et al.* 2005b; Ashford *et al.* 2007). In this way, increased Mn:Ca ratios may reflect an association with the Patagonian Shelf-based environment, and the frontal zones that occur along the shelf-slope interface. Elevated Mn:Ca ratios have also been attributed to low-oxygen conditions (Limburg *et al.* 2015; Heimbrand *et al.* 2020). Research has indicated that Patagonian toothfish have a very low oxygen affinity (Coppola *et al.* 2015), with juvenile Patagonian toothfish occurring in a relatively narrow range of moderate to high dissolved oxygen concentrations throughout their shelf-based life-history (Lee *et al.* 2021). Further, variability in oxygen concentrations has been described as a key factor in the survival of new recruits within their inshore habitats (Lee *et al.* 2021). The oceanic environment associated with the APF is oxygen rich (Ashford and Jones 2007); with the Falklands Current and Subantarctic Front distributing these waters across the western, southern and eastern shelf adjacent to and offshore of the 200 m depth contour around the Falkland Islands. These conditions appear to be reflected in the Mn:Ca ratios across the early life-history for Patagonian toothfish. Patterns in the current study indicate high oxygen conditions (low Mn:Ca ratios) during the first 40 days post-hatch, corresponding with the larval oceanic developmental stages. Increasing Mn:Ca ratios correspond with the dispersal of larval fish with the Falklands and Patagonian Currents onto the shelf by 110 days post-hatch (LHS_{OS}). The subsequent steady decline in Mn:Ca ratios after 130 days post-hatch, may be a reflection of a transition (LHS_{MN}) to a demersal habitat and subsequent ontogenetic migration into deeper, oxygen-rich frontal zones as described above.

Although element-specific patterns were prominent, there were high levels of inter-individual variation that was not explained by the area within which fish were captured, nor the year of birth. This could be a result of the limitations in the methodology used. Elemental markers reflect physiology and growth, as well as environmental exposures (Campana and Thorrold 2001). Otolith growth is complex in Patagonian toothfish and varies greatly within individual otoliths (Horn 2002; Arkhipkin and Laptikhovsky 2010). Further, there is a great deal of

variability in elemental markers, even where the otolith material is laid down fairly evenly, such as along the proximal surfaces (Hoover *et al.* 2012; Hoover and Jones 2013). Within spot-based otolith elemental analyses, these can be stabilized, through the use incorporation of a large number of scans in a particular area of the otolith (e.g. core or edge region). However, this is not possible with a transect line as used in the current study, and variation has to be carefully balanced through the spot size, and the speed at which the spot is scanned across the otolith section. As a result, sources of variability as described above, may overwhelm fine-scale signals of interest (Hoover and Jones 2013). This may be exacerbated through the presence of a complex internal structure that may generate misleading artefacts.

An ecological explanation could be that the early life-history period for Patagonian toothfish individuals around the Falkland Islands occurs over an environmental continuum, as opposed to arising from spatially distinct, discrete spawning grounds. Alternately, high variability may be indicating that mixing from spawning areas, as discrete units, occurs during the protracted egg phase of development, prior to the onset of otolith elemental signatures. Finally, this result may also indicate that inter-individual variability is simply greater than the extent of environmental variability across the region, although, given the results obtained from other studies on otolith chemistry (Ashford *et al.* 2005b; Ashford *et al.* 2012b) and shape analyses (Lee *et al.* 2018) for Patagonian toothfish in the region, this consideration is unlikely. Ashford *et al.* (2012) found strong heterogeneity in elemental concentrations (Sr, Ba, Mg and Mn) between fish captured to the north and south of the Falkland Islands shelf. Given the values of elemental ratios from the otolith core that were presented in their study, spots from which concentrations were taken appear to correspond with the post-settlement, juvenile life-history stage (100 to 120 days post-hatch; see discussion below). This period of the life-history occurs subsequent to the dispersal of individuals from spawning areas into spatially discrete recruitment areas (Lee *et al.* 2021), and the findings of this comparison therefore make intuitive sense (i.e. reflecting separate areas of settlement). Further investigation through a comparison of the current data set with baseline samples acquired from the two known

spawning areas off southern Chile and the Burdwood Bank, is therefore required. The presence of well-defined trends for all elements across the core region of Patagonian toothfish identify the care required in the preparation and subsequent interpretation of otolith spot analyses. In particular consideration should be applied to the relative distance that spots are taken across core profiles from the primordium to avoid the discovery of grouping structures that are based on life-history trends instead of population structures.

5.4.3. Timing of life-history events

The timing of life-history shifts for individual Patagonian toothfish varied according to the five markers, with LHS_{Sr} and LHS_{Ba} (LHS-group 1) occurring between one and two months earlier compared to the LHS_{Mg} , LHS_{Mn} and LHS_{OS} (LHS-group 2). Differences in the predicted markers may be reflective of various physiological and environmental factors being displayed more prominently for each of the otolith elemental and microstructure methods investigated. Such variability among markers was also observed when predicting timing of settlement (egress) for Pacific bluefin tuna which was attributed to a three-month lag effect among Mg:Ca, Mn:Ca and Sr:Ca, and the identification of an independent changepoint from the Ba:Ca marker (Rooker *et al.* 2021). In the current study, the LHS among the two groupings was attributed to be a reflection of two to three distinct early life-history processes taking place; (1) the entrance of larval Patagonian toothfish onto the shelf (LHS-group 1), (2) the settlement of early juveniles from a pelagic to a demersal habitat on the shelf (LHS-group 2) and (3) the ontogenetic migration into deeper waters shortly thereafter, (LHS_{Mn}).

The life-history shifts identified through otolith microstructure observations were typified through the formation of a distinct hyaline band from 106 days post-hatch. In the current study, the initiation of this zone was thought to represent the settlement of early juvenile Patagonian toothfish into the deeper shelf waters indicating a shift to a demersal habitat, and an associated change in diet (Morales-Nin 2000; Hogan *et al.* 2017). Based on a mean birth date

of 3 October, this would suggest the onset of settlement during early January (17th) at the peak of the austral summer, and shortly prior to the first juveniles appearing as bycatch in the bottom-trawl fisheries during years of high recruitment (Lee *et al.* 2021). These results coincide with the observed timing of settlement onto the shelf for a number of other species in the region including southern blue whiting (*Micromesistius australis australis*, 76.5 days post-hatch; Busbridge *et al.*, 2020) and common hake (*Merluccius hubbsi*, 80 days; Buratti and Santos, 2010). The formation of a hyaline zone in the otolith microstructure is indicative of physiological stress as the fish adjusts to the new environment (Morales-Nin 2000). This physiological response coincides with the interpretation of changes in the Mg:Ca profile, indicating that the LHS from these two markers are congruent. In contrast, the later LHS_{Mn} is thought to be a reflection of the ontogenetic migration from an inshore, demersal habitat down the slope into oxygen rich waters. In this context the earlier shifts that occurred for Sr:Ca and Ba:Ca were a result of significant changes in the respective LA profiles dominated by the earlier influence of environmental change as larval Patagonian toothfish were dispersed from cold, offshore oceanic waters to inshore waters of the Falkland Shelf.

Life-history shifts among markers occurred earlier for Patagonian toothfish captured in the west compared to the southern and northeast of the shelf. This may be due to juvenile Patagonian toothfish from the west coming from different spawning areas, or along a more direct dispersal pathways compared to those in the south and northeast. This is consistent with the findings of Ashford *et al.* (2012) who used a combination of oceanographic particle simulation modelling and otolith microchemistry to infer that juvenile Patagonian toothfish to the west of the Falklands came from a southern Chile origin, while those to the south and northeast were from a combined southern Chile and Burdwood Bank spawning population.

The LHS_{int} provided a useful, conservative estimate that summarises the overall transition from oceanic-pelagic to demersal habitat into a singular estimate reflecting the timing of settlement for juvenile Patagonian toothfish in the shelf waters of the Falkland Islands (7

January). The three modal peaks reflected in the individual LHS age-distribution may be indicative of the dominance of environmental (earlier modal peak) over physiological (later modal peak) influences within individual elemental profiles (or vice versa); or an indication of discrete spawning areas or periods, contributing varying rates of larval dispersal onto the shelf.

The results of the current study revealed that ontogenetic shifts during the early life-history of Patagonian toothfish resulted in significant changes in otolith microstructure, and across elemental profiles. Age-specific life-history shifts were clearly identified through changepoint analyses, and complied with known interpretations of environmental, physiological and interactive factors. The provision and interpretation of this novel and important information regarding the early life-history period in juvenile Patagonian toothfish identified some key aspects related to future research needs. The inclusion of multiple changepoints across individual elemental profiles may provide further clarity in terms of the potential for the temporal delineation of life-history shifts. Further, key questions remain in terms of the source population of juvenile Patagonian toothfish around the Falkland Islands and greater Patagonian Shelf. There is a stringent need for improved collaborative research within the region that can address these research questions through the integrated application of current research techniques.

Chapter 6 - General Discussion

Stock identification is an important prerequisite for fishery management (Cadrin 2020). The closer management units reflect biological population structure, the better for achieving management (such as optimum yield) or conservation objectives (Cadrin *et al.* 2014). The general aim of this thesis was to provide an improved understanding of the complex stock structure dynamics of Patagonian toothfish in the southwest Atlantic, specifically related to the Patagonian Shelf, slope and deep-sea plains around the Falkland Islands. Through the use of an integrated approach, a range of complementary (Izzo *et al.* 2017; Kerr *et al.* 2017) methods were applied to assess regional connectivity during key life-history stages wherein knowledge was disparate.

6.1. Connectivity of Patagonian toothfish on the Patagonian Shelf

Patagonian toothfish possess complex life-histories including protracted egg and larval stages (Chapter 5) which leads to high dispersal potential (Álvarez-Noriega *et al.* 2020). Further, they are distributed across vast geographical scales and depths (Collins *et al.* 2010). Patagonian toothfish have pelagic larvae (Evseenko *et al.* 1995; North 2002), inshore demersal early-juveniles (Chapter 3 - Lee *et al.*, 2021), down-slope migratory sub-adults (Péron *et al.* 2016), and deep-sea adults showing high site fidelity (Chapter 2 - Lee *et al.*, 2018). In contradiction to following a unified life-history pattern in the region, however, wide-ranging intra-specific variation is also prevalent, and suggestive of more complex stock structure dynamics. For example, there appears to be variability in the timing of pelagic larval settlement to a demersal habitat (Chapter 5); and significant proportions of deep-sea adults also undertake large-scale movements across vast distances (Chapter 4 - Lee *et al.*, 2022). This variability can be considered as key contributions in life-cycle demographic population connectivity in a spatially complex stock structure.

Analyses of otolith shape from an extensive component of their distribution highlighted distinct separation along the Antarctic Polar Front (APF; Chapter 2 - Lee *et al.*, 2018). Otolith microstructure and microchemistry identified a temporally discrete birth date period along with a protracted period of larval dispersal, and discrete timing of settlement into areas on the shelf (Chapter 5). A series of habitat distribution models were used to infer abundance hotspots, ontogenetic migration pathways, and the nature of these in a spatial-temporal context (Chapter 3 - Lee *et al.*, 2021). Further, through the use of otolith shape analyses (Chapter 2 - Lee *et al.*, 2018), clear evidence of high site fidelity was provided. This extended from the period wherein larval Patagonian toothfish were retained in nursery areas as early juveniles, through their associated ontogenetic pathways to early adult life-history stages (Chapter 3 - Lee *et al.*, 2021). An extensive tag-recapture programme, both highlighted this result depicting a highly constrained adult population, with additional complexities revealed (Chapter 4 - Lee *et al.*, 2022). Large components (9 to 25%) of the adult deep-sea population were identified maintaining connectivity across previously considered oceanographic (e.g. Subantarctic Front, Falklands Current) and physical (e.g. Falkland Trough) boundaries, linking the deep-sea northern foraging grounds with spawning areas across the Patagonian population.

6.2. A hypothetical life-history for Patagonian toothfish

Based on the findings of this research, in combination with material from prior studies of its biology, it is possible to start piecing together a tentative life cycle for Patagonian toothfish on the Patagonian Shelf (Figure 39). This can also identify further gaps in our knowledge that can be used to define future research priorities for improved management.

Throughout the discussion below, the terminology defined by Cadrin (2020), Hawkins *et al.* (2016) and Ciannelli *et al.* (2013) were used, whereby a population refers to a group of interbreeding individuals that exist together in time and space. We therefore refer to the Patagonian toothfish population as that encompassing the full Patagonian range. The

Patagonian toothfish population across the Patagonian Shelf is discussed in the context of a possible stock structure continuum, extending across possible sympatric discrete, spatially complex and panmictic population structures (see a further description of the stock structure continuum in Section 1.3). A spatially complex (meta)population is identified as a population consisting of contingents (sub-populations) that exhibit a degree of independence in local population dynamics containing variable connectivity among them (Hawkins *et al.* 2016; Cadrin *et al.* 2020). Such a structure can range from similar discrete contingents connected by relatively rare dispersal events (classical metapopulation), to a source-sink metapopulation structure. A source-sink population structure is characterised by 'donor' groups contributing to 'receptor' components that, while able to survive and grow successfully, become non-breeding vagrants (Sinclair and Iles 1989). Receptor groups can be a result of both spatial (e.g. dispersal beyond the distributional areas of the population) and energetic (e.g. predation, disease, and starvation) processes (Sinclair and Iles 1989). In a source-sink metapopulation structure, the 'sink' feature stems from poor habitat quality (Hawkins *et al.* 2016).

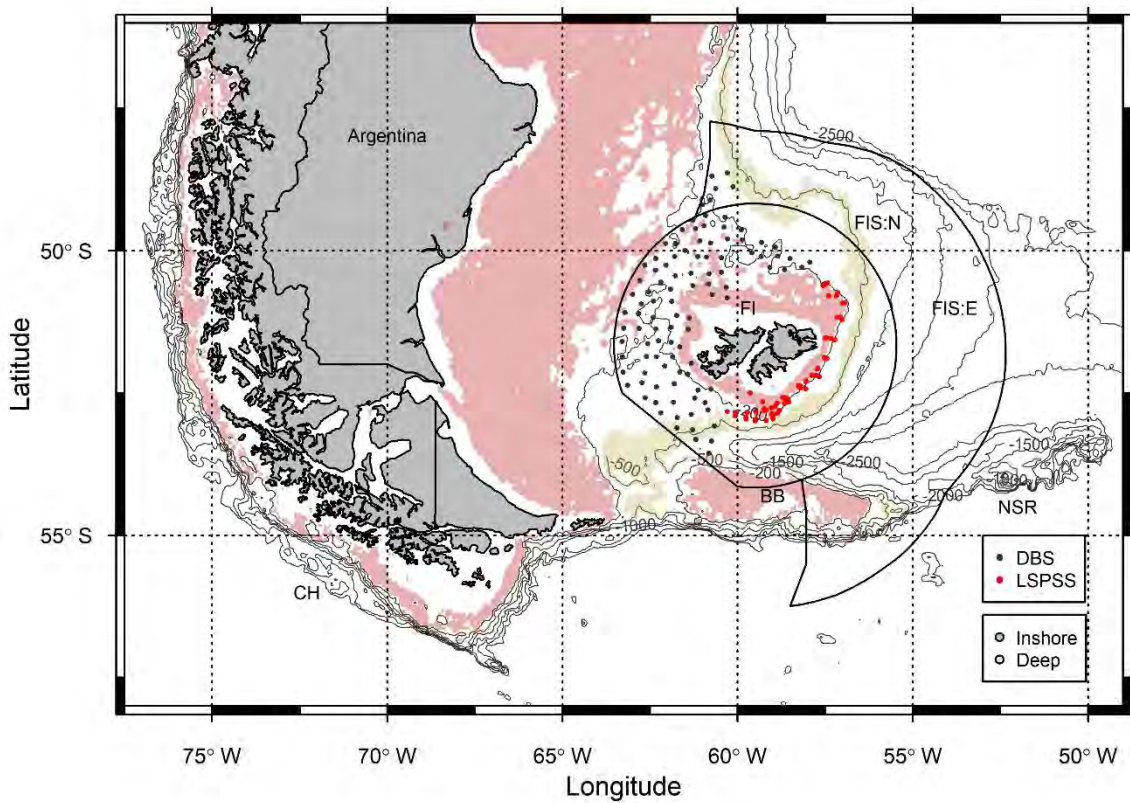


Figure 39: Map depicting the full Patagonian range occupied by Patagonian toothfish across the study area. Solid lines reflect the conservation zones of the Falkland Islands, including juvenile inshore (50 to 150 m) and sub-adult deep-sea areas (401 to 600 m) for which monitoring data are limited. Black points reflect stations from the demersal biomass trawl survey including deep-sea stations used in 2018 (DBS), and red points indicate Lolignid squid pre-season trawl survey stations.

6.2.1. Genetic units

Previous genetic evidence using microsatellites, mitochondrial and nuclear DNA, suggests a single population across the Patagonian region, independent to those to the south of the APF (Smith and McVeagh 2000; Shaw *et al.* 2004; Rogers *et al.* 2006; Canales-Aguirre *et al.* 2018). This clear differentiation in self-sustaining units on either side of the APF was further validated through the use of otolith shape analyses (Chapter 2 - Lee *et al.*, 2018). A recent study I

contributed to at the Falkland Islands Government Fisheries Department (FIFD) suggests two independent evolutionary lineages within the '*D. eleginoides*' complex and their differentiation into two distinct taxonomic entities as separate species based on genomic and morphometric data (Arkhipkin *et al.* 2022). Results of Arkhipkin *et al.* (2022) also implied a complex level of restricted connectivity between local populations of Patagonian toothfish, specifically between fish captured from (1) southern Chile and the Falkland Island; and (2) Falkland Islands and the high seas (North of Falkland Islands), illustrating the Falkland Islands as an intermediate zone of mixing. These findings were initially inferred on the basis of variability (and similarities) in otolith shape among localised regions representing stock contingents on the Patagonian Shelf between Chile, the Burdwood Bank and a Falkland Islands North - High Seas intermediate zone (Chapter 2 - Lee *et al.*, 2018).

6.2.2. Spawning

Evidence from previous research identified two discrete spawning localities off southern Chile, and the Burdwood Bank (Laptikhovsky *et al.* 2006a; Arana 2009). The North Scotia Ridge has also been suggested as a probable spawning area in the region (Laptikhovsky *et al.* 2006a). Spawning has been recorded over May (minor peak) on the Burdwood Bank, and from July to August across both areas (Laptikhovsky *et al.* 2006a; Arana 2009). On the Burdwood Bank, spawning is thought to take place at depths of 900 to 1200 m, during which distinct vertical movements of 150 to 580 m take place (Laptikhovsky *et al.* 2006a; Brown *et al.* 2013a). It remains unclear to what extent the spawning areas are indeed discrete units, or instead comprise a continuum extending from southern Chile, across the entire extent of the Burdwood Bank onto the North Scotia Ridge (see Section 6.4.2: Research Priorities). Results from otolith shape analyses clearly reflect these as discrete population units, although samples from waters intermediate to these areas were not included in the study (Chapter 2 - Lee *et al.*, 2018). In this regard, results from Chapter 5 were inconclusive, with high variability in microchemistry signatures across the early life-history period either being indicative of (1) a

continuous spawning area, (2) the mixing of eggs from discrete areas prior to hatching, or (3) the retention of juveniles around the Falkland Islands from only a single discrete area (Figure 40). No spawning has been observed on the shelf, slope and deep-sea plateau in waters north of the Falklands Trough (ca. 53.5°S) despite extensive monitoring by FIFD fisheries observers since 1994 (Laptikhovsky *et al.* 2006a). Further research is required to understand the extent that adult fish in this region contribute to the spawning stock (Chapter 4 - Lee *et al.*, 2022).

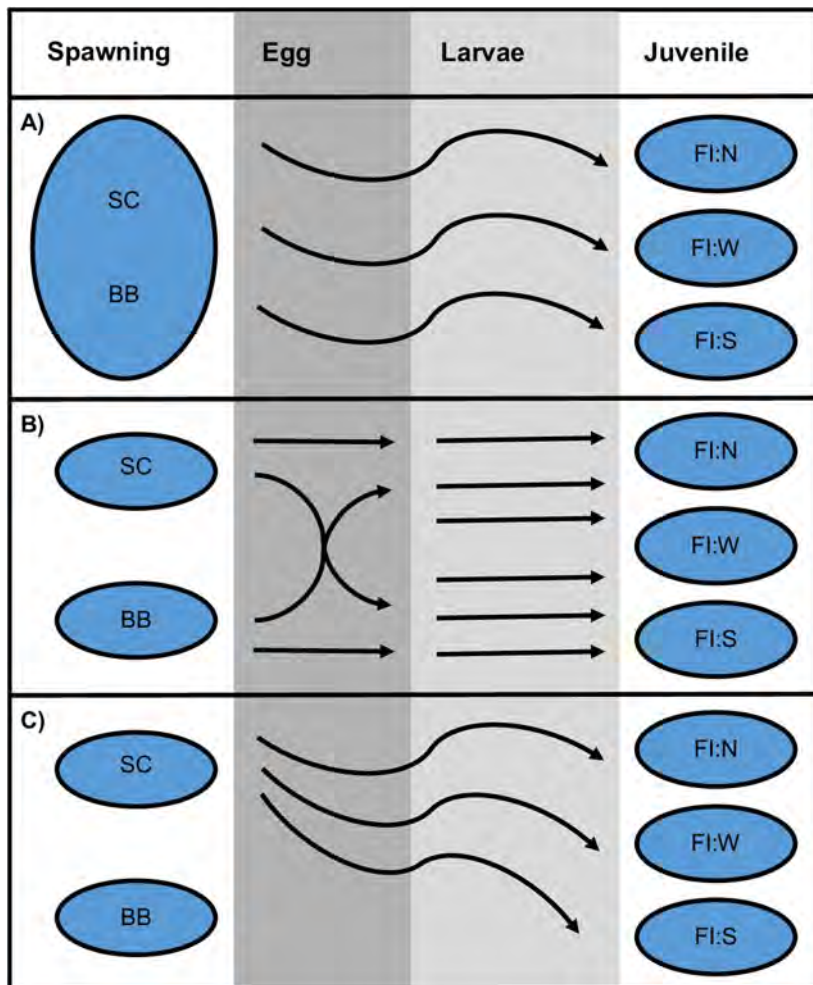


Figure 40: Hypothetical depiction of possible scenarios explaining high variability in microchemistry signatures and what this implies in terms of the retention of juveniles from discrete or continuous spawning areas. A.) Continuous spawning area with eggs and larvae spread evenly across the Falklands Shelf. B.) Discrete spawning areas with mixing taking place during the egg phase, or (C.) retention of early juveniles from a single discrete spawning area.

6.2.3. *Egg and larval dispersal and retention*

The early life-history of Patagonian toothfish is elusive. Indeed, during two research surveys (of which I was a part), undertaken by the FIFD during November 2015 (Pompert *et al.* 2015) and December 2018 (Lee *et al.*, 2019), no Patagonian toothfish eggs or larvae were found, despite the occurrence of 100s of larvae from other species in the region (e.g. *Patagonotothen* spp., *myctophid* spp., *Macrourus* spp., *Sprattus fuegensis*). Until now, the information gathered has largely been based on tank-rearing experiments in Chile (Mujica *et al.* 2016) or from sparsely sampled specimens (n = 43) obtained over extensive time periods (1978 to 2001) predominantly from south of the APF (Evseenko *et al.*, 1995; North, 2002). Specimens sampled during these surveys included three larvae collected from the upper 3 m layer in waters over the northeastern edge of the Burdwood Bank (200 m depth) in December 1997. Based on evidence from the literature, these samples represent the only reliable record of larval Patagonian toothfish attained for the Patagonian population. From the combined sample collected in this study (i.e. across genetically discrete units), the egg and larval period have been described as pelagic, occurring in the upper 250 m of the water column. Further, these results provide an egg phase duration ranging between 30 and 105 days. The timing, depth and dispersal characteristics that occur during the egg phase for the Patagonian population, therefore, remains uncertain.

Through the computation of particle trajectories in an oceanographic simulation model, Ashford *et al.* (2012b) predicted potential dispersal pathways, and retention possibilities for juvenile Patagonian toothfish on the shelf around the Falkland Islands (Table 15). However, due to knowledge gaps, results were wide ranging (0 to 28.5%), depending on the month of release, days at liberty, and retention area. Results obtained from Chapter 3 (Lee *et al.* 2021) and Chapter 5 have therefore provided us with further information that can be used to refine the retention possibilities described by Ashford *et al.* (2012b). We were able to identify the timing of key early life-history events including (1) the hatch date distribution (mid-September

to late October; mean = 3 October); (2) the dispersal period of pelagic larvae until their entry onto the Patagonian Shelf (0 to 40 days post-hatch, dph); (3) the transition phase from the shelf extent to inshore waters (<100 m depth; 40 to 75 days post-hatch); (4) settlement into a demersal habitat (100 days post-hatch); and (5) subsequent migration into juvenile nursery areas (<150 m depth, 120 days post-hatch; Chapter 5). Dispersal periods for recruitment onto the Falklands Shelf that are more than 200 days therefore appear excessive, and given the balance of information, a mid-July to late-August release date is most likely. These refinements seem to provide positive validation for the retention of dispersed eggs and larvae from both spawning areas with a dominance of input from southern Chile to the western shelf, and mixed retention in the south and northeast. Model predictions are indicative that all egg and larval dispersal arising from the North Scotia Ridge would be retained in the High Seas to the north of the Falkland Islands (Ashford *et al.* 2012b).

Results of Chapter 3 (Lee *et al.* 2021) identified spatially and temporally variable retention hotspots that serve as nursery areas for juvenile Patagonian toothfish, specifically to the northeast, west and south of the Falkland Islands. The retention of early juveniles in these areas as discrete units is strongly suggestive of recruitment from distinct spawning areas (Hare and Richardson 2014). Early life-history stages were shown to take place 13 days earlier across the western shelf (Chapter 5). The unique timing of early life-history stages in this area compared to that of the northeast, and southern shelf (areas of mixed retention) may be suggestive of the retention of larvae from a distinct spawning area (i.e. southern Chile).

The spatial-temporal patterns of the nursery areas were largely driven by mesoscale oceanographic features, specifically eddies forming off the northeast of the Burdwood Bank (Chapter 3 - Lee *et al.* 2021). The increased presence of these oceanographic features provides an important link between the Subantarctic Front (and Burdwood Bank spawning area) with the Falklands Shelf leading to higher levels of larval retention and recruitment; specifically, to the southern (2015 and 2017) and northeastern (2015) nursery areas. Results

obtained from spatial-temporal patterns in subsequent year classes indicate that in the absence of retention hotspots, low levels of stable recruitment continue to occur to the northwest of the Falkland Islands, thought to originate from southern Chile (Ashford *et al.* 2012b). Finally, results obtained from Chapter 3 (Lee *et al.* 2021) provide the distinct potential for further refining of model predictions through the provision of known retention areas in a given year (i.e. nursery hotspots), and the inclusion of these in predictions inferred through particle simulation oceanographic models (see section 6.4.2: Research priority 3).

Table 15: Mean percentage (range) of drifters released between May and June 1996–2000 from (a) Burdwood Bank and (b) southern Chile, present in the northern and southern FICZ at 50–300 days (table taken from Ashford *et al.*, 2012b). Refined scenarios based on recent results have been highlighted in grey.

a)						
Month	Destination	Mean % in FICZ at day				
		50	100	200	250	300
May	North	2.6 (0–5)	3 (0–8)	0	0	0
	South	17(0–38.5)	11 (0–26)	1.5 (0–5)	1.5 (0–5)	1.5 (0–5)
June	North	1(0–2.6)	1 (0–5)	1 (0–5)	0	0
	South	16 (5–26)	7 (0–23)	0.5 (0–2.5)	1 (0–5)	1.5 (0–8)
July	North	3.6 (0–13)	0.5 (0–2.6)	0	0	0
	South	15(5–20.5)	11 (5–15)	3 (0–10)	1.5 (0–8)	2 (0–10)
b)						
May	North	1.8 (0–4)	7.5 (3–11)	13 (6–22)	3(1.5–6)	1.5 (0–3)
	South	17(4.5–31)	27 (16–44)	5 (0–10)	2 (0–3)	2.3 (0–6)
June	North	0.8 (0–4)	10(1.5–25)	10 (6–17)	2 (0–6)	1.8 (0–4)
	South	14.5 (3–26)	22.5 (10–40)	3 (0–4)	3 (0–10)	2 (0–4)
July	North	2.4 (0–4)	12 (3–24)	9 (4–19)	3.5 (1.5–9)	3.5(3.5–10)
	South	11 (3–25)	28.5 (15–46)	3.3 (1.5–10)	3.5(1.5–12)	3.5(1.5–10)

6.2.4. Demersal juveniles and sub-adults

Benthic juveniles appear on the shelf for the first time at length of 5 to 15 cm (Arkhipkin and Laptikhovsky 2010). In Chapter 5, settlement into a demersal habitat was identified at 120

days post-hatch (~105 days post-hatch in the west), with a mean date of settlement on 17 January (in the peak of the austral Summer). In Chapter 3 (Lee *et al.* 2021), persistent (stable) nursery area hotspots were identified to the northwest, along with opportunistic (spatially and temporally variable) areas to the south and northeast of the Falkland Islands (see discussion above). Nursery areas were characterised by the presence of quasi-stationary upwelling regions where cold, productive subantarctic waters were pushed up onto the Falklands Shelf.

The recruitment of juveniles into discrete nursery areas proves vital in defining their abundance and ontogenetic migratory pathways over the next three to five years. During their juvenile life-history stages (ages 0+ to 3+), it was shown how a spatially progressive (related to previous age) down-slope ontogenetic migration occurred into deeper waters (Chapter 3 - Lee *et al.* 2021). Predictable pathways were identified adjacent to the areas of initial recruitment. As such, juvenile Patagonian toothfish that were retained in the southern nursery area, migrated southwards; those within the northeast nursery area migrated towards the northern and eastern slope; and those to the west migrated southwest towards the western extent of the Falklands Trough, thus linking up with the southern ontogenetic migratory corridor. By age-4 (50 to 60 cm TL) the majority of juvenile toothfish (>97% by number) had migrated past the shelf edge into waters >400 m. This is indicative that the stock structure, as defined by recruitment patterns, is largely retained throughout the juvenile to sub-adult life-history stages, with no evidence of large-scale mixing taking place on the shelf up to the point of their entrance into deeper waters of the slope.

Difference in the otolith shape of Patagonian toothfish sampled from early adults on the Burdwood Bank and the northern Slope provides retrospective validation of isolation over the course of their life-history from their recruitment into nursery areas, and through their spatially discrete ontogenetic migrations (Chapter 2 - Lee *et al.*, 2018). A second consideration is that these results indicate that abundance on the eastern slope is largely driven by the northeast nursery area; while the southward direction of the ontogenetic migrations of fish from the

southern and western nursery area appear to feed into the southern slope, the Falklands Trough, the Burdwood Bank and possibly even as far as the southern Chilean adult components of the population, respectively.

In the current study, the term sub-adult is defined as juvenile fish that use adult habitats rather than spatially discrete juvenile nursery and ontogenetic pathway habitats (Hare and Richardson 2014). Information on the sub-adult component of the population that occurs between 400 m and 800 m is scarce, mainly due to it forming a gap between the maximum depths targeted by commercial trawlers (400 m) and longline operations (generally >900 m). However, length-frequency data (n = 1588; 2015 to 2021) indicates that this region largely comprised fish with lengths between 35 and 75 cm, reflecting fish between 3 and 5 years old (Chapter 3 - Lee *et al.*, 2021; Figure 41). These sub-adult cohorts can be followed with increasing depths, although a clear convergence with older adult life-history stages occurs at depths between 600 and 1000 m. The sub-adult to adult components of the population are therefore thought to be more or less separated along this depth range (Laptikhovsky *et al.* 2006a; Arkhipkin and Laptikhovsky 2010). These results are indicative that the final stages of the sub-adult ontogenetic migration take place across the same down-slope spatially discrete patterns, as defined in Chapter 3 (Lee *et al.* 2021) until convergence with the adult component of the population.

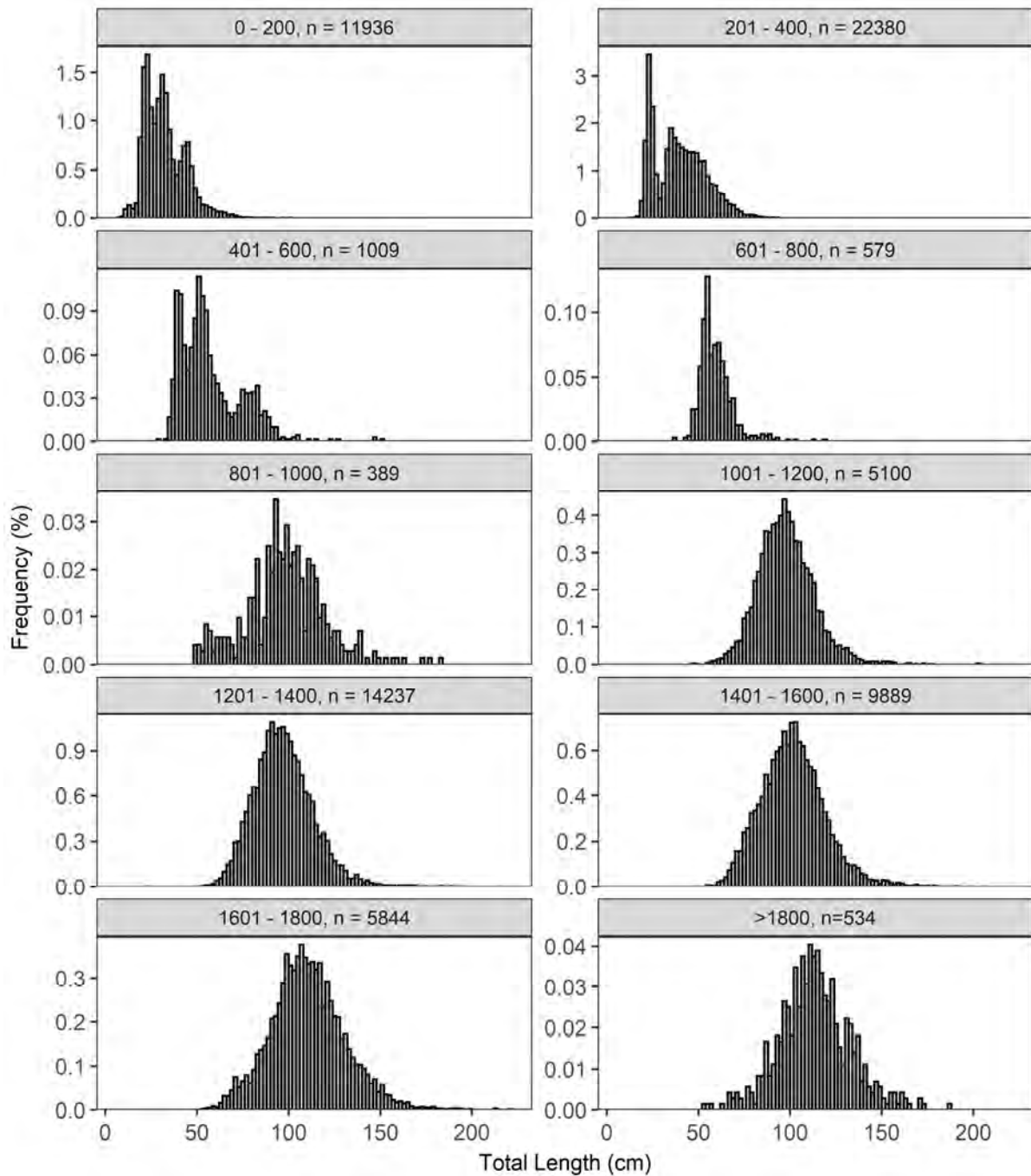


Figure 41: Length frequency distribution at different depths for Patagonian toothfish sampled on the Patagonian Shelf and Slope between 2015 and 2021 ($n = 71897$).

6.2.5. Adults

The length at which 50% of the population reaches maturity for both the Falkland Islands and southern Chile is reported as 81 to 86 cm (male) and 89 to 90 cm (female), respectively

(Laptikhovsky *et al.* 2006a; Arana 2009). Histological evidence suggests that maturity may be reached at smaller sizes (Falkland Islands; females = 79.1 cm), although the majority of individuals (55.8 to 85.6%) are not active participants in spawning on an annual basis (Yates *et al.* 2018; Boucher 2018). On the Kerguelen Plateau, the ontogenetic migration of Patagonian toothfish is thought to stop between 600 and 1200 m where they settle at their preferred depth to feed and grow as they approach maturity (Péron *et al.* 2016). Length-frequency distributions around the Falkland Islands reflect similar patterns (Figure 41). Fish occupying these depths reflect a consolidation of sub-adult cohorts entering the deep-sea adult population (Arkhipkin and Laptikhovsky 2010).

Results of Chapter 2 (Lee *et al.*, 2018), provide little evidence of movement in sub-adult and early adult fish (70 to 120 cm). These indications were further validated by results from tag-recapture data showing high levels of site fidelity across their Falklands distribution (Chapter 4 - Lee *et al.*, 2022). However, despite high site fidelity, small (44.40% of recaptured fish moved between 11 and 50 km) to medium (12.50% of recaptured fish undertook movements of 51 to 200 km) scale movement, defined as foraging activity does seem to occur (Chapter 4 - Lee *et al.*, 2022; Brown *et al.*, 2013a). At this stage in the life-history, the stock structure therefore remains defined according to the dispersal and subsequent retention of larvae within nursery areas, and the associated ontogenetic migratory pathways into adjacent deeper waters. Upon reaching maturity, fish that were retained as larvae on the Burdwood Bank continue their ontogenetic migration into deeper waters for spawning. The extent of their spawning on an annual basis remains uncertain and requires further research (Yates *et al.* 2018; Boucher 2018). Fish that were previously retained as larvae on the west, northeast and southern areas of the Falklands Shelf, consisting of southern Chile and Burdwood Bank contingents, utilise these adult areas on the southern, northern and eastern slope exclusively as feeding zones to grow and increase body condition for migrations to spawning grounds.

Two sets of movement behaviours appear to be initiated when fish reach spawning condition. Fish begin what appears to be (1) a range relocation towards spawning grounds; in combination with (2) a continuation of their ontogenetic migration into deeper waters (Chapter 4 - Lee *et al.*, 2022). Due to the absence of northern spawning grounds, this would suggest a continued southward dispersal and replacement pattern undertaken by larger fish that were retained as larvae on the Falklands Shelf and High Seas. Many fish, however, do not appear to be undertaking this home-range relocation. Either they are unable to reach suitable condition to undertake a migration, or this is attained relatively late in their life-history. While return feeding migrations have been proposed, results from Chapter 2 (Lee *et al.* 2018) indicating clear differences in the otolith shape among local regions, and Chapter 4 (Lee *et al.*, 2022) showing an absence of southward migrations, suggest that this is not a common occurrence. Further, results suggest that natal homing may be apparent in their southward home-range relocations, although this requires further investigation (see Section 6.4.3. Data Collection and Monitoring: Tag-recapture Programme). Given their long-life-history, a tag-recapture program of six years is relatively short, and further patterns may become evident over time.

6.2.6. Stock structure

Large-scale uncertainty remains in our understanding of the stock structure for Patagonian toothfish in the region. The absence of clear genetic structuring across the region suggests that sympatric discrete populations are unlikely (Canales-Aguirre *et al.* 2018). Similarly, high site fidelity as described through results from otolith shape (Chapter 2 - Lee *et al.* 2018) and tag-recapture analyses (Chapter 4 - Lee *et al.*, 2022) appear to indicate a definitive panmictic population structure is also not reflective of the Patagonian toothfish population in the region. The integration of results across studies are suggestive of a spatially complex population, i.e. a metapopulation type structure (Smedbol and Stephenson 2001; Ciannelli *et al.* 2013). Life-cycle connectivity from juvenile retention areas around the Falkland Islands, through

progressive life-history stages to southern spawning locations, suggests deviation from a distinct source-sink model (Chapter 3 - Lee *et al.* 2021; Chapter 4 - Lee *et al.* 2022). Nonetheless, characteristics of this structure do appear to exist as reflected in high site fidelity outside of the spawning areas (Chapter 4 - Lee *et al.* 2022), possibly indicative of vagrants (Sinclair and Iles 1989).

The key question of where along the continuum Patagonian toothfish in the region lie, in terms of a classical metapopulation vs panmictic type stock structure, relates to the extent of connectivity among discrete or continuous spawning areas; specifically to the extent that spawning areas are indeed structured as discrete units as opposed to a continuous zone extending across the southern range. Evidence, however, suggests discrete spawning areas occurring across their southern range are likely. A second interacting factor relates to the extent that return home-range relocations of reproductively capable adults (Chapter 4 - Lee *et al.* 2022) are a reflection of natal homing to discrete spawning areas, or simply a movement to the area most suitable for spawning. The occurrence of natal-homing would suggest a classical metapopulation type structure, even despite the indication of large-scale mixing of contingents during the process of egg and larval dispersal.

Spatially complex population

The stock structure for Patagonian toothfish on the Patagonian Shelf and deep-sea plateau may be a reflection of a spatially complex classical metapopulation type structure with aspects of source-sink dynamics according to the 'member-vagrant hypothesis'. The population structure is comprised of at least three contingents, arising from southern Chile (SC), Burdwood Bank (BB) and North Scotia Ridge (NSR) spawning stocks (Figure 42). Spawning occurs between May and August across the population. A component of the southern Chile contingent is retained within Chilean waters across all life-history stages (Arana 2009; Chapter 2 - Lee *et al.* 2018), also reflecting a distinct member group according to the 'Member-Vagrant

Hypothesis' (Sinclair and Iles 1989). Similarly, a component of the Burdwood Bank contingent is retained within this area from larval, through to the spawning life-history stages (Ashford *et al.* 2012b; Chapter 2 - Lee *et al.* 2018). Egg and larval dispersal from the North Scotia Ridge spawning stock are all retained on the High Seas to the north of the Falkland Islands (Ashford *et al.* 2012b). Early juveniles that are retained on the shelf around the Falkland Islands arise from both the southern Chile and Burdwood Bank spawning areas. The composition of individuals from each contingent are not known, but high levels of mixing are hypothesised.

Early juveniles from the Burdwood Bank spawning area are retained across the southern (Ashford *et al.* 2012b) and northeastern extent (Chapter 5) of the Shelf, with years of high recruitment driven by oceanographic processes (Chapter 3 - Lee *et al.*, 2021). Early juveniles that are retained from the southern Chile spawning therefore appear to be less vulnerable to oceanographic variability and are distributed more consistently across the shelf regions around the Falkland Islands, in particular to the western shelf (Ashford *et al.*, 2012b; Chapter 3 - Lee *et al.*, 2021). The stock structure is largely retained throughout the subsequent nursery and ontogenetic migratory life-history phases until maturity is reached. However, there is some evidence of mixing of contingents on the Falklands Shelf through (1) the merging of the western and southern ontogenetic migratory pathways into a single southern channel; (2) the eastward ontogenetic migration of juveniles from the southern and northeast nursery areas.

Upon reaching maturity, a considerable proportion of the population (9 to 25% covering all contingents) initiate large-scale southern dispersal movements defined as home-range relocations towards what may be their original spawning contingent (natal homing). Many individuals that were dispersed as eggs and larvae to these northern areas, however, do not appear to undertake a home-range relocation, remaining as non-spawning (but spawning capable) inhabitants (i.e. vagrants displaying source-sink characteristics). This means that the stock structure across the adult deep-sea habitats consists of (1) non-spawning (but spawning capable) vagrants retained as larvae from the three spawning contingents; potential migrants

(2) passing through or (3) yet to undertake their home-range relocations to their respective spawning grounds; or (4) individuals that have undertaken a return migration, although there is currently only limited evidence available to support this hypothesis (i.e. a return feeding migration as hypothesised by Laptikhovsky *et al.* (2006a) and Boucher (2018)).

The adult life-history stages occurring on the Burdwood Bank spawning grounds therefore consists of (1) locally retained fish; (2) returnees of Burdwood Bank contingents that were dispersed as eggs and larvae to the High Seas and Falklands Shelf; and (3) North Scotia Ridge and Southern Chile contingents passing through as they undertake home-range relocations towards their respective spawning grounds. This reinforces the importance of the Burdwood Bank population, not only as an important spawning stock contingent driving recruitment across the Patagonian Shelf and slope, but also as a major connectivity hotspot for Southern Chile and North Scotia Ridge contingents as they pass through to their respective spawning grounds.

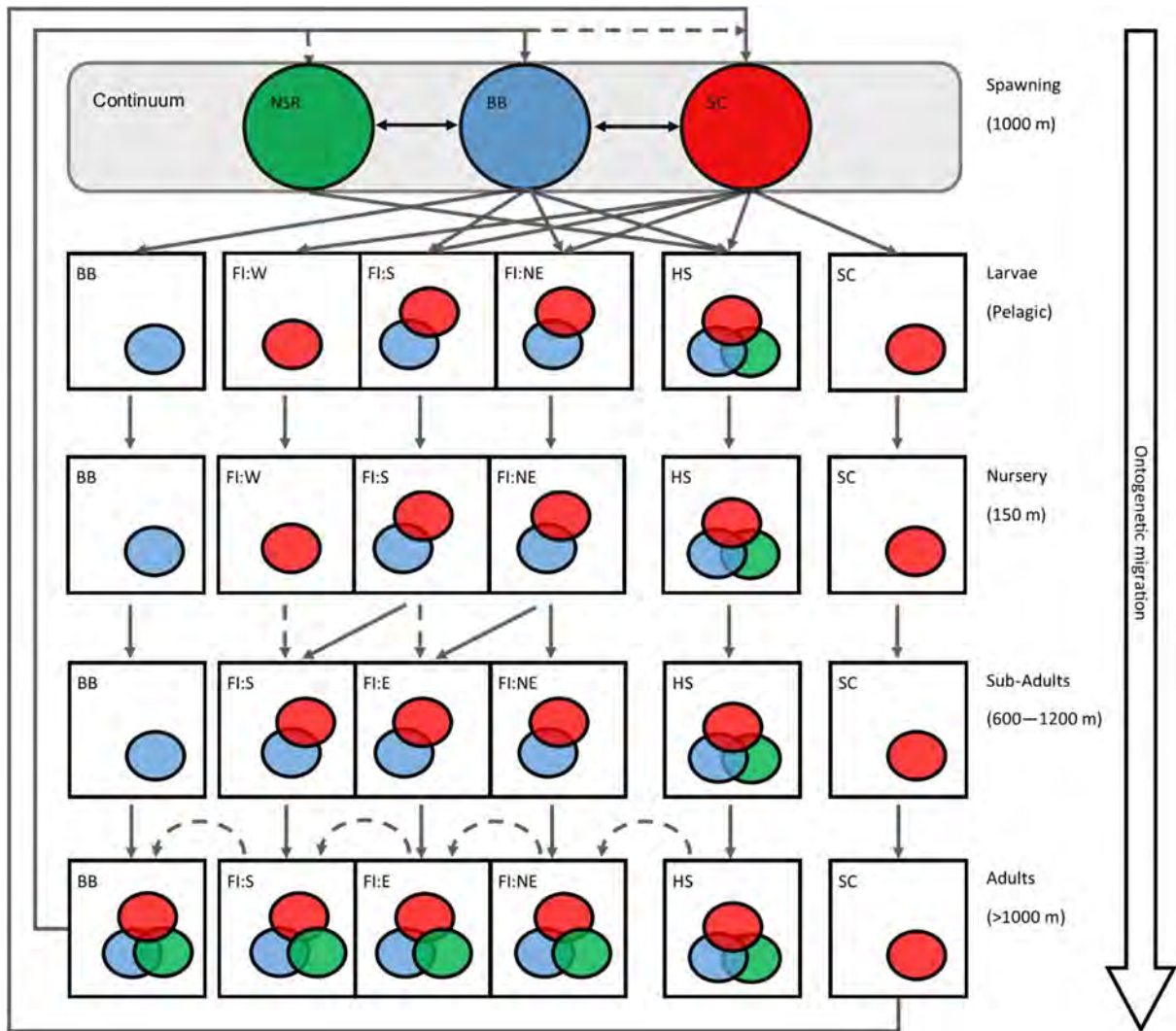


Figure 42: Hypothetical life-cycle for Patagonian toothfish depicting the stock structure based on findings of this thesis. The three spawning stock contingents (NSR = North Scotia Ridge, BB = Burdwood Bank, SC = Southern Chile) that make up the metapopulation are depicted passing through areas of interest across key life-history stages. Regions of interest: BB = Burdwood Bank, FI:W = Falkland Islands west, FI:E = Falkland Islands East, FI:S = Falkland Islands South, FI:NE = Falkland Islands North East, HS = High Seas, SC = Southern Chile. Dashed lines indicate movement across areas.

6.3. Management approaches

Understanding where the Patagonian toothfish population structure lies in terms of a discrete sympatric – spatially complex – panmixia continuum provides a framework in which to define suitable management units (Hawkins *et al.* 2016). For a population displaying sympatric or distinct source-sink characteristics, the emphasis is on management of the source population (i.e. southern Chile, Burdwood Bank and North Scotia Shelf). At the other end of the extreme, a classical metapopulation approaching panmixia requires consideration as an integrated single unit.

While a broad spectrum of potential techniques are available, Kerr *et al.* (2017) described five core approaches that have been applied to integrate new information on complex population structure and mixing of marine fish into assessment and management. These will be discussed below in relation to the findings of the current research and their potential application in the development of improved assessment and management measures for Patagonian toothfish around the Falkland Islands. It is important to note that these management approaches are not mutually exclusive. In the current context, multiple approaches have been incorporated over time, and are noted in the discussion below.

6.3.1. Status quo management

The status quo management approach reflects the situation wherein there is insufficient information to change current management practices, providing a default position. The basis for following this approach involves the situations wherein (1) levels of uncertainty or the reliability of current data is inadequate to provide credible or robust advice for management, (2) the presence of stock units that span international boundaries characterised by complex politics, or (3) a combination of the above. These factors are largely applicable in the current context wherein each geographical area is managed independently according to political

boundaries, with the assumption of no mixing of contingents. The exception applies to the North Scotia Ridge contingent for which catches are estimated for inclusion within FIFD assessments. The degree of stock mixing across these political boundaries is therefore an important source of uncertainty in the assessment of Patagonian toothfish.

Through improved collaborations (see 6.4.1), the achievement of strategic research objectives (see 6.4.2), and enhanced monitoring (see 6.4.3), changes in the relative abundance of unique populations can be tracked. Further, sufficient scientific consensus is available, both in terms of stock structure and life-history dynamics, for the incorporation and implementation of additional approaches for meeting management objectives. These will be further developed in the sections below.

6.3.2. *'Weakest link' management*

The weakest link management approach reflects the situation wherein there is some knowledge of spatial structure, but insufficient information exists to explicitly manage all spawning components. Therefore, the assumed weakest spawning component is protected through management measures. Although not necessarily the 'weakest link', based on management objectives, this would involve the introduction of measures to protect the Burdwood Bank contingent of the stock.

The relative contribution of the Burdwood Bank contingent to the abundance of Patagonian toothfish across life-history stages and areas (see research priority 1) is not known. Further, how this contribution varies on a spatial-temporal scale according to oceanographic processes (see research priority 3) is yet to be identified. However, the occurrence of this contingent in spatial units across the spawning area itself (Burdwood Bank), nursery areas (Burdwood Bank, northeastern and southern shelf), and the ontogenetic pathways that link these (southern and southeast pathway) have been identified. Options for the implementation of

management measures to protect the Burdwood Bank contingent can therefore be pursued using this approach.

At present, management measures have already been implemented for the protection of the Burdwood Bank spawning area. For example, no trawling is permitted on the Burdwood Bank, and longline based commercial fisheries are prohibited from fishing in the area during spawning from June to August (see section 6.3.3 below). In addition, management measures have been initiated with the objective of reducing bycatch of juvenile Patagonian toothfish on the Shelf. These entail a 'move-on rule' in which vessels are required to exit the spatial unit (pre-defined $0.5^{\circ}\text{W} \times 0.25^{\circ}\text{S}$ grid-squares) wherein they are fishing for 10 days, after triggering an action (defined as Patagonian toothfish catch $>1.5\%$ of daily aggregated trawl catch calculated for each respective vessel).

The implementation of a weakest link management approach can be considered as an extreme version of precautionary principles, in the presence of uncertainty. The greatest drawback of this is that it can also lead to an under-utilization of the population, and therefore not be effective in optimizing long-term yield (Punt and Donovan 2007). In contrast, the weakest link management approach can also result in a displacement of effort to contingents that are not being protected, leading to an overall loss of biomass and decrease in yield (Crowder *et al.* 2000; Abbott and Haynie 2012).

6.3.3. *Spatial and temporal closures*

Spatial and temporal closures can be implemented in situations where there is knowledge of spatial structure, but insufficient information exists to alter the scale of assessment. Spatial and temporal closures are usually used to protect vulnerable life-history stages, sometimes at specific times of the year (e.g. spawning populations).

A year-round closure has been implemented on the Burdwood Bank to trawl-activity, as well as to commercial longline operation during the Patagonian toothfish spawning season. However, nursery and juvenile life-history stages remain susceptible to fishing pressure. Based on data from long-term monitoring programs (biomass surveys, pre-season surveys), spatially and temporally variable nursery area hotspots can be reliably predicted. Further, the increasing persistence with age in the abundance of shelf-based juveniles and sub-adults across ontogenetic pathways, reflect stable spatial zones as a focus point for the implementation of management measures (Chapter 3 - Lee *et al.*, 2021). Due to the low abundance of Patagonian toothfish in their nursery areas relative to species targeted by commercial fisheries (*Merluccius hubbsi*, *D. gahi*), along with their small size (6 to 15 cm, 4 to 10 g), newly recruited juveniles are unlikely to be protected by the move-along rule described above. Further, closed areas are likely to create problems due to overlap with other important commercial fisheries across the region. Additional spatial and temporal closures need to be investigated in relation to gear-restrictions (mesh size restriction), and implemented on a proactive basis according to pre-defined thresholds and triggers, defined according to a robust monitoring framework (see section 6.4.3).

6.3.4. Integration of stock composition into management

The incorporation of stock composition into management decisions can be applied in situations where there is knowledge of stock mixing, but insufficient information exists to explicitly model connectivity within a stock assessment. An understanding of the stock composition for Patagonian toothfish around the Falkland Islands is not currently known, although there is a clear potential for this to be achieved (see research priority 1). Understanding stock composition in a given year, may provide higher levels of resolution for the implementation of weakest link management (see section 6.3.2) or spatial and temporal closures (see section 6.3.3), protecting stock components of importance (based on management objectives), without adversely affecting overall yield. Further, the development

of time series of composition data across life-history stages, can subsequently be used to identify oceanographic, anthropogenic or environmental drivers of these changes. Relevant management measures can then be incorporated to mitigate these changes.

6.3.5. *Alteration of stock boundaries*

The alteration of stock boundaries is a management approach wherein sufficient information is available on population structure, which allows updating and redrawing stock boundaries to improve the alignment of biological populations and management units. In the current context, high levels of uncertainty still characterise our understanding of the stock structure within the region. What is evident is high levels of connectivity among the three spawning stock contingents are likely, and there is the potential for a requirement to move towards increased collaborative efforts with Chile and Argentina in terms of a unified framework for assessments. From this broad perspective of unified management, and based on assessments derived from the overall population, improved management objectives can be identified that are based on the incorporation of the approaches described above.

6.4. Management recommendations

The results of this work have filled important gaps and together with prior research, has provided important baseline information in terms of understanding the stock structure for Patagonian toothfish in the region. However, fundamental information is still required to build up a complete picture. These themes described below are based on information requirements pertaining to two key life-history periods that appear to be the driving force in terms of stock structure within the region: the dispersal of eggs and larvae through oceanographic processes and home-range relocations undertaken by spawning capable adults.

6.4.1. Collaborations

A key theme that has arisen across this research reflects the shared Patagonian toothfish population across political boundaries. It is therefore important for increased collaborative research, monitoring and communications to take place between the scientific departments of Chile, Argentina, and the Falkland Islands. This is already starting to occur between Chile and the Falkland Islands, with the development of new research projects in this regard that may provide further clarity in terms of understanding the stock composition in areas south of the spawning grounds (see 6.4.2: Research priority 1). Further, future findings may push for further collaborative efforts in terms of assessments for the Patagonian toothfish population as a combined stock, or the inclusion of data from specified contingents that straddle international boundaries.

6.4.2. Research priorities

Research priority 1: The identification of mixed stock origin on the Patagonian Shelf

The aim of this study would be the identification of markers that can be used to develop a time-series, describing the proportions of each contingent across the population. While otolith shape was shown to be effective in discriminating fish captured across areas, it is unclear to what extent this is a reflection of (1) the stock contingent from which they arise, or the area within which they have spent their lives up to the point of capture (i.e. a reflection of high site fidelity adjacent to the area of larval retention; Chapter 2 - Lee *et al.*, 2018). Otolith microchemistry analysis may provide the key missing component for identifying the stock composition of Patagonian toothfish across the region. The specific objectives for such a study would be to identify elemental signatures in the core region of otoliths from the three spawning contingents (Chile, Burdwood Bank and North Scotia Ridge), and compare these with

signatures from fish dispersed across the Patagonian Shelf. Such a collaborative project has already been initiated between the Falkland Islands and Chile.

Research priority 2: Identification of stock reproductive potential

Key questions pertaining to the reproductive biology for Patagonian toothfish were identified in the current study, with a key focus on the extent of potential skipped spawning in their adult, deep-sea, northern habitats. Further research is required to characterise the active spawning depth, seasons, and maturity schedule in Patagonian toothfish across contingents. In addition, it is essential to estimate the proportion of each spawning stock contingent that fails to undertake home-range relocations, or actively participate in spawning (i.e. skipped spawners as discussed in Chapter 4 - Lee *et al.*, 2022). Related to this, further research should be undertaken to evaluate the extent of spawning periodicity that takes place in Patagonian toothfish among contingents across the Patagonian Shelf.

Research priority 3: Early life-history transport on the Patagonian Shelf

Improving our understanding of oceanic transport and their role in population connectivity during egg and larval dispersal has emerged as a key driver of stock structure dynamics for Patagonian toothfish. Such approaches have already been investigated through the important works undertaken by Ashford *et al.* (2012b) as well as by Mori *et al.* (2016) on the Kerguelen Plateau. The predictive abilities of these works can be enhanced through the incorporation and validation provided by recent research findings, such as the (1) incorporation of known larval retention areas based on spatial-temporal distribution models (Chapter 3 - Lee *et al.*, 2021), (2) improved understanding of spawning behaviour (research priority 2); and updated estimates of the larval period prior to settlement (Chapter 5).

6.4.3. Data collection and monitoring

Fisheries independent surveys

Demersal biomass surveys represent the most important high-resolution data source supporting the evaluation of demersal resources based on fishery-independent data around the Falkland Islands. Together with the Patagonian longfin squid pre-season surveys, annual data has been collected from across the Patagonian Shelf around the Falkland Islands since 2015. There are four aspects that can be considered regarding this data in terms of its ability to be effectively used for monitoring Patagonian toothfish stocks for the implementation of effective management measures. These are specifically related to the monitoring of (1) nursery areas, (2) deep-sea ontogenetic migratory transition zones (3) expansion to encompass a seasonal component and (4) increased alignment among the two survey data collection protocols.

Shallow coastal waters are essential recruitment and nursery grounds for Patagonian toothfish (Chapter 3 - Lee *et al.*, 2021). It is necessary to develop fishery-independent survey protocols to collect reliable information from stratified areas for monitoring recruitment patterns into identified nursery areas. The inclusion of extensive, high intensity bottom trawl stations may have negative effects on habitats in these sensitive ecosystems (Pitcher *et al.* 2017). Careful control of sampling efforts and monitoring of benthic community changes in these areas should therefore be considered. Considerations should also be given for the development and inclusion of zooplankton survey programs for monitoring potential egg and larval retention in nursery areas and species interactions that occur at this life-history stage.

In addition, it is important for the inclusion of deep-sea stations between 400 and 600 m for which data is extremely limited (see Figure 39). The acquisition of data from these depths is critical for understanding the linkages between the juvenile and sub-adult population on the shelf, with the adult population in deeper waters. Such an extension has indeed been

undertaken (for example in 2018), and subsequent surveys can easily be extended to incorporate these stations.

Finally, the inclusion of a winter demersal biomass survey component is essential for obtaining (1) seasonal spatial-temporal patterns in abundance, as well as (2) the provision of reliable data and validation on recruitment strength. These data would significantly reduce uncertainty and provide increased resolution for use in predictive modelling of recruitment, timing, strength, and spatial usage for the implementation of proactive management measures (see section 6.3.2 and 6.3.3).

Each of these aspects mentioned in the paragraphs above can equally be argued along the basis of their importance to many other commercially important fish species, and the species complex surrounding their interactions (Chapter 3 - Lee *et al.*, 2021). For example, results of Chapter 3 - Lee *et al.* (2021) identified inter-specific interactions among juvenile Patagonian toothfish with icefish (competition) and rock cod (predator-prey relationship) across their nursery and shelf-based life-history stages. In the deep-sea environment, very little is known in terms of the population dynamics and life-history for the ridge-scaled grenadier, a species showing strong vulnerabilities to overexploitation, and a key prey source for sub-adult Patagonian toothfish (Arkhipkin *et al.* 2003; Lee *et al.* 2019a). Monitoring changes in a multi-species assemblage in a dynamic environment therefore provides further context into how the effective management of fisheries needs to be considered within an ecosystem-based framework (Link 2010; Franco *et al.* 2020b; Campana *et al.* 2020).

There is an increasing need for the alignment of protocols across the two fisheries independent surveys undertaken by the Falkland Islands Government. Patagonian longfin squid pre-season surveys utilise full commercial fishing gear, longer (two hour) stations with fewer participating staff (see Chapter 3 - Lee *et al.*, 2021). The resolution of data collected from demersal biomass surveys is therefore far greater, given the staff capacity involved, and the

effort applied for stations. Given the multi-faceted approach and multiple objectives applied to both these surveys, greater alignment can only reduce uncertainty and provide an improved ability to monitor Patagonian toothfish spatial and temporal patterns across the region.

Environmental monitoring

Oceanographic factors have been shown to be key drivers of larval dispersal across the region (Chapter 3 - Lee *et al.*, 2021). There is an urgent need for routine analysis of long-term trends of environmental change, and the identification of what this means for Patagonian toothfish recruitment to the Falklands Shelf (see research priority 3). These data can be used as contextual information for the implementation of direct and indirect management measures:

- Direct: the protection of juvenile cohorts as they undertake their migration across the shelf through the implementation of an appropriate spatial management approach.
- Indirect: Reduce the impact of fishing on age truncation through appropriate sustainability measures. Long-lived spawners (such as occurs in toothfish) provides a storage effect whereby a stock will persist as long as enough adults outlive periods unfavourable to successful spawning and recruitment.

Further, the distributional response of Patagonian toothfish and the species and habitats upon which they rely to environmental change is not known. Environmental change is likely to modify spatial and temporal patterns through range expansions and contractions (Campana *et al.* 2020), particularly for species at the extent of their range, like Patagonian toothfish.

Tag-recapture program

The guidelines and protocols that were established for the tagging program have been demonstrated as effective, providing a high-quality data set. Recapture rates have remained

high during the course of the program and consistent patterns are emerging from the data, providing valuable insights into the stock structure and movement patterns of Patagonian toothfish within the Falkland Islands Conservation Zones; and indeed, across the wider southwest Atlantic. From 2023, exploratory analyses on the inclusion of tag-recapture data within the stock assessment will also be initiated. These factors re-assert the importance for maintaining the tag-recapture programme objectives, specifically for the continued tagging of ~1000 toothfish per year within the Falkland Islands Conservation Zones. The best approach for achieving this should be determined through further discussion in collaboration with industry, and the FIFD Patagonian toothfish Scientific team.

According to the current approach, an annual target of 400 toothfish (40%) should be tagged by FIFD observers per year. As stated in the FIFD observer manual for longliners, the specific objective for scientific fisheries observers at sea is to tag an average of 25 fish per week / 4 fish per biological sampling day at sea. This objective should be undertaken according to the following approach:

- Tag the first 4 suitable fish from targeted lines within the first 15 minutes of hauling (landing of first umbrella), i.e. observer is to stop tagging when the first limit is reached (4 tagged fish OR 15 minutes after landing of the first umbrella).
- There should be flexibility regarding the 15-minute time period and the allowance to conduct tagging on multiple lines per day so that the objective can be achieved. This is specifically in cases when the targeted line may have yielded fewer than 4 toothfish suitable for tagging within the first 15-minute time period.

During the first 6 years of the tag-recapture programme this target has not been achieved, and the numbers of fish tagged by FIFD observers has been substantially lower compared to tagging surveys (83.75% for surveys vs 16.25% for FIFD Observers).

Should the decision be made for tagging effort to be driven through the FIFD observer programme, the observer longline protocol would need to be revised to allow for an increased tagging workload. There are a number of options in which this protocol can be adjusted to increase the ratio of fish tagged by FIFD observers, for example:

- The implementation of research lines specifically for tagging according to specified time periods (e.g. one tagging line every fourth day).
- The assignment of sections of lines specifically for tagging according to specified time period (e.g. one section of line each day).
- Other options at the discretion of a collaborative discussion.

It is recommended that a pulsed tagging protocol (see Chapter 4 - Lee *et al.*, 2022) should be included as an objective on further research surveys undertaken on the CFL Hunter. These surveys have been the driver of tagging effort during the first 6-years of the tag-recapture programme. Such surveys can be incorporated into an annual programme as follows:

- Pulsed-tagging as a primary objective: In the absence of increased FIFD observer tagging effort, a single two-week pulsed tagging survey will be required on an annual basis. The intention of such a trip would be to tag up to 1000 fish covering the full spatial extent of the toothfish distribution in the FCZ.
- Tagging as a secondary objective: Should tagging rates be improved by FIFD observers, tagging can be included in future surveys as a secondary objective. Such objectives would be related to covering shortfalls in the number of tags deployed, and the deployment of tags in areas with low sampling effort.

Discussions should further build towards collaborations in this venture with the intention to (1) extend the spatial scale of the study and (2) quantify and improve the reporting of recaptures in areas outside of the Falkland Islands (see section 6.4.1).

6.5. Conclusion

This dissertation applied an integrated approach to define aspects of the stock structure of Patagonian toothfish on the Patagonian Shelf to reveal complex patterns, characterised by high levels of connectivity, largely driven during the early life-history phases of egg and larval dispersal. It further demonstrates that the stock structure arising from the retention of mixed contingents across the Falklands Shelf remains discrete until adult life-history stages. Finally, movement patterns described for the adult component of the stock are providing important contributions to our understanding of the linkages between these mixed contingents and the southern spawning areas.

Data programs initiated and used in the current studies are all relatively short (2015 to 2021), for the acquisition of data and identification of patterns for a long-lived species with well over a 30-year history of exploitation. Nonetheless, the results of this research contribute meaningfully to management through improved confidence in and transparency of the advice. Further, this research provided an important platform for the enhancement and extension of current monitoring programs through key collaborations, and the development of future research priorities to inform management objectives.

The continuing development of our understanding on the life-history of Patagonian toothfish is likely to remain a source of both inspiration and frustration for researchers, managers, and fisheries industry for many years to come. I am excited to have contributed novel pieces to the puzzle.

References

- Abbott, J. K., and Haynie, A. C. (2012). What are we protecting? Fisher behavior and the unintended consequences of spatial closures as a fishery management tool. *Ecological Applications* **22**, 762–777. doi:10.1890/11-1319.1
- Abrantes, J. P., Reygondeau, G., Wabnitz, C. C. C., and Cheung, W. W. L. (2020). The transboundary nature of the world's exploited marine species. *Scientific Reports* **10**, 17668. doi:10.1038/s41598-020-74644-2
- Acha, E. M., Mianzan, H. W., Guerrero, R. A., Favero, M., and Bava, J. (2004). Marine fronts at the continental shelves of austral South America: Physical and ecological processes. *Journal of Marine Systems* **44**, 83–105. doi:10.1016/j.jmarsys.2003.09.005
- Agnew, D. J. (2002). Critical aspects of the Falkland Islands pelagic ecosystem: distribution, spawning and migration of pelagic animals in relation to oil exploration. *Aquatic Conservation: Marine and Freshwater Ecosystems* **12**, 39–50. doi:10.1002/aqc.474
- Agnew, D. J. (2000). The illegal and unregulated fishery for toothfish in the southern Ocean, and the CCAMLR catch documentation scheme. *Marine Policy* **24**, 361–374. doi:10.1016/S0308-597X(00)00012-9
- Agnew, D. J., Moir Clark, J., McCarthy, P. A., Unwin, M., Ward, M., Jones, L., Breedt, G., Du Plessis, S., Van Heerden, J., and Moreno, G. (2006). A study of Patagonian toothfish (*Dissostichus eleginoides*) post-tagging survivorship in Subarea 48.3. *CCAMLR Science* **13**, 279–289.
- Agüera, A., and Brophy, D. (2011). Use of sagittal otolith shape analysis to discriminate Northeast Atlantic and Western Mediterranean stocks of Atlantic saury, *Scomberesox saurus saurus* (Walbaum). *Fisheries Research* **110**, 465–471. doi:10.1016/j.fishres.2011.06.003
- Ainley, D. G., and Blight, L. K. (2009). Ecological repercussions of historical fish extraction from the Southern Ocean. *Fish and Fisheries* **10**, 13–38. doi:10.1111/j.1467-

2979.2008.00293.x

- Allen, R. M., Metaxas, A., and Snelgrove, P. V. R. (2018). Applying Movement Ecology to Marine Animals with Complex Life Cycles. *Annual Review of Marine Science* **10**, 19–42. doi:10.1146/annurev-marine-121916-063134
- Álvarez-Noriega, M., Burgess, S. C., Byers, J. E., Pringle, J. M., Wares, J. P., and Marshall, D. J. (2020). Global biogeography of marine dispersal potential. *Nature Ecology and Evolution* **4**, 1196–1203. doi:10.1038/s41559-020-1238-y
- Anderson, M. J., and Willis, T. J. (2003). Canonical Analysis of Principal Coordinates: A Useful Method of Constrained Ordination for Ecology. *Ecology* **84**, 511–525.
- Andrews, A. H., Ashford, J. R., Brooks, C. M., Krusic-Golub, K., Duhamel, G., Belchier, M., Lundstrom, C. C., and Cailliet, G. M. (2011). Lead-radium dating provides a framework for coordinating age estimation of Patagonian toothfish (*Dissostichus eleginoides*) between fishing areas. *Marine and Freshwater Research* **62**, 781–789. doi:10.1071/MF10225
- Andrews, S., and Leroux, S. J. (2020). Modelling the spatial – temporal distributions and associated determining factors of a keystone pelagic fish. *ICES Journal of Marine Science* **77**, 2776–2789. doi:10.1093/icesjms/fsaa148
- Ansorge, I. J., and Lutjeharms, J. R. E. (2003). Eddies originating at the South-West Indian Ridge. *Journal of Marine Systems* **39**, 1–18. doi:10.1016/S0924-7963(02)00243-9
- Appleyard, S. a., Ward, R. D., and Williams, R. (2002). Population structure of the Patagonian toothfish around Heard, McDonald and Macquarie Islands. *Antarctic Science* **14**, 364–373. doi:10.1017/S0954102002000238
- Arana, P. (2009). Reproductive aspects of the Patagonian toothfish (*Dissostichus eleginoides*) off southern Chile. *Latin American Journal of Aquatic Research* **37**, 381–394. doi:10.3856/vol37-issue3-fulltext-9
- Arkhipkin, A., Brickle, P., and Laptikhovsky, V. (2013). Links between marine fauna and oceanic fronts on the Patagonian Shelf and Slope. *Arquipelago - Life and Marine Sciences* **30**, 19–37.

- Arkhipkin, A., Brickle, P., and Laptikhovsky, V. (2003). Variation in the diet of the Patagonian toothfish with size, depth and season around the Falkland Islands. *Journal of Fish Biology* **63**, 428–441. doi:10.1046/j.1095-8649.2003.00164.x
- Arkhipkin, A. I., and Laptikhovsky, V. V. (2010). Convergence in life-history traits in migratory deep-water squid and fish. *ICES Journal of Marine Science* **67**, 1444–1451. doi:10.1093/icesjms/fsq103
- Arkhipkin, A. I., McKeown, N. J., Brickle, P., Lee, B., and Shaw, P. W. (2022). Taxonomic re-appraisal for toothfish (*Dissostichus*: Notothenioidea) across the Antarctic Polar Front using genomic and morphological studies. *Journal of Fish Biology*, 1–13.
- Arkhipkin, A., Lee, B., Goyot, L., Ramos, J. E., Chemshirova, I., Roberts, G., Costa, M., and Blake, A. (2019). Cruise Report ZDLM3-02-2019: Demersal biomass survey. Stanley, Falkland Islands Government, Fisheries department.
- Armstrong, R. A. (2014). When to use the Bonferroni correction. *Ophthalmic & physiological optics : the journal of the British College of Ophthalmic Opticians (Optometrists)* **34**, 502–508. doi:10.1111/opo.12131
- Ashford, J., Dinniman, M., Brooks, C., Andrews, A. H., Hofmann, E., Cailliet, G., Jones, C., and Ramanna, N. (2012a). Does large-scale ocean circulation structure life history connectivity in antarctic toothfish (*Dissostichus mawsoni*)? *Canadian Journal of Fisheries and Aquatic Sciences* **69**, 1903–1919. doi:10.1139/f2012-111
- Ashford, J., Duhamel, G., Jones, C., and Bobko, S. (2005a). Age, growth and mortality of Patagonian toothfish (*Dissostichus eleginoides*) caught off Kerguelen. *CCAMLR Science* **12**, 29–41.
- Ashford, J., and Jones, C. (2007). Oxygen and carbon stable isotopes in otoliths record spatial isolation of Patagonian toothfish (*Dissostichus eleginoides*). *Geochimica et Cosmochimica Acta* **71**, 87–94. doi:10.1016/j.gca.2006.08.030
- Ashford, J. R., Arkhipkin, A. I., and Jones, C. M. (2006). Can the chemistry of otolith nuclei determine population structure of Patagonian toothfish *Dissostichus eleginoides*? *Journal of Fish Biology* **69**, 708–721. doi:10.1111/j.1095-8649.2006.01144.x

- Ashford, J. R., Arkhipkin, A. I., and Jones, C. M. (2007). Otolith chemistry reflects frontal systems in the Antarctic Circumpolar Current. *Marine Ecology Progress Series* **351**, 249–260. doi:10.3354/meps07153
- Ashford, J. R., Fach, B. A., Arkhipkin, A. I., and Jones, C. M. (2012b). Testing early life connectivity supplying a marine fishery around the Falkland Islands. *Fisheries Research* **121–122**, 144–152. doi:10.1016/j.fishres.2012.01.023
- Ashford, J. R., Jones, C. M., Hofmann, E., Everson, I., Moreno, C., Duhamel, G., and Williams, R. (2005b). Can otolith elemental signatures record the capture site of Patagonian toothfish (*Dissostichus eleginoides*), a fully marine fish in the Southern Ocean? *Canadian Journal of Fisheries and Aquatic Sciences* **62**, 2832–2840. doi:10.1139/F05-191
- Avigliano, E., Alves, N. M., Rico, M. R., Ruarte, C. O., D'Atri, L., Méndez, A., Pisonero, J., Volpedo, A. V., and Borstelmann, C. (2021). Population structure and ontogenetic habitat use of *Micropogonias furnieri* in the Southwestern Atlantic Ocean inferred by otolith chemistry. *Fisheries Research* **240**. doi:10.1016/j.fishres.2021.105953
- Baranov, T. I. (1918). On the question of the biological basis of fisheries. *Nauchnyi Issledovatel'skii Ikhtologicheskii Institut Izvestia* 1 (1): 81--128. *Reports from the Division of Fish Management and Scientific Study of the Fishing Industry.* (English translation by WE Ricker, 1945. Mimeographed.)
- Barbeaux, S. J., and Hollowed, A. B. (2017). Ontogeny matters : Climate variability and effects on fish distribution in the eastern Bering Sea. , 1–15. doi:10.1111/fog.12229
- Barnett, L. A. K., Branch, T. A., Ranasinghe, R. A., and Essington, T. E. (2017). Old-Growth Fishes Become Scarce under Fishing. *Current Biology* **27**, 2843-2848.e2. doi:10.1016/j.cub.2017.07.069
- Barrios, A., Ernande, B., Mahe, K., Trenkel, V., and Rochet, M. J. (2017). Utility of mixed effects models to inform the stock structure of whiting in the Northeast Atlantic Ocean. *Fisheries Research* **190**, 132–139. doi:10.1016/j.fishres.2017.02.005
- Bartes, S., Simpfendorfer, C., Walker, T. I., King, C., Loneragan, N., and Braccini, M. (2021). Conventional tagging of sharks in Western Australia: The main commercial species

- exhibit contrasting movement patterns. *Marine and Freshwater Research* **72**, 1643–1656. doi:10.1071/MF20367
- Beamish, R. J., and Fournier, D. A. (1981). A method for comparing the precision of a set of age determinations. *Canadian Journal of Fisheries and Aquatic Sciences* **38**, 982–983.
- Beebee, T., and Rowe, G. (2008). 'An Introduction to Molecular Ecology' 2nd ed. (Oxford University Press: New York, USA.)
- Begg, G. A., Friedland, K. D., and Pearce, J. B. (1999a). Stock identification and its role in stock assessment and fisheries management : an overview. *Fisheries Research* **43**, 1–8.
- Begg, G. A., Hare, J. A., and Sheehan, D. D. (1999b). The role of life history parameters as indicators of stock structure. *Fisheries Research* **43**, 141–163.
- Begg, G. A., and Waldman, J. R. (1999). An holistic approach to fish stock identification. *Fisheries Research* **43**, 35–44.
- Belchier, M., and Collins, M. A. (2008). Recruitment and body size in relation to temperature in juvenile Patagonian tooth (*Dissostichus eleginoides*) at South Georgia. *Marine Biology* **155**, 493–503. doi:10.1007/s00227-008-1047-3
- Berger, A. M., Deroba, J. J., Bosley, K. M., Goethel, D. R., Langseth, B. J., Schueller, A. M., and Hanselman, D. H. (2021). Incoherent dimensionality in fisheries management : consequences of misaligned stock assessment and population boundaries. *ICES Journal of Marine Science* **78**, 155–171. doi:10.1093/icesjms/fsaa203
- Bergstad, O. A. (1990). Distribution, population structure, growth and reproduction of the roundnose grenadier *Coryphaenoides rupestris* (Pisces: Macrouridae) in the deep waters of the Skagerrak. *Marine Biology* **107**, 25–39. doi:10.1007/BF01313239
- Beverton, R. J. ., and Holt, S. . (1957). 'On the Dynamics of Exploited Fish Populations'. (Chapman and Hall: London.)
- Bialek, D. (2003). Sink or Swim : Measures Under International Law for the Conservation of the Patagonian Toothfish in the Southern Ocean. *Ocean Development and International Law* **34**, 105–137. doi:10.1080/00908320390209609

- Blackwell, B. G., Brown, M. L., and Willis, D. W. (2000). Relative Weight (Wr) Status and Current Use in Fisheries Assessment and Management. *Reviews in Fisheries Science* **8**, 1–44. doi:10.1080/10641260091129161
- Bonnet-Lebrun, A. S., Catry, P., Clark, T. J., Campioni, L., Kuepfer, A., Tierny, M., Kilbride, E., and Wakefield, E. D. (2020). Habitat preferences, foraging behaviour and bycatch risk among breeding sooty shearwaters *Ardenna grisea* in the Southwest Atlantic. *Marine Ecology Progress Series* **651**, 163–181. doi:10.3354/meps13439
- Booth, A. J. (2000). Incorporating the spatial component of fisheries data into stock assessment models. *ICES Journal of Marine Science* **57**, 858–865. doi:10.1006/jmsc.2000.0816
- Boucher, E. M. (2018). Disentangling reproductive biology of the Patagonian toothfish *Dissostichus eleginoides*: skipped vs obligatory annual spawning , foraging migration vs residential life style. *Environmental Biology of Fishes* **101**, 1343–1356.
- Branch, T. A., Jensen, O. P., Ricard, D., Ye, Y., and Hilborn, R. (2011). Contrasting Global Trends in Marine Fishery Status Obtained from Catches and from Stock Assessments. *Conservation Biology* **25**, 777–786. doi:10.1111/j.1523-1739.2011.01687.x
- Brander, K. (2010). Impacts of climate change on fisheries. *Journal of Marine Systems* **79**, 389–402. doi:10.1016/j.jmarsys.2008.12.015
- Brander, K. M. (2007). Global fish production and climate change. *Proceedings of the National Academy of Sciences* **104**, 19709–19714.
- Brickle, P., Arkhipkin, A. I., and Shcherbich, Z. N. (2005). Age and growth in a temperate euryhaline notothenioid, *Eleginops maclovinus* from the Falkland Islands. *Journal of the Marine Biological Association of the UK* **85**, 1217. doi:10.1017/S0025315405012348
- Brickle, P., Arkhipkin, A., and Shcherbich, Z. (2006a). Age and growth of a sub-Antarctic notothenioid, *Patagonotothen ramsayi* (Regan 1913), from the Falkland Islands. *Polar Biology* **29**, 633–639. doi:10.1007/s00300-005-0099-9
- Brickle, P., Mackenzie, K., and Pike, A. (2006b). Variations in the parasite fauna of the Patagonian toothfish (*Dissostichus eleginoides* Smitt, 1898), with length, season, and

- depth of habitat around the Falkland Islands. *Journal of Parasitology* **92**, 282–291.
- Brigden, K. E., Marshall, C. T., Scott, B. E., Young, E. F., and Brickle, P. (2017). Interannual variability in reproductive traits of the Patagonian toothfish *Dissostichus eleginoides* around the sub-Antarctic island of South Georgia. *Journal of Fish Biology* **91**, 278–301. doi:10.1111/jfb.13344
- Brophy, D., Haynes, P., Arrizabalaga, H., Fraile, I., Fromentin, J. M., Garibaldi, F., Katavic, I., Tinti, F., Saadet Karakulak, F., Macías, D., Busawon, D., Hanke, A., Kimoto, A., Sakai, O., Deguara, S., Abid, N., and Santos, M. N. (2016). Otolith shape variation provides a marker of stock origin for north Atlantic bluefin tuna (*Thunnus thynnus*). *Marine and Freshwater Research* **67**, 1023–1036. doi:10.1071/MF15086
- Brown, J. (2011). Ecology and life history of a deepwater notothenid, *Dissostichus eleginoides* Smitt 1898, around the Falkland Islands, SW Atlantic Ocean. University of Aberdeen.
- Brown, J., Brickle, P., Hearne, S., and French, G. (2010). An experimental investigation of the ‘umbrella’ and ‘Spanish’ system of longline fishing for the Patagonian toothfish (*Dissostichus eleginoides*) in the Falkland Islands: Implications for stock assessment and seabird by-catch. *Fisheries Research* **106**, 404–412. doi:10.1016/j.fishres.2010.09.013
- Brown, J., Brickle, P., and Scott, B. E. (2013a). Investigating the movements and behaviour of Patagonian toothfish (*Dissostichus eleginoides* Smitt, 1898) around the Falkland Islands using satellite linked archival tags. *Journal of Experimental Marine Biology and Ecology* **443**, 65–74. doi:10.1016/j.jembe.2013.02.029
- Brown, J., Brickle, P., and Scott, B. E. (2013b). The parasite fauna of the Patagonian toothfish *Dissostichus eleginoides* off the Falkland Islands. *Journal of Helminthology* **87**, 501–509. doi:10.1017/S0022149X12000636
- Brundtland, G. (1987). Our common future: Report of the 1987 World Commission on Environment and Development. Oslo.
- Buratti, C. C., and Santos, B. A. (2010). Otolith microstructure and pelagic larval duration in two stocks of the Argentine hake, *Merluccius hubbsi*. *Fisheries Research* **106**, 2–7.
- Burnham, K. P., and Anderson, D. R. (2002). ‘Model selection and multimodel inference: a

- practical information-theoretic approach'. (Springer-Verlag: New York, USA.)
- Busbridge, T. A. J., Marshall, C. T., Arkhipkin, A. I., Shcherbich, Z., Marriott, A. L., and Brickle, P. (2020). Can otolith microstructure and elemental fingerprints elucidate the early life history stages of the gadoid southern blue whiting (*Micromesistius australis australis*)? *Fisheries Research* **228**, 105572. doi:10.1016/j.fishres.2020.105572
- Cadrin, S. X. (2020). Defining spatial structure for fishery stock assessment. *Fisheries Research* **221**, 105397. doi:10.1016/j.fishres.2019.105397
- Cadrin, S. X., Kerr, L. A., and Mariani, S. (2014). Interdisciplinary Evaluation of Spatial Population Structure for Definition of Fishery Management Units. In 'Stock Identification Methods: Applications in Fishery Science'. (Eds S. X. Cadrin, L. A. Kerr, and S. Mariani.) pp. 566. (Academic Press: London.)
- Cadrin, S. X., Maunder, M. N., and Punt, A. E. (2020). Spatial Structure: Theory, estimation and application in stock assessment models. *Fisheries Research* **229**. doi:10.1016/j.fishres.2020.105608
- Campana, S. E. (2001). Accuracy, precision and quality control in age determination, including a review of the use and abuse of age validation methods. *Journal of Fish Biology* **59**, 197–242. doi:10.1111/j.1095-8649.2001.tb00127.x
- Campana, S. E. (1999). Chemistry and composition of fish otoliths: pathways , mechanisms and applications. *Marine Ecology Progress Series* **188**, 263–297.
- Campana, S. E., and Casselman, J. M. (1993). Stock Discrimination Using Otolith Shape-Analysis. *Canadian Journal of Fisheries and Aquatic Sciences* **50**, 1062–1083. doi:10.1139/f93-123
- Campana, S. E., Stefánsdóttir, R. B., Jakobsdóttir, K., and Sólmundsson, J. (2020). Shifting fish distributions in warming sub-Arctic oceans. *Scientific Reports* **10**, 1–14. doi:10.1038/s41598-020-73444-y
- Campana, S. E., and Thorrold, S. R. (2001). Otoliths, increments, and elements: keys to a comprehensive understanding of fish populations? *Canadian Journal of Fisheries and Aquatic Sciences* **58**, 30–38. doi:10.1139/cjfas-58-1-30

- Canales-Aguirre, C. B., Ferrada-Fuentes, S., Galleguillos, R., Oyarzun, F. X., and Hernandez, C. E. (2018). Population genetic structure of Patagonian toothfish (*Dissostichus eleginoides*) in the Southeast Pacific and Southwest Atlantic Ocean. *PeerJ* **6**, e4173. doi:10.7717/peerj.4173
- Cardinale, M., Kastowsky, M., and Mosegaard, H. (2004). Effects of sex, stock, and environment on the shape of known-age Atlantic cod (*Gadus morhua*) otoliths. *Canadian Journal of Fisheries and Aquatic Sciences* **61**, 158–167. doi:10.1139/F03-151
- Castonguay, M., Simard, P., and Gagnon, P. (1991). Usefulness of Fourier Analysis of Otolith Shape for Atlantic Mackerel (*Scomber scombrus*) Stock Discrimination. *Canadian Journal of Fisheries and Aquatic Sciences* **48**, 296–302. doi:10.1139/f91-041
- Chemshirova, I., Hoving, H. J., and Arkhipkin, A. (2021). Temperature effects on size, maturity, and abundance of the squid *Illex argentinus* (Cephalopoda, Ommastrephidae) on the Patagonian Shelf. *Estuarine, Coastal and Shelf Science* **255**, 107343. doi:10.1016/j.ecss.2021.107343
- Chikov, V. N., and Melnikov, Y. S. (1990). On the question of fecundity of the Patagonian toothfish, *Dissostichus eleginoides*, in the region of the Kerguelen Islands. *Journal of Ichthyology* **30**, 122–125.
- Christensen, V., Coll, M., Piroddi, C., Steenbeek, J., Buszewski, J., and Pauly, D. (2014). A century of fish biomass decline in the ocean. *Marine Ecology Progress Series* **512**, 155–166. doi:10.3354/meps10946
- Ciannelli, L., Fisher, J. A. D., Skern-Mauritzen, M., Hunsicker, M. E., Hidalgo, M., Frank, K. T., and Bailey, K. M. (2013). Theory, consequences and evidence of eroding population spatial structure in harvested marine fishes: A review. *Marine Ecology Progress Series* **480**, 227–243. doi:10.3354/meps10067
- Clark, M. R., and Dunn, M. R. (2012). Spatial management of deep-sea seamount fisheries: balancing sustainable exploitation and habitat conservation. *Environmental Conservation* **39**, 204–214. doi:10.1017/S0376892912000021
- Clarke, A., Barnes, D. K. A., and Hodgson, D. A. (2005). How isolated is Antarctica? *Trends*

- in Ecology and Evolution* **20**, 1–3. doi:10.1016/j.tree.2004.10.004
- Clarke, M. W., Kelly, C. J., Connolly, P. L., and Molloy, J. P. (2003). A life history approach to the assessment and management of deepwater fisheries in the Northeast Atlantic. *Journal of Northwest Atlantic Fishery Science* **31**, 401–411.
- Claude, J. (2008). 'Morphometrics with R'. (Springer Science and Business Media, LLC: New York.) doi:10.1007/978-1-4419-7976-6
- Clausen, L. A. W., Bekkevold, D., Hatfield, E. M. C., and Mosegaard, H. (2007). Application and validation of otolith microstructure as a stock identification method in mixed Atlantic herring (*Clupea harengus*) stocks in the North Sea and western Baltic. *ICES Journal of Marine Science* **64**, 377–385. doi:10.1093/icesjms/fsl036
- Coll, M., Pennino, M. G., Steenbeek, J., Sole, J., and Bellido, J. M. (2019). Predicting marine species distributions: Complementarity of food-web and Bayesian hierarchical modelling approaches. *Ecological Modelling* **405**, 86–101. doi:10.1016/j.ecolmodel.2019.05.005
- Collins, M. A., Brickle, P., Brown, J., and Belchier, M. (2010). The Patagonian Toothfish. Biology, Ecology and Fishery. *Advances in Marine Biology* **58**, 227–300. doi:10.1016/B978-0-12-381015-1.00004-6
- Collins, M. A., Hollyman, P. R., Clark, J., Soeffker, M., Yates, O., and Phillips, R. A. (2021). Mitigating the impact of longline fisheries on seabirds: Lessons learned from the South Georgia Patagonian toothfish fishery (CCAMLR Subarea 48 . 3). *Marine Policy* **131**, 104618. doi:10.1016/j.marpol.2021.104618
- Constable, A. J., de la Mare, W. K., Agnew, D. J., Everson, I., and Miller, D. (2000). Managing fisheries to conserve the Antarctic marine ecosystem: practical implementation of the Convention on the Conservation of Antarctic Marine Living Resources (CCAMLR). *ICES Journal of Marine Science* **57**, 778–791. doi:10.1006/jmsc.2000.0725
- Cooper, D. W., and Nichol, D. G. (2016). Juvenile northern rock sole (*Lepidopsetta polyxystra*) spatial distribution and abundance patterns in the eastern Bering Sea: spatially dependent production linked to temperature. *ICES Journal of Marine Science* **73**, 1138–1146.

- Cope, J. M., and Punt, A. E. (2011). Reconciling stock assessment and management scales under conditions of spatially varying catch histories. *Fisheries Research* **107**, 22–38. doi:10.1016/j.fishres.2010.10.002
- Coppola, D., Giordano, D., Abbruzzetti, S., Marchesani, F., Balestrieri, M., di Prisco, G., Viappiani, C., Bruno, S., and Verde, C. (2015). Functional characterisation of the haemoglobins of the migratory notothenioid fish *Dissostichus eleginoides*. *Hydrobiologia* **761**, 315–333. doi:10.1007/s10750-015-2439-2
- Costello, C., and Ovando, D. (2019). Status, Institutions, and Prospects for Global Capture Fisheries. *Annual Review of Environment and Resources* **44**, 177–200. doi:10.1146/annurev-environ-101718-033310
- Costello, C., Ovando, D., Clavelle, T., Strauss, C. K., Hilborn, R., and Melnychuk, M. C. (2016). Global fishery prospects under contrasting management regimes. *Proceedings of the National Academy of Sciences of the United States of America* **113**, 5125–5129. doi:10.1073/pnas.1520420113
- Costello, C., Ovando, D., Hilborn, R., Gaines, S. D., Deschenes, O., and Lester, S. E. (2012). Status and Solutions for the World's Unassessed Fisheries. *Science* **338**, 517–520. doi:10.1126/science.1223389
- Cowen, R. K., Gawarkiewicz, G., Pineda, J., Thorrold, S. R., Werner, F. E., Simon, R., and Werner, F. E. (2007). Population connectivity in marine systems: An overview. *Oceanography* **20**, 14–21. doi:10.5670/oceanog.2007.26
- Cowen, R. K., and Sponaugle, S. (2009). Larval dispersal and marine population connectivity. *Annual Review of Marine Science* **1**, 443–466. doi:10.1146/annurev.marine.010908.163757
- Crowder, L. B., Lyman, S. J., Figueira, W. F., and Priddy, J. (2000). Source-sink population dynamics and the problem of siting marine reserves. *Bulletin of Marine Science* **66**, 799–820.
- Croxall, J. P., and Nicol, S. (2004). Management of Southern Ocean fisheries: global forces and future sustainability. *Antarctic Science* **16**, 569–584.

doi:10.1017/S0954102004002330

- Croxall, J. P., and Wood, A. G. (2002). The importance of the Patagonian Shelf for top predator species breeding at South Georgia. *Aquatic Conservation: Marine and Freshwater Ecosystems* **118**, 101–118. doi:10.1002/aqc.480
- Danovaro, R., Fanelli, E., Aguzzi, J., Billett, D., Carugati, L., Corinaldesi, C., Anno, A. D., Gjerde, K., Jamieson, A. J., Kark, S., McClain, C., Levin, L., Levin, N., Ramirez-Ilodra, E., Ruhl, H., and Smith, C. R. (2020). Ecological variables for developing a global deep-ocean monitoring and conservation strategy. *Nature Ecology & Evolution* **4**, 181–192.
- Devine, J. A., Baker, K. D., and Haedrich, R. L. (2006). Deep-sea fishes qualify as endangered. *Nature* **439**, 29. doi:10.1038/439029a
- Devine, J. A., Watling, L., Cailliet, G., Drazen, J., Durán Muñoz, P., Orlov, A. M., and Bezaury, J. (2012). Evaluation of potential sustainability of deep-sea fisheries for grenadiers (Macrouridae). *Journal of Ichthyology* **52**, 709–721. doi:10.1134/S0032945212100062
- Dickey-Collas, M., Nash, R. D. M., Brunel, T., Van Damme, C. J. G., Marshall, C. T., Payne, M. R., Corten, A., Geffen, A. J., Peck, M. A., Hatfield, E. M. C., Hintzen, N. T., Enberg, K., Kell, L. T., and Simmonds, E. J. (2010). Lessons learned from stock collapse and recovery of North Sea herring: A review. *ICES Journal of Marine Science* **67**, 1875–1886. doi:10.1093/icesjms/fsq033
- Doonan, I. J., Fu, D., and Dunn, M. R. (2015). Harvest control rules for a sustainable orange roughy fishery. *Deep-Sea Research Part I* **98**, 53–61. doi:10.1016/j.dsr.2014.12.001
- Doyle, M. J., and Mier, K. L. (2016). Early life history pelagic exposure profiles of selected commercially important fish species in the Gulf of Alaska. *Deep-Sea Research II* **132**, 162–193.
- Dray, S., and Dufour, A.-B. (2007). The **ade4** Package: Implementing the Duality Diagram for Ecologists. *Journal of Statistical Software* **22**. doi:10.18637/jss.v022.i04
- Drazen, J. C., and Haedrich, R. L. (2012). A continuum of life histories in deep-sea demersal fishes. *Deep-Sea Research Part I* **61**, 34–42. doi:10.1016/j.dsr.2011.11.002
- Drévillon, M., Lellouche, J.-M., Régnier, C., Garric, G., Bricaud, C., Hernandez, O., and

- Bourdallé-Badie, R. (2021). Quality Information Document: For Global Ocean Reanalysis Products. CMEMS-GLO-QUID-001-030. Available at: <https://catalogue.marine.copernicus.eu/documents/QUID/CMEMS-GLO-QUID-001-030.pdf>
- Duarte, C. M., Agusti, S., Barbier, E., Britten, G. L., Castilla, J. C., Gattuso, J., Fulweiler, R. W., Hughes, T. P., Knowlton, N., Lovelock, C. E., Lotze, H. K., Predragovic, M., Poloczanska, E., Roberts, C., and Worm, B. (2020). Rebuilding marine life. *Nature* **580**, 39–51. doi:10.1038/s41586-020-2146-7
- Eastman, J. T. (1993). 'Antarctic fish biology: evolution in a unique environment.' (Academic Press: San Diego, California.)
- Edwards, J. E., Pratt, J., Tress, N., and Hussey, N. E. (2019). Thinking deeper: Uncovering the mysteries of animal movement in the deep sea. *Deep-Sea Research Part I: Oceanographic Research Papers* **146**, 24–43. doi:10.1016/j.dsr.2019.02.006
- Everson, I., and Murray, A. (1999). Size at sexual maturity of Patagonian toothfish (*Dissostichus eleginoides*). *CCAMLR Science* **6**, 37–46.
- Evseenko, S. A., Kock, K. H., and M, N. M. (1995). Early life history of the Patagonian toothfish, *Dissostichus eleginoides* Smitt, 1898 in the Atlantic sector of the Southern Ocean. *Antarctic Science* **7**, 221–226. doi:10.1017/S0954102095000319
- FAO (2020). 'The State of World Fisheries and Aquaculture 2020. Sustainability in action.' doi:<https://doi.org/10.4060/ca9229en>
- Farrugia, T. J., Goyot, L., and Kuepfer, A. (2018). Toothfish Tagging and Underwater Camera: Cruise Report ZDLK3-11-2018. Stanley, Falkland Islands Government, Fisheries department.
- Farrugia, T. J., and Keningale, B. (2018). Toothfish Tagging and Underwater Camera: Cruise Report ZDLK3-02-2018. Stanley, Falkland Islands Government, Fisheries department.
- Félix-Hackradt, F. C., Hackradt, C. W., Treviño-Otón, J., Segovia-Viadero, M., Pérez-Ruzafa, A., and García-Charton, J. A. (2013). Environmental determinants on fish post-larval distribution in coastal areas of south-western Mediterranean Sea. *Estuarine, Coastal and*

- Shelf Science* **129**, 59–72. doi:10.1016/j.ecss.2013.05.029
- Ferguson, G. J., Ward, T. M., and Gillanders, B. M. (2011). Otolith shape and elemental composition: Complementary tools for stock discrimination of mulloway (*Argyrosomus japonicus*) in southern Australia. *Fisheries Research* **110**, 75–83. doi:10.1016/j.fishres.2011.03.014
- Fernandez, E., and Lellouche, J. M. (2021). Product User Manual: For the Global Ocean Physical Reanalysis product. CMEMS-GLO-PUM-001-030. Available at: <https://catalogue.marine.copernicus.eu/documents/PUM/CMEMS-GLO-PUM-001-030.pdf>
- Fiorentino, F., Garofalo, G., De Santi, A., Bono, G., Giusto, G. B., and Norrito, G. (2003). Spatio-temporal distribution of recruits (0 group) of *Merluccius merluccius* and *Phycis blennoides* (Pisces, Gadiformes) in the Strait of Sicily (Central Mediterranean). *Hydrobiologia* **503**, 223–236.
- Fogarty, M. J. (2014). The art of ecosystem-based fishery management. *Canadian Journal of Fisheries and Aquatic Sciences* **71**, 479–490.
- Fonseca, V. P., Pennino, M. G., de Nóbrega, M. F., Oliveira, J. E. L., and de Figueiredo Mendes, L. (2017). Identifying fish diversity hot-spots in data-poor situations. *Marine Environmental Research* **129**, 365–373. doi:10.1016/j.marenvres.2017.06.017
- Fraile, I., Arrizabalaga, H., Santiago, J., Goñi, N., Arregi, I., Madinabeitia, S., David Wells, R. J., and Rooker, J. R. (2016). Otolith chemistry as an indicator of movements of albacore (*Thunnus alalunga*) in the North Atlantic Ocean. *Marine and Freshwater Research* **67**, 1002–1013. doi:10.1071/MF15097
- Francis, R. C., Hixon, M. A., Clarke, E., Murawski, S. A., and Ralston, S. (2007). Ten Commandments for Ecosystem-Based Fisheries Scientists. *Fisheries* **32**, 217–233. doi:10.1577/1548-8446(2007)32
- Franco, B. C., Combes, V., and González Carman, V. (2020a). Subsurface Ocean Warming Hotspots and Potential Impacts on Marine Species: The Southwest South Atlantic Ocean Case Study. *Frontiers in Marine Science* **7**, 1–13. doi:10.3389/fmars.2020.563394

- Franco, B. C., Defeo, O., Piola, A. R., Barreiro, M., Yang, H., Ortega, L., Gianelli, I., Castello, J. P., Vera, C., Buratti, C., Pájaro, M., Pezzi, L. P., and Möller, O. O. (2020b). Climate change impacts on the atmospheric circulation, ocean, and fisheries in the southwest South Atlantic Ocean: a review. *Climatic Change* **162**, 2359–2377. doi:10.1007/s10584-020-02783-6
- Franco, C., Piola, A. R., Rivas, L., Baldoni, A., and Pisoni, J. P. (2008). Multiple thermal fronts near the Patagonian shelf break. *Geophysical Research Letters* **35**, L02607. doi:10.1029/2007GL032066
- Fraser, C. I., Kay, G. M., Plessis, M., and Ryan, P. G. (2017). Breaking down the barrier: dispersal across the Antarctic Polar Front. *Ecography* **40**, 235–237. doi:10.1111/gcb.13304
- Freeman, N. M., Lovenduski, N. S., and Gent, P. R. (2016). Temporal variability in the Antarctic Polar Front (2002-2014). *Journal of Geophysical Research: Oceans* **121**, 7263–7276. doi:10.1002/2016JC012145.Received
- Fronhofer, E. A., Kubisch, A., Hilker, F. M., Hovestadt, T., and Poethke, H. J. (2012). Why are metapopulations so rare? *Ecology* **93**, 1967–1978.
- Fuglstad, G. A., Simpson, D., Lindgren, F., and Rue, H. (2019). Constructing Priors that Penalize the Complexity of Gaussian Random Fields. *Journal of the American Statistical Association* **114**, 445–452. doi:10.1080/01621459.2017.1415907
- Galaiduk, R., Radford, B. T., Saunders, B. J., Newman, S. J., and Harvey, E. S. (2017). Characterizing ontogenetic habitat shifts in marine fishes: Advancing nascent methods for marine spatial management. *Ecological Applications* **27**, 1776–1788. doi:10.1002/eap.1565
- Godelman, E., Brunetti, E., Palacios, M., Lugo, A., and Cornejo, A. (2021). Preevaluación de la Pesquería de Merluza Negra (*Dissostichus eleginoides*) con Redes de Arrastre de Fondo por Buques de la Flota Congeladora de Bandera Argentina.
- Gras, M., Randhawa, H. S., Blake, A., Busbridge, T., Chemshirova, I., and Guest, A. (2018). Report of the 2018 ground fish survey ZDLM3–02–2018. Stanley, Falkland Islands

- Government, Fisheries department.
- Grilly, E., Reid, K., Lenel, S., and Jabour, J. (2015). The price of fish: A global trade analysis of Patagonian (*Dissostichus eleginoides*) and Antarctic toothfish (*Dissostichus mawsoni*). *Marine Policy* **60**, 186–196. doi:10.1016/j.marpol.2015.06.006
- Grønkvær, P. (2016). Otoliths as individual indicators: A reappraisal of the link between fish physiology and otolith characteristics. *Marine and Freshwater Research* **67**, 881–888. doi:10.1071/MF15155
- Grorud-Colvert, K., and Sponaugle, S. (2009). Larval supply and juvenile recruitment of coral reef fishes to marine reserves and non-reserves of the upper Florida Keys, USA. *Marine Biology* **156**, 277–288. doi:10.1007/s00227-008-1082-0
- Guisan, A., and Zimmermann, N. E. (2000). Predictive habitat distribution models in ecology. *Ecological Modelling* **135**, 147–186.
- Gullestad, P., and Sundby, S. (2020). Management of transboundary and straddling fish stocks in the Northeast Atlantic in view of climate-induced shifts in spatial distribution. *Fish and Fisheries* **21**, 1008–1026. doi:10.1111/faf.12485
- Haddon, M. (2011). 'Modelling and Quantitative Methods in Fisheries' 2nd Editio. (CRC Press: Taylor & Francis Group: Boca Raton.)
- Haedrich, R. L., Merrett, N. R., O'Dea, N. R., and Dea, N. R. O. (2001). Can ecological knowledge catch up with deep-water fishing? A North Atlantic perspective. *Fisheries Research* **51**, 113–122. doi:10.1016/S0165-7836(01)00239-9
- Hall, D. A. (2014). Conventional and Radio Frequency Identification (RFID Tags). In 'Stock Identification Methods: Applications in Fishery Science'. (Eds S. X. Cadrin, L. Kerr, and S. Mariani.) pp. 365–395. (Academic Press: London.)
- Hanchet, S., Dunn, A., Parker, S., Horn, P., Stevens, D., and Mormede, S. (2015). The Antarctic toothfish (*Dissostichus mawsoni*): biology, ecology, and life history in the Ross Sea region. *Hydrobiologia* **761**, 397–414. doi:10.1007/s10750-015-2435-6
- Hanchet, S. M., Rickard, G. J., Fenaughty, J. M., and Dunn, A. (2008). A hypothetical life cycle for Antarctic toothfish (*Dissostichus mawsoni*) in the Ross Sea region. *CCAMLR Science*

15, 35–53.

- Hare, J. A., and Richardson, D. E. (2014). The Use of Early Life Stages in Stock Identification Studies. In 'Stock Identification Methods: Applications in Fishery Science'. (Eds S. Cadrin, L. Kerr, and S. Mariani.) pp. 566. (Academic Press: London.)
- Hawkins, S. J., Bohn, K., Sims, D. W., Ribeiro, P., Faria, J., Presa, P., Pita, A., Martins, G. M., Neto, A. I., Burrows, M. T., and Genner, M. J. (2016). Fisheries stocks from an ecological perspective: Disentangling ecological connectivity from genetic interchange. *Fisheries Research* **179**, 333–341. doi:10.1016/j.fishres.2016.01.015
- Hedges, K. J., Ludsin, S. A., and Fryer, B. J. (2004). Effects of ethanol preservation on otolith microchemistry. *Journal of Fish Biology* **64**, 923–937. doi:10.1111/j.1095-8649.2004.00353.x
- Hegg, J. C., Kennedy, B. P., and Chittaro, P. (2019). What did you say about my mother? The complexities of maternally derived chemical signatures in otoliths. *Canadian Journal of Fisheries and Aquatic Sciences* **76**, 81–94. doi:10.1139/cjfas-2017-0341
- Heimbrand, Y., Limburg, K. E., Hüsey, K., Casini, M., Sjöberg, R., Palmén Bratt, A. M., Levinsky, S. E., Karpushevskaja, A., Radtke, K., and Öhlund, J. (2020). Seeking the true time: Exploring otolith chemistry as an age-determination tool. *Journal of Fish Biology* **97**, 552–565. doi:10.1111/jfb.14422
- Henriquez, V., Licandeo, R., Cubillos, L. A., and Cox, S. P. (2016). Interactions between ageing error and selectivity in statistical catch-at-age models: simulations and implications for assessment of the Chilean Patagonian toothfish fishery. *ICES Journal of Marine Science* **73**, 1074–1090.
- Hernandez, M., Midway, S., West, L., Tillya, H., and Polito, M. (2021). Stable isotopes track the ontogenetic movement of three commercially important fishes along a coastal Tanzanian seascape. *Marine Ecology Progress Series* **670**, 139–154. doi:10.3354/meps13754
- Hilborn, R. (2020). Measuring fisheries management performance. *ICES Journal of Marine Science* **77**, 2432–2438. doi:10.1093/icesjms/fsaa119

- Hilborn, R., Amoroso, R. O., Anderson, C. M., Baum, J. K., Branch, T. A., Costello, C., Moor, C. L. de, Faraj, A., Hively, D., Jensen, O. P., Kurota, H., Little, L. R., Mace, P., McClanahan, T., Melnychuk, M. C., Minto, C., Osio, G. C., Parma, A. M., Pons, M., Segurado, S., Szuwalski, C. S., Wilson, J. R., and Ye, Y. (2020). Effective fisheries management instrumental in improving fish stock status. *Proceedings of the National Academy of Sciences* **117**, 2218–2224. doi:10.1073/pnas.1909726116
- Hilborn, R., Fulton, E. A., Green, B. S., Hartmann, K., Tracey, S. R., and Watson, R. A. (2015). When is a fishery sustainable? *Canadian Journal of Fisheries and Aquatic Sciences* **72**, 1433–1441. doi:10.1139/cjfas-2015-0062
- Hilborn, R., Quinn, T. P., Schindler, D. E., and Rogers, D. E. (2003). Biocomplexity and fisheries sustainability. *Proceedings of the National Academy of Sciences of the United States of America* **100**, 6564–6568. doi:10.1073/pnas.1037274100
- Van Den Hoff, J., Kilpatrick, R., and Welsford, D. (2017). Southern elephant seals (*Mirounga leonina* Linn.) depredate toothfish longlines in the midnight zone. *PLoS ONE* **12**, 1–13. doi:10.1371/journal.pone.0172396
- Hogan, J. D., Kozdon, R., Blum, M. J., Gilliam, J. F., Valley, J. W., and McIntyre, P. B. (2017). Reconstructing larval growth and habitat use in an amphidromous goby using otolith increments and microchemistry. *Journal of Fish Biology* **90**, 1338–1355. doi:10.1111/jfb.13240
- Hollyman, P. R., Hill, S. L., Laptikhovskiy, V. V., Belchier, M., Gregory, S., Clement, A., and Collins, M. A. (2021). A long road to recovery: Dynamics and ecology of the marbled rockcod (*Notothenia rossii*, family: Nototheniidae) at South Georgia, 50 years after overexploitation. *ICES Journal of Marine Science* **78**, 2745–2756. doi:10.1093/icesjms/fsab150
- Hoover, R. R., and Jones, C. M. (2013). Effect of laser ablation depth in otolith life history scans. *Marine Ecology Progress Series* **486**, 247–256. doi:10.3354/meps10328
- Hoover, R. R., Jones, C. M., and Grosch, C. E. (2012). Estuarine ingress timing as revealed by spectral analysis of otolith life history scans. *Canadian Journal of Fisheries and*

- Aquatic Sciences* **1277**, 1266–1277. doi:10.1139/F2012-058
- Horn, P. L. (2002). Age and growth of Patagonian toothfish (*Dissostichus eleginoides*) and Antarctic toothfish (*D. mawsoni*) in waters from the New Zealand subantarctic to the Ross Sea, Antarctica. *Fisheries Research Research* **56**, 275–287.
- Howey, L. A., Wetherbee, B. M., Tolentino, E. R., and Shivji, M. S. (2017). Biogeophysical and physiological processes drive movement patterns in a marine predator. *Movement Ecology* **5**, 16. doi:10.1186/s40462-017-0107-z
- Hussey, N. E., Orr, J., Fisk, A. T., Hedges, K. J., Ferguson, S. H., and Barkley, A. N. (2018). Mark report satellite tags (mrPATs) to detail large-scale horizontal movements of deep water species: First results for the Greenland shark (*Somniosus microcephalus*). *Deep-Sea Research Part I: Oceanographic Research Papers* **134**, 32–40. doi:10.1016/j.dsr.2018.03.002
- Hüssy, K. (2008). Otolith shape in juvenile cod (*Gadus morhua*): Ontogenetic and environmental effects. *Journal of Experimental Marine Biology and Ecology* **364**, 35–41. doi:10.1016/j.jembe.2008.06.026
- Hutchings, J. A. (1996). Spatial and temporal variation in the density of northern cod and a review of hypotheses for the stock's collapse. *Canadian Journal of Fisheries and Aquatic Sciences* **53**, 943–962. doi:10.1139/cjfas-53-5-943
- Izzo, C., Doubleday, Z. A., and Gillanders, B. M. (2016a). Where do elements bind within the otoliths of fish? *Marine and Freshwater Research* **67**, 1072–1076.
- Izzo, C., Doubleday, Z. A., Grammer, G. L., Gilmore, K. L., Alleway, H. K., Barnes, T. C., Disspain, M. C. F., Giraldo, A. J., Mazloumi, N., and Gillanders, B. M. (2016b). Fish as proxies of ecological and environmental change. *Reviews in Fish Biology and Fisheries* **26**, 265–286. doi:10.1007/s11160-016-9424-3
- Izzo, C., Ward, T. M., Ivey, A. R., Suthers, I. M., Stewart, J., Sexton, S. C., and Gillanders, B. M. (2017). Integrated approach to determining stock structure: implications for fisheries management of sardine, *Sardinops sagax*, in Australian waters. *Reviews in Fish Biology and Fisheries* **27**, 267–284. doi:10.1007/s11160-017-9468-z

- Janßen, H., Bastardie, F., Eero, M., Hamon, K. G., Hinrichsen, H. H., Marchal, P., Nielsen, J. R., Le Pape, O., Schulze, T., Simons, S., Teal, L. R., and Tidd, A. (2018). Integration of fisheries into marine spatial planning: Quo vadis? *Estuarine, Coastal and Shelf Science* **201**, 105–113. doi:10.1016/j.ecss.2017.01.003
- Kainge, P., van der Plas, A. K., Bartholomae, C. H., and Wieland, K. (2017). Effects of environmental variables on survey catch rates and distribution by size of shallow- and deep-water Cape hakes, *Merluccius capensis* and *Merluccius paradoxus* off Namibia. *Fisheries Oceanography* **26**, 680–692. doi:10.1111/fog.12227
- Keating, J. P., Brophy, D., Officer, R. A., and Mullins, E. (2014). Otolith shape analysis of blue whiting suggests a complex stock structure at their spawning grounds in the Northeast Atlantic. *Fisheries Research* **157**, 1–6. doi:10.1016/j.fishres.2014.03.009
- Kelly, C. J., Connolly, P. L., and Bracken, J. J. (1997). Age estimation, growth, maturity and distribution of the roundnose grenadier from the Rockall trough. *Journal of Fish Biology* **50**, 1–17. doi:10.1006/jfbi.1996.0272
- Kenny, A. J., Campbell, N., Koen-alonso, M., Pepin, P., and Diz, D. (2018). Delivering sustainable fisheries through adoption of a risk-based framework as part of an ecosystem approach to fisheries management. *Marine Policy* **93**, 232–240. doi:10.1016/j.marpol.2017.05.018
- Kerr, L. A., Hintzen, N. T., Cadrin, S. X., Clausen, L. W., Dickey-Collas, M., Goethel, D. R., Hatfield, E. M. C., Kritzer, J. P., and Nash, R. D. M. (2017). Lessons learned from practical approaches to reconcile mismatches between biological population structure and stock units of marine fish. *ICES Journal of Marine Science* **74**, 1708–1722. doi:10.1093/icesjms/fsw188
- Kerr, L. A., Whitener, Z. T., Cadrin, S. X., Morse, M. R., Secor, D. H., and Golet, W. (2020). Mixed stock origin of Atlantic bluefin tuna in the U.S. rod and reel fishery (Gulf of Maine) and implications for fisheries management. *Fisheries Research* **224**, 105461. doi:10.1016/j.fishres.2019.105461
- Killick, R., and Eckley, I. (2014). “changept: An R Package for Changept Analysis.

- Journal of Statistical Software* **58**, 1–19.
- Kimura, D. K., Shimada, A. M., and Shaw, F. R. (1998). Stock structure and movement of tagged sablefish, *Anoplopoma fimbria*, in offshore northeast pacific waters and the effects of el nino-southern oscillation on migration and growth. *Fishery Bulletin* **96**, 462–481.
- Kloser, R. J., Sutton, C., Krusic-golub, K., and Ryan, T. E. (2015). Indicators of recovery for orange roughy (*Hoplostethus atlanticus*) in eastern Australian waters fished from 1987. *Fisheries Research* **167**, 225–235. doi:10.1016/j.fishres.2015.02.017
- Kock, K.-H. K.-H., Reid, K., Croxall, J., and Nicol, S. (2007). Fisheries in the Southern Ocean: an ecosystem approach. *Philosophical Transactions of the Royal Society B: Biological Sciences* **362**, 2333–2349. doi:10.1098/rstb.2006.1954
- Kock, K.-H., and Kellermann, A. (1991). Reproduction in Antarctic notothenioid fish. *Antarctic Science* **3**, 125–150. doi:10.1017/S0954102091000172
- Koslow, J. A., Boehlert, G. W., Gordon, J. D. M., Haedrich, R. L., Lorance, P., and Parin, N. (2000). Continental slope and deep-sea fisheries: Implications for a fragile ecosystem. *ICES Journal of Marine Science* **57**, 548–557. doi:10.1006/jmsc.2000.0722
- Kraufvelin, P., Pekcan-Hekim, Z., Bergström, U., Florin, A. B., Lehikoinen, A., Mattila, J., Arula, T., Briekmane, L., Brown, E. J., Celmer, Z., Dainys, J., Jokinen, H., Kääriä, P., Kallasvuo, M., Lappalainen, A., Lozys, L., Möller, P., Orio, A., Rohtla, M., Saks, L., Snickars, M., Støttrup, J., Sundblad, G., Taal, I., Ustups, D., Verliin, A., Vetemaa, M., Winkler, H., Wozniczka, A., and Olsson, J. (2018). Essential coastal habitats for fish in the Baltic Sea. *Estuarine, Coastal and Shelf Science* **204**, 14–30. doi:10.1016/j.ecss.2018.02.014
- Kritzer, J. P., and Sale, P. F. (2004). Metapopulation ecology in the sea: from Levins' model to marine ecology and fisheries science. *Fish and Fisheries Fish Fish* **5**, 131–140. doi:10.1111/J.1467-2979.2004.00131.X
- Kruskal, J. B. (1964). Nonmetric multidimensional scaling: A numerical method. *Psychometrika* **29**, 115–129. doi:10.1007/BF02289694
- Kurth, B. N., Peebles, E. B., and Stallings, C. D. (2019). Atlantic Tarpon (*Megalops atlanticus*) exhibit upper estuarine habitat dependence followed by foraging system fidelity after

- ontogenetic habitat shifts. *Estuarine, Coastal and Shelf Science* **225**, 106248. doi:10.1016/j.ecss.2019.106248
- Laptikhovskiy, V., Arkhipkin, A., and Brickle, P. (2006a). Distribution and reproduction of the Patagonian toothfish *Dissostichus eleginoides* Smitt around the Falkland Islands. *Journal of Fish Biology* **68**, 849–861. doi:10.1111/j.0022-1112.2006.00973.x
- Laptikhovskiy, V., Arkhipkin, A., and Brickle, P. (2013). From small bycatch to main commercial species: Explosion of stocks of rock cod *Patagonotothen ramsayi* (Regan) in the Southwest Atlantic. *Fisheries Research* **147**, 399–403. doi:10.1016/j.fishres.2013.05.006
- Laptikhovskiy, V., and Brickle, P. (2005). The Patagonian toothfish fishery in Falkland Islands' waters. *Fisheries Research* **74**, 11–23. doi:10.1016/j.fishres.2005.04.006
- Laptikhovskiy, V. V., Arkhipkin, A. I., and Brickle, P. (2006b). Life history, fishery, and stock conservation of the Patagonian toothfish around the Falkland Islands. *American Fisheries Society Symposium* **49**, 587–594. doi:10.1111/j.1095-8649.2006.00973.x
- Larkin, P. A. (1976). An Epitaph for the Concept of Maximum Sustained Yield. *Transactions of the American Fisheries Society* **19**.
- Lauria, V., Garofalo, G., Fiorentino, F., Massi, D., Milisenda, G., Piraino, S., Russo, T., and Gristina, M. (2017). Species distribution models of two critically endangered deep-sea octocorals reveal fishing impacts on vulnerable marine ecosystems in central Mediterranean Sea. *Scientific Reports* **7**, 1–14. doi:10.1038/s41598-017-08386-z
- Leach, K., Montgomery, W. I., and Reid, N. (2016). Modelling the influence of biotic factors on species distribution patterns. *Ecological Modelling* **337**, 96–106. doi:10.1016/j.ecolmodel.2016.06.008
- Lee, B., Arkhipkin, A., and Randhawa, H. S. (2021). Environmental drivers of Patagonian toothfish (*Dissostichus eleginoides*) spatial-temporal patterns during an ontogenetic migration on the Patagonian Shelf. *Estuarine, Coastal and Shelf Science* **259**, 107473. doi:10.1016/j.ecss.2021.107473
- Lee, B., Brewin, P. E., Brickle, P., and Randhawa, H. (2018). Use of otolith shape to inform stock structure in Patagonian toothfish (*Dissostichus eleginoides*) in the south-western

- Atlantic. *Marine and Freshwater Research* **69**, 1238–1247. doi:10.1071/MF17327
- Lee, B., Cockroft, K., Arkhipkin, A. I., Wing, S. R., and Randhawa, H. S. (2019a). Age , growth and mortality estimates for the ridge-scaled grenadier *Macrourus carinatus* (Günther , 1878) in the south-western Atlantic. *Fisheries Research* **218**, 174–185. doi:10.1016/j.fishres.2019.05.012
- Lee, B., Goyot, L., Castillejos, J. E. R., Hall, J., and Zawadowski, T. (2019b). Research Cruise Report: ZDLT1-12-2018. Patagonian toothfish - juvenile survey. Stanley.
- Lee, B., Skeljo, F., Randhawa, H. S., and Arkhipkin, A. (2022). Deep-sea movement patterns of the Patagonian toothfish *Dissostichus eleginoides* Smitt in the Southwest Atlantic. *Marine and Freshwater Research*, 1–13. doi:10.1071/MF21338
- Legendre, P., Oksanen, J., and ter Braak, C. J. F. (2011). Testing the significance of canonical axes in redundancy analysis. *Methods in Ecology and Evolution* **2**, 269–277. doi:10.1111/j.2041-210X.2010.00078.x
- Lestrel, P. E. (1997). 'Fourier Descriptors and their Applications in Biology'. (Cambridge University Press: Cambridge.)
- Lezama-Ochoa, N., Pennino, M. G., Hall, M. A., Lopez, J., and Murua, H. (2020). Using a Bayesian modelling approach (INLA - SPDE) to predict the occurrence of the Spinetail Devil Ray (*Mobular mobular*). *Scientific Reports* **10**, 18822. doi:10.1038/s41598-020-73879-3
- Libungan, L. A., Óskarsson, G. J., Slotte, A., Jacobsen, J. A., and Pálsson, S. (2015). Otolith shape: A population marker for Atlantic herring *Clupea harengus*. *Journal of Fish Biology* **86**, 1377–1395. doi:10.1111/jfb.12647
- Libungan, L. A., and Pálsson, S. (2015). ShapeR: An R Package to Study Otolith Shape Variation among Fish Populations. , 1–12. doi:10.1371/journal.pone.0121102
- Limburg, K. E., Walther, B. D., Lu, Z., Jackman, G., Mohan, J., Walther, Y., Nissling, A., Weber, P. K., and Schmitt, A. K. (2015). In search of the dead zone: Use of otoliths for tracking fish exposure to hypoxia. *Journal of Marine Systems* **141**, 167–178. doi:10.1016/j.jmarsys.2014.02.014

- Limburg, K. E., Wuenschel, M. J., Hüsey, K., Heimbrand, Y., and Samson, M. (2018). Making the Otolith Magnesium Chemical Calendar-Clock Tick: Plausible Mechanism and Empirical Evidence. *Reviews in Fisheries Science and Aquaculture* **26**, 479–493. doi:10.1080/23308249.2018.1458817
- Lindgren, F., Rue, H., and Lindström, J. (2011). An explicit link between gaussian fields and gaussian markov random fields: The stochastic partial differential equation approach. *Journal of the Royal Statistical Society. Series B: Statistical Methodology* **73**, 423–498. doi:10.1111/j.1467-9868.2011.00777.x
- Link, J. S. (2010). 'Ecosystem-Based Fisheries Management: confronting tradeoffs'. (Cambridge University Press: Cambridge.)
- Link, J. S., Bundy, A., Overholtz, W. J., Shackell, N., Manderson, J., Duplisea, D., Hare, J., Koen-Alonso, M., and Friedland, K. D. (2011). Ecosystem-based fisheries management in the Northwest Atlantic. *Fish and Fisheries* **12**, 152–170. doi:10.1111/j.1467-2979.2011.00411.x
- Liu, O. R., Kleisner, K. M., Smith, S. L., and Kritzer, J. P. (2018). The use of spatial management tools in rights--based groundfish fisheries. *Fish and Fisheries* **19**, 821–838. doi:10.1111/faf.12294
- Leonart, J., Salat, J., and Torres, G. J. (2000). Removing Allometric Effects of Body Size in Morphological Analysis. *Journal of Theoretical Biology* **205**, 85–93. doi:10.1006/jtbi.2000.2043
- Loher, T., and Seitz, A. C. (2008). Characterization of active spawning season and depth for eastern Pacific halibut (*Hippoglossus stenolepis*), and evidence of probable skipped spawning. *Journal of Northwest Atlantic Fishery Science* **41**, 23–36. doi:10.2960/J.v41.m617
- Lowe, W. H., and Allendorf, F. W. (2010). What can genetics tell us about population connectivity? *Molecular Ecology* **19**, 3038–3051. doi:10.1111/j.1365-294X.2010.04688.x
- Ludwig, D., Hilborn, R., and Walters, C. (1993). Uncertainty , Resource Exploitation , and Conservation: Lessons from History. *Ecological Application* **3**, 547–549.

- Mace, P. M. (2001). A new role for MSY in single-species and ecosystem approaches to fisheries stock assessment and management. *Fish and Fisheries* **2**, 2–32. doi:10.1046/j.1467-2979.2001.00033.x
- Mahe, K., Evano, H., Mille, T., and Bourjea, J. (2016a). Otolith shape as a valuable tool to evaluate the stock structure of swordfish (*Xiphias gadus*) in the Indian Ocean. *African Journal of Marine Science* **2338**, 1–8. doi:10.1097/INF.0b013e318211581e
- Mahe, K., Oudard, C., Mille, T., Clausen, L. W., Petursdottir, G., Rasmussen, H., Meland, E., Mullins, E., Schon, P.-J., McCorriston, P., Pinnegar, J. K., Hoinés, Å., and Trenkel, V. M. (2016b). Identifying blue whiting (*Micromesistius poutassou*) stock structure in the northeast Atlantic by otolith shape analysis. *Canadian Journal of Fisheries and Aquatic Sciences* **73**, 1363–1371. doi:10.1139/cjfas-2015-0332
- Maloney, N. E., and Sigler, M. F. (2008). Age-specific movement patterns of sablefish (*Anoplopoma fimbria*) in Alaska. *Fishery Bulletin* **106**, 305–316.
- Mapp, J., Hunter, E., Van Der Kooij, J., Songer, S., and Fisher, M. (2017). Otolith shape and size: The importance of age when determining indices for fish-stock separation. *Fisheries Research* **190**, 43–52. doi:10.1016/j.fishres.2017.01.017
- Marlow, T. R., Agnew, D. J., Purves, M. G., and Everson, I. (2003). Movement and growth of tagged *Dissostichus eleginoides* around South Georgia and Shag Rocks (Subarea 48.3). *CCAMLR Science* **10**, 101–111.
- Martínez-Minaya, J., Cameletti, M., Conesa, D., and Pennino, M. G. (2018). Species distribution modeling: a statistical review with focus in spatio-temporal issues. *Stochastic Environmental Research and Risk Assessment* **32**, 3227–3244. doi:10.1007/s00477-018-1548-7
- Martins, T. G., Simpson, D., Lindgren, F., and Rue, H. (2013). Bayesian computing with INLA: New features. *Computational Statistics and Data Analysis* **67**, 68–83. doi:10.1016/j.csda.2013.04.014
- Matano, R. P., Palma, E. D., and Combes, V. (2019). The Burdwood Bank Circulation. *Journal of Geophysical Research: Oceans* **124**, 6904–6926. doi:10.1029/2019JC015001

- Mbatha, F. L., Yemane, D., Ostrowski, M., Moloney, C. L., and Lipiński, M. R. (2019). Oxygen and temperature influence the distribution of deepwater Cape hake *Merluccius paradoxus* in the southern Benguela: a GAM analysis of a 10-year time-series. *African Journal of Marine Science* **41**, 413–427. doi:10.2989/1814232X.2019.1688681
- Melnichuk, M. C., Peterson, E., Elliott, M., and Hilborn, R. (2017). Fisheries management impacts on target species status. *Proceedings of the National Academy of Sciences of the United States of America* **114**, 178–183. doi:10.1073/pnas.1609915114
- Mérigot, B., Letourneur, Y., and Lecomte-Finiger, R. (2007). Characterization of local populations of the common sole *Solea solea* (Pisces, Soleidae) in the NW Mediterranean through otolith morphometrics and shape analysis. *Marine Biology* **151**, 997–1008. doi:10.1007/s00227-006-0549-0
- La Mesa, M. (2007). The utility of otolith microstructure in determining the timing and position of the first annulus in juvenile Antarctic toothfish (*Dissostichus mawsoni*) from the South Shetland Islands. *Polar Biology* **30**, 1219–1226. doi:10.1007/s00300-007-0281-3
- Möllmann, C., Cormon, X., Funk, S., Otto, S. A., Schmidt, J. O., Schwermer, H., Sguotti, C., Voss, R., and Quaas, M. (2021). Tipping point realized in cod fishery. *Scientific Reports* **11**, 14259. doi:10.1038/s41598-021-93843-z
- Moore, B. R., Bell, J. D., Evans, K., Farley, J., Grewe, P. M., Hampton, J., Marie, A. D., Minte-Vera, C., Nicol, S., Pilling, G. M., Scutt Phillips, J., Tremblay-Boyer, L., Williams, A. J., and Smith, N. (2020). Defining the stock structures of key commercial tunas in the Pacific Ocean I: Current knowledge and main uncertainties. *Fisheries Research* **230**, 105525. doi:10.1016/j.fishres.2020.105525
- Morales-Nin, B. (2000). Review of the growth regulation processes of otolith daily increment formation. *Fisheries Research* **46**, 53–67. doi:10.1016/S0165-7836(00)00133-8
- Morato, T., Watson, R., Pitcher, T. J., and Pauly, D. (2006). Fishing down the deep. *Fish and Fisheries* **7**, 24–34. doi:10.1111/j.1467-2979.2006.00205.x
- Moreno, C. A., Arata, J. A., Rubilar, P., Huckle-Gaete, R., and Robertson, G. (2006). Artisanal longline fisheries in Southern Chile: Lessons to be learned to avoid incidental seabird

- mortality. *Biological Conservation* **127**, 27–36. doi:10.1016/j.biocon.2005.07.011
- Moreno, C. A., Castro, R., Mújica, L. J., and Reyes, P. (2008). Significant conservation benefits obtained from the use of a new fishing gear in the Chilean patagonian toothfish fishery. *CCAMLR Science* **15**, 79–91.
- Mori, M., Corney, S. P., Melbourne-Thomas, J., Welsford, D. C., Klocker, A., and Ziegler, P. E. (2016). Using satellite altimetry to inform hypotheses of transport of early life stage of Patagonian toothfish on the Kerguelen Plateau. *Ecological Modelling* **340**, 45–56. doi:10.1016/j.ecolmodel.2016.08.013
- Morley, S. A., Belchier, M., Dickson, J., and Mulvey, T. (2005). Daily otolith increment validation in larval mackerel icefish, *Champscephalus gunnari*. *Fisheries Research* **75**, 200–203. doi:10.1016/j.fishres.2005.04.008
- Mormede, S., Parker, S. J., and Pinkerton, M. H. (2020). Comparing spatial distribution modelling of fisheries data with single-area or spatially-explicit integrated population models, a case study of toothfish in the Ross Sea region. *Fisheries Research* **221**, 105381. doi:10.1016/j.fishres.2019.105381
- Mujica, A., Peñailillo, D., Reyes, A., and Nava, M. L. (2016). Embryonic and larval development of *Dissostichus eleginoides* (Pisces: Nototheniidae). *Revista de biología marina y oceanografía* **51**, 675–680. doi:10.4067/S0718-19572016000300018
- Murray, T. S., Cowley, P. D., Mann, B. Q., Maggs, J. Q., and Gouws, G. (2019). Movement patterns of an endemic South African sparid, the black musselcracker *Cymatoceps nasutus*, determined using mark-recapture methods. *African Journal of Marine Science* **41**, 71–81. doi:10.2989/1814232X.2019.1574238
- Murua, H. (2003). Population structure, growth and reproduction of roughhead grenadier on the Flemish Cap and Flemish Pass. *Journal of Fish Biology* **63**, 356–373. doi:10.1046/j.1095-8649.2003.00158.x
- Murua, H., and Motos, L. (2000). Reproductive biology of roughhead grenadier (*Macrourus berglax* Lacepède, 1801) (Pisces, Macrouridae), in Northwest Atlantic waters. *Sarsia* **85**, 393–402. doi:10.1080/00364827.2000.10414590

- Nathan, R., Getz, W. M., Revilla, E., Holyoak, M., Kadmon, R., Saltz, D., and Smouse, P. E. (2008). A movement ecology paradigm for unifying organismal movement research. *Proceedings of the National Academy of Sciences* **105**, 19052–19059.
- Neubauer, P., Jensen, O. P., Hutchings, J. A., and Baum, J. K. (2013). Resilience and Recovery of Overexploited Marine Populations. *Science* **340**, 347–350.
- Neves, A., Sequeira, V., Farias, I., Vieira, A. R., Paiva, R., and Gordo, L. S. (2011). Discriminating bluemouth, *Helicolenus dactylopterus* (Pisces: Sebastidae), stocks in Portuguese waters by means of otolith shape analysis. *Journal of the Marine Biological Association of the United Kingdom* **91**, 1237–1242. doi:10.1017/S002531541000189X
- Nikolsky, G. V. (1963). 'Ecology of Fishes'. (Academic Press: London.)
- Norberg, A., Abrego, N., Blanchet, F. G., Adler, F. R., Anderson, B. J., Anttila, J., Araújo, M. B., Dallas, T., Dunson, D., Elith, J., Foster, S. D., Fox, R., Franklin, J., Godsoe, W., Guisan, A., O'Hara, B., Hill, N. A., Holt, R. D., Hui, F. K. C., Husby, M., Kålås, J. A., Lehikoinen, A., Luoto, M., Mod, H. K., Newell, G., Renner, I., Roslin, T., Soininen, J., Thuiller, W., Vanhatalo, J., Warton, D., White, M., Zimmerman, Niklaus E. Gravel, D., and Ovaskainen, O. (2019). A comprehensive evaluation of predictive performance of 33 species distribution models at species and community levels. *Ecological Monographs* **89**, e01370. doi:10.1002/ecm.1370
- Norse, E. A., Brooke, S., Cheung, W. W. L., Clark, M. R., Ekeland, I., Froese, R., Gjerde, K. M., Haedrich, R. L., Heppell, S. S., Morato, T., Morgan, L. E., Pauly, D., Sumaila, R., and Watson, R. (2012). Sustainability of deep-sea fisheries. *Marine Policy* **36**, 307–320. doi:10.1016/j.marpol.2011.06.008
- North, A. W. (2002). Larval and juvenile distribution and growth of Patagonian toothfish around South Georgia. *Antarctic Science* **14**, 25–31. doi:10.1017/S0954102002000548
- Nye, J. A., Link, J. S., Hare, J. A., and Overholtz, W. J. (2009). Changing spatial distribution of fish stocks in relation to climate and population size on the Northeast United States continental shelf. *Marine Ecology Progress Series* **393**, 111–129. doi:10.3354/meps08220

- Ogle, D. H. (2016). 'Introductory Fisheries Analyses with R'. (CRC Press.)
- Pante, E., and Simon-Bouhet, B. (2013). marmap: A Package for Importing, Plotting and Analyzing Bathymetric and Topographic Data in R. *PLoS ONE* **8**, e73051. doi:10.1371/journal.pone.0073051
- Paradinas, I., Conesa, D., López-quílez, A., and Bellido, J. M. (2017). Spatio-Temporal model structures with shared components for semi-continuous species distribution modelling. *Spatial Statistics* **22**, 434–450. doi:10.1016/j.spasta.2017.08.001
- Paradinas, I., Conesa, D., López-Quílez, A., Esteban, A., López, L., Bellido, J., and Pennino, M. (2020). Assessing the spatiotemporal persistence of fish distributions: a case study on two red mullet species (*Mullus surmuletus* and *M. barbatus*) in the western Mediterranean. *Marine Ecology Progress Series* **644**, 173–185. doi:10.3354/meps13366
- Paradinas, I., Conesa, D., Pennino, M. G., Muñoz, F., Fernández, A. M., López-Quílez, A., and Bellido, J. M. (2015). Bayesian spatio-temporal approach to identifying fish nurseries by validating persistence areas. *Marine Ecology Progress Series* **528**, 245–255. doi:10.3354/meps11281
- Park, K. J., Choi, S., and An, D. (2021). Distribution of Fishing Grounds of Korean Bottom Longline and Annual Change of CPUE of the Patagonian Toothfish *Dissostichus eleginoides* in South West Atlantic. *Korean Journal of Aquatic Science* **54**, 129–134.
- Parker, S. J., Stevens, D. W., Ghigliotti, L., La Mesa, M., Di Blasi, D., and Vacchi, M. (2019). Winter spawning of Antarctic toothfish *Dissostichus mawsoni* in the Ross Sea region. *Antarctic Science* **31**, 243–253. doi:10.1017/S0954102019000282
- Parra, H. E., Pham, C. K., Menezes, G. M., Rosa, A., Tempera, F., and Morato, T. (2017). Predictive modeling of deep-sea fish distribution in the Azores. *Deep-Sea Research Part II* **145**, 49–60. doi:10.1016/j.dsr2.2016.01.004
- Pauly, D., Christensen, V., Dalsgaard, J., Froese, R., and Jr, F. T. (1998). Fishing Down Marine Food Webs. *Science* **279**, 860–863.
- Pauly, D., and Froese, R. (2021). MSY needs no epitaph - But it was abused. *ICES Journal of Marine Science* **78**, 2204–2210. doi:10.1093/icesjms/fsaa224

- Pauly, D., and Zeller, D. (2016). Catch reconstructions reveal that global marine fisheries catches are higher than reported and declining. *Nature Communications* **7**, 10244. doi:10.1038/ncomms10244
- Pauly, D., Zeller, D., and Palomares, M. L. D. (2020). Sea Around Us Concepts, Design and Data. Available at: searoundus.org
- Payne, A. G., Agnew, D. J., and Brandão, A. (2005). Preliminary assessment of the Falklands Patagonian toothfish (*Dissostichus eleginoides*) population: Use of recruitment indices and the estimation of unreported catches. *Fisheries Research* **76**, 344–358. doi:10.1016/j.fishres.2005.07.010
- Pennino, M. G., Guijarro-García, E., Vilela, R., Del Río, J. L., and Bellido, J. M. (2019). Modeling the distribution of thorny skate (*Amblyraja radiata*) in the southern grand banks (Newfoundland, Canada). *Canadian Journal of Fisheries and Aquatic Sciences* **76**, 2121–2130. doi:10.1139/cjfas-2018-0302
- Péron, C., Welsford, D. C., Ziegler, P., Lamb, T. D., Gasco, N., Chazeau, C., Sinègre, R., and Duhamel, G. (2016). Modelling spatial distribution of Patagonian toothfish through life-stages and sex and its implications for the fishery on the Kerguelen Plateau. *Progress in Oceanography* **141**, 81–95. doi:10.1016/j.pocean.2015.12.003
- Perruche, C. (2019). Product user manual: For the Global Ocean Biogeochemistry Hindcast. CMEMS-GLO-PUM-001-029. Available at: <https://resources.marine.copernicus.eu/documents/PUM/CMEMS-GLO-PUM-001-029.pdf>
- Perruche, C., Szczypta, C., Paul, J., and Drévilon, M. (2019). Quality Information Document: Global Production Centre. CMEMS-GLO-QUID-001-029. Available at: <https://catalogue.marine.copernicus.eu/documents/QUID/CMEMS-GLO-QUID-001-029.pdf>
- Petrov, A. F., and Tatarnikov, V. A. (2010). New data on migrations of Antarctic toothfish *Dissostichus mawsoni* in the Dumont d'Urville Sea in the 2008/2009 Season. *Journal of Ichthyology* **50**, 140–141. doi:10.1134/S0032945210010170

- Pitcher, C. R., Ellis, N., Jennings, S., Hiddink, J. G., Mazor, T., Kaiser, M. J., Kangas, M. I., McConnaughey, R. A., Parma, A. M., Rijnsdorp, A. D., Suuronen, P., Collie, J. S., Amoroso, R., Hughes, K. M., and Hilborn, R. (2017). Estimating the sustainability of towed fishing-gear impacts on seabed habitats: a simple quantitative risk assessment method applicable to data-limited fisheries. *Methods in Ecology and Evolution* **8**, 472–480. doi:10.1111/2041-210X.12705
- Polis, G. A. (1984). Age structure component of niche width and intra-specific resource partitioning: can age groups function as ecological species?. *American Naturalist* **123**, 541–564. doi:10.1086/284221
- Pompert, J., Lee, B., Blake, A., Jones, J., and Zawadowski, T. (2015). Scientific Report, Fisheries Cruise ZDLT1-11-2015. Technical Report. Stanley.
- Punt, A. E., and Donovan, G. P. (2007). Developing management procedures that are robust to uncertainty: Lessons from the International Whaling Commission. *ICES Journal of Marine Science* **64**, 603–612. doi:10.1093/icesjms/fsm035
- Quinn II, T. J., and Collie, J. S. (2005). Sustainability in single-species population models. *Philosophical Transactions of the Royal Society B: Biological Sciences* **360**, 147–162. doi:10.1098/rstb.2004.1577
- Quinn, T. P., and Brodeur, R. D. (1991). Intra-Specific Variations in the Movement Patterns of Marine Animals. *American Zoologist* **31**, 231–241. Available at: <http://www.jstor.org/stable/3883472>
- R Core Team (2021). R: A Language and Environment for Statistical Computing. Available at: <https://www.r-project.org/>
- Ramesh, N., Rising, J. A., and Oremus, K. L. (2019). The small world of global marine fisheries: The cross-boundary consequences of larval dispersal. *Science* **1196**, 1192–1196.
- Randhawa, H. S. (2020). TOO bycatch report: a review. Efficacy of the 1.5% bycatch threshold. Fisheries Department, Directorate of Natural Resources, Falkland Islands Government.

- Randhawa, H. S., and Lee, B. (2016). Toothfish tagging cruise ZDLC2-06-2016, CFL Gambler. Stanley, Falkland Islands Government, Fisheries department.
- Randhawa, H. S., Lee, B., Farrugia, T. J., and Keningale, B. (2017). Toothfish tagging cruise ZDLK3 – 06/07 – 2017. Stanley, Falkland Islands Government, Fisheries department.
- Riccialdelli, L., Becker, Y., Fioramonti, N., Torres, M., Bruno, D., Raya Rey, A., and Fernández, D. (2020). Trophic structure of southern marine ecosystems: a comparative isotopic analysis from the Beagle Channel to the oceanic Burdwood Bank area under a wasp-waist assumption. *Marine Ecology Progress Series* **655**, 1–27. doi:10.3354/meps13524
- Rideout, R. (2000). Observations on mass atresia and skipped spawning in northern Atlantic cod, from Smith Sound, Newfoundland. *Journal of Fish Biology* **57**, 1429–1440. doi:10.1006/jfbi.2000.1405
- van Rij, J., Wieling, M., Baayen, R., and van Rijn, H. (2020). itsadug: Interpreting Time Series and Autocorrelated Data Using GAMMs. *R package version 2.4*.
- Rindorf, A., Mumford, J., Baranowski, P., Clausen, L. W., García, D., Hintzen, N. T., Kempf, A., Leach, A., Levontin, P., Mace, P., Mackinson, S., Maravelias, C., Prellezo, R., Quetglas, A., Tserpes, G., Voss, R., and Reid, D. (2017). Moving beyond the MSY concept to reflect multidimensional fisheries management objectives. *Marine Policy* **85**, 33–41. doi:10.1016/j.marpol.2017.08.012
- Roberts, C. M. (2002). Deep impact: the rising toll of fishing in the deep sea. *TRENDS in Ecology & Evolution* **17**, 242–246.
- Roberts, J., and Agnew, D. A. (2008). Proposal for an extension to the mark recapture experiment to estimate toothfish population size in Subarea 48.4. *CCAMLR WG-FSA*, 08/46.
- Roberts, J. O. (2012). Ecology and management of range edge populations: the case of toothfish species at the South Sandwich Islands. PhD Thesis: Imperial College.
- Robinson, L. M., Elith, J., Hobday, A. J., Pearson, R. G., Kendall, B. E., Possingham, H. P., and Richardson, A. J. (2011). Pushing the limits in marine species distribution modelling :

- lessons from the land present challenges. *Global Ecology and Biogeography* **20**, 789–802. doi:10.1111/j.1466-8238.2010.00636.x
- Rodgveller, C. J., Hutchinson, C. E., Harris, J. P., Vulstek, S. C., and Guthrie, C. M. (2017). Otolith shape variability and associated body growth differences in giant grenadier, *Albatrossia pectoralis*. *PLoS ONE* **12**, e0180020. doi:10.1371/journal.pone.0180020
- Rodríguez-Marín, E., Ruiz, M., and Sarasua, A. (2002). Validation of roughhead grenadier (*Macrourus berglax*) otolith reading. *Journal of Applied Ichthyology* **18**, 70–80. doi:10.1046/j.1439-0426.2002.00330.x
- Rogers, A. D., Morley, S., Fitzcharles, E., Jarvis, K., and Belchier, M. (2006). Genetic structure of Patagonian toothfish (*Dissostichus eleginoides*) populations on the Patagonian shelf and Atlantic and western Indian Ocean Sectors of the Southern Ocean. *Marine Biology* **149**, 915–924. doi:10.1007/s00227-006-0256-x
- Rogers, T. A., Fowler, A. J., Steer, M. A., Gillanders, B. M., and George, K. (2019). Spatial connectivity during the early life history of a temperate marine fish inferred from otolith microstructure and geochemistry. *Estuarine, Coastal and Shelf Science* **227**, 106342. doi:10.1016/j.ecss.2019.106342
- Rooker, J. R., Wells, R. J. D., Block, B. A., Liu, H., Baumann, H., Chiang, W. C., Sluis, M. Z., Miller, N. R., Mohan, J. A., Ohshimo, S., Tanaka, Y., Dance, M. A., Dewar, H., and Snodgrass, O. E. (2021). Natal origin and age-specific egress of Pacific bluefin tuna from coastal nurseries revealed with geochemical markers. *Scientific Reports* **11**, 14216. doi:10.1038/s41598-021-93298-2
- Rue, H., Martino, S., and Chopin, N. (2009). Approximate Bayesian inference for latent Gaussian models by using integrated nested Laplace approximations. *Journal of the Royal Statistical Society. Series B: Statistical Methodology* **71**, 319–392. doi:10.1111/j.1467-9868.2008.00700.x
- Rueden, C. T., Schindelin, J., Hiner, M. C., DeZonia, B. E., Walter, A. E., Arena, E. T., and Eliceiri, K. W. (2017). ImageJ2: ImageJ for the next generation of scientific image data. *BMC Bioinformatics* **18**, 529–555. doi:10.1186/s12859-017-1934-z

- Rufener, M. C., Kinas, P. G., Nóbrega, M. F., and Lins Oliveira, J. E. (2017). Bayesian spatial predictive models for data-poor fisheries. *Ecological Modelling* **348**, 125–134. doi:10.1016/j.ecolmodel.2017.01.022
- Russell, E. S. (1931). Some theoretical considerations on the overfishing problem. *ICES Journal of Marine Science* **6**, 3–20.
- Salmerón, F., Báez, J., Macías, D., Fernandez-Peralta, L., and Ramos, A. (2015). Rapid fish stock depletion in previously unexploited seamounts: the case of *Beryx splendens* from the Sierra Leone Rise (Gulf of Guinea). *African Journal of Marine Science* **37**, 405–409. doi:10.2989/1814232X.2015.1085902
- Sanchez, P. J., Rooker, J. R., Zapp Sluis, M., Pinsky, J., Dance, M. A., Falterman, B., and Allman, R. J. (2020). Application of otolith chemistry at multiple life history stages to assess population structure of Warsaw grouper in the Gulf of Mexico. *Marine Ecology Progress Series* **651**, 111–123. doi:10.3354/meps13457
- Schindler, D. E., Hilborn, R., Chasco, B., Boatright, C. P., Quinn, T. P., Rogers, L. A., and Webster, M. S. (2010). Population diversity and the portfolio effect in an exploited species. *Nature* **465**, 609–612. doi:10.1038/nature09060
- Shaw, A. K. (2020). Causes and consequences of individual variation in animal movement. *Movement Ecology* **8**, 1–12. doi:10.1186/s40462-020-0197-x
- Shaw, P. W., Arkhipkin, A. I., and Al-Khairulla, H. (2004). Genetic structuring of Patagonian toothfish populations in the Southwest Atlantic Ocean: The effect of the Antarctic Polar Front and deep-water troughs as barriers to genetic exchange. *Molecular Ecology* **13**, 3293–3303. doi:10.1111/j.1365-294X.2004.02327.x
- Shepherd, J. G. (1982). A versatile new stock-recruitment relationship for fisheries, and the construction of sustainable yield curves. *ICES Journal of Marine Science* **40**, 67–75.
- Sinclair, M., and Iles, T. D. (1989). Population regulation and speciation in the oceans. *ICES Journal of Marine Science* **45**, 165–175. doi:10.1093/icesjms/45.2.165
- Skeljo, F. (2020). 2020 Sustainability measures for Patagonian toothfish (*Dissostichus eleginoides*). Fisheries Report SM-2020-TOO. Stanley, Falkland Islands.

- Skeljo, F., and Pearman, T. (2021). Cruise Report ZDLK3-01-2021: Patagonian toothfish (*Dissostichus eleginoides*) tagging and benthic habitat survey. Stanley, Falkland Islands Government, Fisheries Department.
- Skeljo, F., and Winter, A. (2020). 2019 Stock Assessment Report: Patagonian toothfish (*Dissostichus eleginoides*). Fisheries Report SA-2019-TOO. Stanley, Falkland Islands Government, Fisheries department.
- Skjæraasen, J. E., Nash, R. D. M., Korsbrekke, K., Fonn, M., Nilsen, T., Kennedy, J., Nedreaas, K. H., Thorsen, A., Witthames, P. R., Geffen, A. J., Høie, H., and Kjesbu, O. S. (2012). Frequent skipped spawning in the world's largest cod population. *Proceedings of the National Academy of Sciences* **109**, 8995–8999. doi:10.1073/pnas.1200223109
- Smedbol, R. K., and Stephenson, R. (2001). The importance of managing within-species diversity in cod and herring fisheries of the north-western Atlantic. *Journal of Fish Biology* **59**, 109–128. doi:10.1006/jfbi.2001.1765
- Smith, P., and McVeagh, M. (2000). Allozyme and microsatellite DNA markers of toothfish population structure in the Southern Ocean. *Journal of Fish Biology* **57**, 72–83. doi:10.1006/jfbi.2000.1612
- Song, H., Marshall, J., Follows, M. J., Dutkiewicz, S., and Forget, G. (2016). Source waters for the highly productive Patagonian shelf in the southwestern Atlantic. *Journal of Marine Systems* **158**, 120–128. doi:10.1016/j.jmarsys.2016.02.009
- Soriano-Redondo, A., Jones-Todd, C. M., Bearhop, S., Hilton, G. M., Lock, L., Stanbury, A., Votier, S. C., and Illian, J. B. (2019). Understanding species distribution in dynamic populations: a new approach using spatio-temporal point process models. *Ecography* **42**, 1092–1102. doi:10.1111/ecog.03771
- Sovacool, B. K., and Siman-Sovacool, K. E. (2008). Creating legal teeth for toothfish: Using the market to protect fish stocks in Antarctica. *Journal of Environmental Law* **20**, 15–33. doi:10.1093/jel/eqm024
- Spiegelhalter, D. J., Best, N. G., Carlin, B. P., and Van Der Linde, A. (2002). Bayesian measures of model complexity and fit. *Journal of the Royal Statistical Society. Series B:*

- Statistical Methodology* **64**, 583–616. doi:10.1111/1467-9868.00353
- Stevens, J. D., Bonfil, R., Dulvy, N. K., and Walker, P. A. (2000). The effects of fishing on sharks, rays, and chimaeras (chondrichthyans), and the implications for marine ecosystems. *ICES Journal of Marine Science* **57**, 476–494. doi:10.1006/jmsc.2000.0724
- Stock, B. C., Ward, E. J., Eguchi, T., Jannot, J. E., Thorson, J. T., Feist, B. E., and Semmens, B. X. (2020). Comparing predictions of fisheries bycatch using multiple spatiotemporal species distribution model frameworks. *Canadian Journal of Fisheries and Aquatic Science* **163**, 146–163.
- Stransky, C. (2014). Morphometric Outlines. In 'Stock Identification Methods: Applications in Fishery Science'. (Eds S. X. Cadrin, L. A. Kerr, and S. Mariani.) pp. 129–140. (Academic Press: London.)
- Stransky, C., Murta, A. G., Schlickeisen, J., and Zimmermann, C. (2008). Otolith shape analysis as a tool for stock separation of horse mackerel (*Trachurus trachurus*) in the Northeast Atlantic and Mediterranean. *Fisheries Research* **89**, 159–166. doi:10.1016/j.fishres.2007.09.017
- Sturrock, A. M., Hunter, E., Milton, J. A., Johnson, R. C., Waring, C. P., Trueman, C. N., and EIMF (2015). Quantifying physiological influences on otolith microchemistry. *Methods in Ecology and Evolution* **6**, 806–816. doi:10.1111/2041-210X.12381
- Sturrock, A. M., Trueman, C. N., Darnaude, A. M., and Hunter, E. (2012). Can otolith elemental chemistry retrospectively track migrations in fully marine fishes? *Journal of Fish Biology* **81**, 766–795. doi:10.1111/j.1095-8649.2012.03372.x
- Sturrock, A. M., Trueman, C. N., Milton, J. A., Waring, C. P., Cooper, M. J., and Hunter, E. (2014). Physiological influences can outweigh environmental signals in otolith microchemistry research. *Marine Ecology Progress Series* **500**, 245–264. doi:10.3354/meps10699
- Thomas Lin Pedersen (2020). patchwork: The Composer of Plots. *R package version 1.1.1*. Available at: <https://cran.r-project.org/package=patchwork>
- Thompson, A. F. (2008). The atmospheric ocean: eddies and jets in the Antarctic Circumpolar

- Current. *Philosophical Transactions of the Royal Society A: mathematical, physical and engineering sciences* **366**, 4529–4541. doi:10.1098/rsta.2008.0196
- Tolimieri, N., Haltuch, M. A., Lee, Q., Jacox, M. G., and Bograd, S. J. (2018). Oceanographic drivers of sablefish recruitment in the California Current. *Fisheries Oceanography* **27**, 458–474. doi:10.1111/fog.12266
- Toomey, L., Welsford, D., Appleyard, S. A., Polanowski, A., Faux, C., Deagle, B. E., Belchier, M., Marthick, J., and Jarman, S. (2016). Genetic structure of Patagonian tooth fish populations from otolith DNA. *Antarctic Science* **28**, 347–360. doi:10.1017/S0954102016000183
- Torres, G. J., Lombarte, A., and Morales-Nin, B. (2000). Sagittal otolith size and shape variability to identify geographical intraspecific differences in three species of the genus *Merluccius*. *Journal of the Marine Biological Association of the UK* **80**, 333–342. doi:10.1017/S0025315499001915
- Tracey, S. R., Lyle, J. M., and Duhamel, G. (2006). Application of elliptical Fourier analysis of otolith form as a tool for stock identification. *Fisheries Research* **77**, 138–147. doi:10.1016/j.fishres.2005.10.013
- Le Traon, P. Y., Reppucci, A., Alvarez Fanjul, E., Aouf, L., Behrens, A., Belmonte, M., Bentamy, A., Bertino, L., Brando, V. E., Kreiner, M. B., Benkiran, M., Carval, T., Ciliberti, S. A., Claustre, H., Clementi, E., Coppini, G., Cossarini, G., De Alfonso Alonso-Muñoyerro, M., Delamarche, A., Dibarboure, G., Dinessen, F., Drevillon, M., Drillet, Y., Faugere, Y., Fernández, V., Fleming, A., Garcia-Hermosa, M. I., Sotillo, M. G., Garric, G., Gasparin, F., Giordan, C., Gehlen, M., Gregoire, M. L., Guinehut, S., Hamon, M., Harris, C., Hernandez, F., Hinkler, J. B., Hoyer, J., Karvonen, J., Kay, S., King, R., Lavergne, T., Lemieux-Dudon, B., Lima, L., Mao, C., Martin, M. J., Masina, S., Melet, A., Buongiorno Nardelli, B., Nolan, G., Pascual, A., Pistoia, J., Palazov, A., Piolle, J. F., Pujol, M. I., Pequignet, A. C., Peneva, E., Pérez Gómez, B., Petit de la Villeon, L., Pinardi, N., Pisano, A., Pouliquen, S., Reid, R., Remy, E., Santoleri, R., Siddorn, J., She, J., Staneva, J., Stoffelen, A., Tonani, M., Vandenbulcke, L., von Schuckmann, K., Volpe, G., Wettre,

- C., and Zacharioudaki, A. (2019). From Observation to Information and Users: The Copernicus Marine Service Perspective. *Frontiers in Marine Science* **6**, 234. doi:10.3389/fmars.2019.00234
- Troccoli, G. H., Aguilar, E., Martínez, P. A., and Belleggia, M. (2020). The diet of the Patagonian toothfish *Dissostichus eleginoides*, a deep - sea top predator off Southwest Atlantic Ocean. *Polar Biology* **43**, 1595–1604. doi:10.1007/s00300-020-02730-2
- Tuck, G. N., de La Mare, W. K., Hearn, W. S., Williams, R., Smith, A. D. M., He, X., and Constable, A. (2003). An exact time of release and recapture stock assessment model with an application to Macquarie Island Patagonian toothfish (*Dissostichus eleginoides*). *Fisheries Research* **63**, 179–191. doi:10.1016/S0165-7836(03)00073-0
- Tuck, G. N., and Possingham, H. P. (1994). Optimal harvesting strategies for a metapopulation. *Bulletin of Mathematical Biology* **56**, 107–127.
- Ulibarrena, J., and Conzonno, V. H. (2015). Mechanisms involved in the proliferation and distribution of phytoplankton in the Patagonian Sea, Argentina, as revealed by remote sensing studies. *Environmental Earth Sciences* **74**, 439–449. doi:10.1007/s12665-015-4052-0
- Velarde, E., Anderson, D. W., and Ezcurra, E. (2019). Seabird clues to ecosystem health. *Science* **365**, 116–117.
- Venables, W. N., and Ripley, B. D. (2002). 'Modern Applied Statistics with S' Fourth. (Springer: New York.) Available at: <http://www.stats.ox.ac.uk/pub/MASS4>
- Victorero, L., Watling, L., Deng Palomares, M. L., and Nouvian, C. (2018). Out of Sight, But Within Reach: A Global History of Bottom-Trawled Deep-Sea Fisheries From >400 m Depth. *Frontiers in Marine Science* **5**, 1–17. doi:10.3389/fmars.2018.00098
- Vieira, A. R., Neves, A., Sequeira, V., Paiva, R. B., and Gordo, L. S. (2014). Otolith shape analysis as a tool for stock discrimination of forkbeard (*Phycis phycis*) in the Northeast Atlantic. *Hydrobiologia* **728**, 103–110. doi:10.1007/s10750-014-1809-5
- Vignon, M., and Morat, F. (2010). Environmental and genetic determinant of otolith shape revealed by a non-indigenous tropical fish. *Marine Ecology Progress Series* **411**, 231–

241. doi:10.3354/meps08651

- Ward, E. J., Jannot, J. E., Lee, Y. W., Ono, K., Shelton, A. O., and Thorson, J. T. (2015). Using spatiotemporal species distribution models to identify temporally evolving hotspots of species co-occurrence. *Ecological Applications* **25**, 2198–2209. doi:10.1890/15-0051.1
- Watanabe, S. (2010). Asymptotic equivalence of Bayes cross validation and widely applicable information criterion in singular learning theory. *Journal of Machine Learning Research* **11**, 3571–3594.
- Wells, R. . D., Mohan, J. A., Dewar, H., Rooker, J. R., Tanaka, Y., Snodgrass, O. E., Kohin, S., Miller, N. R., and Ohshimo, S. (2020). Natal origin of Pacific bluefin tuna from the California Current Large Marine Ecosystem. *Biology Letters* **16**, 20190878. doi:http://dx.doi.org/10.1098/rsbl.2019.0878
- Wheeland, L. J., and Morgan, M. J. (2020). Age-specific shifts in Greenland halibut (*Reinhardtius hippoglossoides*) distribution in response to changing ocean climate. *ICES Journal of Marine Science* **77**, 230–240. doi:10.1093/icesjms/fsz152
- Wickham, H., Averick, M., Bryan, J., Chang, W., McGowan, L. D., François, R., Golemund, G., Hayes, A., Henry, L., Hester, J., Kuhn, M., Pedersen, T. L., Miller, E., Bache, S. M., Müller, K., Ooms, J., Robinson, D., Seidel, D. P., Spinu, V., Takahashi, K., Vaughan, D., Wilke, C., Woo, K., and Yutani, H. (2019). Welcome to the tidyverse. *Journal of Open Source Software* **4**, 1686. doi:https://doi.org/10.21105/joss.01686
- Williams, R., Tuck, G. N., Constable, A. J., and Lamb, T. (2002). Movement, growth and available abundance to the fishery of *Dissostichus eleginoides* SMITT, 1898 at Heard Island, derived from tagging experiments. *CCAMLR Science* **9**, 33–48.
- Winter, A., Lee, B., Arkhipkin, A., Tutjavi, V., and Büring, T. (2020). 2020 1st Season assessment survey Falkland calamari (*Doryteuthis gahi*): ZDLS3-S1-2020. Stanley, Falkland Islands Government, Fisheries department.
- Wood, S. N. (2017). 'Generalized additive models: an introduction with R' 2nd ed. (Chapman and Hall/CRC.: Boca Raton, Florida.)
- Worm, B., Hilborn, R., Baum, J. K., Branch, T. A., Collie, J. S., Costello, C., Fogarty, M. J.,

- Fulton, E. A., Hutchings, J. A., Jennings, S., Jensen, O. P., Lotze, H. K., Mace, P. M., McClanahan, T. R., Minto, C., Palumbi, S. R., Parma, A. M., Ricard, D., Rosenberg, A. A., Watson, R., and Zeller, D. (2009). Rebuilding Global Fisheries. *Science* **325**, 578–585. doi:10.1126/science.1173146
- Wright, P. J., Régnier, T., Gibb, F. M., and Augley, J. (2018). Assessing the role of ontogenetic movement in maintaining population structure in fish using otolith microchemistry. *Ecology and Evolution* **8**, 7907–7920. doi:10.1002/ece3.4186
- Yates, P., Ziegler, P., Welsford, D., Mclvor, J., Farmer, B., and Woodcock, E. (2018). Spatio-temporal dynamics in maturation and spawning of Patagonian toothfish *Dissostichus eleginoides* on the sub-Antarctic Kerguelen Plateau. *Journal of Fish Biology* **92**, 34–54. doi:10.1111/jfb.13479
- Ye, Y., and Gutierrez, N. L. (2017). Ending fishery overexploitation by expanding from local successes to globalized solutions. *Nature Ecology & Evolution* **1**, 0179. doi:10.1038/s41559-017-0179
- Ying, Y., Chen, Y., Lin, L., and Gao, T. (2011). Risks of ignoring fish population spatial structure in fisheries management. *Canadian Journal of Fisheries and Aquatic Sciences* **68**, 2101–2120. doi:10.1139/F2011-116
- Young, M., and Carr, M. H. (2015). Application of species distribution models to explain and predict the distribution, abundance and assemblage structure of nearshore temperate reef fishes. *Diversity and Distributions* **21**, 1428–1440. doi:10.1111/ddi.12378
- Zemeckis, D. R., Martins, D., Kerr, L. A., and Cadrin, S. X. (2014). Stock identification of Atlantic cod (*Gadus morhua*) in US waters: an interdisciplinary approach. *ICES Journal of Marine Science* **71**, 1490–1506. doi:10.4135/9781412953924.n678
- Zischke, M. T., Litherland, L., Tilyard, B. R., Stratford, N. J., Jones, E. L., and Wang, Y. G. (2016). Otolith morphology of four mackerel species (*Scomberomorus* spp.) in Australia: Species differentiation and prediction for fisheries monitoring and assessment. *Fisheries Research* **176**, 39–47. doi:10.1016/j.fishres.2015.12.003
- Zuur, A. F. (2016). 'A Beginner's Guide to Generalized Additive Models with R' 3rd ed.

(Highland Statistics Ltd.: Newburgh.)

Zuur, A. F., and Ieno, E. N. (2018). 'Beginner's Guide to Spatial, Temporal and Spatial-Temporal Ecological Data Analysis with R-INLA Volume II: GAM and Zero-Inflated Models'. (Highland Statistics Ltd.: Newburgh.)

Zuur, A. F., Ieno, E. N., and Elphick, C. S. (2010). A protocol for data exploration to avoid common statistical problems. *Methods in Ecology and Evolution* **1**, 3–14. doi:10.1111/j.2041-210X.2009.00001.x

Zuur, A. F., Ieno, E. N., and Saveliev, A. A. (2017). 'Beginner's Guide to Spatial, Temporal and Spatial-Temporal Ecological Data Analysis with R-INLA Volume I: Using GLM and GLMM'. (Highland Statistics Ltd.: Newburgh.)

Zuur, A. F., Ieno, E. N., Walker, N. J., Saveliev, A. A., and Smith, G. M. (2009). 'Mixed Effects Models and Extensions in Ecology with R'. (Springer Science and Business Media, LLC: New York.)